CORA Cork Open Research Archive
Cartlann Taighde Oscailte Chorcaí

Title	The bacteriome and virome in social and stress-related disorders
Authors	Ritz, Nathaniel L.
Publication date	2023
Original Citation	Ritz, N. L. 2023. The bacteriome and virome in social and stress-related disorders. PhD Thesis, University College Cork.
Type of publication	Doctoral thesis
Rights	© 2023, Nathaniel Lloyd Ritz. - https://creativecommons.org/licenses/by/4.0/
Download date	2026-11-17 11:37:45
Item downloaded from	https://hdl.handle.net/10468/15971

UCC
University College Cork, Ireland
Coláiste na hOllscoile Corcaigh

University College Cork, Ireland
Coláiste na hOllscoile Corcaigh

Ollscoil na hÉireann, Corcaigh
National University of Ireland, Cork

Department of Anatomy and Neuroscience
Head of Department - Professor Aideen Sullivan

The Bacteriome and Virome in Social and Stress-Related Disorders

Thesis presented by

Nathaniel Lloyd Ritz MSc.

under the supervision of

Professor John F. Cryan
Professor Timothy G. Dinan

for the degree of

Doctor of Philosophy

November 2023

Microbiome Ireland
Interfacing Food & Medicine

Table of contents

Declaration **5**

Author contributions **7**

Acknowledgements **7**

Publications and presentations **8**

Abstract **11**

Chapter 1 Introduction **13**

1.1 The Microbiota-Gut-Brain Axis **14**

1.1.1 Bacteriome-Gut-Brain Axis 16

1.2 Modes of communication **19**

1.2.1 Immune system 19

1.2.2 Microbial metabolites 21

1.2.3 Endocrine signaling 22

1.2.4 Enteric nervous system 23

1.2.5 Vagus nerve 23

1.2.6 Neurotransmitters and neuroactive chemicals 24

1.3 Gut Viruses **26**

1.3.1 Bacteriophages of the gut 34

1.3.2 Viral immune activation and inflammation: A first line of interaction with the microbiota-gut-brain axis 36

1.3.3 Potential of phage therapy and faecal virome transplants 39

1.4 Gut Fungi **41**

1.4.1 Fungi and the microbiota-gut-brain axis 42

1.4.2 Fungi and the immune system 44

1.5 Gut Archaea **45**

1.5.1 Methanogens and gut physiology 46

1.6 Other members of the microbiome 47
1.6.1 Challenges to studying the non-bacteriome field 50
1.7 The Microbiota-Gut-Brain Axis and Brain Disorders 51
1.7.1 Social and Stress-Related Disorders 57
1.7.2 Chronic Stress 59
1.7.3 Social Anxiety Disorder 60
1.8 Aims and objectives 61
Aim 1: Can the virome be used to reduce the effects of chronic stress on brain and behaviour? **61**
Aim 2: Is the microbiome associated with social fear resiliency? **61**
Aim 3: Does microbiota from individuals with social anxiety disorder play a causal role in social fear behaviour? **62**

Chapter 2 The Gut Virome is Associated with Stress-Induced Changes in Behaviour and Immune Responses in Mice 63
2.1 Abstract **64**
2.2 Introduction **64**
2.3 Results **66**
2.4 Discussion **84**
2.5 Methods **93**
2.6 Supplemental Figures **116**

Chapter 3 Social Fear Extinction Susceptibility is Associated with Microbiota-Gut-Brain Axis Alterations 130
3.1 Abstract **131**
3.2 Introduction **132**
3.3 Methods **134**
3.4 Results **145**
3.5 Discussion **155**

3.6 Supplemental Figures **161**

Chapter 4 Social Anxiety Disorder-Associated Gut Microbiota Increases Social Fear **162**

4.1 Abstract **163**

4.2 Introduction **164**

4.3 Results **165**

4.4 Discussion **177**

4.5 Methods Summary **184**

4.6 Supplemental Figures **206**

Chapter 5 Discussion and conclusions **217**

5.1 Summary **218**

5.2 Faecal virome transplant as a tool to elucidate the role of the stressed gut virome **221**

5.3 Limitations of faecal virome transplant studies **223**

5.4 Future of virome therapeutics **224**

5.5 The social fear conditioning paradigm in the context of the microbiota-gut-brain axis **225**

5.6 Social anxiety disorder humanized mice to assess microbiota driving social fear causality **226**

5.7 Limitations of microbiota-gut-brain axis and social fear **227**

5.8 Social anxiety and microbiota: Where are we going **228**

5.9 Conclusions **230**

Declaration

This is to certify that the work I am submitting is my own and has not been submitted for another degree, either at University College Cork or elsewhere. All external references and sources are clearly acknowledged and identified within the contents. I have read and understood the regulations of University College Cork concerning plagiarism and intellectual property.

Author contributions

All the work conducted in this thesis was performed by the author in collaboration with the following.

Chapter 2: N.L.R., L.A.D, V.L.P, A.N.S., G.M.M., T.G.D, C.H., and J.F.C. designed the studies. N.L.R. and V.L.P. performed the experiments with animals. N.L.R., L.A.D., V.L.P. M.v.d.W., K.V., C.F., K.E.G, A.B, and M.D. performed assays, sample collection, and processing. T.F.S.B., L.A.D., C.T., V.L.P., H.H., M.D., F.C., and P.C. generated metagenomic and virome sequencing analyses. T.F.S.B. and G.M.M. generated transcriptomic analyses. N.L.R. and T.F.S.B. analysed the data. N.L.R. and J.F.C. wrote the paper with contributions made from all the authors.

Chapter 3: N.L.R., C.S.M.C., G.M.M., L.A.D, C.H., T.G.D, D.A.S., and J.F.C. designed the studies. N.L.R., C.S.M.C., and N.T. performed the experiments with animals. N.L.R., M.B., and L.A.D., performed assays, sample collection, and processing. L.S., A.N.S., and T.F.S.B. generated metagenomic and virome sequencing analyses and interpretation.

N.L.R., A.N.S., L.S., and T.F.S.B. analysed the data. N.L.R. and J.F.C. wrote the paper with contributions made from all the authors.

Chapter 4: N.L.R., M.I.B., C.S.M.C., L.A.D, V.T., L.M., M.R.A., G.M.M., C.H., G.C., D.A.S., T.G.D, and J.F.C. designed the studies. N.L.R. and M.B. performed the experiments with animals. N.L.R., M.B., M.I.B., C.S.M.C., C.B., L.A.D., V.T., L.M., D.C., C.E.G., A.R., V.S., A.G., and G.M.M. performed assays, sample collection, and processing. C.T., A.N.S., and T.F.S.B. generated metagenomic and virome sequencing analyses. N.L.R., C.T., and T.F.S.B. analysed the data. N.L.R. and J.F.C. wrote the paper with contributions made from all the authors.

Acknowledgements

First, I would like to my thanks supervisors Professor John Cryan and Professor Ted Dinan for giving me the opportunity to pursue a PhD in their lab group. John was always close at hand, day or night, to guide, mentor, and push me in my pursuit as a scientist. I have gained invaluable professional, scientific, and life experience during the process of this PhD work, and I will be forever grateful for their time, patience, and support they generously offered me.

I would also like to thank my close collaborators and colleagues in the Cryan Lab. Being a part of this group has been a great pleasure and there is not a better group of people that I could have shared this experience with. Thank you to the senior research members of the Microbiota-Gut-Brain Axis Group, the research staff in the Dept. of Anatomy and Neuroscience, and lab mates who have helped me along our shared journeys. You all have been a huge source of help and have become many of my closest friends. I would also like to thank my first research mentors Professor Henry Lin and Professor Larry Barton who inspired me to pursue a career in science years ago.

Finally, I would like to extend my thanks to my family back home, who have continued to share their love and excitement in my research pursuits, despite my moving across the world. My love and thanks also go to my family, Minke and Comet, and friends here in Ireland and abroad, who have helped me celebrate the successes, weather the storms, and somehow reach the summit.

Publications and presentations

Accepted and published manuscripts relevant to thesis

Ritz NL, Draper LA, Bastiaanssen TFS, Turkington CJR, Peterson VL, van de Wouw M, Vlckova K, Fulling C, Guzzetta KE, Burokas A, Harris H, Dalmasso M, Crispie F, Cotter PD, Shkoporov AN, Moloney GM, Dinan TG, Hill C, Cryan JF. The Gut Virome is Associated with Stress-Induced Changes in Behaviour and Immune Responses in Mice. Accepted at *Nature Microbiology*.

Ritz NL, Brocka M, Butler MI, Cowan CSM, Barrera- Bugueño C, Draper LA, Turkington CJR, Bastiaanssen TFS, Turpin V, Morales L, Campos D, Gheorghe CE, Ratsika A, Sharma V, Golubeva AV, Aburto MR, Shkoporov AN, Moloney GM, Hill C, Clarke G, Slattery DA, Dinan TG, Cryan JF. Social anxiety disorder-associated gut microbiota increases social fear. Accepted at *Proceedings of the National Academy of Sciences*.

Butler MI, Bastiaanssen TFS, Long-Smith C, Morkl S, Berding K, **Ritz NL**, Strain C, Patangia D, Patel S, Stanton C, O'Mahony SM, Cryan JF, Clarke G, Dinan TG. The gut microbiome in social anxiety disorder: evidence of altered composition and function. *Translational Psychiatry* 2023; 13(1):95.

Gheorghe CE, **Ritz NL**, Martin JA, Wardill HR, Cryan JF, Clarke G. Investigating causality with fecal microbiota transplantation in rodents: applications, recommendations and pitfalls. *Gut Microbes* 2021; 13(1):1941711.

Boehme M, Guzzetta KE, Bastiaanssen TFS, Van de Wouw M, Moloney GM, Gual-Grau A, Spichak S, Olavarría-Ramírez L, Fitzgerald P, Morillas E, **Ritz NL**, Jagger M, Cowan CSM, Crispie F, Donoso F, Halitzki E, Neto MC, Sichetti MS, Golubeva AV, Fitzgerald RS, Claesson MJ, Cotter PD, O'leary OF, Dinan TG, Cryan JF. Microbiota from young mice counteracts selective age-associated behavioral deficits. *Nature Aging* 2021; 1(8):666-76.

Van de Wouw M, Sichetti M, Long-Smith CM, **Ritz NL**, Moloney GM, Cusack A, Berding K, Dinan TG, Cryan JF. Acute stress increases monocyte levels and modulates receptor expression in healthy females. *Brain, Behavior, and Immunity* 2021: 94:463-8

Bastiaanssen TFS, Gururajan A, Van de Wouw M, Moloney GM, **Ritz NL**, Long-Smith CM, Wiley NC, Murphy AB, Lyte JM, Fouhy F, Stanton C, Claesson MJ, Dinan TG, Cryan JF. Volatility as a concept to understand the impact of stress on the microbiome. *Psychoneuroendocrinology* 2021; 124:105047.

Cryan JF, O'Riordan KJ, Cowan CSM, Sandhu KV, Bastiaanssen TFSB, Boehme M, Codagnone MG, Cussotto S, Fulling V, Golubeva AV, Guzzetta KE, Jaggar M,

Long-Smith CM, Lyte JM, Martin JA, Molinero-Perez A, Moloney G, Morelli E, Morillas E, O'Connor R, Cruz-Pereira JS, Peterson VL, Rea K, **Ritz NL**, Sherwin E, Spichak S, Teichman EM, van de Wouw M, Ventura-Silva AP, Wallace-Fitzsimons SE, Hyland N, Clarke G, and Dinan TG. The microbiota-gut-brain axis. *Physiological Reviews* 2019; 99(4):1877-2013.

Submitted manuscripts relevant to thesis

Ritz NL, Bastiaanssen TFS, Cowan CSM, Smith L, Theune N, Brocka M, Moloney GM, Shkoporov AN, Draper LA, Hill C, Dinan TG, Slattery DA, Cryan JF. Social Fear Extinction Susceptibility is Associated with Microbiota-Gut-Brain Axis Alterations. Submitted to *Brain, Behavior, and Immunity*.

Manuscripts in preparation relevant to thesis

Ritz NL, Dinan TG, Hill C, Cryan JF. The microbiota-gut-brain axis: beyond the bacteriome. In preparation.

Other published manuscripts

Birg A, **Ritz NL**, Barton LL, Lin HC. Hydrogen availability is dependent on the actions of both hydrogen-producing and hydrogen-consuming microbes. *Digestive Disease and Sciences* 2023; 68(4):1253-9.

Singh SB, Carroll-Portillo A, Coffman C, **Ritz NL**, Lin HC. Intestinal alkaline phosphatase exerts anti-inflammatory effects against lipopolysaccharide by inducing autophagy. *Scientific Reports* 2020; 10(1):3107.

Lin DM, Koskella B, **Ritz NL**, Lin D, Carroll-Portillo A, Lin HC. Transplanting fecal virus-like particles reduces high-fat diet-induced small intestinal bacterial overgrowth in mice. *Frontiers in Cellular and Infection Microbiology* 2019; 9:348.

Barton LL, Granat AS, Lee S, Xu H, **Ritz NL**, Hider R, Lin HC. Bismuth(III) interactions with Desulfovibrio desulfuricans: inhibition of cell energetics and nanocrystal formation of Bi_2S_3 and Bi^0. *Biometals* 2019; 32(5):803-11.

Birg A, **Ritz NL**, Lin HC. The unknown effect of antibiotic-induced dysbiosis on the gut microbiota. *Microbiome and Metabolome in Diagnosis, Therapy, and other Strategic Applications* 2019; 10.1016/B978-0-12-815249-2.00020-8.

Other manuscripts in preparation

Sharvin BL, Gavioli N, **Ritz NL**, Morley S, Cabre S, Gunnigle E, Warda A, Dinan TG, Stanton C, Ross P, Cryan JF. Probiotic supplementation restores adult brain and behaviour in missing microbes in infants born by caesarian section. In preparation.

Gavioli N, Sharvin BL, **Ritz NL**, Hedayatpour D, Gunnigle E, Warda A, Dinan TG, Stanton C, Ross P, Cryan JF. Probiotic supplementation restores adolescent brain and behaviour in missing microbes in infants born by caesarian section. In preparation.

Conference posters and oral presentations

Ritz NL, Draper LA, Bastiaanssen TFS, Turkington CJR, Peterson VL, van de Wouw M, Vlckova1 K, Fulling C, Guzzetta KE, Burokas A, Harris H, Dalmasso M, Crispie F, Cotter PD, Shkoporov AN, Moloney GM, Dinan TG, Hill C, Cryan JF. The Virome Regulates the Effects of Chronic Stress in Mice. (Poster presentation at European College of Neuropsychopharmacology, Barcelona, Spain, October 2023, *ECNP Excellence Award).

Ritz NL, Cryan JF. Microbiome and the social brain. *IBNS* 2022 (Oral presentation at International Behavioural Neuroscience Society, Glasgow, Scotland, June 2022).

Ritz NL, Cryan JF. Microbiome and the social brain. *WFSBP Congress* 2021 (Virtual oral presentation at 15th World Congress of Biological Psychiatry, Vienna, Austria, June 2021).

Ritz NL, Draper LA, Bastiaanssen TFS, Turkington C, Peterson VL, van de Wouw M, Vlckova K, Burokas A, Harris H, Dalmasso M, Crispie F, Cotter P, Fulling C, Shkoporov AN, Moloney G, Dinan TG, Hill C, Cryan JF. Stress gone viral: Targeting the virome to counter the effects of stress in mice. *TTBD* 2021 (Virtual poster presentation at Targeting Therapeutics for Brain Disorders, Cork, Ireland, June 2021).

Ritz N, Cowan C, Theune N, Smith L, Draper L, Dinan T, Slattery D, Cryan J. P. 225 Differential social fear response in mice is not affected by microbiota depletion. *Eur Neuropsychopharm* 2021;44:S32-S33. (Virtual presentation at European College of Neuropsychopharmacology Workshop for Early Career Scientists in Europe, November 2021).

Abstract

The gastrointestinal microbiota has been shown to influence mammalian health and well-being in many conditions but has also been implicated in a variety of diseases and disorders. The multi-faceted interaction of the microbiota with the host that affects the brain and behaviour is termed the microbiota-gut-brain axis. While this axis plays an important role in stress and social behaviour, research has largely focused on associations with the bacterial fraction of the community. The gut also harbours viruses, fungi, archaea, and other microbial forms of life that can affect the health of the mammalian host. Gut viruses, which are dominated by bacteriophages, are also ubiquitous in the gut and have the ability to infect bacteria and alter their structure and activity. Moreover, these populations of viruses are intimately associated with the bacterial community, but little is known about their involvement within the microbiota-gut-brain axis. Whether bacteriophages are capable of exerting effects on the brain and behaviour is largely unknown. To this end, we tested whether the virome was affected by stress followed by the capability of the virome to prevent stress-related sequelae. We found that the virome is stress sensitive and that restoring the virome to mice undergoing stress reduced anxiety-like behaviour, immune activation, inflammation, and gene expression in the brain. These data provide evidence that the gut virome can be harnessed to improve stress-coping outcomes.

Social diseases and disorders have been implicated in the microbiota-gut-brain axis. Social anxiety disorder is a common but understudied psychiatric condition. Whether specific microbiota communities play a role in social fear responsivity or are capable of

driving social fear behaviour is also unknown. Preclinical animal models of social fear allow for testing translational hypotheses that can then be returned to the clinic. We sought to characterize associations of the microbiota with social fear resiliency and susceptibility. Then, we transferred microbiota from individuals with social anxiety disorder to mice to test whether the microbiota played a causative role in the disorder. We found a strong correlation between microbiota and social fear variability along with differential expression of amygdalar genes involved in social behaviour, immunity, and host-microbe interaction. We also found that microbiota from individuals with social anxiety disorder could drive social fear sensitivity in mice. Mice that received microbiota from social anxiety disorder donors also had impaired cytokine release in the gut, reduced immune cell populations in the mesenteric lymph nodes and circulation, altered basal HPA axis, and diminished oxytocin and oxytocin-related expression of genes in the brain. These data indicate that social fear and anxiety are linked with the microbiota and that the gut-brain axis is a target for future research for social anxiety disorder therapeutics.

Herein we tested whether gut viruses could alter stress response, whether social fear behaviour is associated with differential microbial communities, and whether human microbiota from individuals with social anxiety disorder can drive social fear behaviour in the mouse. Collectively we have shown that stress-related sequelae can be restored by virome transfer and that the microbiota can play a causal role in social anxiety disorder.

Chapter 1

Introduction

1.1 The Microbiota-Gut-Brain Axis

The term microbiota refers to the collection of microbes that live in and on us. Bacteria are the most common and most active but viruses, fungi, archaea, and other microorganisms also exist in this dynamic ecosystem. Microbiota research has vastly grown over the past two decades, thanks in part to new sequencing technology advancements allowing the characterization of microbial nucleic acids motifs[1]. While recent microbiota research and concepts give the feeling that this is a new phenomenon, microbes precede multicellular life and have in fact co-evolved with our earliest ancestors depending on one another in symbiosis for survival[2]. The concept of the holobiont describes the ecological unit of the host and its symbiotic microbiota[3,4]. This symbiotic relationship has far-reaching effects and recent evidence indicates that our neurobiological function, brain, and behaviour depend on the holobiont perspective to better understand factors that promote health and well-being[5].

The complex ecosystem of bacteria that coexist with the human host have been estimated to slightly outnumber human cells by approximately 1.1-fold[6]. However, the total genetic material, known as the microbiome, has been estimated to outnumber the human genome 100-fold[7]. The highest microbial density is found in the distal gut, or large intestine, where the microbes help the breakdown of complex dietary components that allows for optimal digestion and absorption of nutrients for the host (Fig. 1.1.1). However, these microbes also play a fundamental role in the development, immunity, and homeostasis of the host. For these reasons, it is perhaps not unsurprising that the microbes that cohabitate in and on us also play a pivotal role in our health and well-being. The microbiota-gut-brain axis

is a burgeoning field of research that is investigating the bi-directional communication between microbes inhabiting the gastrointestinal tract and the brain[8].

Complex communication and signalling cross the boundaries of neural connections, immune activation, microbe-host interaction, and chemical messaging. It is clear that gut microbes are capable of influencing peripheral systems (e.g. immune and metabolism) and central systems at the level of microglia[9,10], myelination[11], neurotransmission[12], and gene expression[13,14]. Furthermore, there have been many studies associating altered host behaviours with ingestion of specific strains of bacteria[15-17], faecal microbiota transplantation (FMT) of the gut microbiota[18-21], prebiotics[22-25] and microbiota derived metabolites[26-28]. However, most of the research to date has focused on the impact of bacterial members of the microbiota within gut ecosystem and on the human host. Less studied components of the gut microbiota are the viruses, fungi, archaea, and other members that intimately contribute to microbiota community dynamics[29]. Here we focus on the role of the non-bacterial members with special focus on the viruses of the gut microbiota across various diseases and disorders in the gut-brain axis.

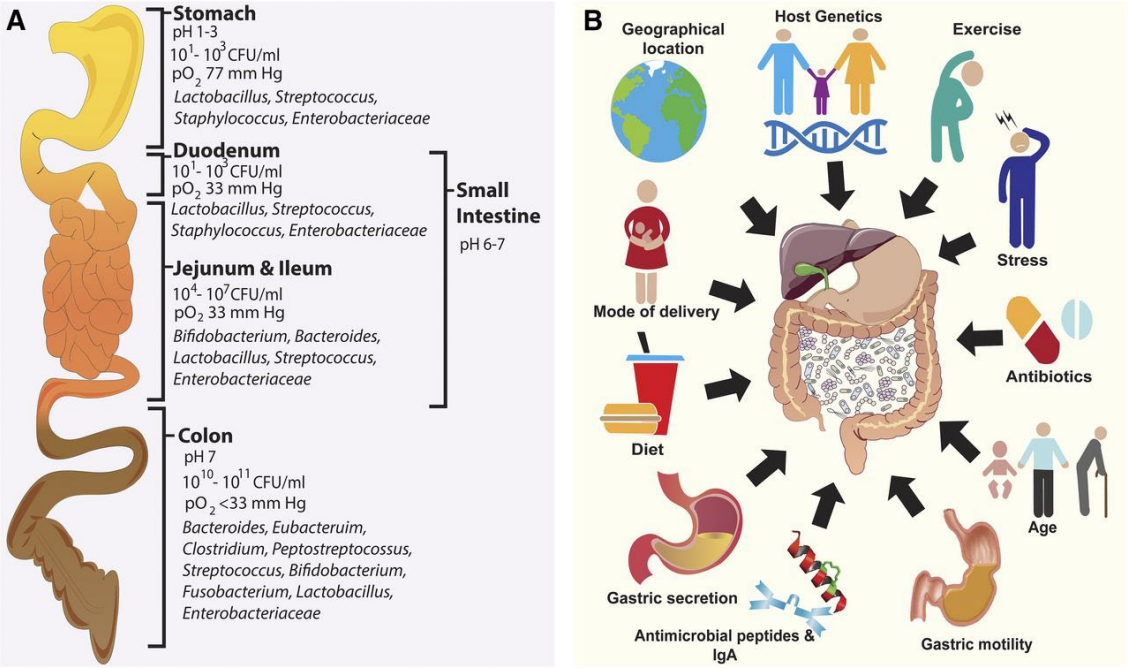


Fig. 1.1.1 Gut biogeography and factors that influence the microbiota. A) *The spatial organization and localization of microbes in the gut depend on many unique features found along the gastrointestinal tract. Microbe-host colonization and interaction largely depend on microniches, pH gradient, and luminal mucosa structure and function along the gut. The density of microbes increases longitudinally along the gut with the lowest numbers found in the acidic stomach and the highest numbers in the distal colon.* ***B)*** *Examples of factors that can affect gut microbiota composition and metabolic function. Some factors are out of our control to change (e.g., host genome, birth mode, aging, etc.) but others are well within reach to optimize microbiota health (e.g., diet, exercise, antibiotics, probiotics, etc.). Figure from Clarke et al., 2019.*

1.1.1 Bacteriome-Gut-Brain Axis

The microbial community in the gut is dominated by the presence and activity of the bacterial community, of which, the collection of genetic material is referred to as the bacteriome. Bacteria number $1x10^{11}$cfu g^{-1} in stool and their nucleic content makes up approximately 93% of the total DNA[6]. The vast majority of the functional activity of the

gut microbial ecosystem is also driven through the bacteriome[30,31]. The functional output of the bacteriome is largely dictated by the diet of the individual, which in turn, affects host metabolite and nutrient availability in addition to modulating inflammatory and immunity[32-34]. The bacteriome has also been shown to be altered in some cases play a causal role in different diseases and disorders such as autism spectrum disorder[20] neurodegenerative disorders[35,36], and stress-related disorders like depression and anxiety[18,37,38]. To unravel the extent of microbial influence there have been various preclinical models designed to fill in the gaps of our understanding (Fig 1.1.2), but since microbial life evolved with mammals from the beginning, perhaps the best place to start is what life looks like in the absence of microbes.

Germ-free (GF) mice, which are lacking any microbiota or microbe exposure and housed in a sterile environment, provide a powerful tool whereby presence (or conventionalised) vs. absence (GF) studies can characterize functions that the microbiota play. In general, GF mice have abnormal development that leads to stark differences in behaviour, immunity, barrier permeability (intestinal epithelium, blood brain barrier, and cerebrospinal fluid barrier), myelination patterns, and neuronal factors[12,39-44]. Furthermore, GF mice do not contain appropriate T cell receptors $CD4^+$ and $CD8^+$ compared to conventionalized animals, indicating inadequate immune development when brought up in the absence of microbes[45]. Indigenous *Clostridium* species have been shown to play a critical role in immune homeostasis through $CD4^+$ T regulatory cells[46]. Microbes, their components, and the products they generate are capable of modulating immune activation[47]. Microbes in the gut have been linked with the release of systemic

proinflammatory cytokines (TNF-α, IL-1β, IL-6, IL-17, *etc*.) which can then activate other response pathways and the brain[48-50].

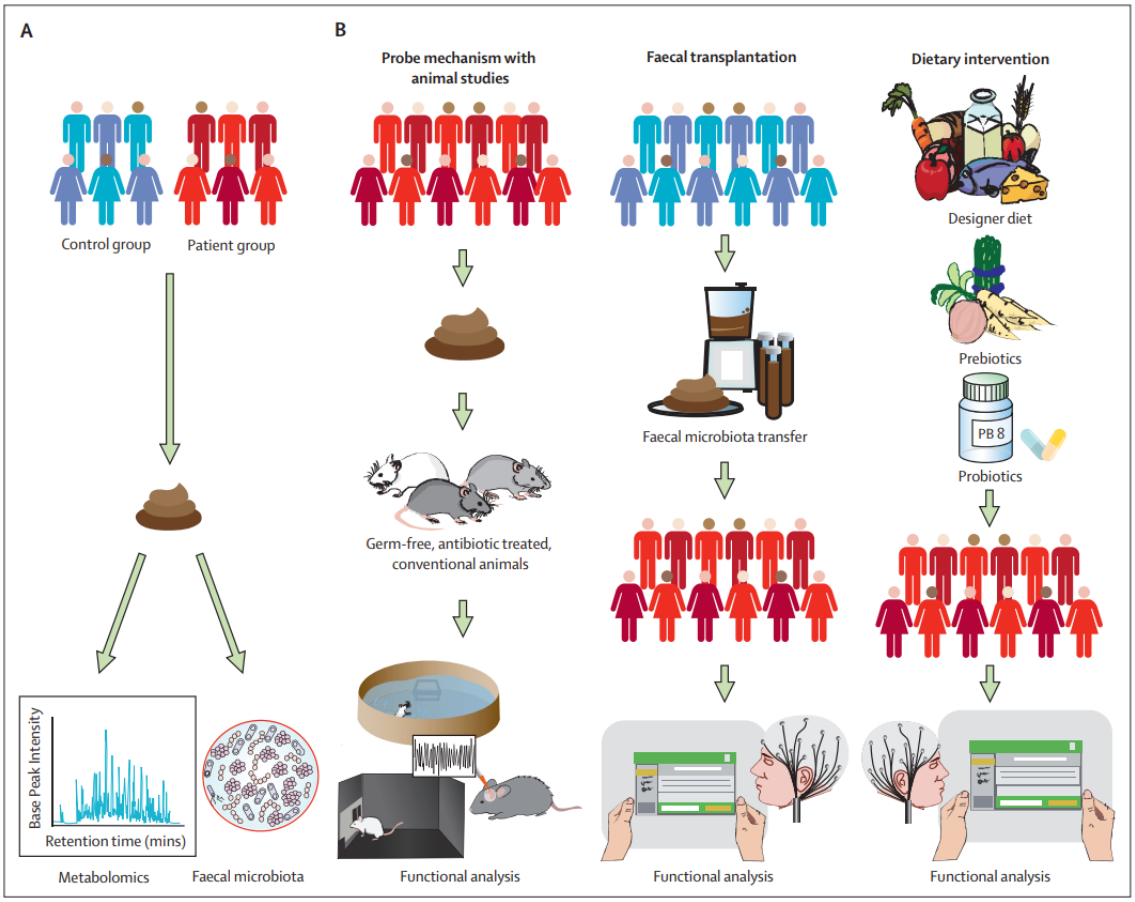


Fig. 1.1.2. Strategies to investigate the role of the human microbiome in disease and disorder. A) *In order to build associations between the microbiota, disease, and disorder, the first step is to characterize the microbiome across the disease or disorder in question and compare it to matched controls to assess microbiota structure and function.* ***B)*** *The next step is to elucidate whether the microbiota plays a causal role in the disease or disorder. This can be done by transferring the microbiota to animal models (typically that have depleted microbiotas either by GF or antibiotic treatment) and testing functions that are associated with the disease or disorder. Then, the following step is to test whether microbiota-based treatments (e.g., FMT, diet, probiotics, etc.) are capable of improving the phenotype. Figure from Cryan et al., 2020.*

1.2 Modes of communication

The bi-directional communication between the brain and gut is crucial in understanding the microbiota-gut-brain axis. There are multiple modes of communication by which the gut microbiota interfaces with the host that can affect the brain. These routes of communication consist of immune activation, the release and absorption of bioactive molecules into circulation, endocrine signalling, enteric nervous system innervation, and directly through the vagus nerve (Fig1.2)[8]. Bacteria have been shown to stimulate gut-brain signalling through each route.

1.2.1 Immune system

The gastrointestinal system is exposed to many external environmental stimuli, xenobiotics, and of course microorganisms and thus it is not surprising that the gut harbors the largest collection of immune cells in the body. The gut epithelium interfaces with this collection of external entities with a single layer of cells that both provide a barrier from the environment, but also allow for digestion and absorption to occur. This is accomplished by a collection of different cell types each providing specific functions to maintain homeostasis. Goblet cells secrete a viscous layer of mucus that coats the luminal lining of the gut, and this luminal-mucosal boundary is the key site of interaction between host and microbes. Therefore, this is also where innate immunity and immune sensing of microbes occur and adaptive immune begins[51]. This information can then be relayed back to the CNS where microbiota-immune-brain interactions then unfold[52].

The intestinal microbiota not only shapes gut function at a local level, it also can stimulate systemic and CNS immunity which can affect mood and behaviour[53]. There are numerous pathways by which specific interactions with gut microbes in the intestinal mucosa can affect host immunity. Toll-like receptors (TLRs) are pattern recognition receptors that play a vital role in immune responses particularly in pathogen recognition. TLRs are broadly activated by various microbial components: TLR-1, 2, 4-6, and 9 are stimulated by bacterial products; TLR-2-4, 6, and 7-9 are stimulated by viral products; TLR-2, 4, 6, and 9 by fungi; and TLR-2, 4, 9 by parasites[54]. Lipopolysaccharide (LPS), a cell membrane component of Gram-negative bacteria, activates TLR-4 and co-receptors CD14 and myeloid differentiation protein 2, which results in the secretion of pro-inflammatory cytokines[55]. Recognition of LPS by epithelial cells leads to immune responses which increase the infiltration of monocytes into the CNS and sickness behaviour[56,57]. Conversely, TLR-9 is activated in response to intracellular viral and bacterial DNA where it then stimulates inflammation and immune activation[58]. Treating GF mice with bacteriophages led to gut immune cell expansion and interferon gamma (IFN-γ) stimulation via nucleotide-sensing TLR-9[59].

The release of specific pro (IL-1β, TNF-α, IFN-γ, IL-6, IL-8, IL-12, IL-17) or anti (IL-4, IL-10, IL-22, TGF-β) -inflammatory or adaptive immunity (IL-2-5, 7, 9) cytokines then determines subsequent immune pathways such as T cell differentiation of type 1 T helper (Th1), Th2, T regulatory, or Th17 cells[60-62]. Specific microbes have been linked to cytokine responses in humans, further increasing our ability to target the microbiota to diagnose individuals and design disease-specific and personalized medical care[63]. In a

TLR-5 deficient murine model of colitis, members of the phylum *Pseudomonadota* (formerly *Proteobacteria*; e.g. *Enterobacteria* spp.) were associated with elevated pro-inflammatory gene expression in the gut and prolonged colitis[64]. There are a number of risk factors that can lead to a proinflammatory microbiota composition such as diet, obesity, disease and disorder[65,66]. As the microbiota is integrally involved in these components of health, further understanding the function and role of microbiota-immune is paramount to designing future microbiota-based therapeutics to improve health and well-being[62,67].

1.2.2 Microbial metabolites

The gut microbiota produces a variety of microbial-derived metabolites. One of the key groups of metabolites produced by bacteria are the short chain fatty acids (SCFAs) primarily composed of acetate, propionate, and butyrate which are readily absorbed by colonocytes and elicit a variety of effects across different tissues, including the brain [68]. The primary source of SCFAs is through microbial fermentation of dietary fibres that are indigestible by the host[69]. SCFAs have been implicated in many physiological processes such as gastrointestinal function[70] and immune function[48]. SCFA reductions have also been associated with chronic stress in both human and murine studies[71]. Furthermore, SCFAs administered to mice undergoing psychosocial stress was shown to alleviate reward-seeking and responsiveness behaviours and protect epithelial barrier function[27]. Another important microbiota influenced metabolite group are branched chain amino acids like valine, leucine and isoleucine which are essential amino acids produced by gut

bacteria in higher amounts than other amino acids. However, the functional and interactive role they play in the microbiota-gut-brain axis is not well understood[72]. Branched chain amino acids have been shown to influence epithelial cells as well as the mucosal immune system[73,74], in addition to showing benefits to well-being and aging[75]. There are also bacterial components like lipopolysaccharide (LPS) and peptidoglycans that elicit host immune responses that play an important role in immune development[76] but also in the brain and behaviour development[77].

1.2.3 Endocrine signalling

The endocrine system, governed by the hypothalamus, uses chemical signals in the form of hormones and neuropeptides to maintain a variety of functions important to the gut-brain axis including metabolism, development, and mood[78,79]. The hypothalamic-pituitary-adrenal axis (HPA axis) is one such example that balances hormones in response to stress, largely through governing the release of cortisol (or corticosterone in rodents), which can be modulated by microbiota-based therapies[80]. Although low in number, enteroendocrine (EE) cells play a crucial sensory role in the gut due to the release of various signalling molecules that help maintain intestinal homeostasis in response to direct and indirect microbiota interactions[81]. The two best studied EE cells are 1) EE L cells which secrete glucagon-like peptide-1 and peptide YY which modulate food intake[82] and 2) enterochromaffin cells which produce most of the serotonin in the body from dietary tryptophan which mediate numerous physiological processes as stated above[83].

1.2.4 Enteric nervous system

The gut is often referred to as the "second brain" because of the extensive neuronal connections throughout the intestinal submucosa and myenteric plexuses that make up the largest component of the autonomic nervous system, the enteric nervous system (ENS). The ENS shares many neurotransmitters and signalling pathways found in the central nervous system (CNS) and is equipped with sufficient circuitry to orchestrate gastrointestinal function independent of CNS input[84]. However, the ENS is linked to the CNS through the vagus nerve which serves as a conduit between the brain and gut[85].

1.2.5 Vagus nerve

Signalling through the vagus nerve (the 10th cranial nerve that links the gut and viscera with the brain) has primarily been studied in the context of hunger, satiety, and stress response. By severing vagal circuits, modulating the gut microbiota, and measuring effects on the brain and behaviour, researchers can show what effects are driven through this pathway. Preclinical animal studies using this technique have shown that stress response, anxiety-like, fear, and cognitive behaviours as well as neurogenesis are impacted by vagus nerve stimulation[86]. *Lacticaseibacillus rhamnosus* (formerly *Lactobacillus rhamnosus*) has been shown to reduce stress-induced corticosterone, anxiety- and depression-like behaviours in mice[15]. Interestingly, these effects were abolished in vagotomised mice- showing evidence that the vagus is a major pathway of communication between gut bacteria and the brain[15]. Similarly, prebiotics have also been shown to have their cognitive and electrophysiological effects blocked by vagotomy[87].

Furthermore, social behaviour that was improved by *Limosilactobacillus reuteri* (formerly *Lactobacillus reuteri*) via oxytocin signalling has been shown to be dependent on vagal innervation[88].

1.2.6 Neurotransmitters and neuroactive chemicals

Through its normal metabolism the microbiota produces a variety of compounds in complex trophic interactions. Many of these products are bioactive and also interact with the host. Neurotransmitters and neuroactive metabolites including, but not limited to, glutamate, glutamine, *N*-acetyl aspartate, γ-aminobutyric acid (GABA), 4-ethylphenylsulfate and catecholamines can be produced by microbes in the gut and can impact host behaviour and physiology[44,89-93]. Gut microbes directly and indirectly influence tryptophan metabolism occurs where serotonin is then synthesised and plays diverse roles including the modulation of mood and behaviour, gastrointestinal motility, hunger, and sleep[94]. Tryptophan catabolism also generates kynurenine, which also modulates neural activity and systemic inflammation. Interestingly, in GF mice there is a reduction in tryptophan metabolism in the kynurenine pathway, which indicates an important role of the microbiota in this pathway network[95,96].

While many microbiota-gut-brain axis communication mechanisms have been described to date, there are still many unknowns in the underlying interplay and signalling mechanisms. Elucidating the biology underpinning these mechanisms will be a top priority in the coming years to better understand the microbiota and modulate its effects in disease and disorder.

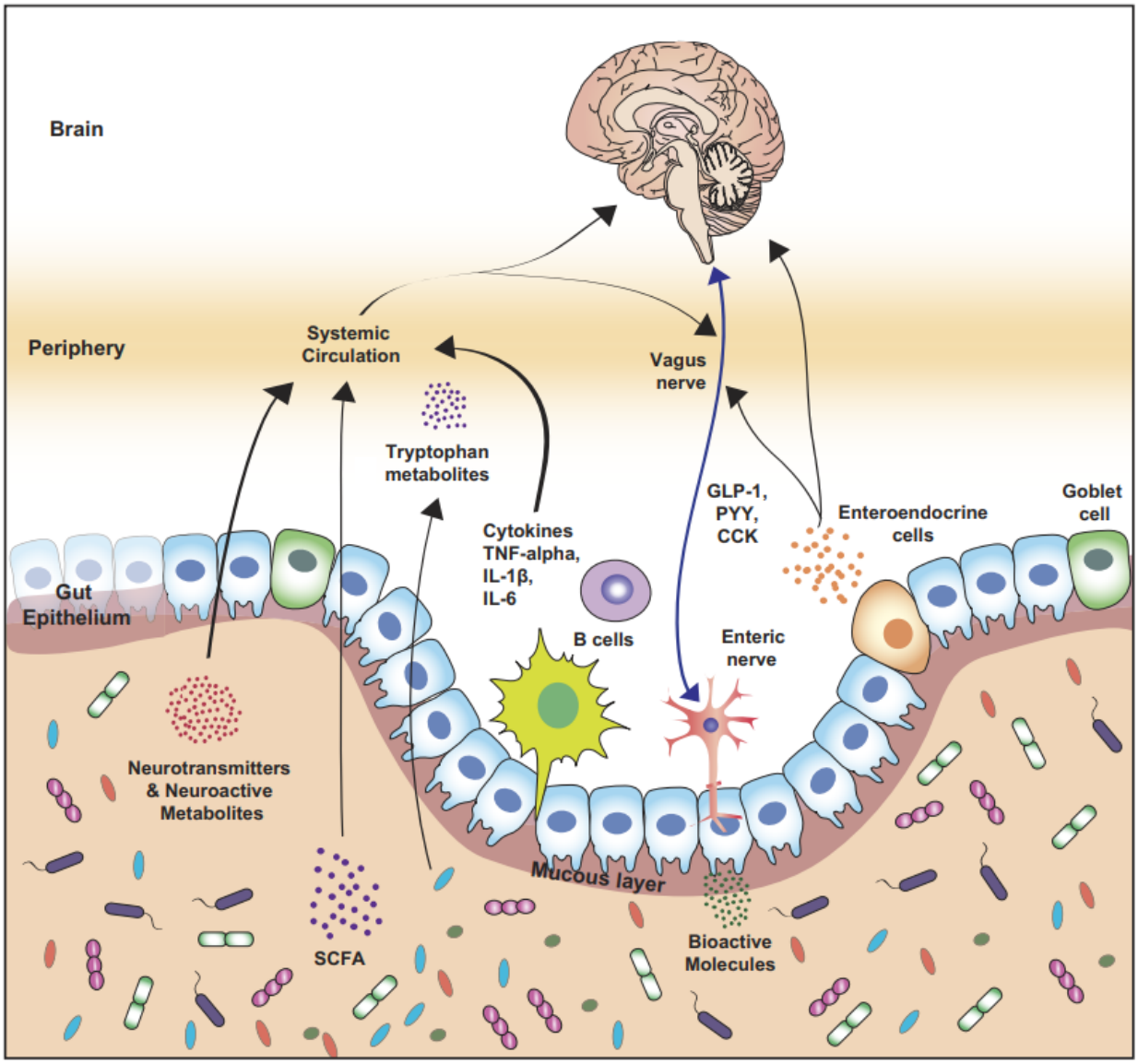


Fig. 1.2 Modes of communication across the microbiota-gut-brain axis. *There are many known pathways by which the microbiota influences the brain and periphery, the work herein primarily explores immune activation through pro-inflammatory cytokine release and endocrine signalling, however there are many mechanisms of communication that need to be further elucidated in the context of the non-bacterial members in chronic and social stress. Figure from Cryan et al., 2019.*

1.3 Gut Viruses

The gut virome research field has been quickly growing as the role of bacteriophages (or simply 'phages') have been found to be increasingly impactful in bacteriome structure and functionality. Phages are viruses that specifically infect bacteria and play an important role in community dynamics of microbial ecosystems. The dynamic coexistence of phages and bacteria in the gut is a subject of active research that comprises a multimodal balance of the biogeography that serves to offer a phage innate immune defence to the mammalian host as well as spatial refuge to bacteria[97,98]. Since phage can infect and reduce specific disease-causing bacteria there has been a renewed interest in using phage therapy to target and remove antimicrobial resistant pathogens, but there is also great potential in using phage to modulate and balance the microbiota to improve the health of the mammalian host. The use of phage to sculpt the microbiota is a complex endeavour as many factors must be taken under careful consideration. First and foremost, the goal of the phage treatment must be identified, whether this is to target a specific bacterial strain, reduce the abundance of a group that produces a particular compound, alter the functionality of specific bacteria, or even to restore the microbiota to promote health.

There are multiple pathways of phage infection (Fig 1.3.1). There are lytic phages which infect, multiply, and lyse their host and lysogenic phages that infect, incorporate their DNA into that of the host as a prophage, and then divide with the host. Phage that are exclusively in the lytic state are referred to as virulent phage, while those which can lysogenize are termed temperate phage[99]. In aquatic and marine ecosystems phage are described as primarily virulent[100], but in the gut the vast majority are temperate[101-103].

There are other phage infection types that are common but not as frequently discussed, these are pseudolysogeny and chronic infection. Pseudolysogeny describes phage that have infected a host but are in a state of stalled development where they have neither begun to multiply or incorporate within the host genome. This typically occurs due to unfavourable host cell growth conditions (*e.g.* starvation). Lastly, there is chronic infection where phage virions are continuously generated and released over time[104].

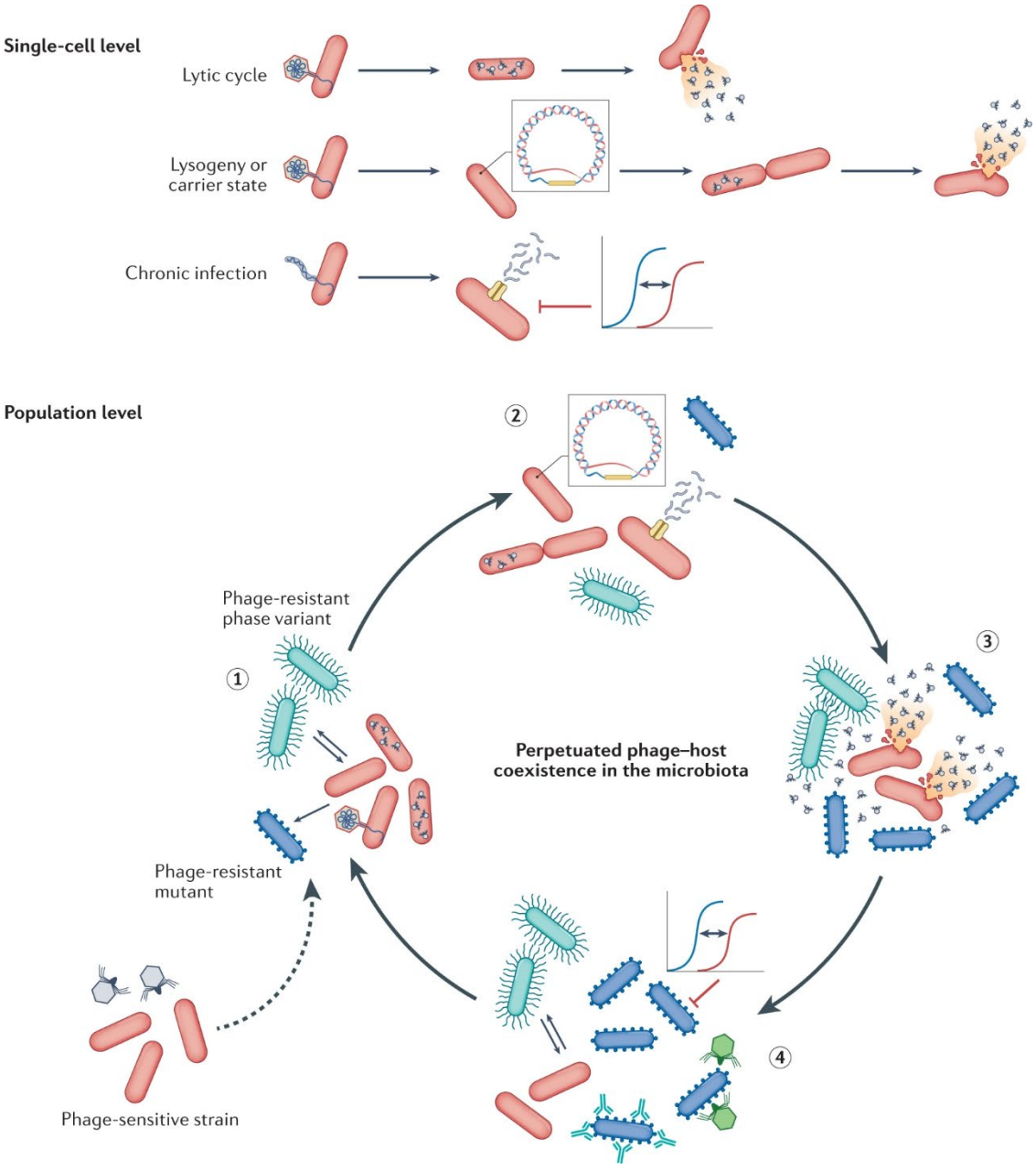


Fig. 1.3.1 Phage-bacterium infections and outcomes. *1) A sensitive population of bacteria is initially infected by phages. 2) Phage infection can follow a number of different pathways. Virulent phages will initiate the lytic cycle where they replicate inside the host until lysis (bursting of the cell) and release large numbers of phages into the environment. Temperate phages can follow the lytic or lysogenic paths, where they incorporate their nucleic acid into the host genome creating a prophage. Then they automatically replicate with the host over time and can re-enter the lytic cycle following environmental triggers. The chronic infection lifestyle (common in archaeal viruses, filamentous phages, and in*

plasmaviruses) slowly shed from the cell over a longer period of time without cell death. 3) Lysis of infected cells reduces the sensitive population and leads to the expansion of insensitive and resistant bacterial populations. 4) There is a decline in phage numbers but metabolic and ecological costs of resistance lead to survival of sensitive populations of bacteria and increased diversification. Figure from Shkoporov et al., 2022.

Many phages are specific to a single species of bacteria, and often infect few strains within the species[105]. Given this high degree of specificity, and the fact that successful phage infection is dependent on random chance encounter with the target bacterial host, an environment rich in potential hosts is required for phage proliferation to occur. Furthermore, since phage are immotile, environments that facilitate these random interactions greatly enhance the probability of encounter and infection. This is one reason that many trends found in aquatic ecosystems do not perfectly translate to that of the gut. The multiple types of phage infection, high degree of specificity, and low probability of encounter are hurdles to widespread use of phage therapy as treating each bacterial infection needs to have these factors optimized for the phage administered to be efficacious.

Viruses are ubiquitous in the mammalian GI tract initially colonized at birth, and the neonatal virome is assembled in a stepwise fashion and important throughout development[106]. The concentration of virus like particles in human faeces, caecal contents, and colonic mucosa have been estimated to reach ~1 x 10^{10} g^{-1} [107-109] with total abundance in the GI tract estimated to be as high as 10^{15} [110]. An alternative quantification method found that phage-bacterial ratios in the human gut are approximately 1:1[111], which would then infer the total abundance to be in the 10^{13} range[6]. Regardless of preferred abundance

estimates, phages represent a large proportion of the biological entities in the gut and their sheer presence in an ecosystem that is constantly removing contents suggests that they play an active role in the gut to adhere and proliferate. While their presence in the gut is known, the specific phages, and their activities and roles within the gut microbiota is not well understood. Thousands of bacterial species have been estimated in human faeces, but the number of phage species in the gut have been estimated as high as 2800[112], however improving technologies and species delineation in the future will likely increase that number. Metagenomic faecal virome analysis has revealed that greater than 80% of the viruses in the GI tract are unknown[101,112]. Currently, the major challenges of phage research and bioinformatics are both not knowing the hosts for specific phages nor genome sequences to taxonomically classify the vast majority of them.

Isolation and characterization of specific phage requires intensive culture technique; bacteria must first be cultured, communities isolated and grown. Once a specific bacterial strain has been isolated, cultivation of potential phage requires identifying plaques in the agar plate. These phage cultures must be propagated for whole genome and electron-microscopy characterization. Most phages that have been isolated, cultured, and characterized are of clinical importance, but the vast majority within the gut microbiota have not yet been identified. Metagenomic sequencing of the microbiome provides a much larger view of the phage community but is yet limited in viral characterization. For focused analysis of the virome, faecal samples must be filtered and refined[113,114]. To date, databases are limited in their ability to classify gut virome sequences, particularly phage. Therefore, current analysis of virome diversity alongside bacteriome sequencing results

provides insights into community structure. Following infection by phage, a small percentage of bacteria will incorporate a short sequence of the genome of the invading phage into a CRISPR (clustered regularly interspersed short palindromic repeats) array, which then will allow Cas (CRISPR-associated proteins) nucleases to target specific phage for destruction. Therefore, one molecular technique to aid in phage-host characterization is to sequence bacterial CRISPR-Cas sequences to identify potential bacteria-phage interactions hosts[115,116].

Phages contribute to the stability and dynamics of bacterial populations and represent a targeted approach to influencing specific populations of bacteria in the gut[117,118]. However, since many microbes may depend on the products produced by others, using phage to knock-down the quantity of one microbe can have cascading effects on others within the ecosystem[119]. Additionally, temperate phages already present in the microbiota are sensitive to cellular stress and oxidation that can be introduced into this dynamic microbial ecosystem[110]. Diet and prescription drugs have been shown to significantly influence the microbiome[120], some of these alterations may be attributed to fluctuations in phage activity. Notably, dietary antioxidants, such as polyphenols, have been shown to reduce viral activity including phages[121]. Since many factors can have positive or negative effects on phage activity their role is an important variable to take into account when considering the microbiota and microbiota-based interventions in health and disease.

Current theories of how phage impact the gut microbiota have been adapted from aquatic ecosystems. The study of gut phages is still in its infancy yet there are some notable similarities and differences between the gut and environmental microbial communities.

Lotka-Volterra predator-prey dynamic models have been used to help describe the "kill the winner" principle that was applied to describe the targeting of the most numerically successful bacteria in an ecosystem by phages[122,123] and has been supported in environmental microbial studies[124] whereby a secondary lytic phage bloom targets and predates upon a bacterial population which is undergoing rapid proliferation[125]. This contrasts with the so-called "Piggyback the Winner" explanation which posits that phage encountering a high concentration of rapidly growing bacteria will lysogenize the host and take part in their many divisions[126]. There is also evidence to support the so-called "Red Queen hypothesis" which describes the constant co-evolutionary arms race between predator and prey that has been applied to describe the infectivity of phage and resistance of the bacterial host[127]. However, currently no evidence of either the "Kill the Winner" principle or the "Red Queen hypothesis" occurring in the gut microbiota has been found. One reason is due to the complex environmental interactions in the mammalian gut. The constant influx of diet, a high diversity of microbes, various host factors (*e.g.* gastric secretion, immune cells, mucus, bile, *etc*.), varied anatomical colonization locations (both longitudinally down the tract and radially within each segment) (Fig 1.3.2), and the constant efflux places many extrinsic pressures on phage identification and infection of bacterial hosts. This complex gastrointestinal environment reduces the expected phage to bacteria ratio from what is seen in marine environments and is one factor in determining phage infection pathway[111].

Intriguingly the mucus lining of the gut binds and concentrates primarily lytic phages which then act as a phage-based innate immune defence against bacterial colonization and

overgrowth[97]. This contrasts with the luminal portion of the gut which contains high concentrations of bacteria and temperate phages[128]. Environment plays a large role in phage lytic-lysogenic infection outcome (Fig 1.3.2). Interestingly, an isolated lytic phage with no known lysogeny genes was found to lyse host bacterial cells on a semi-solid agar lawn, but when introduced into a continuous liquid culture of the same cells it infected but did not impede bacterial cell proliferation[114]. Recently, phages have been shown to be capable of hijacking bacterial quorum sensing molecules and then initialize lysis-lysogeny pathways as a result[129]. As phages are unable to pick up environmental cues on their own, once infection occurs, a series of bacterial host factors dictate the fate determination of the phage.

If phages are lysogenizing rather than lysing their bacterial hosts, their role in modulating the microbiota is more difficult to elucidate. Lysogenic phages have the potential to positively affect the growth of their host by "arming" them with a number of different horizontally transferrable genes that may confer selection advantages such as greater metabolic range, antibiotic resistance, increased adherence, or even factors that may offer protection or weaponization against other bacterial populations[104].

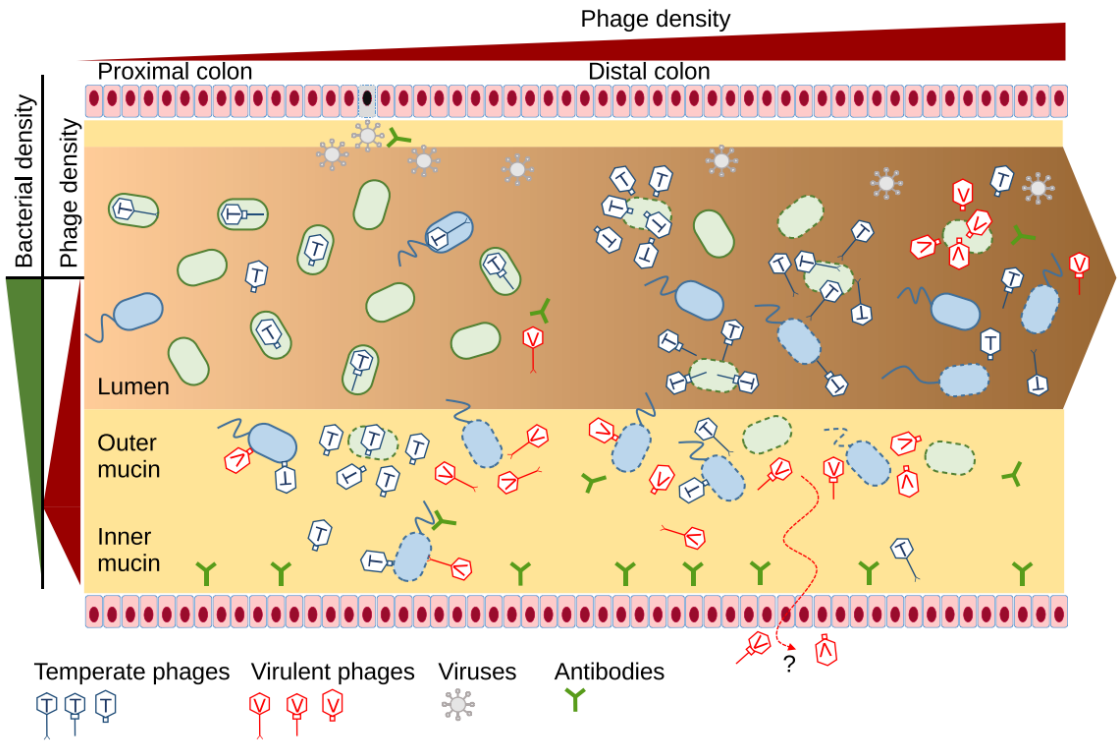


Fig. 1.3.2 phage biogeographical distribution in the gut. *The gut luminal contains high concentrations of bacteria that are pushed through peristaltic action. Temperate lysogeny ("Piggyback the winner") is most common in the lumen as virulent phages quickly become expelled. Moving distally through the gut lysis and prophage induction is more likely due to environmental triggers (e.g., nutrient starvation). In the mucin layer there is lower bacterial density causing a higher proportion of virulent and temperate phage lysis ("Kill the winner"). Many phages stick to the mucin layer where they provide bacteriophage-adherence-to mucus immunity. Figure from Shkoporov and Hill 2019.*

1.3.1 Bacteriophages of the gut

Frequently phages in the gut belong to the class *Caudoviricetes* which infect bacteria and archaea, are primarily temperate and classified by being non-enveloped, having dsDNA genomes, icosahedral heads, and tails. The *Caudovirales* order was previously made up of three families commonly identified in microbiome samples: *Siphoviridae*, *Myoviridae*,

and *Podoviridae*[130]. However, this order has recently been disbanded by the International Committee on Taxonomy of Viruses and reclassified into new taxonomic groups including the *Crassvirales* order and the *Ackermannviridae*, *Chaseviridae* and *Herelleviridae* families[131].

The family *Microviridae* contains phages with icosahedral heads and circular single-stranded DNA genomes. These viruses are relatively modest in both structural (head diameter approximately 26 nm) and genome size (4.5-6 kb) and contain most of the ssDNA phages. The family contains the genera *Microvirus* (infect *Enterobacteria*), and sub-families *Gokushovirinae* (currently known only to infect intra-cellular parasites) and *Alpavirinae* which have been isolated from genera *Prevotella* and *Bacteroides*[132].

CrAssphages, named after the Cross-Assembly software used for their discovery, are phages that have been recently identified as the most ubiquitous and abundant viruses in the gut being found in approximately half of individuals and representing up to 90% of their gut viromes[133,134]. These lytic phages contain an approximately 100-kilobase genome and predicted hosts largely belonging to the order *Bacteroidales*[134,135]. One recently cultured crAssphage (ΦCrAss001) with podovirus-like morphology was isolated from human faecal material and infects the gut symbiont *B. intestinalis*[134]. Interestingly, no prophages or lysogeny-based integrase genes were detected. liquid culture results indicate a complex approach combining an early lytic infection followed by a longer-lived pseudolysogeny-like state with the remaining hosts.

1.3.2 Viral immune activation and inflammation: A first line of interaction with the microbiota-gut-brain axis

The immune system has been implicated as a key signalling hub for microbiota to brain signalling[136,137] thus it is also an important facet in our understanding of how phages interact with host too. Many studies focus on using phages to combat specific antibiotic-resistant pathogens, however, the use of phages to regulate the microbiota of the mammalian host as an extra branch of the innate immune system is still relatively new[138]. Lytic phages are concentrated in the mucus lining of the gut which benefits both the phage through adherence and presentation to potential bacterial hosts and the mammalian host due to an extra level of non-host-derived immunity to potentially invasive bacteria[97]. Phages are found in many different anatomical locations due to their ability to enter the mammalian host through multiple different routes affecting the immune system in both direct and indirect interactions[139]. The most straightforward route of phage entering the mammalian host occurs during gastrointestinal inflammation or damage to the gut epithelium resulting in altered gut permeability which allows phages to directly enter circulation[140]. Phages can also undergo endocytosis directly by eukaryotic cells[141] or indirectly through a bacterium already infected with a phage is engulfed by epithelial cells[142]. Additionally, phages are capable of transcytosis through epithelial layers in cell lines originating from gut, lung, kidney, and brain *in vitro*[143].

While phages do not directly infect and propagate within eukaryotic cells, they can still elicit an effect on cells they encounter. For example, a rodent study tested the effect of administering a phage cocktail for ten sequential days and found that the lactulose-

mannitol ratio increased (a characteristic of increased gut permeability) following phage treatment compared to pre-treatment[144,145]. Moreover, increased levels of lipopolysaccharide (LPS) and inflammation-related cytokines (TNF-α, IL-1β, and IL-6) were found in the serum, however, it is unclear whether the source of the increased serum LPS was a result of gut permeability deficits per se or potentially from the administered phage cocktail itself. 16S rRNA sequencing revealed increased microbial diversity and microbiome compositional changes following the phage cocktail treatment and led the authors to regard phages as potential mammalian pathogens[145].

Further support for phages potentially exacerbating gastrointestinal disease has been linked in intestinal inflammation and colitis[59]. Here it was shown that tumour formation could be prevented when genetically susceptible mice were colonized with tumour-associated adherent invasive *E. coli* (AIEC) were treated with phage targeting the AIEC. Interestingly, phage treated mice displayed heightened immune responses leading authors to test the effect of the phage treatment on germ free (GF) mice. Phage treatment increased CD4+ and CD8+ T cells and IFN-γ production in Peyer's patches in GF mice, indicating a direct effect of phage on the mammalian immune system. Then to identify the pathway by which phage stimulated the immune system the authors tested phage DNA, UV-treated phage, heat-killed phage, and phage capsids and found that UV-treated phage and phage DNA both stimulated IL-12 production through the TLR-9 pathway. Next, they confirmed the TLR-9 immune pathway was affected by phage by administering the phage cocktail with and without dextran sodium sulphate and found that animals with colitis that received phage had lost more weight and had worsened tissue histology scores, however, $TLR9^{-/-}$

animals were resistant to phage-augmented colitis and had a diminished immune response. These experiments are fundamental to our understanding of the potential impact of phage on not only the bacterial fraction of the microbiota, but also the mammalian host.

Further research will need to be conducted to assess whether different types of phages have differing effects on the mammalian host. Greater than ten-fold more phages were found in colon mucosa biopsies in patients with Crohn's disease compared to healthy individuals[108]. Increased phage of the *Caudoviricetes* class have been correlated in patients afflicted with both major clinical subtypes of IBD, Crohn's disease and ulcerative colitis[146]. The phage population in colitis has been associated with phages predicted to infect pathobionts, but not all increased phage population expansions were assigned to a concomitant increase in their bacterial host, indicating that additional unknown mechanisms and roles of phages in gastrointestinal disease are likely[147]. To date, most studies delivering phages in isolation or in multi-phage cocktails have been derived from the pathobiont bacteria [148], while phages from commensal organisms are capable of exerting stimulation of the mammalian host immune system[149], there is a paucity of evidence whether pathobiont versus commensal phages exert varying effects.

Phage likely play a larger role in faecal microbiota transplant (FMT) than currently understood, this has been highlighted as a necessary mechanism to explore alongside other undefined microorganisms and their functional effect on the recipient microbiota[150]. FMTs that have had the bacterial fraction removed by filtration have been shown to still be capable of ameliorating *Clostridioides difficile* infection (CDI)[151]. Moreover, phage transfer during FMT in CDI has been associated with long-term colonisation and the

outcome of the treatment[152,153]. Ulcerative colitis patients undergoing FMT that displayed decreased responsivity and symptom improvement had significantly higher amounts of *Caudoviricetes* compared to FMT responders[59]. Whether future phage-based therapies can be used to modulate the gastrointestinal microbiota and ameliorate disease will also need to consider the direct effect of phage on the mammalian host.

1.3.3 Potential of phage therapy and faecal virome transplants

To date, phage therapy is used in food production[121]and in former Soviet states, such as Georgia, for antibiotic resistant infections[154]. Most phage therapy applications seek to deliver a cocktail of virulent phages to remove specific bacterial pathogens[119,155]. Using this approach to remove or knock down populations of pathobionts in the gut allows for a more specific targeting system than antibiotics, where even the most specific still render many commensal microbial casualties and introduce selection for antibiotic resistant genes. A topic for future research discussion is to use temperate phages (potentially genetically modified) to confer competitive advantage to beneficial commensal and probiotic strains to aid factors such as substrate utilization, adherence, metabolite production and other proliferative strategies to sculpt specific microbes in the gut to optimize health benefits to the host. Another approach that is currently being tested is to attempt to use the entire gut virome population to alter the microbiota rather than the surgical precision of targeting one specific member. This technique has the potential to produce a large shift in the microbial population which may provide greater efficacy when

attempting to treat diseases and disorders that contain a vastly different microbiome compared to healthy controls.

Faecal virome transplant (FVT) is an intriguing technique where faecal samples are purified (usually through numerous steps involving centrifugation, filtration, and reconcentration) to remove the non-viral microbes before administering to the host[156]. Since free viruses rely on a few relatively simple structural compounds and nucleic acids, this technique is more resilient to long-term storage and biobanking practices than standard FMTs. At this time two clinical studies have used a FVT approach as a treatment to CDI[151,153] and three pre-clinical studies have similarly done so to treat type II diabetes[156], post-antibiotic microbiota recovery[157], and small intestinal bacterial overgrowth[158]. Early evidence indicates that FVTs can alter the microbiome and ameliorate various aspects of disease. Since the phageome is highly host specific (both in terms of bacterial and supra-mammalian host) the highest yield alignment between phage-host pairs would come from the microbiome of each individual host. This technique is currently being termed as an autologous (or autochthonous) transfer and refers to the use of the indigenous microbiota population (from oneself). Heterologous (or heterochthonous) transfers, from one host to another, can also be used, but will not reach the same bacterial infection limit across the microbiota due to high inter-individual variability.

1.4 Gut Fungi

Gut fungi are another understudied group included in the gut microbiota that have increasingly been correlated with different diseases and disorders. In a subsequent study from the Human Microbiome Project dataset, the gut mycobiota was found to be far less diverse than the bacteriome, have higher inter- and intra-subject variability, and are largely dominated by yeasts (*e.g. Saccharomyces*, *Malassezia*, and *Candida*)[159].

Fungi in the gut have not been studied to the same extent that bacteria have due to their lower numbers and less understood role. Fungal genes have been estimated to account for 0.01-0.1% of genes in stool samples[160]. The major phyla in the gut are *Ascomycota* and *Zygomycota* and the most abundant genera found in human stool samples belong to *Saccharomyces*, *Candida*, and *Cladosporium* [161]. Fungal diversity is highest in infants and the elderly and lowest during adulthood[162,163], interestingly this is the opposite of the diversity trend seen in bacterial populations[164]. The most abundant species in the newborn mycobiota are *Candida parapsilosis*, *Candida tropicalis*, *Candida albicans*, *Saccharomyces cerevisiae*, *and Candida orthopsilosis*[161,163].

There are over 150 species of *Candida* in the gut[165], most of which are commensals, but ten percent are known opportunistic pathogens[166]. The most common *Candida* spp. are *C. albicans, C. glabrata, C. parapsilosis,* and *C. tropicalis*[165]. *C. albicans* is found on mucosal surfaces of the gastrointestinal tract, urogenital tract, mouth, and skin of 60% of healthy individuals[166]. *C. kefyr* has been shown to protect mice from developing autoimmune encephalomyelitis, an animal model of multiple sclerosis[167]. Yeasts, primarily of the genus *Saccharomyces*, are also associated with the human gut microbiota.

S. cerevisiae (also known as baker's yeast) has potential as a probiotic as it has been shown to aid immune system maturation and cytokine production[168]. *S. boulardii*, another yeast with probiotic potential, can increase IgA production[169]and is able to secrete enzymes that can inactivate toxins produced by gut pathogens like *C. difficile* and *E. coli*[170,171].

1.4.1 Fungi and the microbiota-gut-brain axis

The mycobiota has been identified as a component of the microbiota that can affect neurological health in a range of diseases and disorders[172,173]. Fungi in the gastrointestinal tract are capable of synthesizing and releasing neurochemicals that can potentially affect both local tissue physiology and the brain[174]. *C. albicans* is capable of producing histamine[174], a molecule involved in mast cell mediated immune responses and a neurotransmitter regulating many physiological functions. Interestingly it appears that neurotransmitters can also elicit effects on the gut mycobiota population, indicating a level of shared coevolved interactions. Evidence suggests that *C. albicans* is capable of increased virulence and germ tube formation in the presence of gamma-aminobutryic acid (GABA)[175] or decreased virulence in the presence of serotonin [176].

There have been links between certain fungi proliferation and different psychiatric and non-psychiatric central nervous diseases. More than 80% of samples from individuals with autism spectrum disorder contain yeast strains[173,177,178]. In addition to an increased *Bacillota/Bacteroidota* (formerly *Firmicutes/Bacteriodetes*) ratio in autistic individuals, *Candida* spp. were also found to be twice as abundant compared to controls[179]. Perhaps

this increased trend of *Candida* spp. in autism is due to the ability of members of the genus being capable of producing ammonia and toxins[180]. Moreover, IBS is a prototypical disorder of the brain-gut axis and has been associated with gut fungal dysbiosis[181]. Indeed, small intestinal fungal overgrowth is characterised by an influx of fungal organisms in the small intestine which has been associated with gastrointestinal symptoms and autism-spectrum disorder[182].

Anorexia is another psychiatric disorder linked with gut fungal changes, in this case evidence links increased diversity when compared to healthy controls[183]. Rhett syndrome is a progressive neurological genetic disorder where individuals often display comorbidities associated with general gastrointestinal dysfunction and constipation in addition to having increased abundance of *Candida* spp.[162]. The presence of *C. albicans* antibodies was associated with gastrointestinal disorders and lower scores on cognitive tests[184]. Interestingly, probiotic supplementation (*Lacticaseibacillus rhamnosus* and *Bifidobacterium animalis*) led to reduced blood antibody levels and improved psychiatric symptoms[185]. Recently fungi have been identified as contributing to depression episodes where increased *Candida spp.* and decreased *Penicillium spp.* quantities were observed[186]. An altered mycobiota has been reported in schizophrenia patients where increased abundances of *C. albicans* and *S. cerevisiae* have been reported[184,187]. In autism spectrum disorder *Saccharomyces spp.* and *Apergillus spp.* were identified to be altered from that of neurotypical controls[188]. Additionally, a disruption of the bacteria-fungi correlation network was reported which brings up the interesting topic of the role of interkingdom interactions of the microbiota[189,190]. The controversial dysbiosis term has been used to

describe altered mycobiotas in different scenarios which demonstrates the necessity of not only defining a healthy bacteriome but all the kingdoms that comprise the microbiome as well as their metabolomic profile and functional potential.

Immune activation and neuroinflammation are increasingly being linked with the microbiota in neurological diseases[191]. Integrity of both the blood brain barrier and tight junctions of the gut have been proposed to play a key role in the progression of neurological and psychiatric diseases and disorders[192] and fungi play a role here as well[193,194]. Presence of polymicrobial pathobionts, including fungi, have been detected in the brains of patients with Alzheimer's and Parkinson's diseases[195,196]. Mycobiota composition driving compromised barrier integrity could also play a role in multiple sclerosis[197]. This evidence supports the purported role of the immune response to fungal pathobionts.

1.4.2 Fungi and the immune system

Specific mycobiota compositions can lead to immune activation and inflammation that has been associated with different diseases[198]. Antifungal treatments can actually lead to an overgrowth of more resistant species such as *Aspergillus amstelodami, Epicoccom nigrum,* and *Wallemia sebi* and while diminishing commensals *Penicillium brevicompactum* and *C. tropicalis*[199]. These alterations of the gut mycobiota have been associated with an increased incidence of allergic airway disease and pre-clinical administration of the increased strains listed above reproduced effects seen in the disease[199].

Normally commensal fungi can exacerbate inflammation in the gut of mice with genotypes that are sensitized to inflammatory bowel disease (IBD)[198]. Furthermore, a link between the mycobiota and IBD has been established over thirty years ago when anti- *C. cerevisiae* antibodies were found in Crohn's disease patients[200]. Anti- *Saccharomyces* antibodies were also detected in IBD patients and are used to predict disease progression[201,202]. A polysaccharide component of fungal cell walls (1,3-B-D-glucan) is associated with IBD [203,204]. Additionally, psychiatric comorbidities that occur with IBD, such as depression, have been associated with systemic inflammation[205]. These studies indicate that in individuals with gut and systemic immunological disorders the commensal mycobiota can potentially exacerbate inflammation and further drive disease states.

1.5 Gut Archaea

Archaea, who are more commonly known for their extremophile life styles[206], have also adapted to a more mesophile life in the mammalian gut, and while small in number, they are very frequently found in the microbiotas of most individuals. They share some properties with bacteria (similar morphologies, circular chromosomes lacking introns with similar post-transcriptional modifications) while other properties are shared with eukaryotes (molecular machinery for DNA replication, RNA translation, and protein translation)[207]. Yet many properties, such as their membrane composition (made up of L-glycerol ethers and isoprenoid), are unique to archaea[208]. However, what gut archaea are best known for is metabolic hydrogenotrophic methanogenesis, which use by-products from bacterial fermentation to generate methane[209,210]. These archaeal methanogens play

a crucial role in the gut by consuming hydrogen generated by microbial fermentation which thereby further optimizes metabolic pathways that fermentative bacteria utilize [211]. This hydrogenotrophic role is shared with sulphate-reducing bacteria and acetogens[212,213]. Furthermore, methane is a physiologically active gas shown to increase intestinal contractility in a non-peristaltic manner thereby slowing gastrointestinal transit which affect both host health and microbiota composition and function[214].

1.5.1 Methanogens and gut physiology

The gut methanogen is *Methanobrevibacter smithii* which predominantly inhabits the right colon and is present in over sixty percent of the population[215-217] but largely depends on the population studied as a range of 25-95% has been reported[218]. *M. smithii* can use either hydrogen or formate as substrates for methanogenesis[219,220]. Interestingly, *M. smithii* has been shown to be capable of affecting gene expression of other microbes, notably well-known fermentative bacterium *Bacteriodes thetaiotaomicron*[221]. The next most common methanogen is *Methanosphaera stadtmanae* which uses hydrogen to reduce methanol[222,223]. As high levels of methane can slow transit and have been associated with constipation predominant irritable bowel syndrome in addition to colorectal cancer[224], clinical diagnoses involves using breath tests to measure exhaled methane in the breath of patients. Additionally, increased methanogen abundance has been associated with IBD[225] and obesity[226].

Methanogens have also been found to increase in prevalence and diversity with age of the human host[218,222]. Methane excretion is higher in adults than in children[227]. The increase

of methanogens in aging could be due to antimicrobial resilience as many antibiotics specifically target bacterial membranes, cell walls, or DNA/RNA related machinery and methanogens inherently contain different components[228,229]. Or the increased abundance of methanogens could potentially be due to the slower gastrointestinal transit time compared to of adults and the elderly compared to children[229,230].

As with the bacteriome, diet is a key predictor in determining microbial presence and abundance. Diets high in carbohydrates were associated with increased *Candida* and *Methanobrevibacter* spp[161]. A possible syntrophic guild has been proposed involving potential polydomain interactions between archaea, fungi, and bacteria. In this example, *Candida* spp. first liberate simple sugars by breaking down carbohydrates, which then allows for fermentation by bacteria like *Prevotella* and *Ruminococcus.* The bacterial derived metabolites (like hydrogen and formate) can then be utilized by *Methanobrevibacter* to produce methane[161,231]. The potential multidomain interactions between microbes of the gut highlight the importance of metagenomic sequencing and metabolomics analyses in studies to gain more complete information about the microbiome in health and disease.

1.6 Other members of the microbiome

There are still other members within the gut microbiota that, while uncommon, can impact the gut microbiota and host (Fig 1.6). These are mostly stories of individual microbes, but how they have evolved and their lifestyles are worth exploring to better understand both

their adaptive traits and potential consequences on the host. These primarily include the kingdom *Protista* and parasites (helminths and protozoa). *Naegleria fowleri* is known for infecting the CNS of individuals exposed to water containing the protist and lead to naegleriasis[232]. *Toxoplasma gondii* is an obligate intracellular protozoan that can infect a wide range of mammalian and avian species but the definitive host are felids. Infection typically occurs after exposure to infected cat faeces and lead to a variety of behavioural alterations in rodents including learning and memory, locomotion, anxiety-like, depression-like, and novelty preference behaviours[233-235]. Furthermore, the nematode *Trichuris muris* induces gastrointestinal inflammation and anxiety-like behaviour in mice[236]. While we know of the role and function of many of these other members through infection and disease, there is potential for more to be uncovered as we elucidate the lifecycle of the commensal non-bacteriome population.

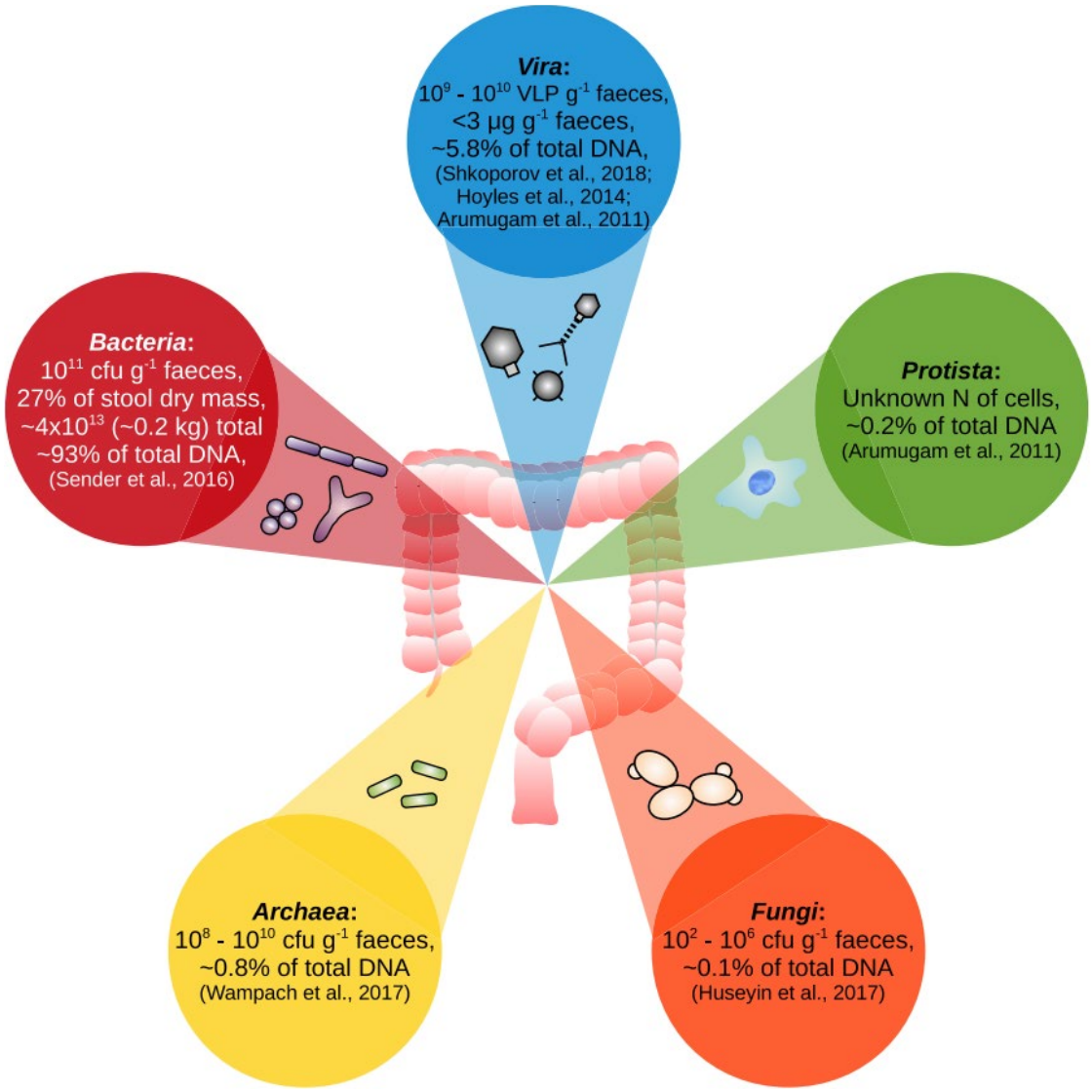


Fig. 1.6 Primary taxonomic microbial groups of the human microbiome. *Bacteria are the most abundant organisms in the gut in terms of DNA followed by viruses, archaea, protists, and fungi. Viral particle counts estimate a phage:bacteria ratio of roughly 1:1* [111] *but with the enormous unknown quantity of the gut virome this may change in years to come. Figure from Shkoporov and Hill 2019.*

1.6.1 Challenges to studying the non-bacteriome field

There are many hurdles in microbiome studies in general, but when studying the non-bacteriome members these difficulties are in some cases increased. The first and foremost challenge across the board is identification. While bacteria contain a universal gene allowing for more convenient labelling (16S rRNA) viruses have no such conserved gene, and there are many unknown viral sequences that have to be individually identified with some estimates as high as 93% of the virome as currently not classified[112]. Furthermore, the vast majority of phage-host pairs are similarly unknown[101,128], meaning that in addition to not knowing who is there, we also do not know who they infect. Viral nucleic acid purification techniques have also been called into question recently with the addition of new insights into virome sequencing[237]. The practice of first purifying phages from the rest of the sample may introduce a bias for free phages rather than prophages incorporated in the genome or plasmid of the host, therefore moving forward the best practice may be to sequence the entire metagenome of samples and identify viral sequences within the total[238]. Prophages are an important consideration when planning for faecal virome transplant studies since the purified viromes will be biased towards free and lytic phage. This is not necessarily counterproductive, since the goal is typically to use phages to alter the bacteriome, however, researchers should be aware that the entire faecal virome population may not be in full attendance.

Gut fungi and archaea are similarly not as well characterized in the gut as bacteria, however both do have conserved genes which aid identification[239,240]. The difficulty is characterizing members within these groups since cultivation of these anaerobes ranges

from complex to currently impossible [241,242]. This is a common issue across the microbiome since many microbes are present in dynamic cross feeding consortia.

1.7 The Microbiota-Gut-Brain Axis and Brain Disorders

The link between perturbations in the gut and disorders of the brain have gradually been growing in evidence with the microbiota often capable of modulating effects[243] (Table 1.7). Many of the interactions that drive these effects between the microbiota and host have been involved with the formation and function of physiological and neurological systems. The concept of sensitive periods, or critical windows of heightened plasticity between neurodevelopment and the microbiota has been suggested as a potential mechanism to explain the association between disorders and the microbiota-gut-brain axis[244]. While still largely theoretical, it stands to reason that if a microbiota perturbation occurs (*e.g.*, acute infection, antibiotic use, stress, *etc.*) during critical windows at heightened developmental susceptibility to extrinsic pressures, that specific functional and neuroanatomical pathways could be negatively influenced.

Autism spectrum disorder (ASD) is one such example where there have long been associations between gut function and severity of symptoms[245,246]. Functional abdominal pain is one such gastrointestinal symptom that has been correlated with microbiome-neuroimmune signatures[247]. Additionally, gastrointestinal comorbidities are found at a higher rate in children with ASD, further implicating that the microbiota-gut-brain axis may contribute to the development of the disorder[248,249]. Furthermore, a microbiota

transfer therapy by FMT showed clinical improvement of gastrointestinal and ASD behaviour symptoms, along with improved diversity of bacterial and viral taxa[250]. FMT is actively being explored in this space and other immune-related pathologies, however there are also risks to this treatment to further expose patients with immune dysfunction to unknown immune challenges where the role of the microbial community is also unknown such as in allergic disease, IBD, autoimmune diseases, *etc*.[251,252].

In ASD microbiome research there are many differing reports on definitive microbial patterns or signatures. Frequently studies find differences in microbiome species diversity and richness, while finding evidence of specific taxa abundance being altered[177,253-255]. To date, *Desulfovibrio* spp. *Lactobacillus*, *Clostridium*, *Bacteroides vulgatus*, *Caloramator*, and *Sarcina* have all been recorded to be upregulated in individuals with autism[177,253,256,257]. Compared to neurotypical controls, ASD individuals have been reported to harbour increases in total numbers and diversity of *Clostridia*[177,254,258]. Evidence that the gut microbiota plays a causal role in ASD has been shown in a study that transferred the faecal microbiota from patients with ASD to germ free mice resulting in increased repetitive behaviour and reduced social interaction and locomotor activity in the animals[20]. Using microbiome and metabolome profiles to identify microbial metabolites that were reduced in the ASD FMT recipient mice, the authors went on to treat the ASD mouse model with the missing microbial metabolites and found improvement in behavioural abnormalities and neuronal excitability in the brain[20].

The two most common neurodegenerative disorders Alzheimer's disease (AD) and Parkinson’s disease (PD) have both been linked with gut microbes. AD classically known

for causing cognitive deficits linked with the generation of amyloid plaques in the brain has also been shown to be associated with the gut microbiota in a mouse model of AD[259]. The microbiota has also been implicated to have a causal role in AD progression as FMT from patients with AD to rats showed increased cognitive deficits and reduced hippocampal neurogenesis[260]. PD has similarly been linked to microbiota alterations with distinct signatures associated along the vagus nerve, α-synuclein in the ENS, intestinal permeability alterations, and inflammation[261,262]. Since PD is frequently preceded by gastrointestinal symptoms with accompanying ENS, taxonomic, and SCFA alterations, the role of the microbiota in the progression of the disorder is a target for therapeutic diagnosis and intervention[263].

Both neurodegenerative diseases AD and PD have been associated with specific taxa. Pathogens *Chlymydia pneumoniae* and *Helicobacter pylori* have been reported to correlate with AD as the bacteria were found in close proximity to plaques and neurofibrillary tangles and associated with proinflammatory cytokines and oxidative stress[264,265]. Within the gut microbiota, increased abundances of *Odoribacter* and *Butyricimonas* spp. have been identified in populations with Alzheimer's[266]. Interestingly, mice that overexpress α-synuclein that were colonized with the microbiota from individuals with Parkinson's disease displayed increased physical impairments compared to mice colonized with microbiota from healthy human donors[267]. Furthermore, dopamine production and intestinal permeability are major factors in Parkinson's disease symptom pathogenesis and could be attributed to shifts in the phage-bacteria ratio in lactic acid bacteria[268].

Table 1.7 Microbiota alterations associated with brain disorders. *There are numerous examples of bacteria, viruses, fungi, and archaea that are involved with neurological and psychiatric disease and disorder. Understanding their role in health and disease will provide alternative options for treatment strategies.*

Microbial group	**Disease and disorder**	**Effect**	**References**
Bacteria	Major depression	Alterations in bacteriome have been shown, however inconsistently, along with reduction in SCFA producing bacteria.	Kelly et al., 2016[19] Yang et al., 2020[269] Muller et al., 2021[270] Zhou et al., 2023[271]
	General anxiety	Elevated anxiety has been recorded in patients with reduced bacteriome richness and diversity and in small intestinal bacterial overgrowth.	Dong et al., 2021[272] Kossewska et al., 2022[273]
	Social anxiety disorder	Changes in bacteriome composition and specific taxa has been shown in individuals with SAD.	Butler et al., 2023[274]
	Autism spectrum	Alterations have been shown in ASD in regard to specific bacterial taxa likes increased *Faecalibacterium prausnitzii* and reduced *Bifidobacterium longum.* FMT can improve symptoms associated with autism.	Strati et al., 2017[179] Coretti et al., 2018[275] Kang et al., 2019[276]
	Schizophrenia	Altered SCFAs, tryptophan, and neurotransmitters have been shown alongside increased *Veillonella* and decreased *Ruminococcus* and *Roseburia.*	Zhu et al., 2020[191] Li et al., 2021[277]

Microbial group	Disease and disorder	Effect	References
	Irritable bowel syndrome	The bacteriome is modulated by diet in IBS with enrichments in *Clostridiales* or *Prevotella* species. Longitudinal sampling indicates that alterations in microbiome and microbial metabolites underlie flaring of IBS symptoms.	Tap et al., 2017[278] Mars et al., 2020[279] Tap et al., 2021[280]
	Inflammatory bowel disease	Microbial signatures are different across IBD subtypes (Crohn's disease and ulcerative colitis) but also different from healthy controls. These differences have been associated with higher host inflammatory transcriptomics and epigenomics, higher bacteriome fluctuation, and increases in *Bacteroides* and *Enterobacteriaceae* with reductions in *F. prausnitzii,* and *B. longum.*	Halfvarson et al., 2017[281] Vila et al., 2018[282] Clooney et al., 2021[283]
	Alzheimer's and Parkinson's disease	Altered bacteriome composition and specific taxa have been shown in both AD and PD.	Petrov et al., 2017[284] Zhuang et al., 2018[285]
Viruses	Major depression and general anxiety	Phages that target prominent bacterial pathogens have been associated with MDD. Chronic infections with viral pathogens *Cytomegalovirus* and Epstein-Barr virus have also been linked with MDD and general anxiety.	Fagundes et al., 2014[286] Jones-Brando et al., 2020[287] Yang et al., 2020[269]
	Autism spectrum	ASD has been associated with viral infections during gestation and early life development.	Al-Beltagi et al., 2023[288] Karlsson et al., 2022[289]

Microbial group	Disease and disorder	Effect	References
	Inflammatory bowel disease	In Crohn's disease the healthy core of virulent phages is replaced with temperate phages. There is also increased expansion and lowered diversity of *Caudovirales* in the mucosa.	Clooney et al., 2019[290] Zuo et al., 2019[291]
	Alzheimer's	Human Herpesvirus 6 has been detected in transcriptomic and genomic AD brains while innate viral immunity proteins have been shown to be upregulated in AD tissue.	Allnutt et al., 2020[292] Hur et al., 2020[293]
Fungi	Alzheimer's disease	Specific fungal taxa, diet, and inflammatory markers have been correlated in progressive AD.	Ling et al., 2020[294] Nagpal et al., 2020[295] Ye et al., 2022[296]
	Irritable bowel syndrome	Diarrhea-predominant IBS has been linked with specific fungal taxa in IBS.	Hong et al., 2020[297] Thiel et al., 2022[298]
	Inflammatory bowel disease	Fungal taxa drive niche-specific inflammatory and immunity in IBD. IL-17A producing T helper cells (T_H17) respond to specific fungal toxins in host-fungal interactions.	Qiu et al., 2017[299] Chiaro et al., 2017[300] Li et al., 2022[301]
	Autism spectrum	Fungal dysbiosis and *Candida* spp. have been associated with GI symptoms in ASD.	Strati et al., 2017[179] Zou et al., 2020[188] Alookaran et al., 2022[302]

Microbial group	Disease and disorder	Effect	References
Archaea	Irritable bowel syndrome	Increased methanogen abundance and methane production is linked to microbiota composition in constipation-predominant IBS.	Wang et al., 2022[303] Villanueva-Millan et al., 2022[304]
	Inflammatory bowel disease	Increased *Methanobrevibacter smithii* is recorded in Crohn's disease and ulcerative colitis and methanogen depletion was found in colorectal cancer.	Ghavami et al., 2018[305] Coker et al., 2020[306]

1.7.1 Social and Stress-Related Disorders

Among extrinsic factors that lead to the development of neuropsychiatric disorders, stress may be the most prevalent in modern society. Stress-related disorders, of which depressive and anxiety disorders being the most common, were leading causes of the global health-related burden before the occurrence of the COVID-19 pandemic in 2020[307]. During the pandemic the prevalence of both depression and anxiety disorders increased by 27.6% and 25.6% respectively[308]. Chronic stress leads to adverse alterations in the gut, such as colitis, increased proinflammatory cytokine IL-6, decreased anti-inflammatory cytokine IL-10, intestinal mucosa damage, and a pro-inflammatory state of the microbiota[309,310]. Stress stimuli lead to the release of cortisol/corticosterone via the HPA axis, but murine GF studies have shown that exaggerated HPA axis responses occur in the absence of microbiota but can be restored with conventionalization[311]. Furthermore, it has been shown in mice that the microbiota composition can affect how well the animal responds to stress[312].

Social behaviour has been shown to be intricately linked to microbiota composition across the animal kingdom[313]. GF mice have been shown to have remarkably different social behaviour compared to colonized animals[314]. While colonization of children with ASD and animals with *Bifidobacterium* and *Lactobacillus* strains has been shown to improve social behaviours across fruit flies, honeybees, and mice[315-319]. Interestingly, the microbiota has been shown to regulate social behaviour through the stress and the HPA axis, and a specific bacterial species, *Enterococcus faecalis*, can promote social activity and reducing corticosterone levels in mice following a social-derived stressor[320]. Additionally, social submissiveness has been linked with less diverse microbiota, increased genera *Mycoplasma*, *Anaeroplasma, Prevotella*, and families *Rikenellaceae* and *Clostridiaceae*[321]. This was further supported by the submissive behaviour phenotype being transferred to GF mice by FMT from the submissive group [321]. Social anxiety disorder (SAD) is a common psychiatric disorder with a lifetime prevalence of 12.1%[322,323] that is defined by an individual experiencing intense fear and avoidance of various benign social situations[324]. SAD has been shown to have alterations in immune function and the kynurenine pathway[325] and we have shown distinct changes in microbiome composition and specific taxa in SAD compared to matched healthy controls[274].

In addition to major depressive disorder and general anxiety disorder, there are a number of other disorders associated with social impairments and stress including SAD, post-traumatic stress disorder, and acute stress disorder. To better understand the underlying

aetiology of these conditions, various preclinical animal models have been designed to study elucidate roles and mechanisms of different biological contributors.

1.7.2 Chronic Stress

Murine models of chronic stress

Preclinical studies have generated essential insights that have deepened our understanding of the neurobiology of stress and the microbiota. While individual elements of the microbiota-gut-brain axis can be divided and approached using combinations of *in vitro* and *in silico* approaches and patient cohorts can be observed and associations garnered, the mosaic interplay of microbial communities in the gut with the host and the resulting effect on brain and behaviour can only be tested in animal models. In order to design better tools for diagnoses and therapeutics for depression and anxiety disorders seen in patients, translational animal models are designed to mirror the symptomology and phenotype as closely as possible within a controlled and ethical manner. Common rodent models for anxiety-related behaviour include exposure to early life stress[326], transgenic modifications[327], and chronic stress in adulthood[328].

For the objective of elucidating the role of microbial members both in chronic stress response and then testing therapeutics to reduce the effects of stress, chronic stress models in adulthood are highly suitable. Probiotics, prebiotics, and FMT have all been shown to have protective effects against chronic stress in murine models[22,329-332]. Intriguingly, the effects of stress on the microbiota appears to drive the community towards a virulence-

associated state whereby the following immune response of the host may exacerbate physiology further[333]. These findings indicate that microbiota-based therapies designed to restore beneficial taxa, functions, and metabolites would be highly advantageous.

1.7.3 Social Anxiety Disorder

Social fear conditioning as a model of social anxiety disorder

Individuals with SAD can range from mild affects and avoidance of social situations to extreme conditions where those with the disorder are unable to establish relationships, hold jobs, or even leave their homes[334]. Currently, the most effective treatment for SAD is cognitive-behavioural therapy which, over time, gradually leads to extinction of social phobia[335]. However, SAD is often an under/misdiagnosed condition and current medication is unspecific, despite appreciable efforts, which calls to attention the need for new diagnostic criteria and therapies to be developed. The social fear conditioning (SFC) paradigm was created this past decade and is the first translational rodent model designed to model SAD[336]. SFC establishes a negative stimulus (an electric foot-shock) association with social interaction and then is followed by measuring how long it takes for social fear behaviour to extinguish. In this way it mirrors SAD where afflicted individuals with neuropsychiatric sensitivity to the disorder are also exposed to a negative social context and develop a heightened social fear response. Using this model as a tool allows for a preclinical modelling system to further test and understand the underlying neurobiology and contributing factors to SAD.

1.8 Aims and objectives

It has become clear that microbiota-gut-brain axis is integrally linked to stress and social behaviour and well-being, however the causal mechanisms underlying the roles of the bacteriome and virome are not known. The overarching purpose of this thesis is to assess and test the role of the bacteriome and virome in social and stress-related disorders (Table 1.8).

Aim 1: Can the virome be used to reduce the effects of chronic stress on brain and behaviour?

Stress-related disorders like anxiety and depression are among the most prevalent psychiatric conditions and are continuously increasing[337,338]. The microbiota has been associated with stress, but thus far only the bacteriome has been explored[339]. In this study we characterise the bacteriome and virome differences in mice that have been subjected to chronic social stress. Then, we sought to test whether an autochthonous faecal virome transplant was capable of restoring the brain and behaviour of stressed mice.

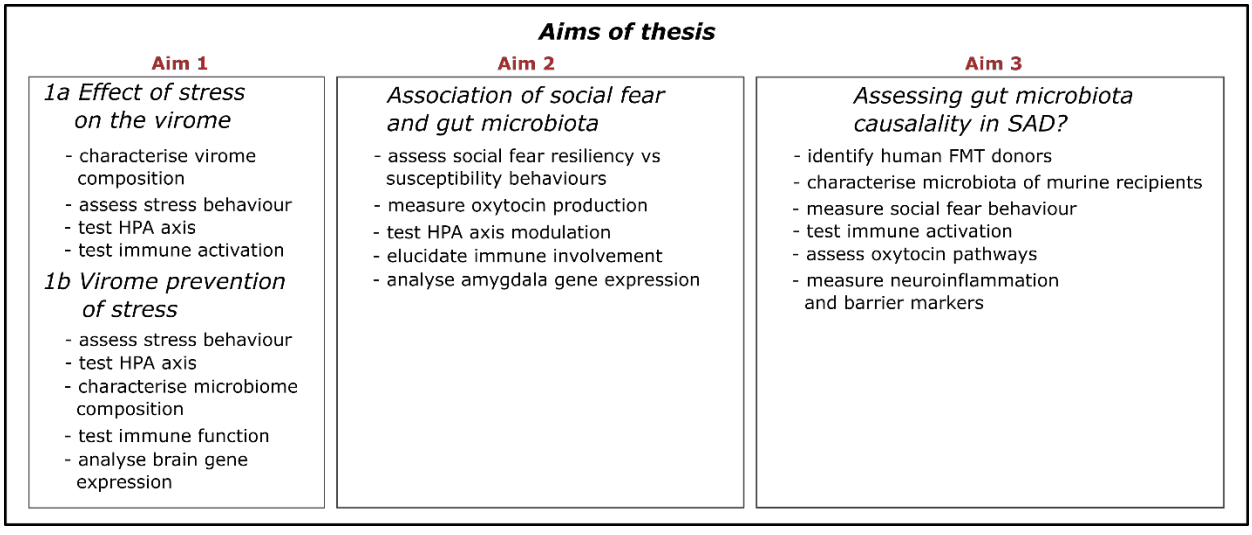
Aim 2: Is the microbiome associated with social fear resiliency?

The biological factors underpinning social fear development are not well understood. We know that there are differences in the neurobiology of social fear[340-342], however it is unknown why some individuals are resilient while others are susceptible to developing heightened social fear. In this study we sought to elucidate the potential role of the microbiota-gut-brain axis in social fear development.

Aim 3: Does microbiota from individuals with social anxiety disorder play a causal role in social fear behaviour?

Social anxiety disorder (SAD) is a very common but understudied psychiatric condition[322,343]. We have shown that microbiota composition is altered between individuals with SAD and healthy controls. However, it is not known whether the microbiota plays a role in the aetiology of the disorder. Therefore, we sought to test whether transfer of the SAD microbiota was capable of eliciting social fear behaviour from humans to mice.

Table 1.8 Diagram representing general aims of the thesis. *The three aims of the thesis are to test the role of the virome in stress, assess whether there are associations between social fear and the gut microbiota, and elucidate if the microbiota-gut-brain axis plays a causal role in social anxiety disorder (SAD).*



Chapter 2

The Gut Virome is Associated with Stress-Induced Changes in Behaviour and Immune Responses in Mice

Nathaniel L Ritz[1,2], Lorraine A Draper[1,3#], Thomaz FS Bastiaanssen[1,2#], Christopher JR Turkington[1,3], Veronica L Peterson[1,2], Marcel van de Wouw[1,2†], Klara Vlckova[1], Christine Fulling[1], Katherine E Guzzetta[1,2‡], Aurelijus Burokas[1§], Hugh Harris[1], Marion Dalmasso[1,3¶], Fiona Crispie[1,4], Paul D Cotter[1,4], Andrey N Shkoporov[1,3], Gerard M Moloney[1,2], Timothy G Dinan[1,5], Colin Hill[1,3], John F Cryan[1,2*]

Affiliations:
[1]APC Microbiome Ireland, University College Cork, Cork, Ireland.
[2]Dept. of Anatomy & Neuroscience, University College Cork, Cork, Ireland.
[3]School of Microbiology, University College Cork, Cork, Ireland.
[4]Dept. of Food Biosciences, Teagasc Food Research Centre, Moorepark, Fermoy, Ireland.
[5]Dept. of Psychiatry and Neurobehavioural Science, University College Cork.

[#]These authors contributed equally: Lorraine A Draper, Thomaz FS Bastiaanssen.

Accepted for publication at *Nature Microbiology*

2.1 Abstract

The microbiota-gut-brain axis has been shown to play an important role in stress response, however, previous work has focused primarily on the role of the bacteriome. The gut virome constitutes a major portion of the microbiome, with bacteriophages having the potential to remodel bacteriome structure and activity. Here, we use a mouse model of chronic social stress, and employ 16S rRNA and whole metagenomic sequencing on faecal pellets to determine how the virome is modulated by and contributes to the effects of stress. We find that chronic stress led to behavioural, immune, and bacteriome alterations in mice that were associated with changes in the bacteriophage class *Caudoviricetes* and unassigned viral taxa. To determine if these changes were causally related to stress-associated behavioural or physiological outcomes, we conducted a faecal virome transplant from mice before stress and autochthonously (ȯ-ˈtäk-thə-nəslē) transferred it to mice undergoing chronic social stress. The transfer of the faecal virome protected against stress-associated behaviour sequelae, and restored stress-induced changes in select circulating immune cell populations, cytokine release, bacteriome alterations and gene expression in the amygdala. These data provide evidence that the virome plays a role in the modulation of the microbiota-gut-brain axis during stress, indicating that these viral populations should be considered when designing future microbiome-directed therapies.

2.2 Introduction

Stress-related psychiatric disorders such as depression and anxiety are among the highest in lifetime prevalence across the globe and are significant societal burdens[307,322,344]. Thus, understanding the biological consequences of chronic stress is an important avenue in developing novel strategies for stress-related disorders. Increasing evidence suggests that brain-gut interactions may gate the response to stress[345]. In tandem, the gut microbiota, the community of microorganisms including bacteria, viruses, archaea, protozoa and fungi that inhabit the intestine, has been shown to influence the development and function of the immune and nervous systems through the microbiota-gut-brain axis[8,2]. Bacteria make up the vast majority and metabolic capability of the cellular microorganisms in the gut and have been shown to modulate stress responses[80]. Although less studied, intestinal viruses, which are predominantly composed of bacteriophages (or phages), infect bacteria and can multiply and lyse or incorporate into their host genome and replicate alongside them[109,346]. These phages can modulate the structure and function of the microbiota and contribute towards diversity, stability, and resilience of microbiota at the community level[103]. Faecal virome transplants (FVT) prepared from faecal filtrate, composed largely of viral (primarily phage) particles and devoid of cellular microbes, have been used as microbiota-based treatments to improve clinical symptoms of *Clostridioides difficile* infection and preclinical models of type 2 diabetes, antibiotic-induced microbiota perturbation, necrotizing enterocolitis, and small intestinal bacterial overgrowth[151,156,347-349].

Numerous stress-related disorders have been associated with alterations in the gut bacteriome[269,350-352], and there is evidence that the transfer of bacterial microbiota from

patients with major depression and general anxiety disorders to rodents can transfer symptoms related to the phenotypes[18,19,37]. As the virome is intimately linked to the composition of the bacteriome[103], it also changes in response to the environment and psychological state of the host[102,269,353,354]. Recently, phages from the class *Caudoviricetes* have been linked with executive function of the host across species which supports the theory that viral members of the microbiota can impact host behaviour[355]. While the gut bacteriome has gained attention and is currently the subject of growing research, the dynamic involvement of how the virome interacts with its bacterial hosts and how both entities, in conjunction, affect stress-related health and disease status is largely unexplored. Herein, we assess the impact of stress on the virome and demonstrate that an autochthonous (*i.e.,* indigenous origin) virome transfer can prevent the manifestation of stress-related behavioural, immune, and neurobiological changes in mice.

2.3 Results

A workflow summary is provided in the supplement to outline how the virome is modulated by stress (Fig. S1a) and how the virome was leveraged to prevent the effects of stress (Fig. S1b).

2.3.1 The virome and gut-brain axis are modulated by stress

First, mice underwent chronic social stress (chronic psychosocial defeat stress; *i.e.,* unpredictable chronic social defeat and single housing with periods of overcrowding)

while control mice were similarly handled and group housed, then stress-coping behaviour, immune modulation, and microbiome composition were tested (Fig. 1a). To assess the impact of chronic social stress on virome and bacteriome composition, viral metagenomic sequencing was combined with 16S bacterial rRNA gene sequencing on faecal pellets before (pre) and following the imposition of stress (post; Fig. S2a-d). Faecal bacteriome Aitchison beta-diversity was significantly altered by stress (Fig. 1b). Qualitatively, stress markedly affected virome composition at the beta-diversity level but due to the use of pooled groups this only showed a trend between groups despite a clear visual separation (Fig. 1c). For the virome analysis, groups of n=10 and 9 (Ctr and Stress, respectively), were pooled to ensure adequate nucleic acid content. Bacterial and viral alpha-diversity metrics were not affected by stress (Fig. 1d, e). However, twelve phages were found to be differentially abundant following stress, five of which were identified as class *Caudoviricetes* (Fig. 1f).

Chronic social stress affected behaviour and immune responses in line with previous murine research[22,328,356]. There was a distinct reduction in social interaction behaviour following stress (Fig. 1g). Immobility time in the forced swim test and, correspondingly, basal corticosterone concentration were increased in the stress recipient group in addition to a trend for increased corticosterone post-FST (Fig. 1h-j). Additionally, there was increased inflammatory cytokine release (IL-6 & IL-10) from Concanavalin A (ConA) stimulated splenocytes (Fig. 1k, l) as commonly seen following chronic social stress in mice (Table S1a)[357,358]. Increased inflammatory cytokine release following stress from splenocyte cultures has been previously linked with anxiety-like behaviour[357], and

stimulation with ConA indicates humoral-based immune activation capable of driving inflammation.

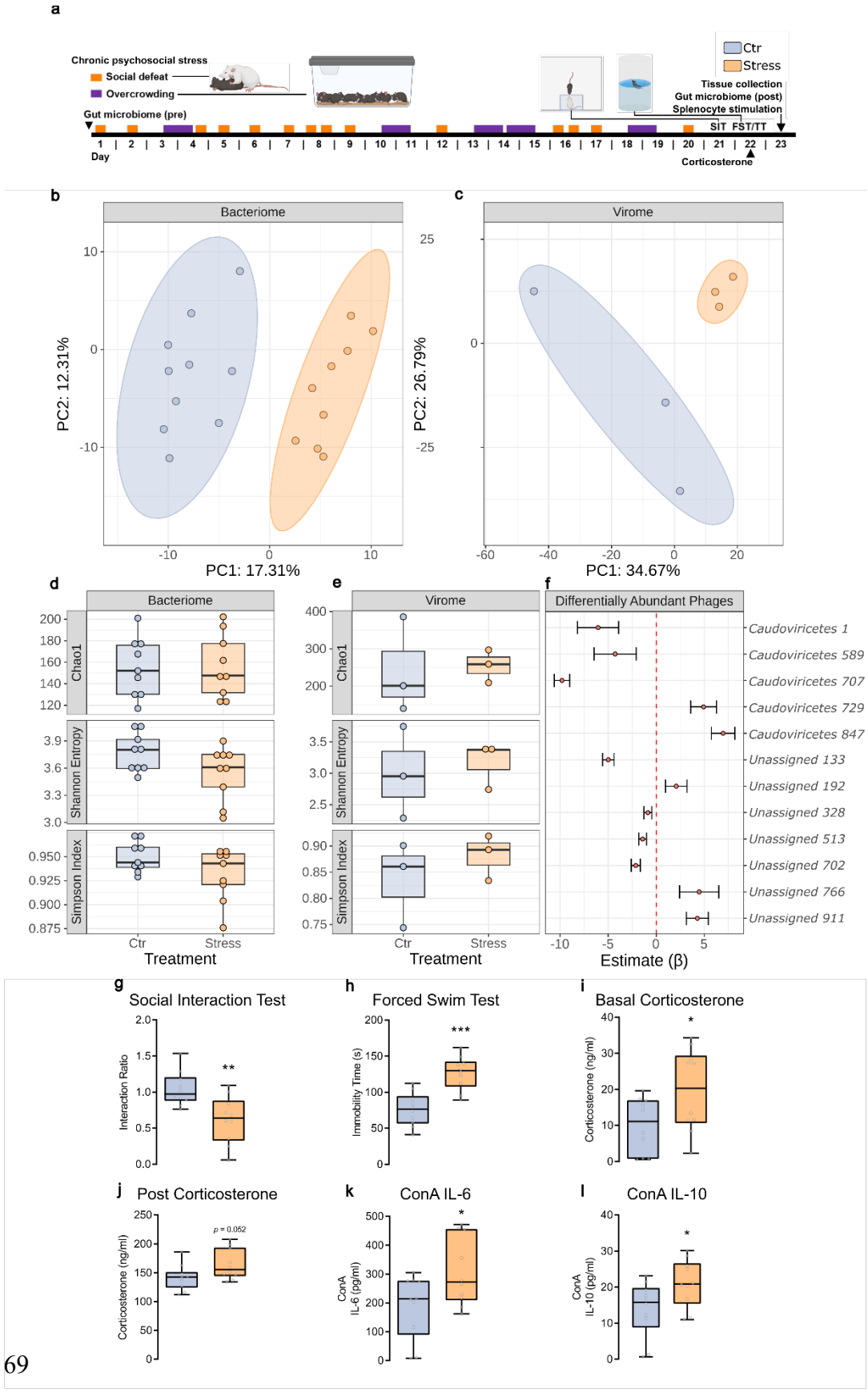

a
Chronic psychosocial stress
Social defeat
Overcrowding
Gut microbiome (pre)
Ctr
Stress
Tissue collection
Gut microbiome (post)
Splenocyte stimulation
SIT FST/TT
1 2 3 4 5 6 7 8 9 10 11 12 13 14 15 16 17 18 19 20 21 22 23
Day
Corticosterone
b
Bacteriome
PC2: 12.31%
PC1: 17.31%
c
Virome
PC2: 26.79%
PC1: 34.67%
d
Bacteriome
Chao1
Shannon Entropy
Simpson Index
Ctr
Stress
Treatment
e
Virome
Chao1
Shannon Entropy
Simpson Index
Ctr
Stress
Treatment
f
Differentially Abundant Phages
Caudoviricetes 1
Caudoviricetes 589
Caudoviricetes 707
Caudoviricetes 729
Caudoviricetes 847
Unassigned 133
Unassigned 192
Unassigned 328
Unassigned 513
Unassigned 702
Unassigned 766
Unassigned 911
Estimate (β)
g
Social Interaction Test
Interaction Ratio
h
Forced Swim Test
Immobility Time (s)
i
Basal Corticosterone
Corticosterone (ng/ml)
j
Post Corticosterone
Corticosterone (ng/ml)
p = 0.052
k
ConA IL-6
ConA IL-6 (pg/ml)
l
ConA IL-10
ConA IL-10 (pg/ml)

Fig. 1. Chronic psychosocial stress leads to microbiome, behavioural, physiological, and immune alterations.

*(**a**) Chronic psychosocial stress experimental timeline. (**b**) Faecal bacteriome Aitchison beta diversity was significantly different between stress and control groups assessed by PERMANOVA (R^2=0.1693, p<0.01; Ctr n=10, Stress n=9). (**c**) There was a trend for a difference in pooled faecal virome Aitchison beta-diversity between stress and control groups assessed by PERMANOVA (R^2=0.3011, p=0.1; Ctr n=10 pooled in 3 samples, Stress n=10 pooled in 3 samples). (**d, e**) No differences were found in bacteriome (Ctr n=9, Stress n=9) or virome alpha-diversity metrics (Ctr n=10 pooled in 3 samples, Stress n=10 pooled in 3 samples). (**f**) Differentially abundant phages of the Stress group compared to Ctr identified at the class taxonomical level; data are presented as mean with 95% confidence intervals of β-estimate (Ctr n=10 pooled in 3 samples, Stress n=10 pooled in 3 samples). (**g**) In the social interaction test (SIT), stress significantly reduced social interaction as measured by percentage of time in interaction zone with CD1 divided by the time spent in the interaction zone without the CD1 (t(18)=3.317, p<0.01; Ctr n=10, Stress n=10). (**h**) In the forced swim test (FST) stress-coping behaviour measured by time spent immobile was significantly increased by stress (t(18)=-4.946, p<0.001; Ctr n=10, Stress n=10). (**i**) Stress caused a significant increase in basal plasma corticosterone collected by tail tipping (TT) before FST (t(15.68)=-2.224, p<0.05; Ctr n=10, Stress n=10). (**j**) There was a trend for corticosterone measured 45min post FST to be increased in the Stress group (t(18)=-2.077, p=0.052; Ctr n=10, Stress n=10). Inflammatory cytokine analysis revealed significant increases collected from supernatant after 24h ex vitro ConA splenocyte stimulations of IL-6 (**k**) and IL-10 (**l**) in the Stress group compared to the Control (t(18)=-2.316, p<0.05; t(18)=-2.257, p<0.05, respectively; Ctr n=10, Stress n=10). Data in d.-l. were compared by independent-samples two-sided T test (* p<0.05, ** p<0.01, *** p<0.001). Data presented as box plots display the minimum, first quartile, median, third quartile, and maximum.*

2.3.2 Stress behaviour is attenuated by faecal virome transplant

Following the observation that chronic social stress alters behaviour and the population structure of both bacteriome and virome, we next sought to determine if a virome intervention could modulate the microbiota and improve stress-related behavioural sequelae. To accomplish this, we collected faeces from healthy non-stressed mice,

purified the viral fraction, and prepared it for subsequent administration to animals via oral gavage. Then, we subjected the same animals to chronic social defeat stress (while housed singly) with and without autochthonous faecal virome transplant (FVT). We removed the overcrowding periods of the stress model to prevent coprophagia, as the specificity of the FVT would be hindered if there were additional microbiota crossover events. After ten days of stress and treatment, animals began behaviour tests to assess social (social interaction test), anxiety-like (elevated plus maze), and stress-coping (forced swim test) behaviours while conjointly going through the stress paradigm (Fig. 2a). We confirmed the behavioural stress phenotype in control mice receiving a buffer oral gavage and additionally found that there was a restoration effect of stress-induced social investigatory deficits by stress and FVT treatment (Fig. 2b, c), in addition to significant improvement in locomotor (Fig. 2d) and anxiety-like behaviours (Fig. 2e, f). No stress effects were observed in immobility time during the forced swim test (a measure of stress-coping behaviour; Fig. 2g), we attribute this to the co-administration of the buffer solution to the unstressed controls by oral gavage in an attempt to account for handling stress effects. However, we did observe increased circulating stress hormone corticosterone in the Stress group at basal and 90min post stress, and a restoration effect in the area under the curve data in response to the forced swim test stressor (Fig. 2h, i).

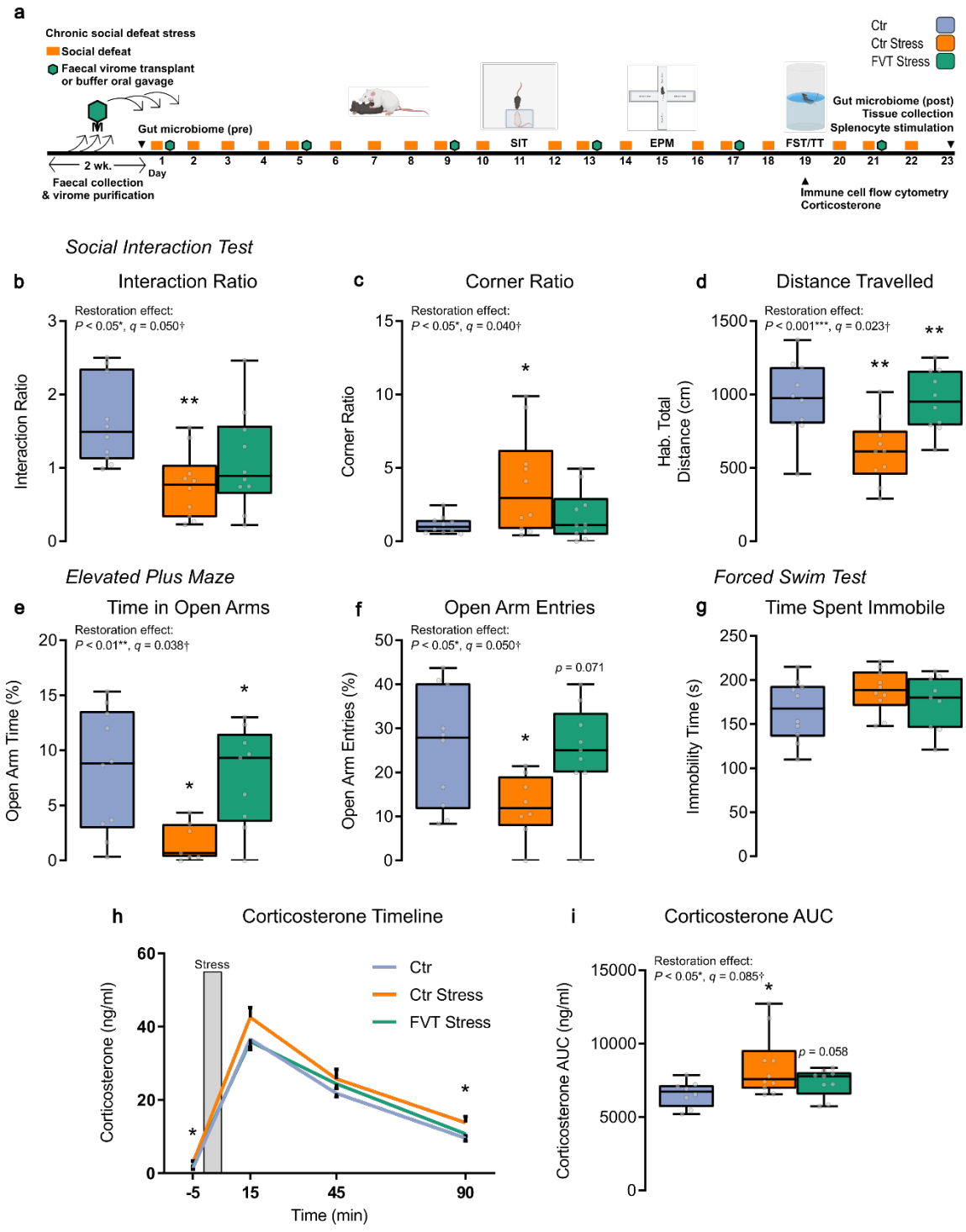


Fig. 2. Faecal virome transplant attenuates stress-related behaviours.

(a) *Experimental timeline.* ***(b)*** *In the social interaction test (SIT), stress significantly reduced the social interaction ratio in the Ctr Stress group (P<0.05, q=0.050, t(27)=9.395, p<0.01, p=0.427, respectively; n=10/group).* ***(c)*** *The corner ratio*

*significantly increased by stress (P<0.05, q=0.040, t(27)=6.067, p<0.05, p=0.111; n=10/group). (**d**) The distance travelled during the habituation phase of the test was significantly reduced by stress and restored in the FVT group (P<0.001, q=0.023, t(27)=17.761, p<0.01, p<0.01; n=10/group). (**e**) In the elevated plus maze (EPM), stress significantly increased the percentage of time spent in the open arms and the FVT restored this effect (P<0.01, q=0.038, t(23)=4.818, p<0.05, p<0.05; Ctr n=10, Ctr Stress n=7, FVT Stress n=9). (**f**) Entries into the EPM open arms were reduced in the stress group followed by a trend for restoration by FVT (P<0.05, q=0.050, t(23)=7.254, p<0.05, p=0.071; Ctr n=10, Ctr Stress n=7, FVT Stress n=9). (**g**) In the forced swim test (FST), there were no effects recorded. (**h**) Plasma corticosterone was measured -5min (basal), +15min, +45min, and +90min from FST initiation collected by tail-tipping (TT); data are presented as mean with standard error. There was increased corticosterone in the Ctr Stress group compared to Ctr at the basal and 90min-post FST timepoints assessed by orthogonal contrast followed by Tukey's two-sided pairwise post hoc (P<0.05, t(16)=2.673, p<0.05, t(16)=2.386, p<0.05, respectively; Ctr n=8, Ctr Stress n=10, FVT Stress n=9). (**i**) Area-under-curve (AUC) of corticosterone was increased in the stress group followed by a trend for reduction by FVT (P<0.05, q=0.085, t(26)=26.703, p<0.05, p=0.058; Ctr n=8, Ctr Stress n=10, FVT Stress n=9). The restoration effect was measured in b.-g. and i. by planned orthogonal contrast followed by Tukey's post hoc (two-sided pairwise comparisons of Ctr–Ctr Stress, and Ctr Stress–FVT Stress), and BH-FDR adjusted. Data are presented in the following order: P=restoration effect measured by orthogonal contrast; q=BH-FDR adjusted P-value; p=Tukey's post hoc. Tukey's pairwise post hoc p-values were calculated for Ctr-Ctr Stress and Ctr Stress-FVT Stress. Significant effects are denoted by: *p<0.05, **p<0.01, ***p<0.001, †q<0.2. Data presented as box plots display the minimum, first-quartile, median, third-quartile, and maximum.*

2.3.3 FVT inocula and virome characterization

FVT is a technique where free viral particles, which are dominated by phages, are extracted from the rest of the microbiota and other particulate material. By using phages to target the bacteriome, this treatment both specifically targets the microbiota-gut-brain axis and is safer than comparable faecal microbiota transplants due to the removal of live cellular microorganisms. FVT has previously been used to specifically target the murine

bacteriome with phages from another source[156,347-349]. Phage infection of bacterial hosts consists of highly specific targeting in most cases being governed by strain level precision. This contributes to the high inter-individual variability of the phageome[101,112,128,353]. We used an autochthonous FVT model since it theoretically provides the highest probability of active phage infections of bacteriome members due to high accordance between phage-host pairs.

Images were taken of FVT samples and confirm that the FVT inocula was free of larger microorganisms (representative image depicted in Fig. 3a). Approximately $2.2x10^8$ virus-like particles per ml were counted in the FVT solution (Fig. 3b). Furthermore, the FVT solution was characterized by virome sequencing (with known concentrations of lactococcal phage Q33 spiked to calculate absolute abundance) and approximately $3.5x10^7$ PFU/ml viruses were enumerated. The incongruity in count data metrics can be explained by the methods of detection as sequencing-based read enumeration is limited by the requirement of next generation sequencing library preparation methods to match viral contigs to a known viral gene; while the epifluorescent microscopy method functions through SYBR staining of FVT inocula samples where nucleic acids fluoresce upon binding. However, the presence of larger cellular microorganisms was not detected by either of the FVT inocula characterization approaches.

We found an assortment of phages present in the FVT preparations – in most cases dominated by members of the class *Caudoviricetes* and the family *Microviridae*, however there are large portions of the viral population that are currently unassigned (Fig. 3c). There were twenty differentially abundant bacterial species that were altered by stress but

restored when FVT was performed. Fifteen bacterial species were depleted by stress and protected by FVT, while five bacterial species were increased by stress and reduced by FVT (Fig. 3d, S3a). Despite differences in individual species in the bacteriome, no changes were found in alpha- and beta-diversity metrics in the bacteriome or virome (Fig. S4a-d), indicating that the bacteriome and virome did not undergo a large shift in community profile but rather, in low abundance members and functionality.

The FVT oral gavage preparation underwent virome sequencing allowing for the viral inputs to be characterized. Viral host pairs were predicted using a comprehensive collection of viral databases which cover the currently available bacteriophage community; however, these tools are still limited by the vast unknown portion of the bacteriophage virome[128]. Therefore, our bacteriophage sequencing data contains a small percentage of phage contigs that had a predictive host. Predicted-hosts of the FVT inocula are reported at the phylum, order, and family levels (Fig. S3b-d). Phages targeting the phylum *Deferribacterota* and *Bacteroidota* (previously *Bacteroidetes*) were the most common, followed by *Bacillota* (previously *Firmicutes*), and to a lesser extent *Pseudomonadota* (previously *Proteobacteria*), and *Halobacteriota*. The most common phages targeted the orders *Deferribacterales*, *Bacteroidales*, *Lachnospirales*, *Lactobacillales*, and *Oscillospirales*. Lastly, the most common phages targeted the families *Mucispirillaceae, Bacteroidaceae*, *Erypsipelotrichaceae*, *Lachnospriaceae*, *Muribaculaceae*, *OLB10*, and *Streptococcaceae*. However, the majority of the phage-host pairs in the murine microbiome are unknown.

Phage-host pairs from the FVT preparation were then cross-referenced with the differentially abundant taxa from faecal bacteriome sequencing data that were affected by stress and restored by FVT. The identified viral taxa that overlapped with the differentially abundant bacterial species were depicted with the predicted phage-hosts at the phyla level (Fig. 3e). At the phylum level, eighteen of the twenty differentially abundant bacterial species were represented in the predicted phage-host pairs. There were six *Pseudomonadota*, six *Bacillota*, three *Bacteroidota*, and one *Verrucomicrobiota*, *Actinobacteriota*, and *Cyanobacteria* pairs. At the order level, there were two *Burkholderiales*, one *Erysipelotrichales*, and one *Bacteroidales* pairs. At the family level, there was one *Lachnospiraceae* and one *Erysipelotrichaeceae* pair. This evidence supports bacteriome modulation by FVT, which in turn aided the restorative effects of the phage-derived treatment of stress. Given that phage infections in the gut are overwhelmingly temperate, the phage-host pair associations could be lytic or lysogenic in nature depending on environmental conditions, which can then have direct and/or indirect effects on bacterial host proliferation[103,113]. Phage-bacterial cascading interactions are shown as a correlational phage-host network plot (Fig. S5). All phage-bacterial correlations depicted significantly associate (q<0.1) and specifically *Caudoviricetes* 48-*Geofilum rubicundum*, *Unassigned class 38-Kriegella aquimaris*, and *Unassigned class 38-Odoribacter splanchnicus* show significant restoration effects following stress and FVT treatment (p<0.05).

Across the differentially abundant *Pseudomonadota* taxa, the individual species increased in abundance following FVT compared to stress (*Advenella mimigardefordensis*, *alpha*

proteobacterium AAP38, *Archangium gephyra*, *Nitrosomonas aestuarii*, *Paraburkholderia kururiensis*, and *Sinorhizobium medicae*), indicating that FVT was a positive regulator. Five *Bacillota* taxa displayed increased abundance (*Bacillus aurantiacus*, *Bacillus campisalis*, *Butyrivibrio sp. WCD3002*, *Cohnella laeviribosi*, and *Erysipelotrichaeceae bacterium NK3D112*). Conversely, the *Bacteroidota* species (*Paludibacter sp. 47-17*, *Pontibacter akesuensis*, *Thermonema rossianum*) decreased in abundance following FVT as well as a single *Bacillota* species (*Paenibacillus sp. 1-49*) and the single *Cyanobacteria* species (*Oscillatoria sp. PCC 10802*), indicating that in these cases FVT was a negative regulator. These changes are attributable to stress modulation and either protection or reduction by the FVT treatment. Our data provide evidence that phage-host pairs are present and potentially involved in the attenuation of stress-coping behaviours within our experimental parameters.

To assess the functional potential of the FVT inocula and bacteriome following the different treatments, gut-brain modules (GBM) and gut-metabolic modules (GMM) were characterized [38,359]. In the FVT inocula viral reads there were three GBMs and ten GMMs identified (Fig. S6a, b). Interestingly, the capacity for S-adenosylmethionine synthesis was found in each FVT inoculum and was significantly restored in the bacteriome GBM following stress and FVT. S-adenosylmethionine plays roles in a multitude of biochemical pathways both in the microbiota and across different tissues, including synthesis and metabolism of monoamine neurotransmitters[360-363]. We also assessed the restoration of GBM and GMM abundance by FVT in the bacteriome, but no other modules were found to be statistically significant following false discovery rate adjustment (Tables S2, S3).

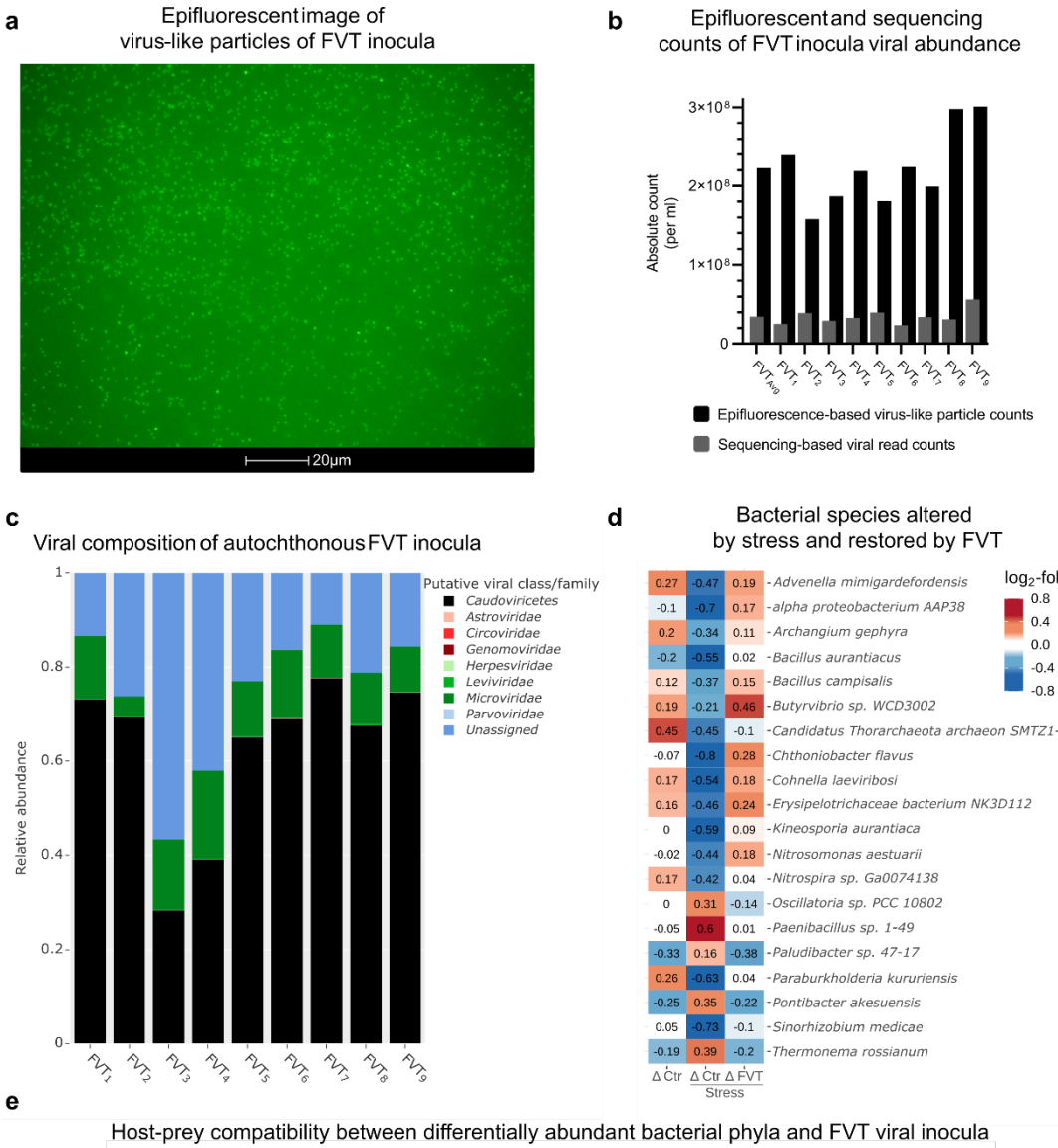

a
Epifluorescent image of virus-like particles of FVT inocula
20µm
b
Epifluorescent and sequencing counts of FVT inocula viral abundance
Absolute count (per ml)
3×10⁸
2×10⁸
1×10⁸
0
FVT_Anc
FVT1
FVT2
FVT3
FVT4
FVT5
FVT6
FVT7
FVT8
FVT9
Epifluorescence-based virus-like particle counts
Sequencing-based viral read counts
c
Viral composition of autochthonous FVT inocula
Relative abundance
1
0.8
0.6
0.4
0.2
0
Putative viral class/family
Caudoviricetes
Astroviridae
Circoviridae
Genomoviridae
Herpesviridae
Leviviridae
Microviridae
Parvoviridae
Unassigned
d
Bacterial species altered by stress and restored by FVT
log2-fold change
0.8
0.4
0.0
-0.4
-0.8
0.27 -0.47 0.19 Advenella mimigardefordensis
-0.1 -0.7 0.17 alpha proteobacterium AAP38
0.2 -0.34 0.11 Archangium gephyra
-0.2 -0.55 0.02 Bacillus aurantiacus
0.12 -0.37 0.15 Bacillus campisalis
0.19 -0.21 0.46 Butyrvibrio sp. WCD3002
0.45 -0.45 -0.1 Candidatus Thorarchaeota archaeon SMTZ1-83
-0.07 -0.8 0.28 Chthoniobacter flavus
0.17 -0.54 0.18 Cohnella laeviribosi
0.16 -0.46 0.24 Erysipelotrichaceae bacterium NK3D112
0 -0.59 0.09 Kineosporia aurantiaca
-0.02 -0.44 0.18 Nitrosomonas aestuarii
0.17 -0.42 0.04 Nitrospira sp. Ga0074138
0 0.31 -0.14 Oscillatoria sp. PCC 10802
-0.05 0.6 0.01 Paenibacillus sp. 1-49
-0.33 0.16 -0.38 Paludibacter sp. 47-17
0.26 -0.63 0.04 Paraburkholderia kururiensis
-0.25 0.35 -0.22 Pontibacter akesuensis
0.05 -0.73 -0.1 Sinorhizobium medicae
-0.19 0.39 -0.2 Thermonema rossianum
Δ Ctr
Δ Ctr Δ FVT
Stress
e
Host-prey compatibility between differentially abundant bacterial phyla and FVT viral inocula
Pseudomonadota, n=4
Cyanobacteria, n=1
Bacteroidota, n=53
Bacillota, n=126
Actinobacteriota, n=7
Unassigned class, n=10
Malgrandaviricetes, n=3
Caudoviricetes, n=178
Vedamuthuvirus, n=1
Unassigned genus, n=165
Oengusvirus, n=14
Eponavirus, n=10
Arawnvirus, n=1
Bacterial Host Phylum
Viral Class
Viral Genus

Fig. 3. Viral characterization of the faecal virome transplant and the effect on recipient microbiome.

*(**a**) Representative epifluorescence microscopy image of virus-like particles from a FVT inoculum stained with SYBR Gold at 100x magnification. No other microbes were observed using this method and viral counts were assessed for each FVT inoculum (FVT Stress n=9). For quantification 4 representative images per sample were taken at predefined quadrant fields of view of the slide and the mean count was used to calculate total number of virus-like particles per sample. (**b**) Absolute counts of virus-like particles calculated using epifluorescent microscopy (black) and sequencing reads (grey) using a Q33 Lactococcal phage spike (FVT Stress n=9). (**c**) Autochthonous FVT inocula relative abundance of viral taxa for each individual FVT treatment (FVT Stress n=9). (**d**) Longitudinal measure of differential bacterial species affected by stress and restored by FVT study assessed by linear mixed effect models (Ctr n=10, Ctr Stress n=8, FVT Stress n=9). (**e**) Predicted phage-host pairs present in FVT inocula and faecal bacteriome phyla of the FVT Stress group analysed at end of study (FVT Stress n=9).*

2.3.4 Stress-induced inflammation and immunity are protected by FVT

Stress-induced changes in immune cell populations and inflammatory cytokines provide evidence that stress-coping behaviour was impacted by prolonged immune activation. Peripheral immune cells and cytokines are known to be altered by stress and inflammation, which has been linked with increased anxiety-like behaviour in murine models[364-366]. Furthermore, both stress and corticosterone induce a redistribution of immune cells whereby myeloid cells migrate from reservoirs (*e.g.*, bone marrow, spleen) to facilitate surveillance and protection of immune-privileged tissues like the brain[367-369]. Characterizing the peripheral blood immunophenotype, we found that the populations of inflammatory monocytes and neutrophils were reduced by stress and improved by FVT (Fig. 4a, b). Interestingly, the monocytes present in the FVT recipient group strongly expressed the CD62-ligand (Fig. 4c), which is linked to lymphoid tissue migration shown

in mice[370]. A chemokine measured in plasma (IP-10) and a series of proinflammatory cytokines in splenocyte cultures (TNF-α, IL-6, and IL-12) were elevated by stress and reduced by FVT indicating a restoration effect of treatment (Fig. 4d-f; Table S1b, c).

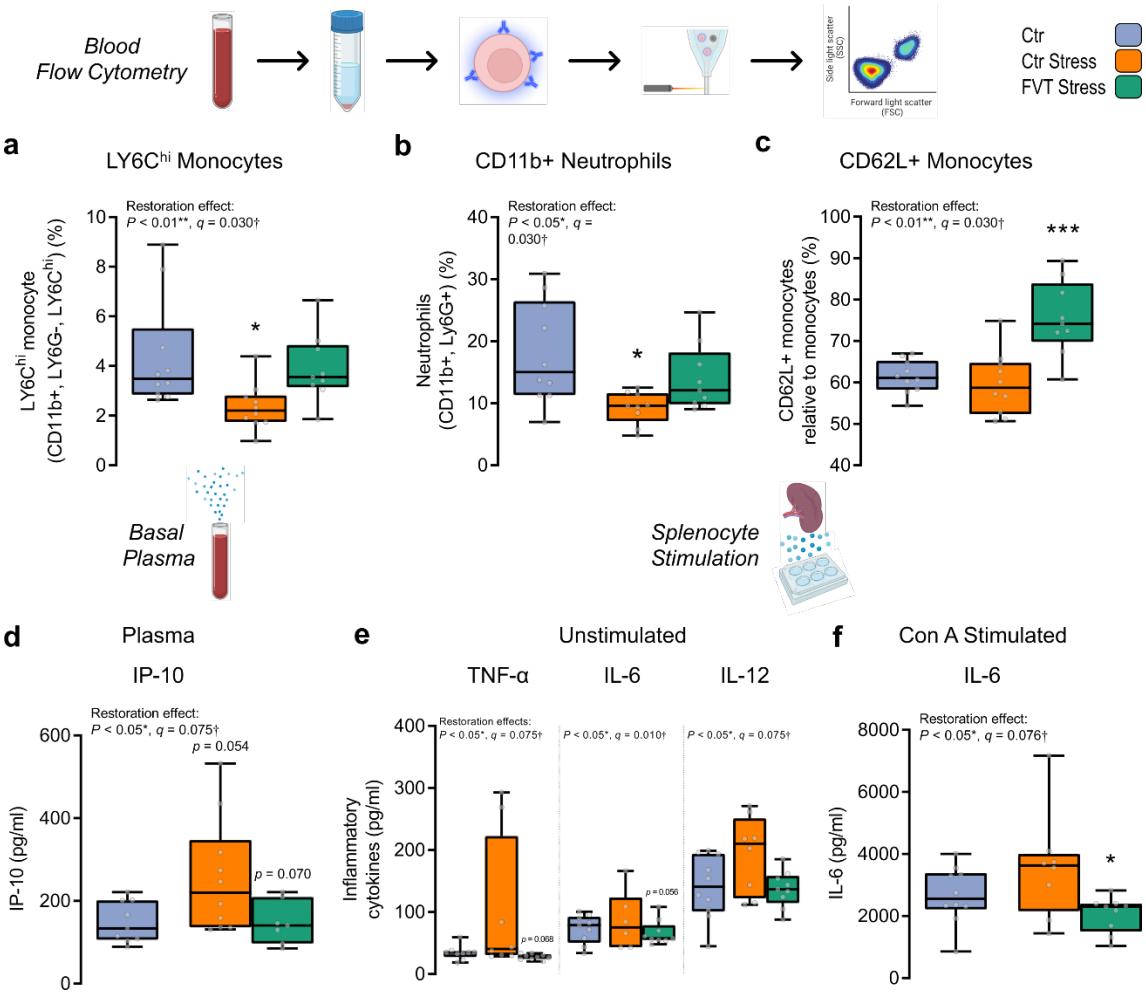


Fig. 4. Effects of FVT on immune activation and inflammation.

*Blood immune cell populations were assessed by flow cytometry after sixteen days of chronic social defeat. (**a**) There was a restoration effect of relative LY6C^{hi} monocytes that were reduced by stress and recovered by FVT (Restoration effect P<0.01, BH FDR adjusted p-value q=0.030, t(26)=-2.867, Tukey's pairwise comparisons p<0.05, p=0.0106, respectively; Ctr n=10, Ctr Stress n=10, FVT Stress n=9). (**b**) There was a restoration effect of relative neutrophils that were reduced by stress and improved by FVT (P<0.01, q=0.030, t(25)=-2.788, p<0.05, p=0.231; Ctr n=10, Ctr Stress n=9, FVT Stress n=9). (**c**) There was a restoration effect of LY6C^{hi} monocytes carrying CD62-ligand which*

*were not affected by stress but were strongly increased by FVT (P<0.05, q=0.030, t(26)=-3.18, p=0.845, p<0.001; Ctr n=10, Ctr Stress n=10, FVT Stress n=9). Inflammatory cytokines were measured in plasma (**d**) where there was a restoration effect for plasma IP-10 to be increased by stress and reduced by FVT (P<0.05, q=0.075, t(23)=2.828, p=0.054, p=0.070; Ctr n=9, Ctr Stress n=10, FVT Stress n=7). Inflammatory cytokines were also measured in unstimulated splenocyte culture supernatants and cultures that were stimulated with ConA or LPS. **(e, f)** There were restoration effects for unstimulated splenocyte culture inflammatory cytokines of TNF-α (P<0.05, q=0.075, t(23)=2.68, p=0.086, p=0.056; Ctr n=9, Ctr Stress n=8, FVT Stress n=9), IL-12/IL23p40 (P<0.05, q=0.075, t(24)=2.634, p=0.079, p=0.068; Ctr n=10, Ctr Stress n=8, FVT Stress n=9), and IL-6 (P<0.05, q=0.010, t(22)=2.328, p=0.162, p=0.091; Ctr n=9, Ctr Stress n=6, FVT Stress n=9); and for IL-6 ConA stimulation of splenocytes (P<0.05, q=0.076, t(24)=2.517, p=0.24, p<0.05; Ctr n=10, Ctr Stress n=8, FVT Stress n=9). The restoration effect was measured in a.-f. by planned orthogonal contrast followed by Tukey's post hoc (two-sided pairwise comparisons of Ctr–Ctr Stress, and Ctr Stress–FVT Stress), and BH-FDR adjusted. Data are presented in the following order: P=restoration effect measured by orthogonal contrast; q=BH-FDR adjusted P-value; p=Tukey's post hoc. Tukey's pairwise post hoc p-values were calculated for Ctr-Ctr Stress and Ctr Stress-FVT Stress. Data presented as box plots display the minimum, first-quartile, median, third-quartile, and maximum. Significant effects are denoted by: *p<0.05, **p<0.01, ***p<0.001, †q<0.2.*

2.3.5 FVT restores gene expression in the hippocampus and amygdala

Finally, to confirm that the FVT could also impact brain circuits underpinning anxiety and stress-coping, we performed deep RNA sequencing in the hippocampus and amygdala of all animals. These stress-sensitive brain regions were selected based on previous studies indicating these regions were susceptible to stress and responsive to modulation by the microbiota[371-373]. The top enriched Gene Ontology (GO)[374] terms from genes affected by stress and restored by FVT were selected to specifically target functions directly involved with stress, social behaviour, the virome, and the microbiota-gut-brain axis. These GO terms consist of genes associated with fear response, immune system processes,

neurotransmitter level modulation, postsynaptic neurotransmitter receptor functionality, stress response, social behaviour, and viral processes.

In the hippocampus, immune system processes were significantly increased, while in the amygdala, all GO terms were significantly increased (Fig. 5a). This finding corresponds with the behaviour alterations observed by stress and FVT treatment and provides evidence that there is a differential regional response within the brain. Intriguingly, amygdalar genes that were affected by stress and restored by FVT (4852) were largely upregulated (4833 genes) rather than downregulated (19 genes; Fig. 5b, d). Hippocampal genes displayed an approximately equal number of genes positively and negatively modulated by stress and restored by FVT (441), 233 were upregulated and 208 were downregulated (Fig. 5c, e). This indicates that there is a mechanism by which stress and FVT treatment impacts neural gene expression, that is particularly sensitive in the amygdala.

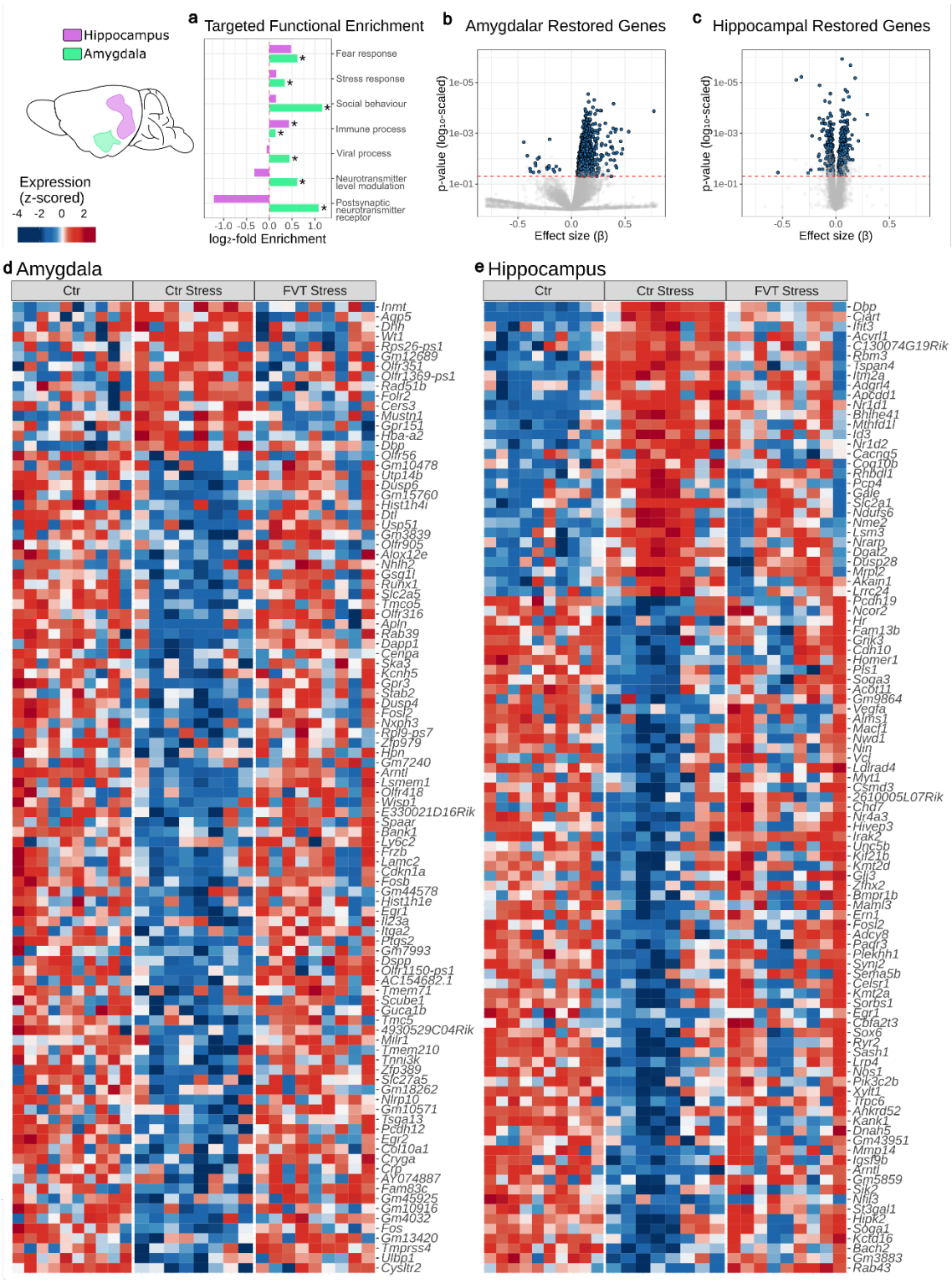


Fig. 5. Amygdalar and hippocampal transcriptomic targeted gene ontology.

*Amygdala and hippocampus brain regions were selected for deep transcriptomic analysis for genes altered by stress and restored by FVT (restoration effect). (**a**) Stress, social behaviour, and microbiota-gut-brain axis targeted gene ontology of functional enrichment in genes restored in the hippocampus (purple) and the amygdala (green; Ctr n=10, Ctr Stress n=8, FVT Stress n=9; Significant effects are denoted by *p<0.001). (**b**, **c**) Volcano plots showing the genes most significantly affected by stress and restored by FVT in the amygdala (**b**, 4852 genes; 4833 upregulated, 19 downregulated) and the hippocampus (**c**, 441 genes; 223 upregulated, 208 downregulated; Ctr n=10, Ctr Stress n=8, FVT Stress n=9). Genes (blue dots) right of "0" represent genes upregulated, while genes to the left of "0" represent genes downregulated following stress and FVT treatment. (**d**, **e**) Heat plots showing the most significantly restored genes in the amygdala (**d**) and hippocampus (**e**). Differentially expressed gene ontology clusters and individual genes were assessed by linear models followed by Storey's FDR.*

2.4 Discussion

The gastrointestinal virome comprises an enormous and diverse population of mostly unclassified bacteriophages that can potentially modulate bacterial community structure and functionality[103,128]. Our study shows a permissive effect of stress on virome composition which can attenuate stress-related sequelae by targeting the bacteriome. First, we showed that chronic social stress affected both gut bacteriome and virome, in addition to eliciting stress-coping behaviour and deficits in immune function in mice. These findings correspond with previously described stress behaviour phenotypes[80]. Interestingly, stress increased the bacteriome and virome beta-diversity distance from controls in the faecal samples. This data highlights a potential link between stress-related behaviours and the gut bacteriome and virome. This led us to pursue the hypothesis that if the virome is permissive to the effects of stress, then we should be able to target the virome to attenuate the effects of stress.

We found that an autochthonous FVT could elicit protective effects against stress-coping behaviours through microbiota-mediated mechanisms. Following chronic social stress, FVT treatment improved social measures in the social interaction test and fully prevented the locomotor deficit observed in stressed animals. Anxiety-like behaviour measured by time spent and number of entries into the open arms of the elevated plus maze was similarly attenuated by FVT compared to the effects of stress. Moreover, there was a restoration effect of stress-induced elevations in circulating corticosterone following chronic stress and FVT treatment in response to acute stress. These findings indicate that there was a measurable stress behavioural response similar to previous reports from chronic social stress despite no differences observed in immobility time measured in the forced swim test[28,29]. Taken together, we show a reduction in anxiety-like behaviour, improved exploratory behaviour, and attenuated stress-coping in animals treated with FVT following stress.

The effects of the FVT on the bacteriome and virome were assessed through a combination of metagenomic and virome sequencing. These associated bacterial taxa have not previously been described in terms of chronic social stress or the microbiota-gut-brain axis at the species level. However, shared genera, which are more commonly characterized via 16S rRNA gene sequencing, provide some interesting context. Members of the *Bacillus* genus have been associated with social aggression prevention, alleviation of neuronal cell death, and health improvement[375-377]. Moreover, a *Bacillus* species was found to attenuate high-fat diet-induced social deficits, anxiety-like behaviour, hippocampal oxidation stress, and inflammation[378]. *Butyrivibrio* species are common

producers of butyrate, which is a key short chain fatty acid product with diverse roles across the microbiota-gut-brain axis[379,380]. *Erysipelotrichaceae*, which had phage-host pair confirmation at every level assessed, was found to be differentially abundant following stress and FVT, and has been linked to inflammatory bowel diseases, metabolic disorders, and enteral nutrition[381]. This family has been shown to be reduced in patients with recurrent or inflammatory conditions in Crohn's disease[382,383] and is a key taxon involved in bile salt metabolism[384]. However, there is also evidence that *Erysipelotrichaceae* is capable of driving inflammation during infection[385,386]. *Nitrosomonas* and *Nitrospira* species are involved in the nitrogen cycle in the gut and help to oxidize ammonia, which at elevated levels has been associated with reduced growth and immune dysfunction[387,388], and can inhibit hippocampal synaptic transmission[389]. Interestingly, *Paenibacillus* produces a range of antimicrobials and insecticides- since this microbe was increased following stress it may indicate opportunistic and indirect pathobiont behaviour in that it has the potential to suppress other microbiota members[390]. There is evidence that members of the genus *Paraburkholderia* may become depleted following stress[391,392]. *Pontibacter*, also depleted by stress and restored by FVT, was previously associated with depression-like phenotypes[393]. In addition to these alterations in specific bacterial taxa, the FVT treatment has the capability to specifically change the dynamic activity of the microbiota. The FVT inocula was found to contain three gut-brain modules[38] including quinolinic acid degradation, S-adenosylmethionine synthesis, and dopamine synthesis. Furthermore, the FVT inocula also contained ten distinct gut-metabolic modules[359] including arabinoxylan degradation, homoacetogenesis, methionine degradation I, mucin degradation, pectin degradation I, starch degradation, and sulphate

reduction (dissimilatory). These findings indicate that the faecal virome administered autochthonously during stress contains elements of both neuroactive and metabolic potential which can play a role in the functional output of the microbiota.

The predicted phage-host pairs from the FVT solution overlapped with ninety percent of the cross-referenced differentially abundant bacterial species in response to stress and FVT at the phylum taxonomical level. However, only ten percent similarly overlapped at the family level (*Lachnospiraceae* and *Erysipelotrichaceae*), given the vast yet undetermined portion of the gut virome and the focus of viral analysis tools on human rather than murine datasets[394,395]. Currently, bacteriophage databases are limited as precise genetic determinants of phage host range are both highly specific and susceptible to mobile elements. For example, nominal amino acid changes in a tail fibre can alter receptor-binding domains of bacterial capsular structures and thereby change phage-host tropism[396,397]. Our data provide evidence that the FVT treatment contained phages that overlapped with bacterial hosts, indicating that there are phage-host pairs present, however due to the aforementioned classification and sensitivity limitations we cannot infer what the true percentage of the host-prey pairs were present in our microbial communities. Two options potentially explain our relatively low phage-host pair numbers and lack of larger effects of FVT treatment on species differential abundance. First, the phage-host interactions in the gut are predominantly temperate with an inclination towards lysogeny, which did not result in community-wide alterations and fits with current gut bacteriophage models[103,113,123]. Second, it could be that the FVT exerted a controlling force over microbial community through mutualistic interplay, this could

occur by governing the growth of susceptible species in response to stress and selecting for species containing protective elements against predation[103,398]. Classically it is perceived that phages are restricted to specifically infect bacteria and therefore do not elicit effects on mammalian cells. However, there is evidence that immune activation can occur following phage challenge[59,145]. Thus, the effects seen in our model are driven through FVT, and presumably, phage modulation of the microbiota first followed by the gut-brain axis, but direct effects of the phages can potentially occur. Furthermore, there is evidence that phage predation of susceptible bacteria can additionally have cascading effects on other species through interbacterial interactions[119]. Phage-host network correlational analysis of our dataset supports this dynamic cascade as there are many phage-bacteria correlations that are not known phage-host pairs, moreover some of the phage-bacteria associations differentially coordinate between groups and may play a role in stress prevention and recovery.

In contrast to short-term models[367], our chronic social stress model induced a reduction of peripheral inflammatory monocytes and neutrophils that coincide with increased levels of inflammatory cytokines, similar to previously seen chronic stress-induced immunosuppression effects[399]. Interestingly, there was a drastic increase in CD62L+ monocytes in circulation following FVT; this cell surface molecule plays an essential role redistributing and guiding the migration of monocytes into inflamed tissue in stress, suggesting that peripheral monocytes were actively being recruited[368]. Plasma IP-10 underwent a significant restoration effect following an elevation by stress and reduction by FVT. This cytokine belongs to the CXC chemokine family and has been shown to be

induced by TLR-9 stimulation and in turn to stimulate monocytes, T-cell migration, and other immune cells to promote viral clearance[59,400,401]. The spleen is an immune cell reservoir and splenocyte culture allows *ex vivo* testing to assess cytokine production of the immune cell population including monocytes, macrophages, T and B lymphocytes, and dendritic cells[369]. Similar restoration effects following stress and FVT were seen in unstimulated splenocyte production of inflammatory cytokines TNF-α, IL-6, and IL-12. IL-6 was the only cytokine reduced by FVT following ConA splenocyte stimulation, further indicating that the FVT treatment was able to reduce antigenicity hyper-response following stress. Here, our collective cytokine data suggests that the FVT Stress group did not show signs of immune activation, viral detection, or active infection. Immune cell signalling is a key mechanism by which the gut microbiome influences the brain, including in stress[364], and it is plausible that the ability for FVT to mitigate the stress response is driven through immune-mediated pathways[402], although more mechanistic research would need to be done to fully elucidate specific microbe-immune-brain pathways involved.

Transcriptomics of the hippocampal and amygdalar regions of the brain revealed many genes that were stress and FVT sensitive. Both the amygdala and hippocampus are brain regions highly involved in coordinating stress response and are sensitive to the gut[39,371,403]. The amygdala has been shown previously by our group to be particularly sensitive to anxiety, social behaviour, and the microbiota interactions[13,403]. We observed that the expression of the vast majority (99.6%) of amygdalar genes were reduced by stress and restored by FVT, while in the hippocampus, gene expression levels were more evenly

distributed (52.8% were upregulated following stress and FVT). In the hippocampus and amygdala, GO immune terms were restored; in the amygdala genes associated with endogenous viral processes were additionally increased. These viral processes include viral multi-organism interactions such as host cell infection, viral genome replication, and/or assembly of virus particle progeny. Since the brain is an immune-privileged organ protected from microbial infection, the viral processes are likely endogenous retroviral assemblage historically incorporated into the genome of the host. In other contexts, these sequences of retroviral origin have been associated with homeostatic and inflammatory responses promoted by the microbiota[404]. Furthermore, amygdalar GO behavioural terms displayed genes associated with social, stress, and fear behaviours were restored. Lastly, neurotransmitter and postsynaptic membrane neurotransmitter receptor levels were additionally restored in the amygdala.

It is worth noting that one of the challenges facing current phage research is that phage sequence databases are primarily made up of industrially relevant, pathogen-associated, and/or cultivatable phages. Given that the majority of sequenced samples in our study are unknown murine phages, it limits our ability to classify all the viral sequences found. Another limitation is that ssDNA and RNA viruses are frequently not captured in sequencing analyses. To account for this, we used a reverse transcription step to convert ssDNA/RNA to cDNA, which is double-stranded and therefore can be incorporated in the library preparation. No viruses were identified taxonomically in the initial virome sequencing (characterising Ctr vs. Stress) to belong to viral taxa that have RNA genomes. However, in the second virome analysis (the FVT study) putative signals belonging to

taxa with RNA genomes were observed (*e.g.* ssRNA viruses *Astroviridae* and *Fiersviridae*- formerly *Leviviridae*) albeit at very low levels in comparison to those for viruses with DNA genomes. Putative signals corresponding to ssDNA viral taxa were also identified in the FVT viromes (*e.g. Circoviridae*, *Genomoviridae*, *Microviridae*, *Parvoviridae*). It should also be noted that a considerable number of viral contigs within both datasets could not be classified to belong to known viral taxa (*i.e.* 'Unassigned'), and while this does not mean these are additional RNA/ssDNA viruses, it neither excludes this as a possibility.

By characterizing the FVT inocula with epifluorescent microscopy and shotgun sequencing we show that the purified FVT inocula were comprised of virus-like particles and viral reads, but as we primarily selected phages based on size it is comprehensible that the smallest bacteria at the extremes of life may have also been transferred. However, the purification steps used herein specifically isolated and concentrated viruses that were between 100kDa (~3.05nm) and 45μm using centrifugation, extensive filtering, and dialysis which would remove larger microbes, and smaller metabolites, proteins, and extracellular milieu. The next consideration is the temperate life cycle, which has the capability to elicit both lytic and lysogenic pathways dependent on environmental conditions and is the predominant phage life cycle type in the gut[103]. This makes it challenging to ascertain whether phages are impacting their bacterial hosts in direct lytic action or through the multimodal optionality of lysogeny. We can infer that since the FVT was derived from excreted faeces that the phages were predominantly temperate, as it is theorized that phages in the top mucin layer primarily follow "piggyback the winner"

dynamics whereby incorporated phages multiply as a result of bacterial division and increase in abundance together[126]. Furthermore, the FVT would also have a bias towards the free viral fraction since incorporated plasmids and lysogenized viral nucleic acid motifs are not readily collected in the sample preparation. This would mean that there are elements of the original donor virome that would not be transferred. Lastly, administration of the FVT by oral gavage is an inherently stressful technique which we balanced by also performing a gavage of buffer to the control groups, but this could potentially impact outcomes as an additional stress-related measure.

FVT as a technique is still in its infancy but there are increasing data supporting its efficacy in disease models[156,349,405-407] and it is burgeoning as an alternative microbiota-based treatment[407-409]. Recently, there is evidence suggesting that it is possible to inactivate different strata of the FVT[406] which may increase specificity of treatment by targeting specific hosts. By using this approach, it is possible to further dissect what groups are driving phage-bacteria-host interactions. Furthermore, it is also necessary to assess what effects a fully inactivated FVT would have on the microbiota and mammalian host. Alternatively, as the role and function of specific microbial taxa are uncovered, phage cocktails targeting pathobionts can be assembled and delivered to ameliorate associated maladies. Our goal for this study was to determine whether the gut virome could elicit a therapeutic effect to prevent stress-related behaviours and then to perform a deep phenotyping analysis to describe the effects in the context of the microbiota-gut-brain axis. Under the specific conditions of our study, we observed protective effects of an autochthonous FVT against stress, however the specific agents that drive these effects

and the targets they interact with are yet unknown and will require future studies to unravel this nuanced interplay. There are yet many intriguing possibilities and directions for future research including whether an inactivated FVT can elicit effects, characterising how an FVT affects the host in lieu of a host microbiota (such as with germ free or gnotobiotic models), whether a FVT from a stressed animal could elicit a stressed phenotype, and whether specific phages can have anti-stress potential.

In conclusion, we show that the virome plays a permissive role to the microbiota-gut-brain axis response to stress. This can be targeted through the virome (*i.e.*, FVT) to ameliorate the effects of stress on the host at a multitude of levels. Bacteriophage treatment demonstrates a utility of harnessing individual strata within the microbiota-gut-brain axis to protect against stress. As gut phage research progresses, characterization of the dynamic interplay between phage and host within the microbiota will unlock even greater potential to promote gut and brain health.

2.5 Methods

Animals

In the first study twenty male C57Bl/6J mice (n=10 per group) and twenty male CD1 non-experimental resident aggressor mice were used and then in the second study thirty male C57Bl/6J mice (n=10 per group) and fifty male CD1 mice were used and housed within the Biological Services Unit, University College Cork. Mice were received at eight weeks of age from Envigo (UK) and randomly assigned to groups. Animals were habituated for

one week after which the 'stress' groups were single housed while the control (Ctr) groups remained group housed. Food and water were provided *ad libitum* throughout the study. The holding room was under a 12-hour light/dark cycle (light cycle began at 07:00h), with a temperature of 21±1°C and humidity 55±10%. Body weight was monitored twice per week. To provide an adequate sample size number to detect changes, a priori power analysis was performed using the Software G*Power (version 3.1) considering a power of 80% (1-beta-error) and a 0.05 alpha-error. Investigators were not blinded during allocation of experiments; however, analyses were conducted in a manner blinded to the experimenter. All experiments were approved by the Animal Experimentation Ethics Committee of University College Cork and conducted in accordance with the European Directive 86/609/EEC and the Recommendation 2007/526/65/EC.

Experimental timeline and behaviour testing

There were two groups, Stress and control (Ctr), used in the first experiment to test whether chronic social stress changed the bacteriome and virome. Animals (assigned randomly) in the Stress group underwent chronic psychosocial defeat stress which consisted of a semi-randomized sequence of social defeat and overcrowding stressors over a period of twenty days (see Fig. 1a). Behavioural tests were performed between 9:00h and 12:00h in the order: (1) Day 21 - social interaction test; (2) Day 22 - forced swim test. At the end of study animals were euthanised on Day 23 by decapitation and tissues were collected for subsequent analyses.

Animals were randomly assigned to one of three groups used in the second experiment: control (Ctr), control stress (Ctr Stress), and faecal virome transplant stress (FVT Stress).

At the start of chronic social stress animals additionally received treatment by oral gavage; Ctr and Ctr Stress groups received vehicle SM buffer, and FVT stress received the purified autochthonous faecal virome from the pre-stress faecal collection. Animals in the 'Stress' groups underwent chronic social defeat stress (CSDS) nineteen times over twenty-two days (animals were not stressed on the three behaviour testing days). Controls did not receive stress but were handled evenly by researchers at the same time. Behavioural tests were performed between 9:00h and 12:00h in the order: (1) Day 11 - social interaction test; (2) Day 15 - elevated plus maze; (3) Day 19 - forced swim test (see Fig. 2a). At the conclusion of the study animals were euthanised on Day 23 by decapitation and tissues were collected for subsequent analyses.

Faecal virome purification

Faecal samples were collected in a PBS-glycerol (20%) solution, frozen (-80^{o}C), and later used to generate phage-rich material used for FVT oral gavage. Approximately 2.5g of faecal pellets were resuspended in 10ml filter sterilized SM buffer (50mM Tris-HCl; 100mM NaCl; 8.5mM mgSO4; pH 7.5) and 2ml 1M NaHCO3 (to reduce stomach acidity). The faecal slurry was vigorously vortexed and then centrifuged at 5,000g for 20min. The supernatant was then filter sterilized (0.45μm filter) and before undergoing overnight dialysis (SpectraPor® Float-A-Lyzer Dialysis Device G2 100kDa, Repligen).

Chronic psychosocial stress

In the first experiment, mice underwent twenty days of chronic psychosocial stress which was comprised of social defeat stress and/or overcrowding (see Fig. 1a for experimental timeline) [328]. Experimental mice were stressed over a consecutive twenty-day period in

an unpredictable social defeat/overcrowding schedule. Social defeats sessions (described below) included exposure to an aggressive CD1 and attack or submissive posture. Overcrowding sessions included co-housing for 24h in a standard holding cage with n=10 per cage.

Chronic social defeat stress

In the second experiment, chronic social defeat stress was carried out daily for nineteen consecutive days (excluding behaviour test days; see Fig. 2a for experimental timeline)[410]. Chronic social defeat stress was selected to eliminate potential coprophagy events that may occur during the overcrowding portion of the chronic psychosocial stress paradigm that may confound the effects of FVT treatment. CD1 mice were screened for aggression over two days prior to social defeat sessions. CD1 mice with the shortest attack latencies were selected as the aggressors to be used in subsequent social defeats. For each social defeat session, a CD1 novel to the experimental mouse was used. The session would involve an initial exposure to the CD1 mouse in a clean cage with fresh bedding to reduce coprophagy. The session would last until the first attack, expression of submissive posturing by the experimental mouse, or until 5min had passed. The latency to attack or submission was recorded. The mice were then separated by a clear Plexiglas® perforated wall that allowed non-physical contact for 2h. After 2h the separator was removed, a second defeat session was conducted, then mice were returned to their home cages. Social defeat sessions were carried out in the afternoon during the light cycle. Control mice were handled an equal amount daily in lieu of social defeat.

Social interaction test

For study one, animals underwent the social interaction test[411] after twenty days of chronic psychosocial stress; for study two, animals were tested after ten consecutive days of chronic social defeat stress. Experimental animals were placed in a rectangular plastic box ($31x39cm^2$) containing an empty wire mesh cage ($9.5x7.5cm^2$) and allowed to freely explore for 2.5min, then the mouse was removed and placed in its home cage for 1min while a novel CD1 mouse was placed into the wire mesh cage. The experimental animal was then returned to the social interaction box and allowed to freely explore for 2.5min while the CD1 mouse was in the wire mesh cage. At the conclusion of the test, the mice were returned to their home cages and the box and wire mesh cage were cleaned with 70% ethanol. Trials were recorded with a ceiling-mounted camera and evaluated using Ethovision 11.5 (Noldus, the Netherlands). Social interaction and corner ratios were calculated by taking the ratio of time spent in the interaction zone (area around the mesh cage) or corner (the two furthest points from the mesh cage) during the habituation versus when the CD1 was present.

Elevated plus maze test

The elevated plus maze test was used to assess anxiety-like behaviour and was conducted[22]. The maze apparatus was elevated 1m above ground and consisted of a grey plus (+) shaped maze with two opposing open arms and closed arms (50x5cm arm length, 15cm closed wall height, 1 cm open wall height). Experiments and habituation were conducted in red light (5lux). Mice were habituated to the room for 1h prior to the test, then allowed to explore the maze for 5min. The maze was cleaned with 70% ethanol between each animal trial. Experiments were videotaped from a ceiling-mounted camera

and videos were scored blind for time spent in open arms and open arm entries (entrance defined as all paws in arm).

Forced swim test

The forced swim test was used to assess depressive-like stress-coping behaviour and was conducted[22]. A glass cylinder (21cm diameter) was filled up with 24±1ºC water to a height of 15cm, water was emptied and replaced after each individual. Experimental animals were placed in the water for 6min while being recorded by a ceiling-mounted camera. After each test, animals were gently dried off with a towel and replaced back in their home cage. The last 4min of the 6min test was used to manually score immobility behaviour from the video recorded by a researcher blinded to the experimental groups. Mice were judged to be immobile when only making movements necessary to keep its head above water.

Repeated blood sampling for stress and immune measures

Plasma from each animal was sampled by tail tip five minutes prior to the forced swim test, then fifteen, forty-five, and ninety minutes after the start of the test. The tail was securely restrained, and a diagonal incision was made approximately 1-2mm from the tip of the tail. Approximately 40ul of whole blood was collected in an EDTA-lined capillary tube (Fisher Scientific, 749311) per timepoint. Samples were deposited in an Eppendorf and centrifuged for 10min at 3500g at 4ºC. Plasma was collected and stored at -80ºC for later corticosterone quantification. The remaining blood cells were used for immune flow cytometry analysis.

Corticosterone stress response timeline

Samples were analysed in duplicate in a single assay using 10ul plasma per sample; the threshold detection was less than 32pg/ml; coefficient of variation limit=20%; the concentration units are expressed in ng/ml. Light absorbance was read with a multi-mode plate reader (Synergy HT, BioTek Instruments, Inc.) at 405nm.

Flow cytometry

Flow cytometry was performed on blood samples collected prior to and 45min post forced swim test and samples were processed on the same day. Staining, gating, and analysis were performed according to the following methods[410] and a gating strategy is provided in the supplement (Fig. S7). Blood was resuspended in 10ml of red blood cell lysis buffer for 3min (15.5mM NH_4Cl, 1.2mM $NaHCO_3$, 0.01mM tetrasodium EDTA, diluted in deionized water). Samples were then centrifuged (1500g, 5min), and resuspended in 45µl staining buffer (autoMACS Rinsing Solution, Miltenyi 130-091-222, supplemented with MACS BSA stock solution, Miltenyi 130-091-376) for staining procedure. Then, 5ul of FcR blocking reagent (Miltenyi, 130-092-575) was added to each sample. Next, samples were incubated with a mix of antibodies at a 2:71 dilution (CD11b+ Miltenyi 130-113-234, LY6G Miltenyi, 130-117-500, LY6C Miltenyi 130-111-917, CD62L BioLegend 104418, MHC-II Biolegend 107632, CD4 Biolegend 100548, CD44 BD Biosciences 563736, CD69 Miltenyi 130-115-575) and incubated for 30min on ice. After, samples were fixed in 4% PFA for 30min on ice. Fixed samples were resuspended in staining buffer and analysed the subsequent day on the FACSCelesta flow cytometer (BD Biosciences, Germany) with FACSDiva (version 8.0, BD Biosciences) and CellQuest Pro

(version 5.2, BD, Biosciences). Data were analysed using FlowJo (version 10). Cells were gated based on FSC-height and SSC-height; subsequently LY6C^{hi} monocytes (CD11b^{+}, LY6C^{hi}), neutrophils (CD11b^{+}, LY6C^{+}, LY6G^{+}), and T helper cells (CD11b^{-}, LY6G^{-}, CD4^{+}) were selected. Next, LY6C^{hi} monocytes and neutrophils that contained CD62L or MHC-II were assessed in their relative proportion to the respective parent population. Then, T helper cells that were either CD69^{+} or CD44^{hi} were similarly assessed in their relative proportion of the total parent cell population.

Splenocyte stimulations

Spleens were collected during tissue harvest, trimmed of fat, and placed in RPMI medium (R8758, supplemented with 10% Foetal Bovine Serum (F7524, Sigma), and 1% penicillin-streptomycin-glutamine 100x (10378-016, Biosciences Ltd.). They were then treated with Red Blood Cell Lysis Buffer (R7757, Sigma), passed through a 70µm filter, and then resuspended in fresh supplemented RPMI medium. Next, 4ml of splenocytes were seeded in 6-well plates at a concentration of 16x10^{6} cells/well. After a 2.5h rest period, cells were stimulated with lipopolysaccharide (2µg/ml, tlrl-eblps, Invivogen) and concanavalin A (2.5µg/ml, C5275, Sigma) for 24h to induce ceiling antigenicity. Then supernatant was collected and used for inflammatory cytokine analysis.

Inflammatory cytokine analysis

Cytokine levels from plasma and splenocyte supernatant samples were collected during euthanasia and quantified using the V-PLEX Proinflammatory Panel 1 Mouse Kit (MSD, K15048D, United States) measuring IFN-y, IL-6, IL-12/IL-23p40, TNF-a, IP-10 on the MESO QuickPlex SQ 120 SECTOR Imager 2400 (MSD). Cytokine quantification was

done according to the manufacturer's guidelines. Samples below the detection limit of each assay were excluded.

Faecal bacteriome collection and sequencing

In the first experiment, the QIAamp DNA Stool Mini Kit (Qiagen, Hilden, Germany) was used to extract bacterial DNA using the manufacturer's handbook (Second Edition 2012) Isolation of DNA from Stool for Pathogen Detection protocol. Samples were prepared for 16S sequencing using the Nextera XT DNA Library Prep Kit (Illumina, San Diego, CA, USA), as described in the Illumina 16S rRNA gene library preparation workflow. 16S bacterial rRNA gene was amplified using primers targeting the V3-V4 hypervariable region (Forward: 5'TCGTCGGCAGCGTCAGATGTGTATAAGAGACAGCCTACGGGNGGCWGCAG ; Reverse: 5'GTCTCGTGGGCTCGGAGATGTGTATAAGAGACAGGACTACHVGGGTATCT AATCC) (Sigma Aldrich Ireland ltd., Wicklow, Ireland). The Illumina V3–V4 primers were selected for their high coverage (94.5% bacteria) while remaining in the amplicon size necessary for sequencing[412]. 16S rRNA amplicons were sequenced on the Illumina MiSeq platform (Teagasc, Moorepark, Ireland).

In the second experiment, The QIAamp Fast DNA Stool Mini Kit (Qiagen, Hilden, Germany) was used to extract DNA from faecal pellets. This was performed following the manufacturer's guidelines. Before extraction, however, 20µl the ZymobIOMICs spike-in control 1 (Zymo Research, Irvine, CA, United States) was added to aid in calculating absolute abundances. DNA concentrations were then measured using the

Qubit High Sensitivity assay (Thermo Fisher Scientific) before adjustment to 0.2ng/µl for the Nextera XT library preparation (Illumina, San Diego, CA, United States). Library quality was assessed using the 4200 Agilent Tapestation (Agilent Technologies, Santa Clara, CA, United States) using the High Sensitivity D1000 ScreenTape assay (Agilent Technologies) before whole metagenomic sequencing was performed on an Illumina Novaseq platform using 2 × 150nt paired-end chemistry (Genewiz, Germany).

Faecal virome collection and sequencing

Faecal viromes in the initial experiment were processed using a verified protocol[113,114]. Briefly, the samples from control and stress groups were pooled (n=3-4 per pool) to create a 1-2g faecal samples. Pooled samples were resuspended in 10ml saline magnesium (SM) buffer, vortexed for 5min, cooled for 5min on ice, and centrifuged 5,000g for 10min at 4ºC to remove large particulate and bacterial cells, then supernatants were transferred to new tubes and centrifugation was repeated. Supernatant was filtered twice through a 0.45µm pore ceramic filter. Following further refinement and treatment with proteinase K and Phage Lysis Buffer, sample DNA was extracted using the phenol-chloroform method. After DNA extraction, samples were processed for shotgun metagenomic sequencing using the Nextera XT DNA Library Prep Kit (Illumina, San Diego, CA, USA). Virome metagenomic sequencing was performed on the Illumina MiSeq platform (Teagasc, Moorepark, Ireland).

In the second experiment, an updated protocol described by Shkoporov *et al.*, 2022[413] was used. For FVT gavage samples 400µl were processed, and to enable comparisons of viral load across samples, 10µl of 10^8 plaque-forming units per millilitre of lactococcal phage

Q33 were added to each sample. For faecal samples, a single faecal sample from each mouse was pooled per group in 650µl of SM buffer. Fresh 0.5M dithiothreitol was prepared in 1ml of SM buffer. A volume of 16µl of the dithiothreitol stock was added to samples to achieve a final concentration of 12mM, and samples were incubated at 37°C for 30min. Centrifugation at 4,000g for 30min at room temperature was used to pellet debris and bacterial cells. Subsequently, 400µl of liquid was removed and treated with 40µl of DNase/RNase buffer (50 mM MgCl2, 10 mM CaCl2), 12µl (24 U) of Turbo DNase (Thermo Fisher) and 4µl (40 U) of Fermentas RNase I (Fisher Scientific) at 37°C for 1h. Nucleases were inactivated by incubating at 65°C for 10min. With free nucleic acids now removed virus-like particles (VLPs) were lysed using the QIAgen Blood and Tissue Kit following the manufacturer's guidelines. However, an elution volume of 30µl of Qiagen AE elution buffer (10mM Tris-HCl, 0.5mM EDTA, pH 9.0) was used to increase the final concentration of nucleic acid obtained.

A reverse transcription reaction was performed using SuperScript IV First Strand Synthesis System (Invitrogen/Thermo Fisher Scientific) with 11µl of purified VLP nucleic acids sample and random hexamer oligonucleotides according to the manufacturer's protocol. The concentration of DNA purified using a DNeasy Blood & Tissue kit (Qiagen) was determined using the Qubit dsDNA HS kit and the Qubit 3 fluorometer (Invitrogen/Thermo Fisher Scientific). DNA/cDNA yields varied between 0.05 and 29ng μl^{-1}, with some samples being below the detection limit. Prior to library preparation, 22µl of each sample underwent reverse transcription using the Superscript

IV kit (Invitrogen/Thermo Fisher Scientific) according to the manufacturer's protocol in order to include any RNA viruses in the analysis.

Subsequently, samples were sonicated following adjustment of the volume to 52.5µl with low-EDTA TE buffer. Shearing of unamplified DNA/cDNA mixture was performed on a M220 Focused-Ultrasonicator (Covaris) with the following settings: peak power of 50W, duty factor of 20%, 200 cycles per burst, total duration of 35s. Samples were then concentrated using the Genomic DNA Clean & Concentrator-10 kit from Zymo Research and eluted in 16µl. Library preparation was then carried out using the Accel-NGS 1S Plus kit (Swift Biosciences) according to the manufacturer's instructions. However, a final and additional bead clean-up step of 0.8 DNA/AMPure beads v/v ratio was included. Library QC to determine fragment length distribution and quantitation was performed using the 4200 Agilent Tapestation (Agilent Technologies, Santa Clara, CA, United States) using the High Sensitivity D1000 ScreenTape assay (Agilent Technologies) and Invitrogen Qubit. The normalised pooled library was then sequenced using 2×150 nucleotide paired-end sequencing chemistry on the Illumina HiSeq platform at Genewiz (Leipzig, Germany).

Analysis of bacteriome sequencing data

We performed quality checks on raw sequences from all faecal samples using the FastQC program with a quality score of 30 as a threshold. Shotgun metagenomic sequencing data were then cleaned and host genome sequences were filtered using Bowtie2 via the Kneaddata wrapper program with following parameters: ILLUMINACLIP:/NexteraPE-PE.fa:2:30:10, SLIDINGWINDOW:5:25, MINLEN:60, LEADING:3, TRAILING:3.

Reads were aligned to the Web of Life database using Bowtie2 and taxonomic and functional profiling of the microbial community was performed using Woltka. Next, the uniref90-based gene abundance matrix was further collapsed by KEGG Orthology (KO) term mapping via the "woltka tools collapse" function provided within Woltka. Woltka SOP is available online (https://github.com/qiyunzhu/woltka/blob/master/doc/wolsop.sh). Gut-Brain Modules (GBMs)[38] and Gut-Metabolic Modules (GMMs)[359] were calculated using the R version of the Gomixer tool.

Analysis of gavage virome sequencing data

Virome reads were processed to remove adaptors, trim low-quality bases, and filter reads for quality and length using fastp v0.23.2[414] with the flags '*-length_required 60–detect_adapter_for_pe –cut_front –cut_tail –cut_window_size 4 –cut_mean_quality 20–trim_front1 10*'. Eukaryotic reads were then identified and removed by mapping reads to the *Mus musculus* and *Homo sapiens* genomes (GCF_000001635.27_GRCm39 and GCF_009914755.1_T2T-CHM13v2.0 respectively) using Kraken v2.1.2[415]. At each step read quality was assessed using FastQC v0.11.9[416].

Reads passing the trimming and filtering steps were then assembled on a per sample basis using MEGAHIT v1.2.9[417] with default parameters. The resulting contigs from all samples were then pooled and filtered to retain only those contigs ≥ 3Kbp in length. Redundant contigs were then removed following an all-vs-all BLASTn (v2.12.0+) comparison (*e*-value cut-off of $\leq 1 \times 10^{-20}$) where the shortest contig was removed for all

pairs of a hit contigs that shared ≥ 90% identity over ≥ 90% of the shortest length of the contig.

Putative viral contigs from the non-redundant contig pool were then identified using the following criteria: Firstly, contigs were compared to the viral nucleotide sequences within the National Center for Biotechnology Information (NCBI) RefSeq database release 211, the Gut Virome Database[238], the Joint Genome Institute (JGI) IMG/VR v3 (release #5; 12-10-2020)[418], and our in-house crAss-like bacteriophage genome database using BLASTn (v2.12.0+) with an *e*-value cut-off of ≤ 1 x 10$ˆ[-10]. For these nucleotide comparisons, any contig found to have ≥ 85% of its length covered by any combination of hits with at least 50% identity to sequences within these databases were deemed as a potential viral sequence. As phages are particularly heterogeneously distributed among microbiomes if a feature is absent (or unobserved) in approximately half of samples, inclusion in subsequent analysis greatly increases the risk of spurious associations[419]. Potential viral contigs were also identified based on protein homology. For this, open reading frames (ORFs) were called within each contig with Prodigal v2.6.3[420] using the '*-meta*' option with the resulting ORFs compared to the NCBI RefSeq viral protein database (release 211) using BLASTp (v2.12.0+; *e*-value cut-off of ≤ 1 x 10$ˆ[-10]). ORFs were also compared to the hidden Markov models (HMMs) of the Prokaryotic virus Remote Homologous Groups (PHROGs; release v3) database[421] and the JGI's inovirus protein families (iPFs) database[422] using hmmscan (HMMER v3.3.2; *e*-value cut-off of ≤ 1 x 10$ˆ[-5]). Contigs were denoted as potentially viral from the results of protein comparisons if the contig encode for at least 2 ORFs that were hit by any combination of

the protein comparisons where this accounted for at least 50% of the total of the contig ORF count. Two stand-alone viral identification tools were also used to identify putative viral contigs from the contig pool, namely VirSorter2 v2.2.3[423] (with '*–include-groupsdsDNAphage,RNA,ssDNA*' and DeepVirFinder v1.0[424]; default paramaters). Finally, any circular contigs identified by the ViRal and Circular content from metAgenomes tool (VRCA; https://github.com/alexcritschristoph/VRCA) was also included in the list of potentially viral contigs.

Contigs that met any of these viral identification criteria were then examined for the presence of rRNA genes using barrnap v0.9 (https://github.com/tseemann/barrnap) with default parameters, with any contigs found to contain rRNA hits then removed from the list of potential viral contigs. Finally, the potential viral contigs were then examined for quality using CheckV v1.0.1 and its sequence database v1.2[425]. In cases where a contig was identified as proviral by CheckV, the contig sequence was refined to that within the viral start and end positions suggested by CheckV for that contig. As this refinement altered some of the viral contig lengths contigs where again re-filtered to remove contigs ≤ 3Kbp in length.

From the list of viral contigs the assembled contig corresponding to the lactococcal phage Q33 used as in internal viral standard was identified by BLASTn of the phage Q33 genome (GenBank accession: JX564242.1) and the corresponding contig replaced with the reference genome sequence for Q33. Viral contigs were then clustered into viral clusters using vCon- TACT2 v0.11.1[426] with the options '–rel-mode Diamond –db ProkaryoticViralRefSeq207-Merged–pcs-mode MCL –vcs-mode ClusterONE'. Viral

family information was also assigned to contigs using Demovir (https://github.com/feargalr/Demovir). Where vContact2 was able to cluster viral contigs with a known virus, the taxa information of the known virus was assigned to the contig, otherwise the information from Demovir was used. The lifestyle of each viral contig (*i.e.* virulent vs. temperate) was predicted using BACPHLIP v0.9.6[427]. If BACPHLIP assigned a lifestyle with a confidence value of ≥ 0.95 that lifestyle was assigned to the contig, else the lifestyle of the contig was denoted as 'unassigned'. Putative bacterial host assignments for each contig were achieved using iPHoP v1.1.0[395] using the 'Sept_2021_pub' host database and default 'predict' parameters.

Quantitative analysis of the faecal virome inocula were achieved by first mapping the per sample reads passing trimming and filtering onto the final database of putative viral contigs using bowtie v2.4.5[428] in '–end-to-end' mode. Read coverage and mapping counts were then collected using SAMTools v1.15.1[429]. Spurious read mapping counts to viral contigs were eliminated from the count data by setting mapped read counts to 0 for any viral contig found to have 1x coverage over < 75% of its length. Putative viral contigs were only included in the quantitative analysis if the contig had been determined to have ≥ 50% completeness by CheckV, the number of CheckV-identified viral genes was ≥ 1, and if the number of genes classified as 'viral' by CheckV was ≥ 10% of the total gene count. For all samples, the abundance for each viral contig in a sample was estimated by normalising the number of reads mapping to a contig by the length of the contig followed by normalisation for library size via 'total-sum scaling'[430] (*i.e.*, length normalised read count / total number of reads used for mapping in a sample). Absolute viral counts were

calculated by comparing the relative abundances of normalised read counts to that for the spiked lactococcal phage Q33 contig. Gut-brain modules (GBMs) and gut-metabolic modules (GMMs) were screened for within the assembled virome sequences by first annotating viral genes using eggNOG-mapper v2.1.11 then searching the output KEGG ko against the GBM database.

Analysis of total viral sequences within the bulk metagenomic sequencing data

Quantitative analysis of the total viral sequence information within the bulk metagenomic sequencing data followed a similar process used in the analysis of viral gavage samples. Namely, reads that passed trimming and filtering by fastp for each sample were mapped to the database of putative viral contigs obtained from the gavage samples as described above. Mapping results were then converted to total-sum scaled read counts as described above. Again, only those viral contigs that passed the CheckV filtering conditions described earlier were included in read count table.

Bioinformatics and statistical analysis of microbiome data

Further data-handling of microbiome measures was undertaken in R (version 4.2.2) using the Rstudio GUI (version 2022.7.2.576).

Inter-plate biases were recalibrated using the Metacal package in R[431]. As a consequence, taxa with a minimal count of < 5 were excluded from the bacterial analysis and taxa with a prevalence of < 50% were excluded from the phage analysis as ratios are invariant to subsetting and this study employs compositional data analysis techniques[432,433]. This approach is used since phages are heterogeneously distributed among microbiomes and if

a feature is absent (or unobserved) in approximately half of samples, then inclusion in subsequent analysis greatly increases the risk of spurious associations[419]. Principal component analysis was performed on centred log-ratio transformed (clr) values. Zeroes were replaced using the 'const' approach described by Lubbe and colleagues[434]. Beta-diversity was computed in terms of Aitchison distance, or Euclidean distance between clr-transformed data, and assessed by PERMANOVA using the vegan package. Alpha-diversity was computed using the iNEXT library[435].

Differential microbial abundance was assessed using generalised linear mixed-effects models using the lme4 framework[436]. Custom functions and scripts are available online at https://github.com/thomazbastiaanssen/Tjazi. Where appropriate, post-hoc pairwise comparisons were performed using one-tailed Tukey's procedures with a *p*-value cutoff of 0.05 in addition to a *P*-value for the orthogonal restoration comparisons with a threshold of 0.05 and a Benjamini-Hochberg adjusted *q*-value cutoff of 0.2.

Restoration of microbial taxa was assessed using orthogonal contrasts in a generalized linear mixed-effects model, weighing the 'Ctr' and 'FVT Stress' group against the 'Ctr Stress' group. Figures were generated using ggplot2, ggforce and patchwork within R.

Phage epifluorescent quantification

VLPs in the FVT solution were stained with SYBR gold adapted from a previous method[437]. Briefly, the FVT solution was diluted and passed through an all-glass vacuum filter onto an Anodisc (25mm diameter, 0.02µm pore size; Whatman®) for 60sec. Then the Anodisc was stained with SYBR Gold for 20min before antifade was added and allowed to dry in the dark. Images were taken on a fluorescent upright microscope

(Olympus BX53 Upright Research Microscope, Japan) at 100x magnification and VLPs in images were quantified using a Python script (script available in supplementary materials).

Transcriptomic sequencing

Hippocampus and amygdala RNA was extracted using the mirVANA kit (Qiagen). mRNA sequencing was conducted by Source Bioscience on the Illumina NovaSeq 6000 (S4 flow cell, 150bp paired-end lane yielding 2.5 billion read pairs). Reference genome of obtained sequences was performed using the reference annotation: *Mus musculus* (organism), GRCm38, UCSC, genome browser (GRCm38.p6), Ensemble[438]. Reads were assessed and filtered for quality using fastqc using default parameters. Genes were annotated and counted using kallisto[439] using default parameters.

Differential gene expression and GO term enrichment analyses

Further handling of transcriptomic data was undertaken in R (version 4.2.2) using the Rstudio GUI (version 2022.7.2.576). Principal component analysis was performed on centred log-ratio transformed (clr) values. Zeroes were replaced using the 'const' approach described by Lubbe and colleagues[434]. Differences in overall gene expression was computed in terms of Aitchison distance (Euclidean distance between clr-transformed data) and assessed by PERMANOVA using the vegan package.

Differential gene expression was assessed using generalised linear models using the base R stats lm framework. Custom functions and scripts are available online at https://github.com/thomazbastiaanssen/Tjazi[440,441]. Before statistical testing,

hippocampal gene transcripts were filtered by variance using the genefilter library in R[442], with 0.5 set as the cutoff. Restoration of gene expression was assessed using orthogonal contrasts in a generalized linear model, weighing the 'Ctr' and 'FVT Stress' group against the 'Ctr Stress' group for the hippocampus and amygdala individually.

In order to assess whether the subset of genes that altered by stress and restored to control levels post FVT, we employed the enrichR framework[443] on the Gene Ontology (GO) database[444]. In parallel, we identified seven terms in the gene ontology database that corresponded with the objectives of the study design. These seven terms were additionally assessed for enrichment using the base R stats phyper implementation of the hypergeometric test. Figures were generated using ggplot2 and patchwork within R.

Statistical analyses

16S rRNA, metagenomic and transcriptomic data were analysed using R, and remaining statistical analyses were carried out using SPSS version 28. Measurements were taken from distinct samples and not measured repeatedly, in outputs where multiple technical replicates were performed (*e.g.* corticosterone and inflammatory cytokine analysis) the mean per individual was used. The restoration effect of features by FVT altered by stress was analysed by planned orthogonal contrast (*P*), followed by Benjamini-Hochberg's adjusted false discovery rate (BH-FDR) of the calculated *P*-value (*q*), and Tukey's post hoc (*p*; pairwise comparison of Ctr-Ctr Stress, followed by comparison of Ctr Stress-FVT Stress). For the phage-host network (Fig.S5) the Anansi package[445] was used whereby data was compared using linear models followed by BH-FDR and Pearson's correlation coefficient to plot the phage-host pairs. Unless otherwise noted, significant effects are

denoted by: *p<0.05, **p<0.01, ***p<0.001, and †q<0.2. Technical outliers were removed prior to statistical analyses (*e.g.*, animals that did not complete tests, samples not available for assays, values outside limits of detection, *etc.*). Values that were 2.5 standard deviations from the mean were considered statistical outliers and excluded from the related analyses (maximum of 2 statistical outliers per test). Data distribution was assumed to be normal, but this was not formally tested. Analyses were conducted in a manner blinded to the experimenter.

Data availability

Metagenomic sequencing data can be found in Sequence Read Archive (SRA) NCBI under BioProject accession PRJNA970614. Transcriptomic sequencing data can be found in European Nucleotide Archive (ENA) under accession PRJEB67706. 16S rRNA sequencing data can be found in the supplementary material. Source data that support the findings of this study are available from the corresponding author upon request.

Code availability

The scripts used for processing and generating the 16S rRNA, metagenomic, and transcriptomic sequencing data sets are available in the extended data section. Additional material describing the microbiome conceptual bioinformatic approaches used in this study can be found here[440,441].

Acknowledgements

The authors would like to thank Drs. K.J. O'Riordan, A. Lavelle, P. Zizka, M. Schverer, O.W. Bayfield, A. Golubeva, S. Stockdale, A. Clooney, and R. Cabrera-Rubio for their technical assistance in the study, and P. Fitzgerald, C. Manley, and J. O'Rielly for their assistance with mouse husbandry. APC Microbiome Ireland is a research centre funded by Science Foundation Ireland (SFI), through the Irish Governments' national development plan (grant no. 12/RC/2273_P2). The authors acknowledge the use of the APC Microbiome Ireland Flow Cytometry Platform. A.N.S. was supported by a Wellcome Trust Research Career Development Fellowship [220646/Z/20/Z], and the European Research Council (ERC) under the European Union's Horizon 2020 research and innovation programme (grant agreement No 101001684).

Author contributions

N.L.R., L.A.D, V.L.P, A.N.S., G.M.M., T.G.D, C.H., and J.F.C. designed the studies. N.L.R. and V.L.P. performed the experiments with animals. N.L.R., L.A.D., V.L.P. M.v.d.W., K.V., C.F., K.E.G, A.B, and M.D. performed assays, sample collection, and processing. T.F.S.B., L.A.D., C.T., V.L.P., H.H., M.D., F.C., and P.C. generated metagenomic and virome sequencing analyses. T.F.S.B. and G.M.M. generated transcriptomic analyses. N.L.R. and T.F.S.B. analysed the data. N.L.R. and J.F.C. wrote the paper with contributions made from all the authors. Illustrations were adapted, in part, using graphics created with BioRender.com (YW260Q7D5T), Servier Medical Art, and Inkscape Project.

Competing interests

The authors declare no competing interests.

2.6 Supplementary Figures

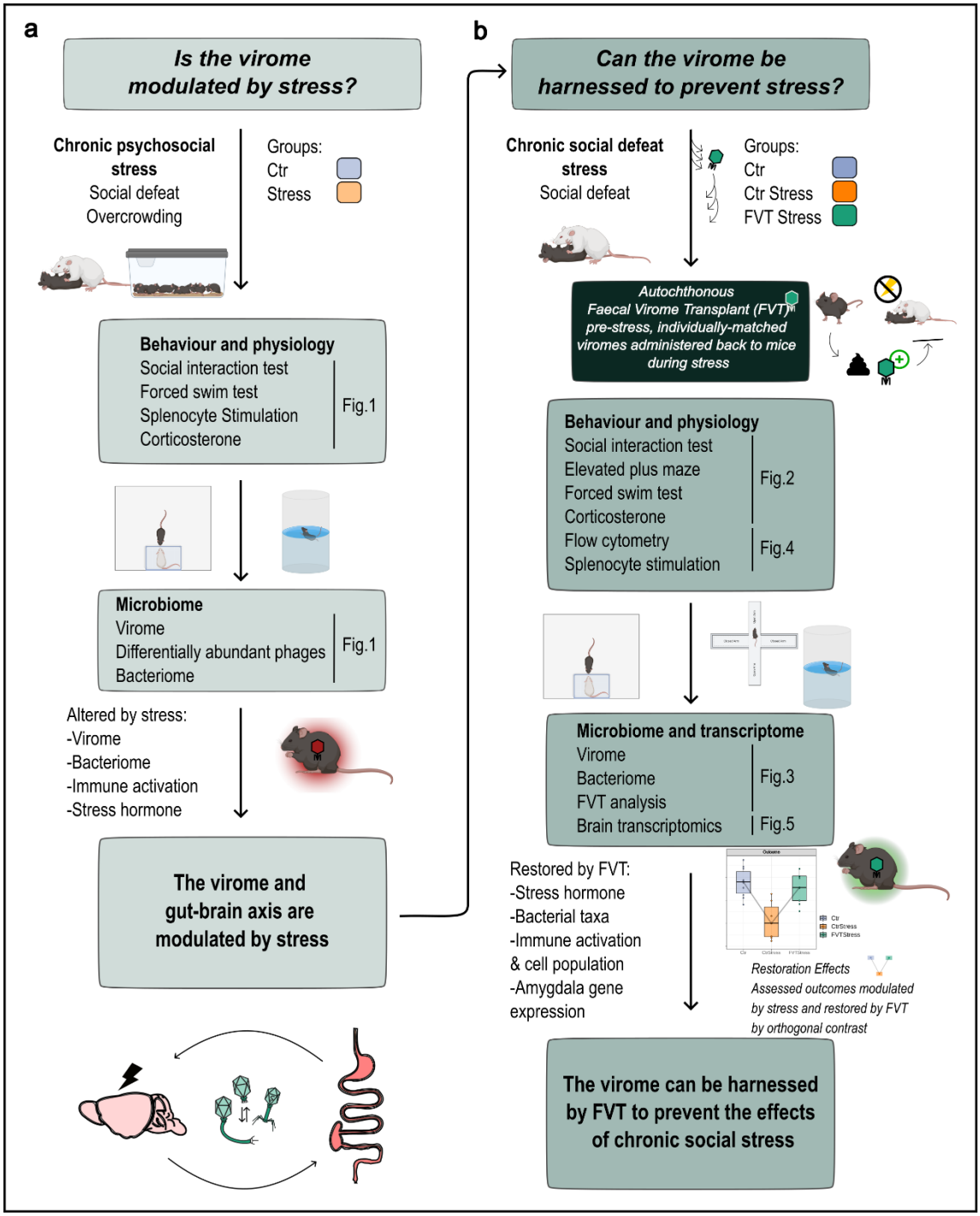


Fig. S1. Study workflow summary.

*(**a**) First, to answer whether the gut virome is affected by stress we assessed behaviour, physiology, and microbiome alterations following chronic psychosocial stress. (**b**) Then, to determine if the virome can be harnessed to prevent stress, we administered an autochthonous faecal virome transplant (FVT) treatment to mice as they underwent stress and found that the FVT attenuated stress effects on behaviour, physiology, microbiome, and brain transcriptomics.*

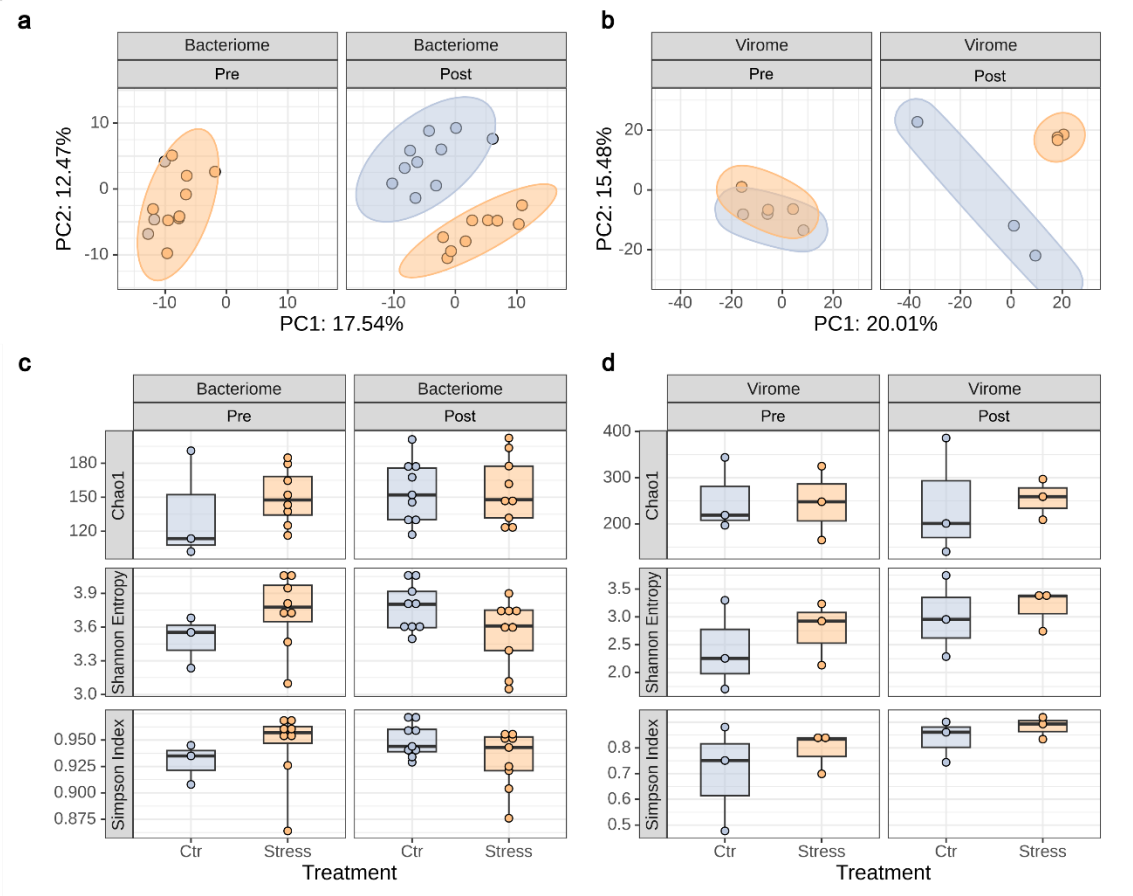


Fig. S2. Before and after chronic psychosocial stress microbiome comparisons.

*(**a**) Bacteriome Aitchison beta diversity measures before (Pre) and after (Post) chronic psychosocial stress, no differences were found in Pre, however there was a significant alteration found in Post assessed by PERMANOVA (R2=0.1693, p<0.01) (n=10 Ctr, pooled in 3 in Pre timepoint; n=9 Stress). (**b**) Virome Aitchison beta diversity measures before (pre) and after (post) chronic psychosocial stress, no differences were found in Pre, however there was a trend for alteration found in Post assessed by PERMANOVA (R2=0.3011, p=0.1) (n=10 Ctr pooled in 3; n=10 Stress pooled in 3). (**c**) Bacteriome alpha diversity measures (Chao1, Shannon Entropy, and Simpson Index), no significant*

*differences were found Pre or Post assessed by independent-samples two-sided T test (n=10 Ctr, pooled in 3 in Pre timepoint; n=9 Stress). (**d**) Virome alpha diversity measures (Chao1, Shannon Entropy, and Simpson Index), no significant differences were found Pre or Post assessed by independent-samples two-sided T test (n=10 Ctr pooled in 3; n=10 Stress pooled in 3). Data presented as box plots display the minimum, first quartile, median, third quartile, and maximum.*

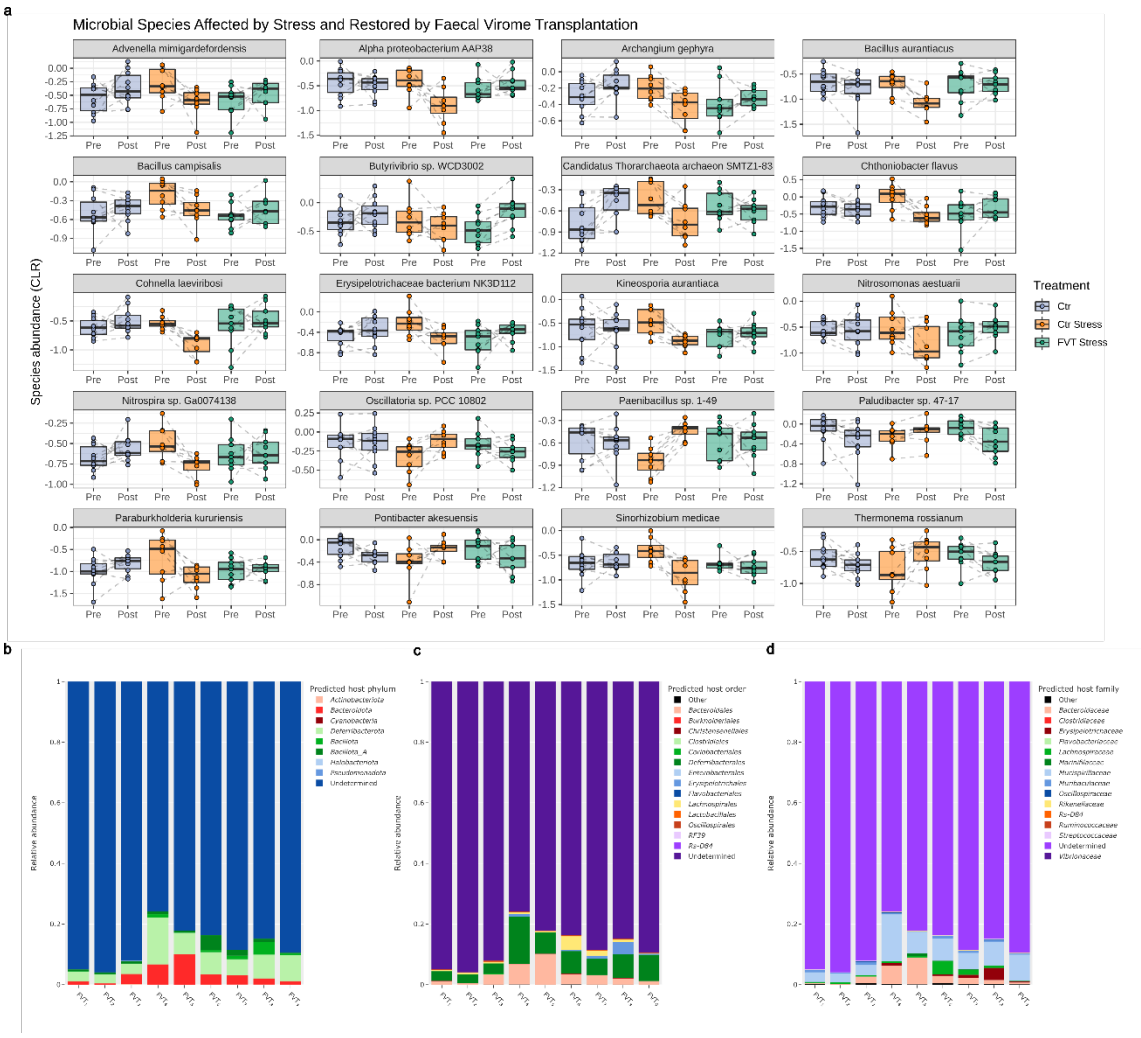


Fig. S3. Bacterial species altered by stress and restored by FVT and predicted host taxa of FVT inocula.

*(**a**) Differentially abundant bacterial species affected by stress and restored by FVT before (pre) and after (post) study compared by a linear mixed effects model followed by Storey's FDR testing (Ctr n=10, Ctr Stress n=8, FVT Stress n=9). (b-d) Predicted phage hosts of FVT inocula at phyla (**b**), order (**c**), and family levels (**d**) (FVT Stress n=9). Data*

presented as box plots display the minimum, first quartile, median, third quartile, and maximum.

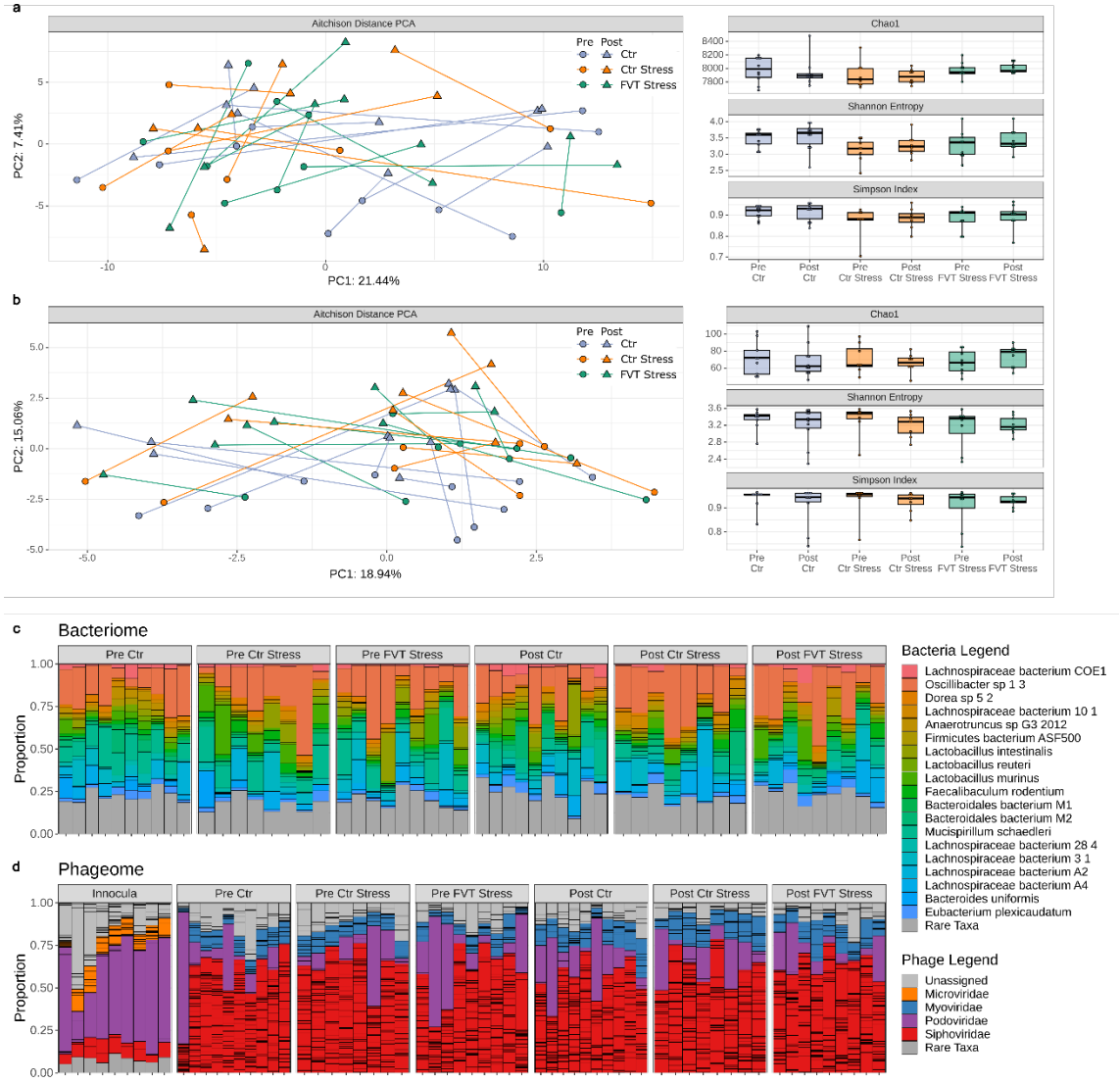


Fig. S4. Diversity and community microbiome measures following chronic stress and FVT.

*(**a**, **b**) Aitchison beta diversity distance, Shannon entropy, and Simpson index of bacteriome (**a**) and virome (**b**) (Ctr n=10, Ctr Stress n=8, FVT Stress n=9). (**c**, **d**) Faecal bacteriome (**c**) and FVT inocula and faecal virome (**d**) community profiles (Ctr n=10, Ctr Stress n=8, FVT Stress n=9). Data presented as box plots display the minimum, first quartile, median, third quartile, and maximum.*

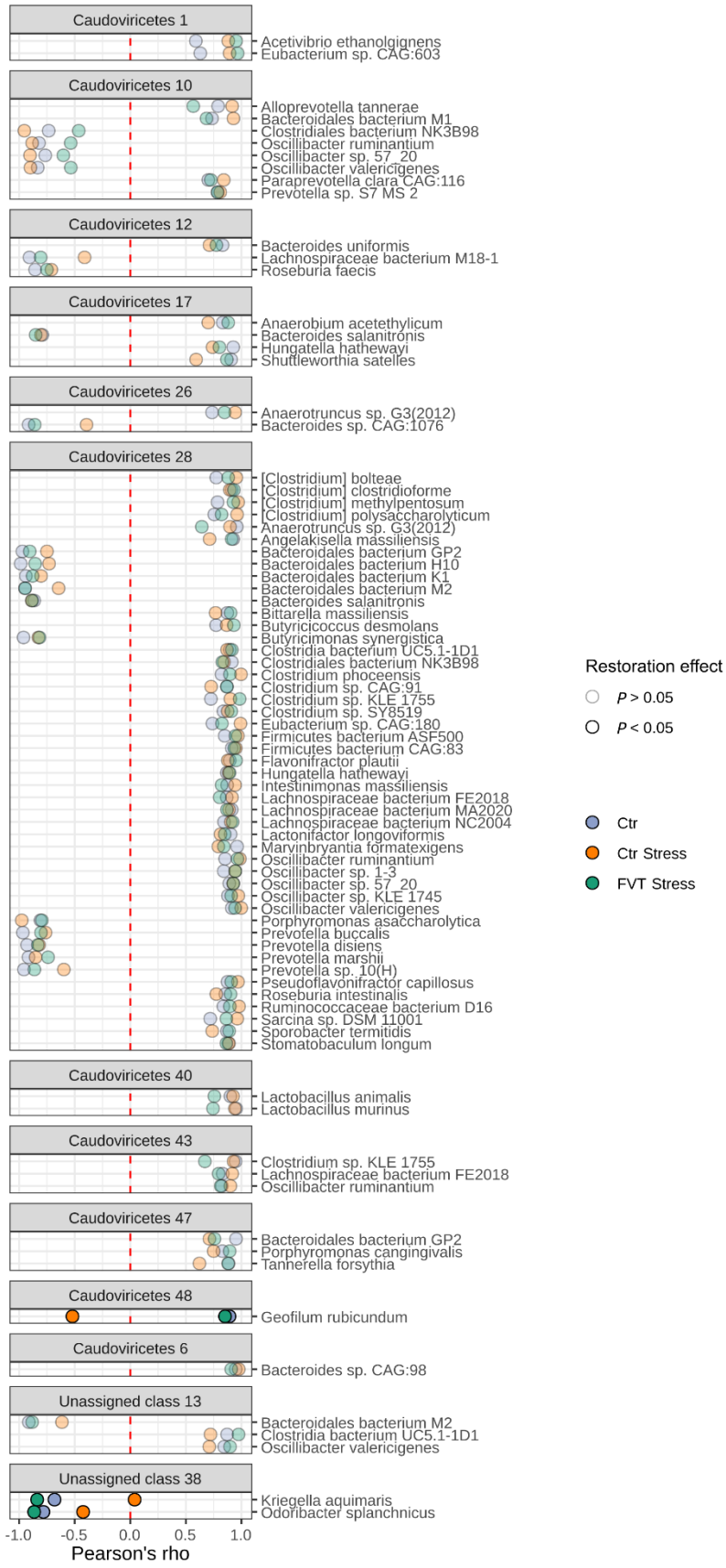
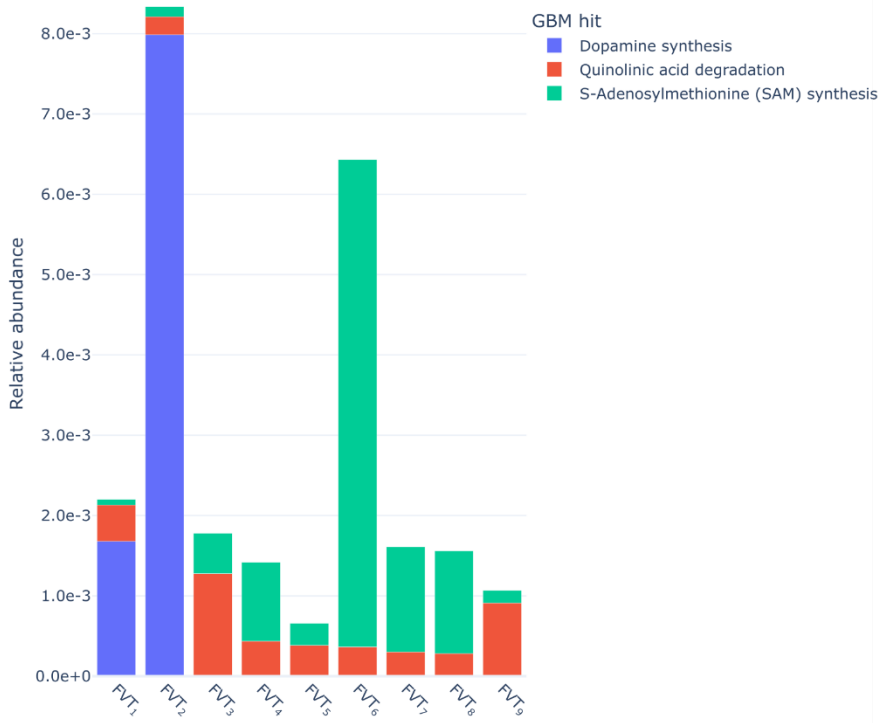

Caudoviricetes 1
Acetivibrio ethanolgignens
Eubacterium sp. CAG:603
Caudoviricetes 10
Alloprevotella tannerae
Bacteroidales bacterium M1
Clostridiales bacterium NK3B98
Oscillibacter ruminantium
Oscillibacter sp. 57_20
Oscillibacter valericigenes
Paraprevotella clara CAG:116
Prevotella sp. S7 MS 2
Caudoviricetes 12
Bacteroides uniformis
Lachnospiraceae bacterium M18-1
Roseburia faecis
Caudoviricetes 17
Anaerobium acetethylicum
Bacteroides salanitronis
Hungatella hathewayi
Shuttleworthia satelles
Caudoviricetes 26
Anaerotruncus sp. G3(2012)
Bacteroides sp. CAG:1076
Caudoviricetes 28
[Clostridium] bolteae
[Clostridium] clostridioforme
[Clostridium] methylpentosum
[Clostridium] polysaccharolyticum
Anaerotruncus sp. G3(2012)
Angelakisella massiliensis
Bacteroidales bacterium GP2
Bacteroidales bacterium H10
Bacteroidales bacterium K1
Bacteroidales bacterium M2
Bacteroides salanitronis
Bittarella massiliensis
Butyricicoccus desmolans
Butyricimonas synergistica
Clostridia bacterium UC5.1-1D1
Clostridiales bacterium NK3B98
Clostridium phoceensis
Clostridium sp. CAG:91
Clostridium sp. KLE 1755
Clostridium sp. SY8519
Eubacterium sp. CAG:180
Firmicutes bacterium ASF500
Firmicutes bacterium CAG:83
Flavonifractor plautii
Hungatella hathewayi
Intestinimonas massiliensis
Lachnospiraceae bacterium FE2018
Lachnospiraceae bacterium MA2020
Lachnospiraceae bacterium NC2004
Lactonifactor longoviformis
Maryinbryantia formatexigens
Oscillibacter ruminantium
Oscillibacter sp. 1-3
Oscillibacter sp. 57_20
Oscillibacter sp. KLE 1745
Oscillibacter valericigenes
Porphyromonas asaccharolytica
Prevotella buccalis
Prevotella disiens
Prevotella marshii
Prevotella sp. 10(H)
Pseudoflavonifractor capillosus
Roseburia intestinalis
Ruminococcaceae bacterium D16
Sarcina sp. DSM 11001
Sporobacter termitidis
Stomatobaculum longum
Caudoviricetes 40
Lactobacillus animalis
Lactobacillus murinus
Caudoviricetes 43
Clostridium sp. KLE 1755
Lachnospiraceae bacterium FE2018
Oscillibacter ruminantium
Caudoviricetes 47
Bacteroidales bacterium GP2
Porphyromonas cangingivalis
Tannerella forsythia
Caudoviricetes 48
Geofilum rubicundum
Caudoviricetes 6
Bacteroides sp. CAG:98
Unassigned class 13
Bacteroidales bacterium M2
Clostridia bacterium UC5.1-1D1
Oscillibacter valericigenes
Unassigned class 38
Kriegella aquimaris
Odoribacter splanchnicus
-1.0
-0.5
0.0
0.5
1.0
Pearson's rho
Restoration effect
P > 0.05
P < 0.05
Ctr
Ctr Stress
FVT Stress

Fig. S5. Phage-host network.

Bacteriophage and bacterial abundance significant associations (q<0.1). Phage-host pair associations that have a significant restoration effect are fully opaque (P<0.05). Data was compared using two-sided linear models followed by Benjamini & Hochberg's procedure for FDR and Pearson's correlation coefficient to plot the phage-host pairs.

a


GBM hit
Dopamine synthesis
Quinolinic acid degradation
S-Adenosylmethionine (SAM) synthesis
Relative abundance
8.0e-3
7.0e-3
6.0e-3
5.0e-3
4.0e-3
3.0e-3
2.0e-3
1.0e-3
0.0e+0
FVT1
FVT2
FVT3
FVT4
FVT5
FVT6
FVT7
FVT8
FVT9

b

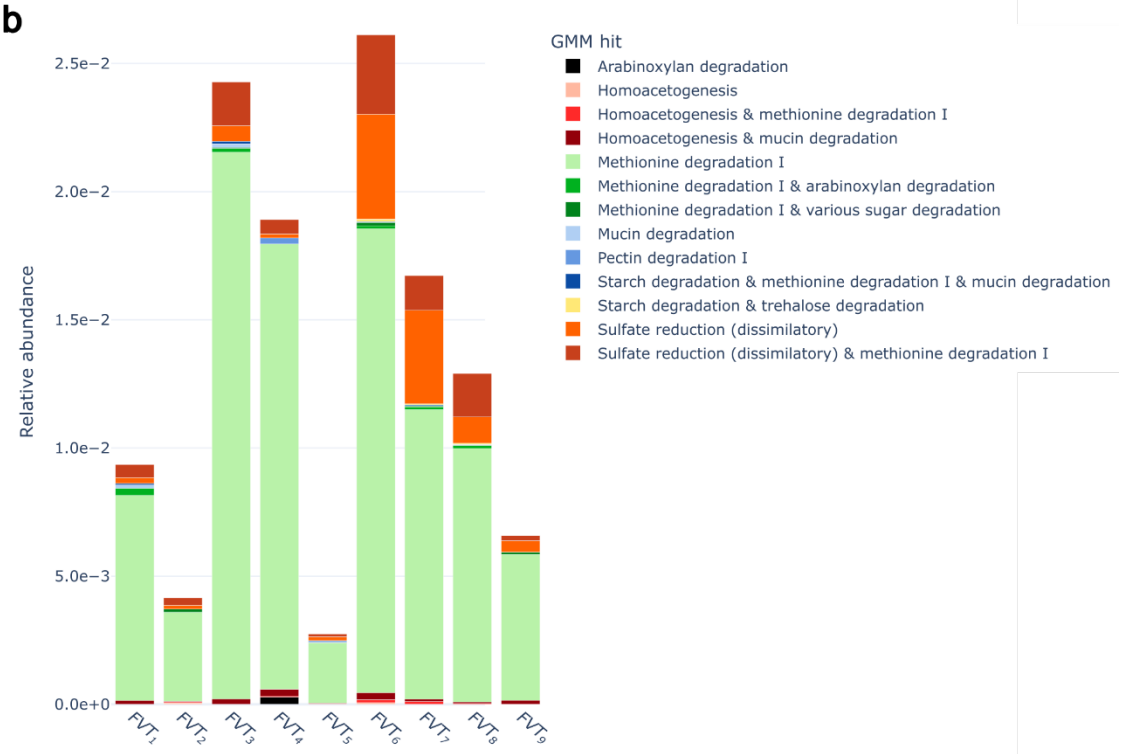

GMM hit
Arabinoxylan degradation
Homoacetogenesis
Homoacetogenesis & methionine degradation I
Homoacetogenesis & mucin degradation
Methionine degradation I
Methionine degradation I & arabinoxylan degradation
Methionine degradation I & various sugar degradation
Mucin degradation
Pectin degradation I
Starch degradation & methionine degradation I & mucin degradation
Starch degradation & trehalose degradation
Sulfate reduction (dissimilatory)
Sulfate reduction (dissimilatory) & methionine degradation I
Relative abundance
2.5e−2
2.0e−2
1.5e−2
1.0e−2
5.0e−3
0.0e+0
FVT1
FVT2
FVT3
FVT4
FVT5
FVT6
FVT7
FVT8
FVT9

Fig. S6. FVT inocula gut-brain and gut-metabolic modules.

*Faecal virome transplant (FVT) inocula were assessed for gut-brain module (GBM) and gut-metabolic module (GMM) functional carriage. (**a**) The GBMs found in the FVT inocula were dopamine synthesis, quinolinic acid degradation, and S-adenosylmethionine (SAM) synthesis. (**b**) The GMMs found in the FVT inocula were arabinoxylan degradation, homoacetogenesis, methionine degradation I, mucin degradation, pectin degradation I, starch degradation, and sulfate reduction (dissimilatory).*

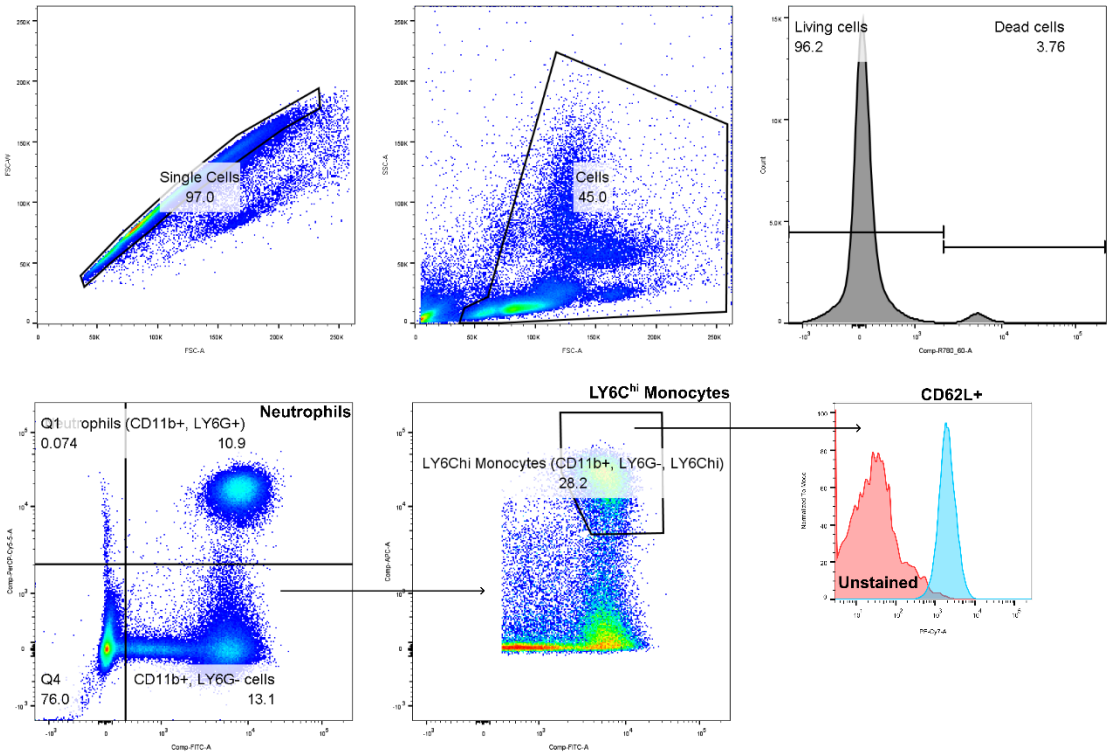


Fig. S7 Immune cell flow cytometry gating strategy.

A panel of whole blood markers was used to assess circulating immune cell populations on the FACSCelesta. This approach enabled initial gating for singlets, followed by the selection of the peripheral blood mononuclear cells, and live cells (using FVS780). Neutrophils were selected based on LY6G+ (PerCP-Vio700-conjugated) and CD11b+ (FITC-conjugated) . Monocytes were selected as being Ly6G−, CD11b+ and LY6C^{hi} (APC-conjugated), after which CD62L+ cells (Pe-Cy7-conjugated) were quantified.

Table S1. Inflammatory cytokine and circulating immune cell population data.

*(**a**) Chronic social stress (Stress) and control (Ctr) inflammatory cytokine data measured in splenocyte stimulation supernatants collected and stimulated at end of study. Mean data presented with independent-samples two-sided T test (*p<0.05, #p<0.1) (Ctr n=10, Stress n=10). (**b**) Inflammatory cytokine data from basal plasma and splenocyte cultures for control (Ctr), chronic social stress (Stress), and stress with faecal virome transplant (FVT Stress) groups. (**c**) Circulating immune cell population data from basal plasma and 45min post stress for Ctr, Stress, and FVT Stress groups. Mean data presented with Tukey's post hoc sequential two-sided pairwise comparison between Stress and other groups (***p<0.001, **p<0.01, *p<0.05, #p<0.1). Benjamini-Hochberg adjusted orthogonal stress effect (q). Flow cytometry mean data 45-min post stress is additionally tested by paired-sample T-test to basal data (†††p<0.001, ††p<0.01, †p<0.05, ‡p<0.1) (n=6-10 per group for each measure).*

a

Splenocyte Stimulations

Inflammatory Cytokines (pg/ml)	Vehicle		ConA		LPS	
	Ctr	Stress	Ctr	Stress	Ctr	Stress
TNF-α	5.00	6.07	177.20	215.80	91.59	124.0
IL-1β	0.49	0.55	1.75	2.57	3.48	4.6
IL-6	20.38	26.92	189.50	307.90*	875.40	1209.00#
IL-10	3.74	4.67	13.86	21.10*	124.70	155.70

b

	Splenocyte Stimulations									Blood Plasma		
	Vehicle			ConA			LPS			Basal		
Inflammatory Cytokines (pg/ml)	Ctr	Stress	FVT Stress	Ctr	Stress	FVT Stress	Ctr	Stress	FVT Stress	Ctr	Stress	FVT Stress
TNF-α	34.4	102.0#	27.9#	1696	2038	1406	1684	1420	1549	17.6	15.9	13.0
IFN-γ	0.44	0.29	0.32	458.7	1747	841.1	201.7	716.4	1884	0.64	0.78	0.94
IL-6	72.6	85.4	66.6#	2673	3573	2051*	12991	14180	15353	24.8	31.4	-
IL-12/IL-23p40	139.9	192.8#	136.9#	139.4	207.6	180.7	231.4	264.3	301.2	1076	837.5	840.7
IP-10	50.7	69.3	28.7	5361	5007	5241	5543	4958	6927	148.9	256.1#	146.9#

c

Flow Cytometry

Immune cell populations Percent of parent population	Basal			45 min post stress		
	Ctr	Stress	FVT Stress	Ctr	Stress	FVT Stress
LY6C^{hi} Monocytes (CD11b^{+}, LY6G^{-}, LY6C^{hi})	4.38	2.35*	3.91	2.47†	2.37*	2.75#‡
CD62L^{+} LY6C^{hi} Monocytes	61.4	59.6	75.5***	71.1‡	73.7†	75.4#
MHC-II^{+} LY6C^{hi} Monocytes	4.62	2.13***	2.25	2.68†††	1.14#††	1.56†
Neutrophils (CD11b^{+}, LY6G^{+})	18.0	9.27*	14.0	23.5†	20.7*†††	22.1†††
CD62L^{+} Neutrophils	55.2	54.6	53.0	61.3	62.3‡	53.4
MHC-II^{+} Neutrophils	1.50	1.43	0.98	0.53††	0.65††	0.73*
T helper cells (CD4^{+})	12.7	11.6	12.1	12.8	13.4**†	13.5‡
CD44^{hi} T helper cells	7.92	7.18	8.58#	6.75††	7.64	8.50
CD69^{+} T helper cells	1.52	2.43**	2.28	3.40	2.75	4.09‡

Table S2. FVT gut-brain modules.

The faecal bacteriome was assessed for carriage of gut-brain modules (GBMs) at the end of the study. The restoration effect was measured for each GBM altered by stress and restored by FVT by linear models (p-value) and Storey's false discovery rate was performed for all measures (q-value).

Gut-Brain Modules		
	Restoration Effect	
GBM	*p*	*q*
ClpB (ATP-dependent chaperone protein)	0.008773839	0.317968219
S-Adenosylmethionine (SAM) synthesis	0.013824705	0.317968219
Nitric oxide synthesis I (NO synthase)	0.058803157	0.682088395
Acetate synthesis I	0.066308307	0.682088395
Quinolinic acid degradation	0.074140043	0.682088395
GABA degradation	0.118651693	0.779009796
Inositol degradation	0.142021899	0.779009796
Isovaleric acid synthesis II (KADC pathway)	0.168188954	0.779009796
DOPAC synthesis	0.17291172	0.779009796
p-Cresol synthesis	0.19012192	0.779009796
Inositol synthesis	0.194350303	0.779009796
Dopamine synthesis	0.215440522	0.779009796
17-beta-Estradiol degradation	0.220154942	0.779009796
Glutamate synthesis I	0.277038963	0.800058766
Propionate synthesis II	0.288975947	0.800058766
Propionate synthesis III	0.294849146	0.800058766
Quinolinic acid synthesis	0.296510144	0.800058766
Nitric oxide synthesis II (nitrite reductase)	0.365925475	0.800058766
Butyrate synthesis II	0.369681956	0.800058766
GABA synthesis II	0.380191762	0.800058766
Tryptophan synthesis	0.394949751	0.800058766
Propionate degradation I	0.405075101	0.800058766
GABA synthesis III	0.409058921	0.800058766
Kynurenine synthesis	0.417421965	0.800058766
Menaquinone synthesis (vitamin K2) II (alternative pathway: futalosine pathway)	0.481993941	0.810041562
Glutamate degradation II	0.487333126	0.810041562
Butyrate synthesis I	0.507401226	0.810041562
Isovaleric acid synthesis I (KADH pathway)	0.516029147	0.810041562
Acetate synthesis IV	0.523423263	0.810041562
GABA synthesis I	0.528287975	0.810041562
Dopamine degradation	0.555789624	0.824720087
Histamine degradation	0.636450845	0.914898089
Glutamate degradation I	0.686481745	0.94383984
Glutamate synthesis II	0.697620751	0.94383984
Acetate degradation	0.767212997	0.948787438
Acetate synthesis II	0.78791645	0.948787438
Acetate synthesis III	0.792452387	0.948787438

Table S3. FVT gut-metabolic modules.

The faecal bacteriome was assessed for carriage of gut-metabolic modules (GMMs) at the end of the study. The restoration effect was measured for each GMM altered by stress and restored by FVT by linear models (p-value) and Storey's false discovery rate was then performed for all measures (q-value).

Gut-Metabolic Modules		
	Restoration Effect	
GMM	*p*	*q*
alanine degradation II	0.010306	0.489963
glycine degradation	0.016662	0.489963
cysteine degradation I	0.038126	0.489963
glycolysis (preparatory phase)	0.048755	0.489963
melibiose degradation	0.089611	0.489963
4-aminobutyrate degradation	0.099229	0.489963
xylose degradation	0.107153	0.489963
mucin degradation	0.11046	0.489963
arginine degradation I	0.127518	0.489963
glycerol degradation III	0.133433	0.489963
fucose degradation	0.137017	0.489963
aspartate degradation II	0.164606	0.489963
arginine degradation V	0.164822	0.489963
glyoxylate bypass	0.183752	0.489963
trehalose degradation	0.186747	0.489963
urea degradation	0.189385	0.489963
nitrate reduction (dissimilatory)	0.192476	0.489963
arginine degradation III	0.200253	0.489963
ethanol production I	0.211651	0.489963
mannose degradation	0.212521	0.489963
ethanol production II	0.233931	0.489963
alanine degradation I	0.243362	0.489963
propionate production II	0.245139	0.489963
aspartate degradation I	0.246817	0.489963
lactate consumption II	0.248919	0.489963
pentose phosphate pathway (non-oxidative branch)	0.250257	0.489963
arabinoxylan degradation	0.252814	0.489963
cysteine degradation II	0.263711	0.489963
tyrosine degradation I	0.264442	0.489963
succinate production	0.266326	0.489963
acetyl-CoA to crotonyl-CoA	0.274638	0.489963
galacturonate degradation I	0.278466	0.489963
histidine degradation	0.278534	0.489963
methionine degradation I	0.280417	0.489963
proline degradation	0.282483	0.489963
threonine degradation I	0.298996	0.489963
lactose and galactose degradation	0.319196	0.489963

Chapter 3

Social Fear Extinction Susceptibility is Associated with Microbiota-Gut-Brain Axis Alterations

Nathaniel L Ritz[1,2], Thomaz FS Bastiaanssen[1,2], Caitlin SM Cowan[1†], Linda Smith[1,3], Nigel Theune[1], Marta Brocka[1], Gerard M Moloney[1,2], Andrey N Shkoporov[1,3], Lorraine A Draper[1,3], Colin Hill[1,3], Timothy G Dinan[1,4], David A Slattery[5], John F Cryan[1,2*]

[1]APC Microbiome Ireland, University College Cork, Cork, Ireland T12YT20
[2]Dept. of Anatomy and Neuroscience, University College Cork, Cork, Ireland T12YT20
[3]School of Microbiology, University College Cork, Cork, Ireland T12K8AF
[4]Dept. of Psychiatry and Neurobehavioural Science, University College Cork, Cork, Ireland T12YT20
[5]Dept. of Psychiatry, Psychosomatics and Psychotherapy, University Hospital Frankfurt, Frankfurt, Germany 60528

Submitted for publication to *Brain, Behavior, and Immunity*

3.1 Abstract

Social anxiety disorder is a common psychiatric condition that severely affects individual quality of life and is a significant societal burden. Although many risk factors for social anxiety exist, it is currently unknown how social fear sensitivity manifests biologically. Furthermore, since some individuals are resilient and others are susceptible to social fear, it is important to interrogate the mechanisms underpinning individual response to social fear situations. The microbiota-gut-brain axis has been associated with social behaviour, has recently been linked with social anxiety disorder, and may serve as a therapeutic target for modulation. Here, we assess the potential of this axis to be linked with social fear extinction processes in a murine model of social anxiety disorder. To this end, we correlated differential social fear responses with microbiota composition, central gene expression, and immune responses. Our data provide evidence that microbiota variability is strongly correlated with alterations in social fear behaviour. Moreover, we identified altered gene candidates by amygdalar transcriptomics that are linked with social fear sensitivity. These include genes associated with social behaviour (*Armcx1*, *Fam69b*, *Kcnj9*, *Maoa*, *Met*, *Serinc5*, *Slc6a17*, *Spata2*, and *Syngr1*), inflammation and immunity (*Cars*, *Ckmt1*, *Klf5*, *Maoa*, *Map3k12*, *Met*, *Pex5*, *Serinc5*, *Sidt1*, *Spata2*), and microbe-host interaction (*Klf5*, *Map3k12*, *Serinc5*, *Sidt1*). Together, these data provide further evidence for a role of the microbiota-gut-brain axis in social fear responses.

3.2 Introduction

Social anxiety disorder (SAD) is a heterogeneous psychiatric condition defined by fear and avoidance of social scenarios due to the preconception of possible scrutiny by others[324]. Like other anxiety disorders, SAD can manifest in different intensities and symptoms. Although it is commonplace for many to experience fear or anxiety of specific social situations, individuals with SAD typically have a stronger response to negative stimuli that may trigger their anxiety in a manner they are unable to effectively cope with[446]. Research into SAD is sparse compared to other psychiatric disorders and more specific therapeutics are needed that target the underlying neurobiology as opposed to minimizing the symptoms, such as SSRIs. While cognitive behavioural therapy has proven to be an effective option for long-term treatment of SAD there is a need for novel treatment directions and options[447].

The gut microbiota has been increasingly associated with social behaviour and has been shown to be capable of modulating a variety of social interactions across the animal kingdom[313]. Previously, stress has been shown to incur social deficits restored by gut microbiota administration and specifically associated with *Enterococcus faecalis* introduction[320]. Resilience to chronic social defeat stress has been linked with corticotrophin-releasing factor expression in the brain and immune cells in circulation[410]. Microbiota volatility, or stress-induced changes in microbiota composition over time, was elevated in individuals with higher stress markers in humans and mice[352]. Such volatility was also associated with resilience and susceptibility to behavioural response in a post-traumatic stress model[448]. These data indicate that the microbiota is involved in social

behaviour[313] and resilience to various stressors, suggesting that social fear response is also likely sensitive to microbiota composition. The microbiota-gut-brain axis, which describes the multidirectional influence of these systems on one another, is one such potential therapeutic target for SAD. Previously we have shown that the gut microbial community is altered in individuals with SAD[274] and that microbiota transfer from individuals with SAD to mice increases social fear sensitivity (Ritz et al., *in press*). However, the underlying etiology of how some individuals are predisposed to heightened social fear and anxiety is unclear, especially after a social stressor.

There is a wide range of individual responses to different stressors, and indeed stress resilience is a phenomenon driven by multiple systems, including the immune, endocrine, and central nervous systems[410,449,450]. To develop novel diagnostic and therapeutic options, it is advantageous to identify factors that are associated with social fear resilience and elimination in addition to understanding what may predispose some individuals to increased sensitivity and susceptibility to social anxiety. Herein, we have adapted the validated social fear conditioning paradigm[336,451], a preclinical murine model of SAD, to untreated (*i.e.*, control) mice and stratified them dependent on their social behaviour measured during extinction to further explore the biological underpinnings of social fear.

3.3 Methods

Animals

This study used male C57Bl/6J mice (*N*=48; 8 weeks of age on arrival; Envigo). Animals were habituated for 2 weeks after which treatments began. The holding room was under a 12-hour light/dark cycle (7:00-19:00), with a temperature of 21ºC and humidity of 10%. Standard rodent chow (Teklad Global 18% Protein Rodent Diet, sterilised) and water were available *ad libitum* throughout the experiments. To determine probable effect sizes for the behavioural readout as a consequence of social fear conditioning an examination of the literature, our publications, and in-house data were carried out. Procedures for the study took place over 3 days: on day 1, mice underwent social fear conditioning; on day 2, social fear extinction took place immediately followed by faecal pellet collection for microbiota analysis; on day 3, animals were euthanised by rapid decapitation and tissues were collected for secondary analyses. All procedures involving animals were conducted in accordance with the European Directive 2010/63/EC, the requirements of the S.I. No 543 of 2012 and approved by the Animal Experimentation Ethics Committee of University College Cork and the Health Products Regulatory Authority (HPRA AE19130 P118).

Social fear conditioning

Social fear learning and social fear extinction were assessed in the social fear conditioning (SFC) test (Fig.1f,g)[451]. One week before SFC, mice were singly housed and continued to be for the remainder of the study. The SFC paradigm consisted of a single conditioning

session on the first day, followed by a single extinction session on the following day. The conditioning chamber consisted of a transparent box (29x25x25cm) enclosed in a wooden chamber to reduce external noise and visual stimulation. The floor consisted of a removable stainless-steel grid connected to a shock delivery unit used for manual application of foot shocks. A video camera positioned above the chamber enabled recording.

During conditioning, mice were placed in the conditioning chamber with an empty wire mesh cage (10x8x7cm) placed in a corner as a non-social stimulus. Mice were allowed to freely explore the chamber and the non-social stimulus for 3min, then it was replaced by an identical cage containing a novel conspecific (the social stimulus). After 2s of interaction (defined by sniffing of the social stimulus), the experimental mouse was manually administered a 1s electric foot shock (0.6mA). This was repeated each time the experimental animal returned to interact with the social stimulus. When no further social contact was made for a 2min period, mice were returned to their home cage. The first social contact and food shock occurred within 30s for all experimental mice, and all mice received between 1- and 5-foot shocks over a maximum 5min interval. Locomotor activity, as measured by distance traveled during habituation, and the time mice spent investigating the non-social stimulus, as a pre-conditioning measure of anxiety, were analysed using an automated tracking program (Ethovision 11.5, Noldus, the Netherlands). Wire mesh cages were cleaned with Trigene disinfectant between each extinction session.

On the next day, social fear extinction (SFE) was assessed in the home cage of each experimental mouse. There was a total of 9 trials in the extinction session, each consisting of a 3min exposure to a social or non-social stimulus (placed on a short wall of the home cage), with a 3min inter-trial interval. For the first 3 trials, experimental mice were exposed to three non-social stimuli identical to the cage used during conditioning. Then mice were exposed to six novel conspecifics (social stimuli) enclosed within the wire mesh cages. To reduce conditioned fear responses to the non-social stimulus, a clean wire mesh cage was placed in the home cage overnight between conditioning and extinction days. Wire mesh cages were cleaned with 70% ethanol between each extinction session. Stimulus investigation, defined as time spent interacting within 7cm of social stimulus, was analysed using an automated tracking program (Ethovision 11.5, Noldus, the Netherlands) and assessed as a readout of social fear during each trial of extinction.

Mice were stratified into 3 groups, Control Extinction (Con. Ext.), Resilient Extinction (Res. Ext.), or Susceptible Extinction (Sus. Ext.) dependent on their social investigatory behaviour measured during SFE. The stratification threshold for Con. Ext. versus Res. Ext. was determined by the experimental mouse spending less than 60% of the time during the 2nd trial in social investigation (Fig. 1a). The stratification threshold for Con. Ext. versus Sus. Ext. was determined by the experimental mouse scoring a total extinction investigation time less than 50% (Fig. 1b).

Corticosterone stress marker

Corticosterone quantification of plasma samples (10µl) collected during euthanasia was performed using a corticosterone ELISA and carried out according to manufacturer's

guidelines (catalogue no. ADI-901-097, Enzo Life Sciences, Invitrogen, USA). Samples were analysed in duplicate in a single assay, the threshold detection was less than 32pg/mL; coefficient of variation limit=20%; the concentration units are expressed in ng/mL. Light absorbance was read with a multi-mode plate reader (Synergy HT, BioTek Instruments, Inc., USA) at 405nm.

Hypothalamic gene expression

The hypothalamus was dissected fresh and snap frozen for storage. Total RNA was extracted using the mirVANA kit (catalogue no. AM1561; Qiagen®, Germany) according to manufacturer's instructions. RNA concentrations were quantified using a Nanodrop^{TM} spectrophotometer (Thermofisher Scientific®, USA). Complementary DNA (cDNA) was then synthesized using High-Capacity cDNA Reverse Transcription Kit (catalogue no. 4368814; Thermofisher Scientific®).

Oxytocin receptor (*Oxtr*) and vasopressin receptor 1a (*Avpr1a*) genes were selected for analysis. Then RT-qPCR was performed using SYBR® Green real-time PCR on the cDNA samples using SYBR green (KAPA SYBR® FAST Kit; catalogue no. KK4602; Sigma, USA) to evaluate gene expression levels. Gene expression levels were then analysed on an AB7300 system (Applied Biosystems, Thermofisher®). Expression levels were calculated as the average of three replicates for each biological sample from Control Extinction, Resilient Extinction, and Susceptible Extinction groups (n=11-13 per group) relative to β-actin expression. Then, fold changes were calculated using the $2^{-\Delta\Delta CT}$ method[452].

Transcriptomic sequencing

Hippocampus and amygdala RNA was extracted using the mirVANA kit (catalogue no. AM1561; Qiagen®, Germany). Source Bioscience conducted mRNA sequencing on the Illumina NovaSeq 6000 (S4 flow cell, 150bp paired-end lane yielding 2.5 billion read pairs). Reference genome of obtained sequences was performed using the reference annotation: *Mus musculus* (organism), GRCm38, UCSC, genome browser (GRCm38.p6), Ensemble[453]. Reads were assessed and filtered for quality using fastqc using default parameters. Genes were annotated and counted using kallisto using default parameters[439].

Processing of transcriptomics sequencing data

Further handling of transcriptomic data was undertaken in R (version 4.2.2) using the Rstudio GUI (version 2022.7.2.576). Principal component analysis was performed on centred log-ratio transformed (clr) values. Zeroes were replaced using the 'const' approach described by Lubbe and colleagues[434]. Differences in overall gene expression was computed in terms of Aitchison distance (Euclidean distance between clr-transformed data) and assessed by PERMANOVA using the vegan package. Differential gene expression was assessed using generalised linear models using the base R stats lm framework. Custom functions and scripts are available online at https://github.com/thomazbastiaanssen/Tjazi[454]. Before statistical testing, gene counts were filtered by variance using the genefilter library in R[442], with 0.5 set as the cutoff.

Inflammatory cytokine analysis

Cytokine levels from plasma and splenocyte supernatant samples was collected during euthanasia and were quantified using the U-PLEX Custom Biomarker Group 1 (mouse) Assays (K15069M-2, Meso Scale Discovery, USA) measuring IFN-γ, TNF-α, IL-1β, IL-

6, IL-10. Cytokine quantification was carried out according to the manufacturer's guidelines. Samples below the detection limit of each assay were excluded. The lower threshold detection limits for each cytokine were: IFN-γ= 0.16 pg/mL, TNF-α= 1.3pg/mL, IL-1β= 3.1pg/mL, IL-6= 4.8pg/mL, and IL-10= 3.8pg/mL.

Faecal bacteriome collection and sequencing

Murine faecal bacteriomes were analysed to assess the differences in community level composition across Control Extinction, Resilient Extinction, and Susceptible Extinction groups (the Sham Extinction group was excluded). Full metagenomic sequencing was conducted on faecal samples following social fear extinction.

A single faecal sample from each mouse per group (Control Extinction, Resilient Extinction, and Susceptible Extinction groups) was collected and used for analysis. The QIAamp Fast DNA Stool Mini Kit (Qiagen, Germany) was used to extract DNA from faecal pellets. This was performed following the manufacturer's guidelines. Before extraction, however, 20µL the ZymoBIOMICs spike-in control 1 (Zymo Research, USA) was added to aid in calculating absolute abundances. DNA concentrations were then measured using the Qubit High Sensitivity assay (Thermo Fisher Scientific, USA) before sequencing libraries were created using the Nextera XT Library Prep Kit (Illumina, USA). Library quality was assessed using the 4200 Agilent Tapestation (Agilent Technologies, USA) using the High Sensitivity D1000 ScreenTape assay (Agilent Technologies) before whole metagenomic sequencing was performed on an Illumina Novaseq 6000 platform using 2 × 150nt paired-end chemistry (Genewiz/Azenta, USA).

Faecal virome collection and sequencing

Murine faecal viromes were analysed to assess the differences in community level composition across Control Extinction, Resilient Extinction, and Susceptible Extinction groups (the Sham Extinction group was excluded). Full metagenomic sequencing was conducted on faecal samples following social fear extinction.

A single faecal sample from each mouse per group (Control Extinction, Resilient Extinction, and Susceptible Extinction groups) were collected and pooled in 650µl of SM buffer. Fresh 0.5M dithiothreitol was prepared in 1mL of SM buffer. A volume of 16µl of the dithiothreitol stock was added to samples to achieve a final concentration of 12mM, and samples were incubated at 37°C for 30min. Centrifugation at 4,000g for 30min at room temperature was used to pellet debris and bacterial cells. Subsequently, 400µl of liquid was removed and treated with 40µl of DNase/RNase buffer (50mM MgCl2, 10mM $CaCl_2$), 12µl (24U) of Turbo DNase (Thermo Fisher) and 4µl (40U) of Fermentas RNase I (Fisher Scientific) at 37°C for 1h. Nucleases were inactivated by incubating at 65°C for 10min. With free nucleic acids now removed virus like particles (VLPs) were lysed using the QIAgen Blood and Tissue Kit following the manufacturer's guidelines. However, an elution volume of 30µl of Qiagen AE elution buffer (10mM Tris-HCl, 0.5mM EDTA, pH 9.0) was used to increase the final concentration of nucleic acid obtained.

Prior to library preparation, samples were adjusted to a volume of 52.5µL sheared with a M220 Focused-Ultrasonicator (Covaris, Austria) applying the 350bp DNA fragment length settings (peak power 50W, duty factor 20%, 200 cycles per burst, total duration of 65s). Samples were then concentrated using the Genomic DNA Clean and Concentrator kit from Zymo Research and eluted in 16µl. Library preparation was then carried out using

xGen ssDNA and Low-Input DNA Library Prep Kit (Integrated DNA Technologies, USA) according to the manufacturer's instructions. However, a final and additional bead clean-up step of 0.8 DNA/AMPure beads v/v ratio was included. Library QC to determine fragment length distribution and quantitation was performed using the 4200 Agilent Tapestation (Agilent Technologies, USA) using the High Sensitivity D1000 ScreenTape assay (Agilent Technologies) and Invitrogen Qubit. The normalised pooled library was then sequenced using 2 × 150 nucleotide paired-end sequencing chemistry on the Illumina NovaSeq 6000 platform at Genewiz (Leipzig, Germany).

Analysis of bacteriome sequencing data

Raw reads quality was assessed using FastQC (v0.11.8) (https://github.com/s-andrews/FastQC) and adapters were trimmed using Trimmomatic (v0.39) (https://github.com/usadellab/Trimmomatic) with parameters ILLUMINACLIP:/data/programs/trimmomatic/adapters/NexteraPE-PE.fa:2:30:10 SLIDINGWINDOW:4:20 MINLEN:60 HEADCROP:10 CROP:230. Trimmed reads were pooled and assembled using metaSPAdes (SPAdes v3.13.1) (https://github.com/ablab/spades) in paired-end metagenomic mode specified by parameters: --meta. Assembled contigs from each extinction cohort were pooled and contigs <1000kb and redundant contigs were removed. Taxonomy and functional capacity of bacterial reads were generated using Woltka's OGU classification pipeline (https://github.com/qiyunzhu/woltka/blob/master/doc/ogu.md). Analysis was done in RStudio following steps in the Bugs as Features pipeline[440,441].

Analysis of total viral sequences within the bulk metagenomic sequencing data

In addition to the contigs assembled by metaSPAdes in the bacteriome analysis, metaSPAdes was run again using the –metaviral parameter to ensure assembly of all viral contigs present. Viral contigs assembled from this step were pooled with contigs assembled in metagenomic mode and redundant sequences were removed. Contigs were identified as viral using VirSorter (version 2.2.3) following the viral sequence identification protocol (https://www.protocols.io/view/viral-sequence-identification-sop-with-virsorter2-5qpvoyqebg4o/v3). CheckV was used to assess the completeness of viral genomes. The final sequences were selected if they were circular (complete), deemed "high" in aai_completeness by CheckV or were filtered based on criteria recommended in aforementioned viral-id-sop pipeline where a contig is deemed potentially viral if viral_gene >0, viral_gene =0 AND (host_gene =0 OR score >=0.95 OR hallmark >2). Viral read counts and coverage per sample was calculated using bowtie2 (version 2.4.2) A breadth of coverage filter was applied to the read counts, removing sequences with <75% coverage per sample. Viral contigs were aligned at nucleotide level using Blastn (v2.11.0+) against an in-house Crassvirales database as well as the GVD, GPD, MGV, IMGVR and RefSeq viral databases (-evalue 1e-10). Viral sequences were translated using Prodigal (V2.6.3) with parameters -p meta and default translation table. Taxonomic classification of viral proteomes was assigned by Crassify (https://github.com/linda5mith/crassify).

Bioinformatics and statistical analysis of microbiome data

Data-handling of microbiome measures was undertaken in R (version 4.2.2) using the Rstudio GUI (version 2022.7.2.576). Principal component analysis was performed on

centred log-ratio transformed (clr) values as a visual companion to the beta diversity analysis. Alpha-diversity metrics were calculated using scikit-bio (v0.5.8; http://scikit-bio.org/). For all analysis beyond alpha-diversity, taxa with a prevalence of < 5% (at the species level for bacteria and vOTU level for viruses) were excluded from analysis as ratios are invariant to sub-setting and this study employs compositional data analysis techniques[432,433]. Zero values were then imputed for using the 'const' approach[434]. Count data were then centred log-ratio (clr) transformed using scikit-bio. Differential abundance estimates were computed using the analysis of composition of microbiomes (ANCOM)[455] method within scikit-bio. Beta diversity was computed in terms of Aitchison distance (Euclidean distance of clr-transformed counts) and differences in beta diversity were assessed using the PERMANOVA implementation from the vegan library using 1000 permutations[456]. Plotting was handled using ggplot2 and the Python implementation of plotly (https://plotly.com/).

Statistics

Behavioural, immune, and gene expression data were assessed for outliers, defined as being outside of 2.5x standard deviations of the mean, and were subsequently excluded from analysis. Data was first assessed by a 1-way ANOVA across groups (Control Extinction, Resilient Extinction, Susceptible Extinction), then Tukey's post hoc analysis was used for pairwise comparisons. False discovery rate (FDR) analysis was performed using Storey's FDR test of metagenomic and transcriptomic sequencing of differentially abundant taxa and expressed genes, respectively. Further statistical analysis was handled

in R (v4.2.2) using the R Studio GUI (version 2022.7.2.576) and in Python with SciPy (v1.9.3). In all cases, an alpha threshold of 0.05 was used to denote significance.

3.4 Results

Social fear behaviour response undergoes typical, resilient, or susceptible extinction behaviours.

Social fear conditioning (SFC) was conducted on all mice (*N*=48) followed by social fear extinction (SFE) 24hr later. SFC, in brief, consisted of a habituation phase (exposure to the chamber environment), immediately followed by a conditioning phase where mice received an aversive stimulus (foot-shock exposure) upon interaction with a novel conspecific. The Sham Extinction group of mice underwent the same procedure but received no foot-shock upon social interaction (*n*=11). The next day, during SFE, experimental mice were exposed to 9 home cage trials, each 3min in duration with 3min breaks between each trial. During the first 3 trials mice were exposed to an empty conspecific cage (non-social stimuli; ns1-3), then in the next 6 trials they were exposed to 6 novel conspecifics (social stimuli; s1-6; all different from the SFC conspecific) and the percent time spent investigating each stimulus was measured. Mice were then stratified into three different behavioural response groups dependent on their social behaviour measured during the 2nd extinction trial (Fig. 1a) and the total extinction (Fig. 1b) social investigation times. Animals that underwent the expected gradient-based increase in social investigatory behaviour[336] (Ritz et al., *in press*) over subsequent trials were placed in the group termed "Control Extinction" (Con. Ext.; *n*=13). Animals that rapidly extinguished social fear were termed "Resilient Extinction" (Res. Ext.; *n*=13) and animals that did not extinguish social fear were termed "Susceptible Extinction" (Sus. Ext.; *n*=11). The Con. Ext. group was unique in this test in that they began with social fear behaviour

indiscernible from the Sus. Ext. group in the first trial (s1), but then gradually improved over each subsequent trial until the end of the test where they resembled the Res. Ext. group. The Res. Ext. group quickly abolished social fear by the second trial (s2) and then displayed a ceiling effect whereby on average they spent >80% of the time in social interaction akin to the sham SFC control group. The Sus. Ext. group did not increase the time spent in social interaction within the 6 social stimuli trials (Fig. 1c).

Prior to SFC, mice were habituated to the conditioning chamber and locomotor activity and investigation time of the empty conspecific cages (non-social stimuli) were recorded. No differences were observed in locomotor activity as measured by total distance traveled during habituation (Fig. S1a). There also were no differences found in investigation time of the non-social stimuli (Fig. S1b). Last, the number of foot-shock exposures administered to inhibit repeated social approaches and interactions (minimum 1, maximum 5) was not different across groups (Fig. S1c). These data show that there were no measured inherent behavioural differences across the groups.

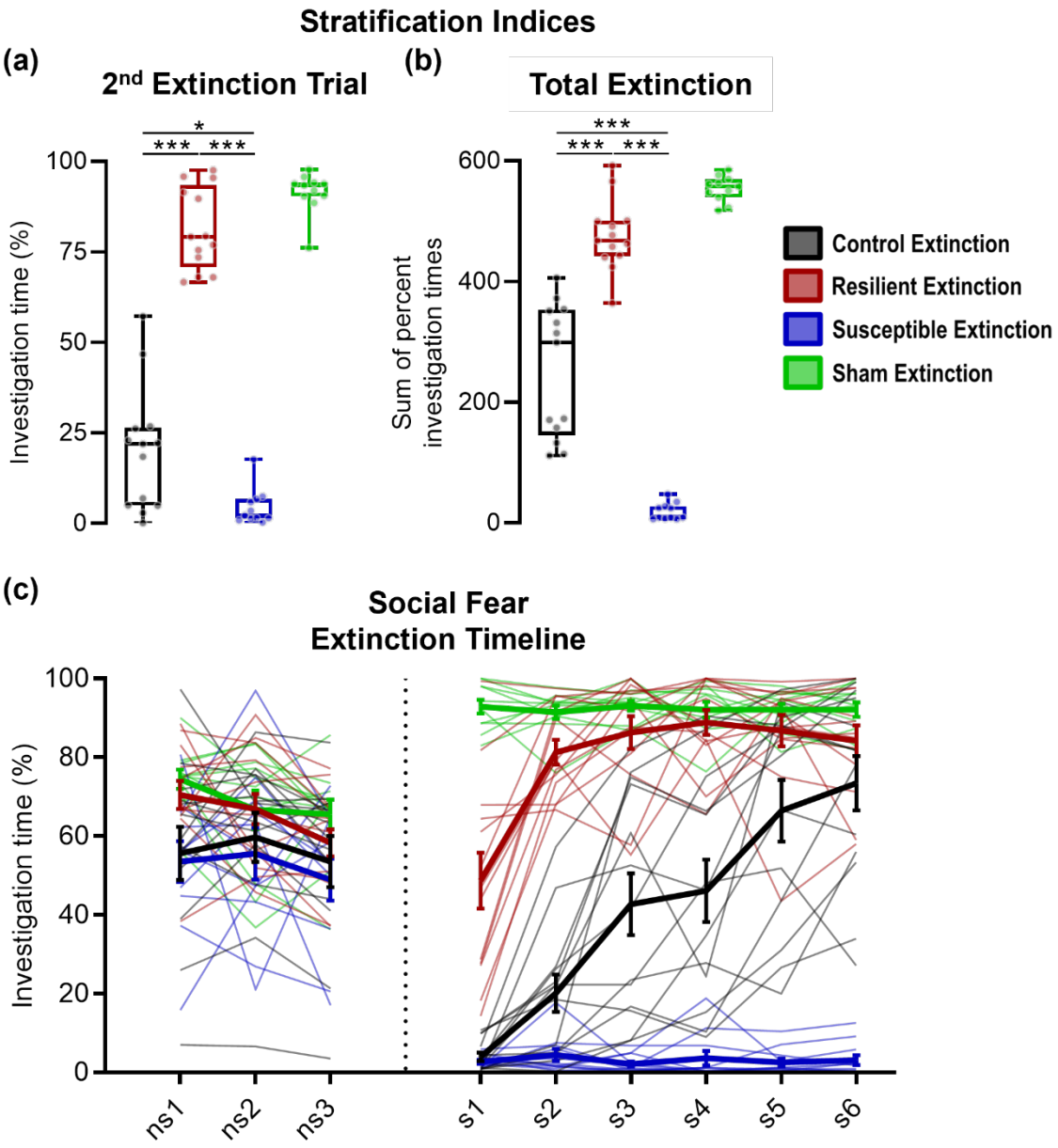


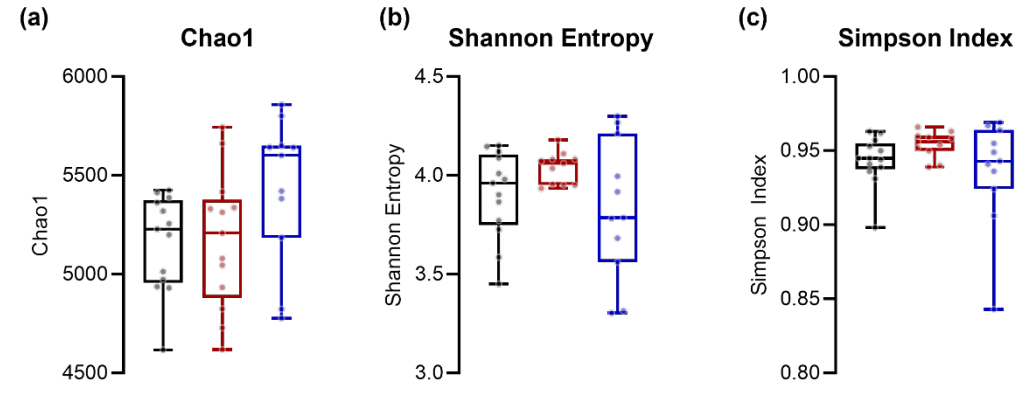
Fig. 1 Social fear extinction behaviour response following social fear conditioning.

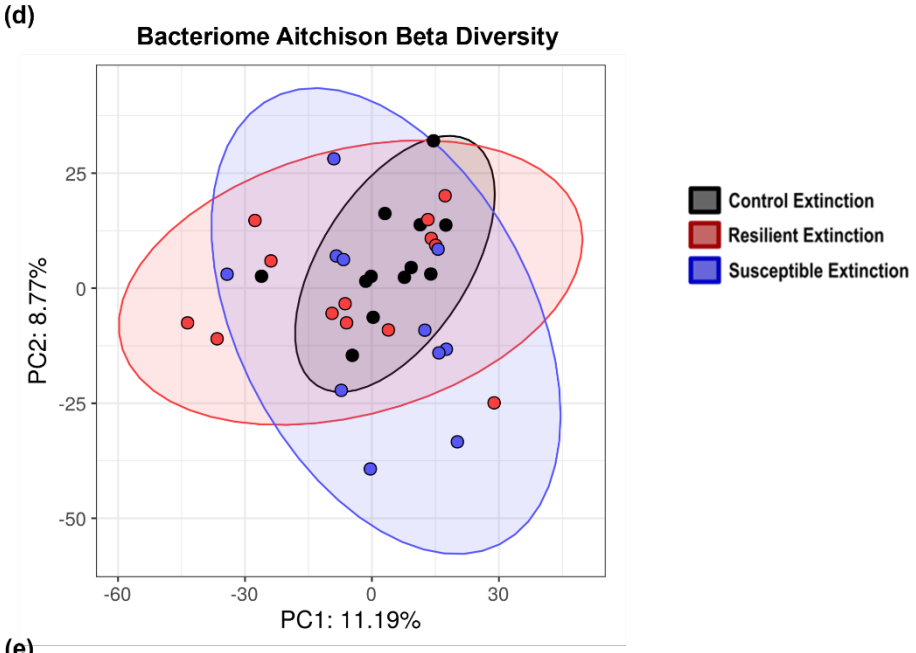
Mice were stratified into three groups dependent on their social fear behaviour during the ***(a)*** *2nd extinction trial and* ***(b)*** *total extinction. The sham group went through the same procedures but received no foot shock.* ***(a)*** *The 2nd trial social investigation percent time of each group during social fear extinction.* ***(b)*** *The area under the curve for the social investigation percent time of each group during social fear extinction.* ***(c)*** *The social fear extinction timeline showing the 3 non-social investigation trials (ns1-3) and the social*

investigation trials (s1-6). Control Extinction n=13, Resilient Extinction n=13, Susceptible Extinction n=11, and Sham Extinction n=11; p<0.05, p<0.001***.*

Social fear behaviour and bacteriome composition variability are positively associated.

The faecal bacteriome and virome were assessed by whole genome metagenomic sequencing collected after social fear extinction. There was a trend for the bacteriome alpha diversity metric Chao1 (species richness) to be different across groups (F=2.748, p=0.078) (Fig. 2a). No differences were observed in Shannon Entropy (Fig. 2b) or Simpson Index (Fig. 2c). There was also no difference found in the bacteriome or virome Aitchison beta diversity distances between groups (Fig. 2d, 3a). However, we observed a strong correlation between bacteriome Aitchison distance from the centroid and distance from the mean total extinction social investigation time measured during SFE (R=0.463, t(34) = 3.64, p<0.0001; Fig. 2e). We also observed a trend in the correlation between virome Aitchison distance from the centroid and distance from the mean total extinction social investigation time (R=0. 266, t(34) = 3.64, p=0.1171; Fig. 3b). The correlation calculations were measured across all samples independent of group. These associations reveal a link between social fear behaviour and microbiome composition.


(a)
Chao1
Chao1
6000
5500
5000
4500
(b)
Shannon Entropy
Shannon Entropy
4.5
4.0
3.5
3.0
(c)
Simpson Index
Simpson Index
1.00
0.95
0.90
0.85
0.80


(d)
Bacteriome Aitchison Beta Diversity
PC2: 8.77%
25
0
-25
-50
-60
-30
0
30
PC1: 11.19%
Control Extinction
Resilient Extinction
Susceptible Extinction

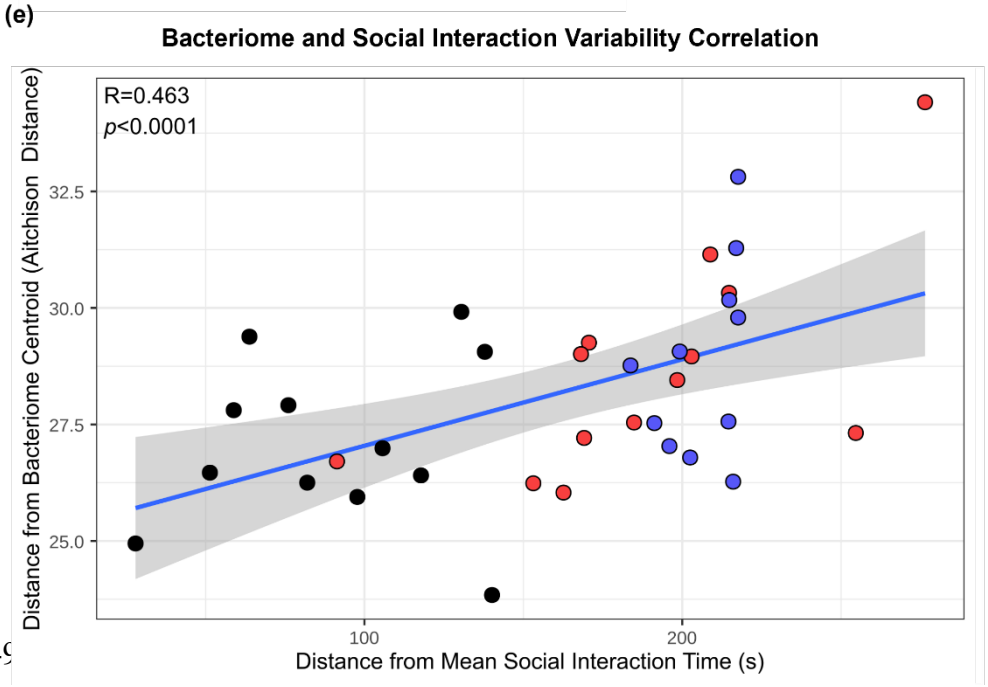

(e)
Bacteriome and Social Interaction Variability Correlation
R=0.463
p<0.0001
Distance from Bacteriome Centroid (Aitchison Distance)
32.5
30.0
27.5
25.0
100
200
Distance from Mean Social Interaction Time (s)

Fig. 2 Social fear response and the bacteriome.

*(**a-c**) No statistical differences were found in bacteriome alpha diversity between groups, however there was a trend for (**a**) Chao1 to be increased in the susceptible group (F=2.748, p=0.078). (**d**) No differences were found in bacteriome Aitchison beta diversity between groups. (**e**) There was a significant correlation between bacteriome distance from the centroid and social fear distance from the average total extinction (R=0.463, t(34) = 3.64, p<0.0001).*

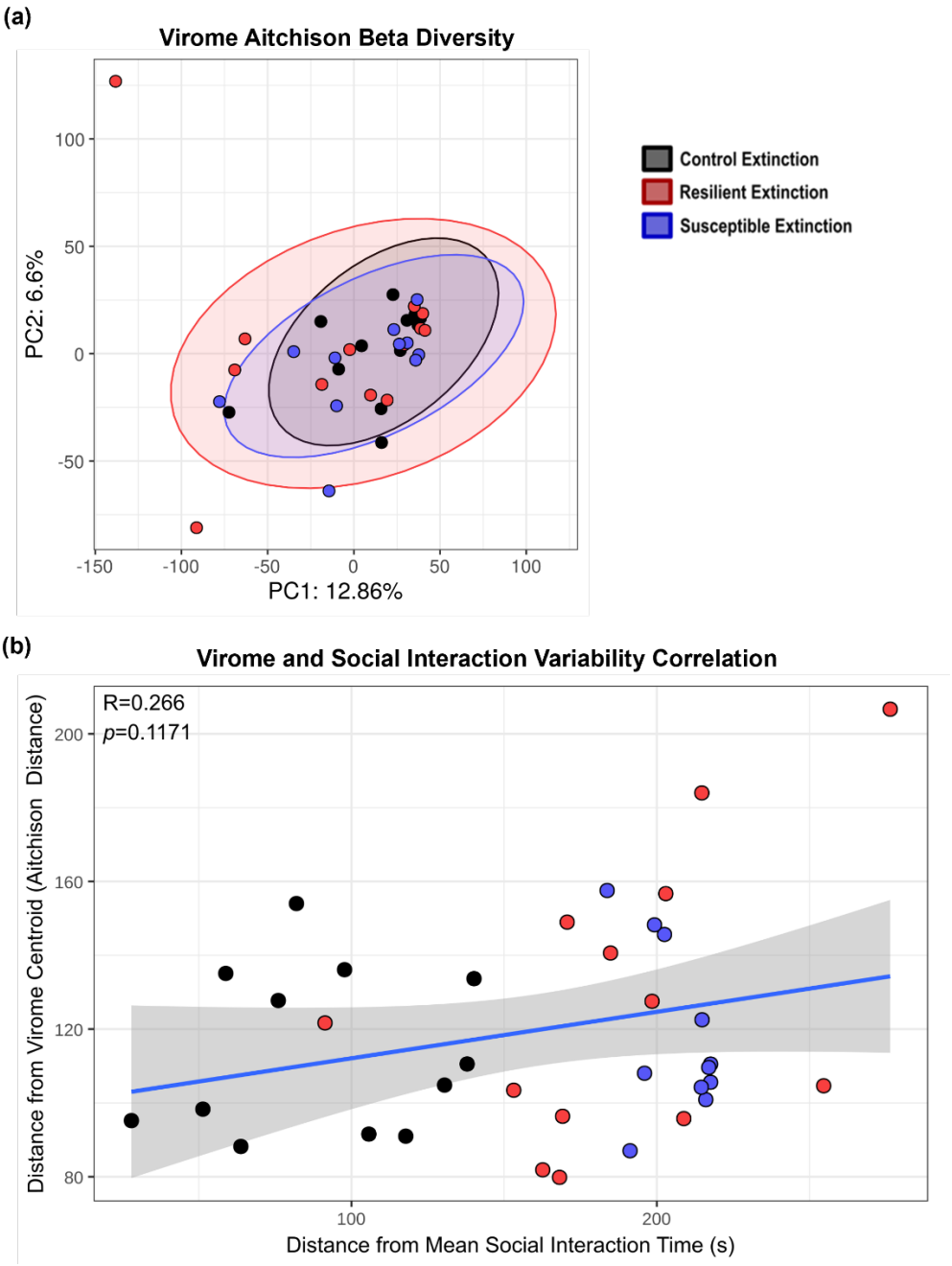
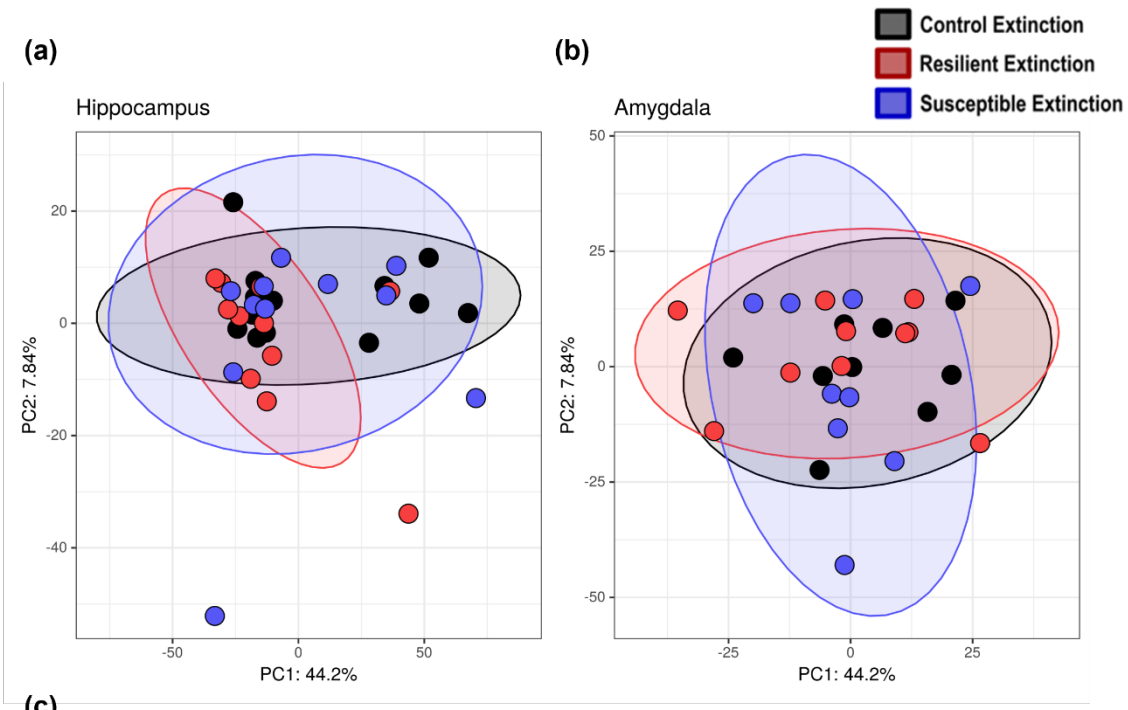


Fig. 3 Social fear response and the virome.

*(**a**) No differences were found in virome Aitchison beta diversity between groups. (**b**) There was a trend in the correlation between virome distance from the centroid and social fear distance from the average total extinction (R=0.266, t(34) = 3.64, p=0.1171).*

Group stratifications can be distinguished via differentially expressed genes in the amygdala.

In order to understand differences present in the brain at the transcriptional level, RNA sequencing was performed on the hippocampus and amygdala, collected 24hr after SFE. No group differences were found in principle coordinate analyses of each brain region (Fig. 4a, b). However, in the amygdala 19 genes were found to be altered across groups (Fig. 4c; statistics included in figure). These genes have been associated with social behaviour (*Armcx1*, *Fam69b*, *Kcnj9*, *Maoa*, *Met*, *Serinc5*, *Slc6a17*, *Spata2*, and *Syngr1*), inflammation and immunity (*Cars*, *Ckmt1*, *Klf5*, *Maoa*, *Map3k12*, *Met*, *Pex5*, *Serinc5*, *Sidt1*, *Spata2*), and microbe-host interaction (*Klf5*, *Map3k12*, *Serinc5*, *Sidt1*). These data reveal differences in amygdalar gene expression that accompany the social fear behaviour alterations across groups.


(a)
Hippocampus
PC2: 7.84%
PC1: 44.2%
(b)
Amygdala
PC2: 7.84%
PC1: 44.2%
Control Extinction
Resilient Extinction
Susceptible Extinction

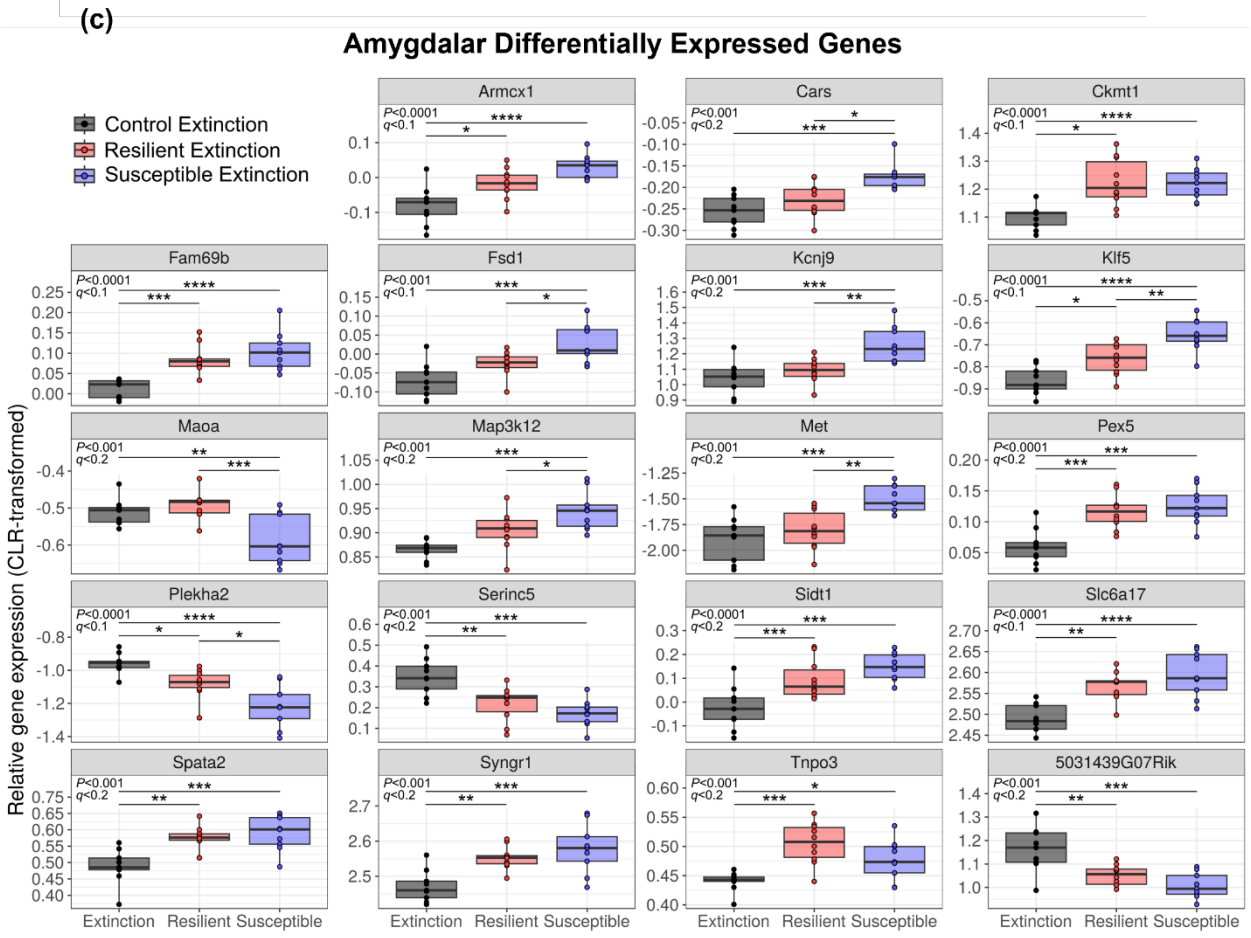

(c)
Amygdalar Differentially Expressed Genes
Control Extinction
Resilient Extinction
Susceptible Extinction
Relative gene expression (CLR-transformed)
Armcx1
Cars
Ckmt1
Fam69b
Fsd1
Kcnj9
Klf5
Maoa
Map3k12
Met
Pex5
Plekha2
Serinc5
Sidt1
Slc6a17
Spata2
Syngr1
Tnpo3
5031439G07Rik
Extinction
Resilient
Susceptible

Fig. 4 Differentially expressed genes in the amygdala between social fear extinction, resilient, and susceptible groups.

*(**a**) PCA of hippocampal gene expression. (**b**) PCA of amygdalar gene expression. (**c**) Differentially expressed genes in the amygdala (P=1-way ANOVA. q=Storey's FDR, p=pairwise Tukey's posthoc; p<0.05*, p<0.01**, p<0.001***, p<0.0001****).*

No differences were observed in social and stress neuropeptide hormones and inflammatory cytokines.

To narrow down the mechanism by which social fear responsivity occurs, we measured social and stress -related neuropeptides. Corticosterone was measured in basal-state plasma the day after SFE, however, there was no difference across groups (Fig. 5a). Then, we measured basal-state plasma oxytocin, but again there were no differences (Fig. 5b). Next, we measured expression of oxytocin and vasopressin receptors in the hypothalamus, a key region that both produces and is activated by these hormones, but we observed no differential effects (Fig. 5c, d). Last, we measured basal-state plasma inflammatory cytokines, but no differences were observed across groups in tumour necrosis factor alpha (TNF-α; Fig. 5e), interferon gamma (IFN-γ; Fig. 5f), or anti-inflammatory cytokine interleukin 10 (IL-10; Fig. 5g). The lack of effects in these data point away from oxytocin-related or corticosterone neuropeptide modulation or peripheral immune activation as the mechanisms driving social fear response.

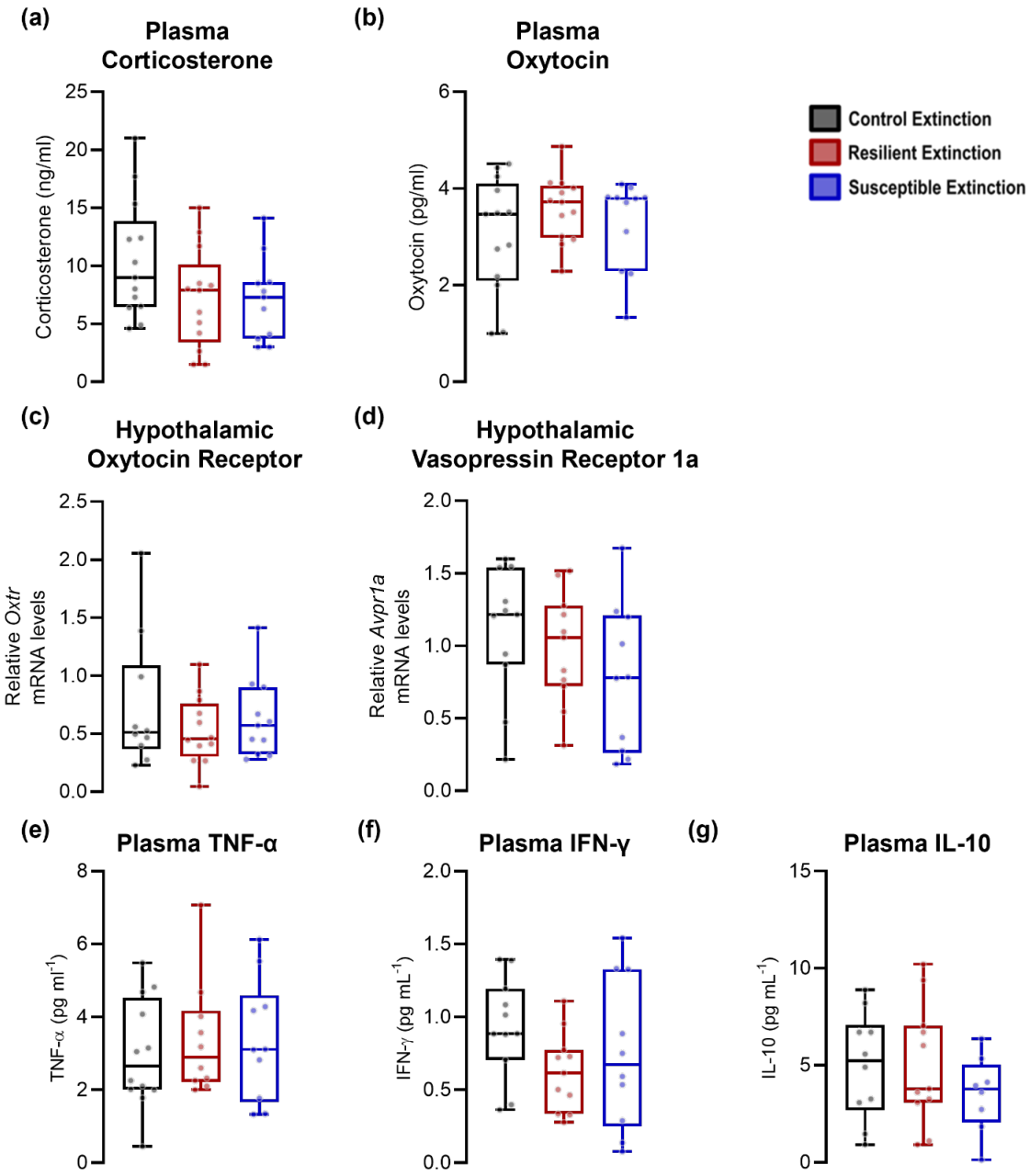


Fig. 5 No differences were observed in social and stress neuropeptide hormones and inflammatory cytokines.

Plasma collected at the end of the study was analysed for ***(a)*** *corticosterone and* ***(b)*** *oxytocin levels across groups, but no differences were found. There were also no differences in hypothalamic* ***(c)*** *oxytocin receptor (Oxtr) and* ***(d)*** *vasopressin receptor 1a (Avpr1a) gene expression. Additionally, no differences were observed in plasma inflammatory cytokines* ***(e)*** *tumour necrosis factor alpha (TNF-α),* ***(f)*** *interferon gamma (IFN-γ), or* ***(g)*** *interleukin 10 (IL-10).*

3.5 Discussion

There is a growing body of literature implicating the host microbiota modulating the brain and behaviour[8,243,457] and especially the social brain[313,458]. Here, we show that microbiota composition and amygdala gene expression correlate with social fear extinction behaviour following conditioning, in a murine model of SAD. These data further posit the microbiota-gut-brain axis as a key biological factor that is relevant to social fear responses and is a potential therapeutic target.

In our model of social fear conditioning, we administered a foot-shock to mice following approximately 2 seconds of social interaction, then an additional foot-shock each time a repeated social interaction approach occurred (up to a maximum of 5 times). The next day, we tested the social interaction time of conditioned mice during social fear extinction where they were exposed to novel conspecifics in 6 sequential trials. We found that mice could be stratified into three general social fear response categories: typical extinction, resilient, and susceptible. Mice that underwent typical extinction, high social fear in the beginning trials as defined by low social interaction time that gradually increased throughout the test, were placed in the "Control Extinction" group[336]. Mice that had high social interaction time (low social fear) within the first 2 trials were termed "Resilient Extinction" and quickly extinguished their social fear. Lastly, mice that had low social interaction time throughout the test were termed "Susceptible Extinction". Of note, there were no differences recorded in baseline locomotor and investigatory behaviours measured during the habituation phase of SFC (prior to any negative stimuli) nor any significant differences in the total number of foot-shock exposures per group.

Both the bacteriome and virome measured across the three social fear categorical groups were similar with no major deviations in alpha or beta diversities or individual strains. However, we found an intriguing correlation between the difference from the mean social interaction total extinction scores versus the distance from average bacteriome composition (Aitchison distance from the bacteriome centroid). This correlation suggests the more divergent the bacteriome the further the individual social fear response will be from typical fear extinction. Interestingly, there was also a trend in the same analysis when looking at the virome, however it was not as strong of a correlation, and it did not reach statistical significance. This finding is similar to a previous finding by our group where the volatility of a microbiome, defined as Aitchison distance between longitudinal measures in a single individual (*i.e.*, temporal variability), positively correlated with stress severity measures both in human and mice[352]. Together, these findings indicate that microbiota stability and centrality in a neutral and healthy setting are informative to mental health in terms of stress response and social fear behaviour.

To better understand how social fear response manifested at the transcriptional level in the brain we conducted RNA sequencing on the hippocampus and amygdala regions. These regions are responsive to stress, social interaction, fear, and learning and memory in addition to being sensitive to microbiota influence[371,459-462]. Furthermore, these regions were previously shown to contain differences in oxytocin receptor binding following SFC[340]. The hippocampus displayed few changes across groups in this study and did not survive false-discovery rate analyses, however the amygdala had 19 genes that were differentially expressed following SFC, extinction, and behaviour-based stratification.

Armcx1 was downregulated in the Con. Ext. group in comparison to the other groups, this gene region overlaps with the quantitative trait loci of *Memor13* and *Memor14,* both of which have been implicated in social behaviour in rats[463]. *Kcnj9* was upregulated in the Sus. Ext. group and has been identified as a risk locus in psychiatric disorders[464]. *Fam69b*, reduced in the Con. Ext. group, localises to the endoplasmic reticulum[465] and has been implicated in neurological disorders[466]. *Maoa* was significantly reduced in the Sus. Ext. group and has been involved in abuse exposure and antisocial behaviour[467,468]. *Met* was also overexpressed in the Sus. Ext. group and has been associated with social communication in autism spectrum disorder[469]. *Serinc5* was reduced in expression in the Res. Ext. and Sus. Ext. groups compared to the Con. Ext. group and is involved in myelination, a reduction of which has been characterized by lack of social interaction in psychiatric disorders[470]. *Slc6a17* was upregulated in the Res. Ext. and Sus. Ext. groups, mutations of which have been shown to cause speech impairment and behavioural problems[471]. *Spata2* is an immune-related gene that was also upregulated in the Res. Ext. and Sus. Ext. groups and has been associated with autistic traits[472]. Last, *Syngr1* was upregulated in the Res. Ext. and Sus. Ext. groups and has been identified to undergo altered expression in depressed humans[450]. Furthermore, *Armcx1*, *Cars*, *Ckmt1*, and *Maoa* have also been associated with mitochondrial function which can play a role in neuropsychiatric diseases[473-476].

There were also genes associated with inflammation and immunity as well as host-microbe interaction. For example, Krupple-like factors (such as *Klf5*), which were increased in the Sus. Ext. and reduced in the Con. Ext group, contribute to numerous

diseases such as cerebrovascular, neurodegenerative, and cardiovascular diseases as well as inflammatory conditions and has been shown to mediate immunity to both bacterial and viral pathogen challenges[477-480]. *Maoa*, reduced in the Sus. Ext. group, has been implicated as a marker for monocytes and macrophages[481] capable of regulating psychosocial behaviour and stress response[482,483]. *Map3k12*, increased in the Sus. Ext. group, has been shown to modulate neuronal injury and neurodegeneration and also modulate antiviral immunity[484,485]. *Pex5*, reduced in the Con. Ext. group, has been linked with inflammation and NF-κB regulation in innate immune signalling response to bacteria and viruses[486-488]. *Serinc5*, increased in the Con. Ext. group, has also been identified as an antiviral factor in addition to being associated with borderline personality disorder[470,489]. *Sidt1*, also increased in the Con. Ext. group, has been shown to play a role in interferon-1 response and associated with antiviral activity[490,491]. Lastly, *Spata2*, reduced in the Con. Ext. group, is involved in TNF and NF-κB signalling modulating inflammation[492,493]. The differential involvement of these genes in social fear response suggests that complex microbiota-gut-brain axis interactions may underly the development of the social anxiety phenotype.

Corticosterone and oxytocin have been shown to be modulated in social stress models and can affect social behaviour[494,495] and intracerebroventricular administration of oxytocin receptor antagonist has previously been reported to attenuate social preference[496] and SFC[340]. These findings suggesting involvement of neuroendocrine hormones in social behaviour. Therefore, we explored whether social or stress hormones were altered between our group designations but found no significant effects. There were no

differences across groups in basal plasma oxytocin, or oxytocin or vasopressin receptor gene expression in the hypothalamus. Basal plasma corticosterone and circulating cytokines were similarly unchanged across groups. Social behaviour has been shown to be regulated by oxytocin[497] which is particularly sensitive in the dorsolateral septum and has previously been shown to modulate social fear[340]. We also did not observe any altered oxytocin-related genes in the hippocampal and amygdalar transcriptomic dataset. These data suggest that an oxytocin neuroendocrine mechanism underlying the differential social response is unlikely mediated in the hippocampus and amygdala, but rather, governed by the hypothalamus and septum[340]. Future research is necessary to further elucidate the underlying mechanism driving the connection between social fear response and the microbiota-gut-brain axis.

Social fear is a multifactorial behaviour that can be attributed to genetic, environmental, and host perception of social contexts. Despite these many factors, there is a relatively narrow diagnostic and treatment approach for individuals with SAD at present. Here we provide evidence in an empirical social fear model that extinction of social fear is variable, even in a controlled environment with a genetically identical single-housed strain of mice. We explored the potential for microbiota-related variability to be associated with social fear responsivity and found that microbiota variability strongly correlated with categorical extinction behaviour. These findings suggest that further research into microbiota-based diagnostics and treatments may provide novel therapeutic potential for the alleviation of SAD symptoms.

Acknowledgements

The authors would like to thank P. Fitzgerald, C. Manley, J. Riley, and A. Markewinski for their assistance with mouse husbandry. The authors would also like to thank P. Fitzgerald, J. Nagpal, M.R. Aburto, and E. Myers for their knowledge sharing and technical assistance. APC Microbiome Ireland is a research centre funded by Science Foundation Ireland (SFI), through the Irish Governments' national development plan (grant no. 12/RC/2273_P2). A.N.S. was supported by a Wellcome Trust Research Career Development Fellowship [220646/Z/20/Z], and the European Research Council (ERC) under the European Union's Horizon 2020 research and innovation programme (grant agreement No 101001684).

N.L.R., C.S.M.C., G.M.M., L.A.D, C.H., T.G.D, D.A.S., and J.F.C. designed the studies. N.L.R., C.S.M.C., and N.T. performed the experiments with animals. N.L.R., M.B., and L.A.D., performed assays, sample collection, and processing. L.S., A.N.S., and T.F.S.B. generated metagenomic and virome sequencing analyses and interpretation. N.L.R., A.N.S., L.S., and T.F.S.B. analysed the data. N.L.R. and J.F.C. wrote the paper with contributions made from all the authors.

3.6 Supplementary Figures

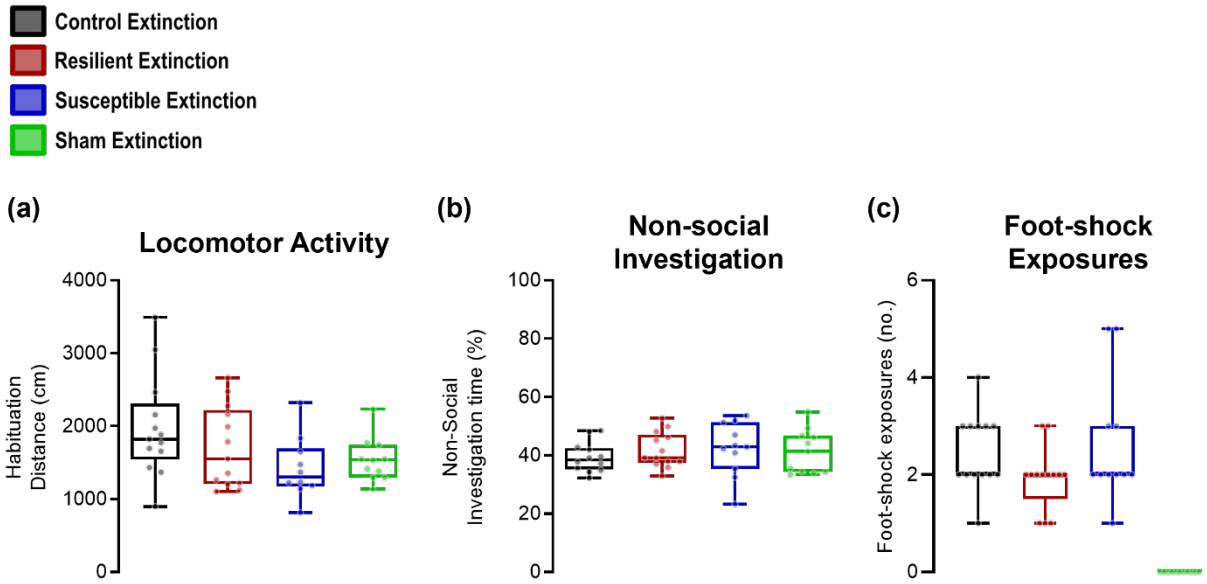


Fig. S1 Baseline behaviours measured during social fear conditioning.

*(**a**) Locomotor activity measured by distance travelled by mice during the habituation phase of the social fear conditioning (SFC) procedure. (**b**) The percent time of investigation of the empty conspecific cage (non-social stimulus) during the habituation phase of SFC. (**c**) Total number of foot-shock exposures of mice in each group. Mice received a foot-shock following the initial social interaction and an additional foot-shock following repeat approach of social stimulus during SFC (total number of foot-shock exposures was between 1-5). No statistically significant differences were observed across groups in locomotor and non-social investigation behaviours. There was no difference in the number foot-shock exposures observed across the conditioned groups. Numbers per group: control extinction n=13, resilient extinction n=13, susceptible extinction n=11, and sham extinction n=11.*

Chapter 4

Social Anxiety Disorder-Associated Gut Microbiota Increases Social Fear

Nathaniel L Ritz[1,2], Marta Brocka[1#], Mary I Butler[1,3#], Caitlin SM Cowan[1†#], Camila Barrera-Bugueño[1], Christopher JR Turkington[1,4], Lorraine A Draper[1,4], Thomaz FS Bastiaanssen[1,2], Valentine Turpin[1], Lorena Morales[1], David Campos[1], Cassandra E Gheorghe[1,3], Anna Ratsika[1,2], Virat Sharma[1,4], Anna V Golubeva[1], Maria R Aburto[1,2], Andrey N Shkoporov[1,4], Gerard M Moloney[1,2], Colin Hill[1,4], Gerard Clarke[1,3], David A Slattery[5], Timothy G Dinan[1,3], John F Cryan[1,2*]

[1]APC Microbiome Ireland, University College Cork, Cork, Ireland T12YT20
[2]Dept. of Anatomy and Neuroscience, University College Cork, Cork, Ireland T12YT20
[3]Dept. of Psychiatry and Neurobehavioural Science, University College Cork, Cork, Ireland T12YT20
[4]School of Microbiology, University College Cork, Cork, Ireland T12K8AF
[5]Dept. of Psychiatry, Psychosomatics and Psychotherapy, University Hospital Frankfurt, Frankfurt, Germany 60528

[#]These authors contributed equally

Accepted for publication at *Proceedings of the National Academy of Sciences*

4.1 Abstract

Social anxiety disorder (SAD) is a crippling psychiatric disorder characterized by intense fear or anxiety in social situations and their avoidance. However, the underlying biology of SAD is unclear and better treatments are needed. Recently, the gut microbiota has emerged as a key regulator of both brain and behaviour, especially those related to social function. Moreover, increasing data supports a role for immune function and oxytocin signalling in social responses. To investigate whether the gut microbiota plays a causal role in modulating behaviours relevant to SAD, we transplanted the microbiota from SAD patients to mice that was identified by 16S rRNA sequencing to be of a differential composition. Although the mice that received the SAD microbiota had normal behaviours across a battery of tests designed to assess depression and general anxiety-like behaviours, they had a specific heightened sensitivity to social fear, a model of SAD. This distinct heightened social fear response was coupled with changes in central and peripheral immune function and oxytocin expression in the bed nucleus of the stria terminalis. This work demonstrates an interkingdom basis for social fear responses and posits the microbiome as a potential therapeutic target for SAD.

Significance statement

Understanding the biological basis of social anxiety disorder (SAD), one of the most disabling of the anxiety disorders, will allow for novel treatment strategies to be developed. Here we show the gut microbiota may be such a target. Mice that received

SAD patient microbiota had a specific heightened sensitivity to social fear without affecting other behaviours tested. This distinct deficit in normal social fear responses was coupled with changes in immunity and the brain.

4.2 Introduction

Social anxiety disorder (SAD) is a common psychiatric disorder characterized by intense fear or anxiety in social scenarios. The onset of SAD typically occurs early in life (childhood or adolescence), and it frequently has a lifelong impact being associated with considerable functional disability and reduced quality of life[447,498-500]. Current pharmacological treatment options for SAD are limited and often ineffective, and new models are necessary to understand the underlying etiology and treatment targets[446]. Recent data has implicated the gut microbiota in brain and behavioural function related to social processes across the animal kingdom[313]. Intriguingly, we recently showed that patients with SAD have a different microbiota composition than age-matched healthy controls (HC)[274]. However, such correlative analysis requires insight to understand if the compositional changes observed may be mechanistically related to social fear or anxiety. To test causal mechanisms, faecal microbiota transplantation (FMT) studies have emerged as an effective technique to understand how the microbiota can potentially elicit phenotypic changes in the host. Furthermore, our approach adheres to both the recommended practice and to the Guidelines for Reporting on Animal Fecal Transplantation (GRAFT)[501,502]. Previous research in major depression, anxiety comorbid with irritable bowel syndrome, and schizophrenia show that transfer of the microbiota via

FMT is sufficient to transfer selective psychological and physiological traits of these disorders, including depression- and anxiety-like behaviour, to the recipient[18,19,37,191,503,504].

To further elucidate the role of the microbiota in SAD, we designed a translational study to test the hypothesis that the microbiota may play a causal role in promoting host social fear behaviour (Fig.1a). Faecal inocula from individual HC and SAD donors were anaerobically processed for cryogenic storage and later use whereby adult male C57Bl/6J mice received FMT from each donor (Fig.1b). Following antibiotic depletion of the microbiota, mice received the specified donor FMT, and were subsequently tested for social fear, sociability, social cognition, and stress-coping behaviours, as well as gastrointestinal transit and motility (Fig.1c).

4.3 Results

Social anxiety disorder leads to alterations in the bacteriome.

Gut microbiota composition was characterized using 16S rRNA sequencing performed on microbial DNA extracted from stool from individuals with SAD and matched HCs (Fig.1d). This analysis confirmed a distinct compositional difference as noted previously based on a metagenomic analysis (R^2=0.03477, p< 0.05, 1,000 permutations)[274]. We selected six SAD and six HC individuals based on host parameters and metrics including microbiota, Liebowitz Social Anxiety Scale score, age, body mass index, sex, and an absence of psychotropic or microbiota medications (*i.e.*, antidepressants, anxiolytics,

antibiotics, probiotics, prebiotics, *etc*.; Table S2). In addition to measuring the bacteriome (the collective bacterial genome) which makes up the majority of the active portion of the microbiome, we also measured the virome (the collective viral genome) which is primarily made up of bacteriophages which specifically infect bacteria[103].

Murine recipient bacteriome beta diversity was significantly altered between SAD and HC groups measured at the end of the study (Fig.1e; R^2=0.02767, p< 0.001, 1,000 permutations). There were three bacterial species that were differentially abundant in the SAD and HC groups at the end of the study, *Bacteroides nordii*, *Bacteroides cellulosiyticus*, and *Phocaeicola massiliensi* (Fig.S1a-c). No group differences were found in alpha diversity metrics at the end of the study (Chao1, Shannon, and Simpson; Fig.S1d-f), but each alpha diversity metric was reduced at the end of study compared to the pretreatment measures (Fig.S1g-i). While no group differences were observed in virome alpha or beta diversity metrics (Fig.S2). This alteration in bacteriome community composition confirms that the FMT from SAD and HC donors led to differential microbiotas recolonizing and engrafting following antibiotic microbiota depletion.

Social anxiety disorder faecal microbiota transplant specifically increases sensitivity to social fear.

Social fear, sociability, anxiety-like, and stress-coping behaviours were assessed in mice following recolonization with SAD or HC microbiota. Social fear conditioning was applied followed by extinction learning on the next day whereby social behaviour was measured by interaction time during repeated exposure to non-social and novel social stimuli (Fig.1f). There was a significant reduction in social interaction over the 6 social

stimuli trials ($W(1)=3.239$, $p<0.05$) and no difference in non-social investigatory behaviour. This reduction in social fear extinction rate provides evidence that the SAD microbiota is capable of increasing sensitivity to social fear stimuli. However, general sociability and social novelty preference were not affected by SAD FMT (Fig.1g,h; Fig.S3c,d). Furthermore, other tests of stress-coping behaviours and gastrointestinal transit were similarly unaffected (Fig.S3a-f), demonstrating that social fear sensitivity was specifically transferred by SAD FMT.

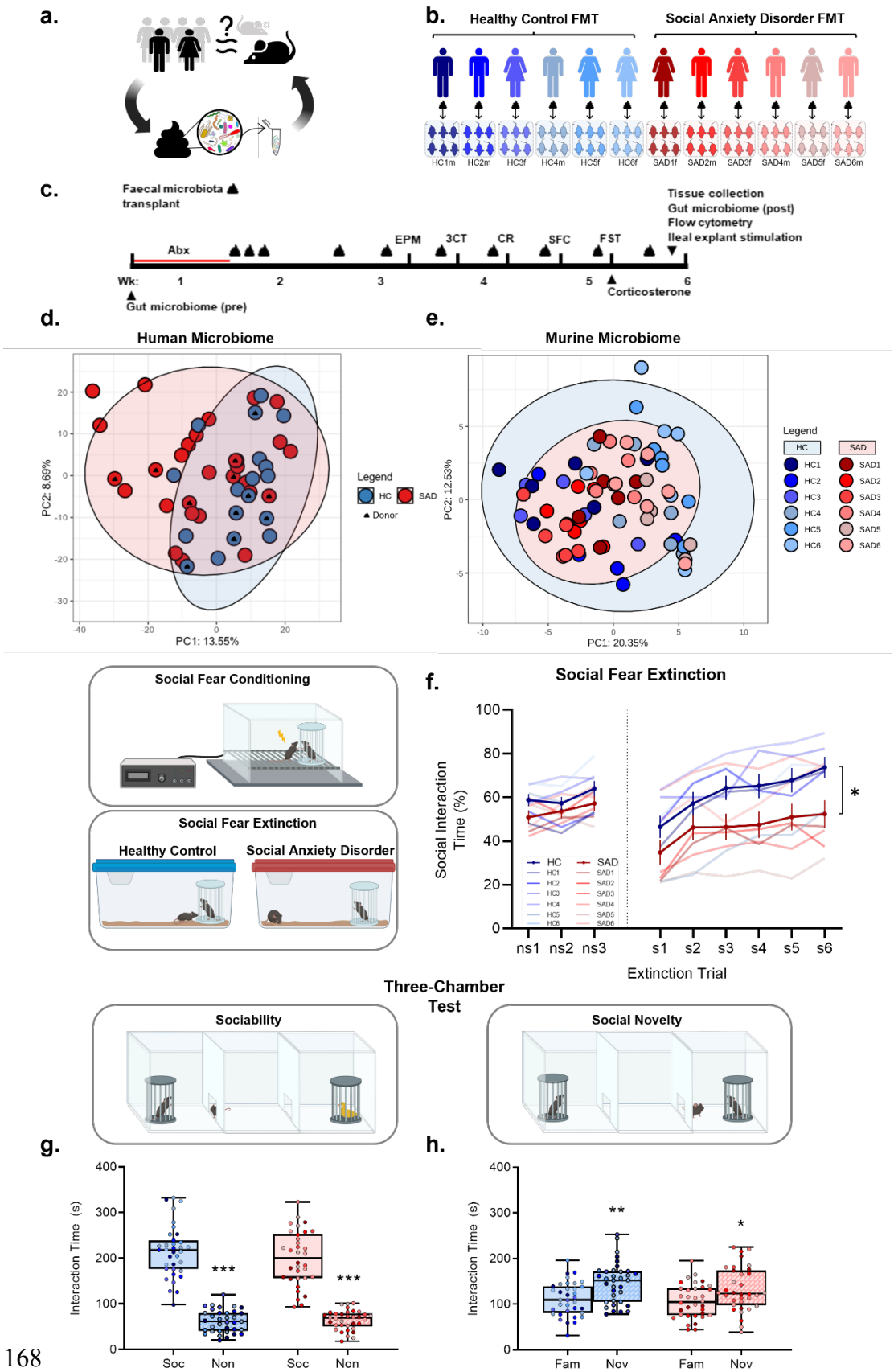

a.
b.
Healthy Control FMT
Social Anxiety Disorder FMT
HC1m HC2m HC3f HC4m HC5f HC6f SAD1f SAD2m SAD3f SAD4m SAD5f SAD6m
c.
Faecal microbiota transplant
Tissue collection
Gut microbiome (post)
Flow cytometry
Ileal explant stimulation
Abx
EPM
3CT
CR
SFC
FST
Wk: 1 2 3 4 5 6
Gut microbiome (pre)
Corticosterone
d.
Human Microbiome
PC2: 8.69%
PC1: 13.55%
Legend
HC
SAD
Donor
e.
Murine Microbiome
PC2: 12.53%
PC1: 20.35%
Legend
HC
SAD
HC1 HC2 HC3 HC4 HC5 HC6
SAD1 SAD2 SAD3 SAD4 SAD5 SAD6
Social Fear Conditioning
Social Fear Extinction
Healthy Control
Social Anxiety Disorder
f.
Social Fear Extinction
Social Interaction Time (%)
ns1 ns2 ns3 s1 s2 s3 s4 s5 s6
Extinction Trial
*
Three-Chamber Test
Sociability
Social Novelty
g.
Interaction Time (s)
***
***
Soc Non Soc Non
h.
Interaction Time (s)
**
*
Fam Nov Fam Nov

Fig. 1 Human gut microbiota from social anxiety disorder (SAD) promotes social fear behaviour in mice but does not alter other general social behaviours.

(a.) *In order to test whether the microbiota plays a causal role in SAD, the microbiota of individuals with SAD was transferred by faecal microbiota transplantation (FMT) to rodent recipients to assess phenotypic characteristics compared to FMT from healthy control.* ***(b.)*** *Study diagram and human donor and rodent recipient group legend, male (m) and female (f).* ***(c.)*** *Experimental design: animals first received an antibiotic cocktail (Abx) for 1wk to deplete the resident microbiota, before receiving FMTs, behavioural assessment (elevated plus maze - EPM, three-chamber test - 3CT, carmine red gastrointestinal transit and motility test - CR, social fear conditioning - SFC, and forced swim test - FST). Faecal samples were collected and microbiota analysed at the beginning and end of study. Corticosterone was measured before and after the FST. At the end of the study animals were euthanised, tissue was collected; then flow cytometry, and ileal explants were stimulated with lipopolysaccharide, concanavalin A, and CD3/CD28.* ***(d.)*** *Aitchison beta diversity of SAD human faecal microbiota in comparison to healthy controls (R^2=0.03477, p< 0.05, 1,000 permutations). Donors (indicated by the faecal symbol) were selected based on microbiota, Liebowitz Social Anxiety Scale score, age, body mass index, sex, and an absence of psychotropic or microbiota medications to treat SAD.* ***(e.)*** *Murine faecal bacteriome beta diversity was significantly different between SAD and HC groups at the end of the study (R^2=0.02767, p< 0.001, 1,000 permutations).* ***(f.)*** *Diagram represents social fear conditioning and social fear extinction, which takes place over two days. Social fear behaviour is increased in mice that receive SAD FMT (W(1)=3.239, p<0.05). Social fear extinction data showing interaction percent with either non-social stimulus (ns1-3) or six novel social stimuli (s1-6). Transparent lines represent each individual donor group (SAD5 and HC3 n=5; other groups n=6) while bold lines show mean±SE of the total HC and SAD groups (n=35 per group).* ***(g.)*** *Diagrams represent the three-chamber social interaction test. Following habituation, sociability was assessed by preference for a novel social stimulus over an inanimate, non-social object (rubber duck), then social novelty preference was assessed by preference for a novel conspecific over the now-familiar conspecific used in the sociability phase. There were no significant group differences in sociability; both groups spent significantly more time interacting with the social (Soc) stimulus over the non-social (Non) stimulus (t(68)=12.01, 11.64, p<0.001).* ***(h.)*** *There were no significant group differences in social novelty preference; both groups spent significantly more time interacting with the novel (Nov) over the familiar (Fam) social stimulus (t(68)=3.158, p<0.01; t(68)=2.513, p<0.05) (n=35 per group).*

Social anxiety disorder faecal microbiota transplant diminishes stress and immune function.

The glucocorticoid stress hormone corticosterone was measured in plasma of mice before and after the forced swim test. The basal plasma concentration of corticosterone was found to be significantly reduced by SAD FMT treatment ($t(64)=-1.858$, $p<0.05$) but no differences were found in corticosterone following stress (Fig.2a,b). Following euthanasia, small intestinal ileal tissue was explanted and stimulated with lipopolysaccharide (LPS), concanavalin A (ConA), T cell receptor clusters of differentiation 3 and 28 (CD3/CD28), or vehicle (buffer) to assess gut immune function in response to paradigmatic antigens between groups. Inflammatory cytokine supernatant concentration from the ileal tissue explants was then assessed. The SAD group displayed reduced IL-17A in response to stimulation by LPS ($t(30)=-2.297$, $p<0.05$) and ConA ($t(32)=-2.457$, $p<0.05$) and trends for reduced IL-17A in the vehicle ($t(32)=-1.804$, $p=0.081$) and CD3/CD28 stimulation ($t(30)=-1.813$, $p=0.100$) (Fig.3a). Mesenteric lymph nodes (MLNs) and blood were also harvested, and immune cell populations were assessed using flow cytometry. In the MLNs F4/80+ macrophages were significantly reduced ($t(30)=-2.602$, $p<0.05$) following SAD FMT while there was a trend for T helper cells to be increased following SAD FMT ($t(34)=1.953$, $p=0.079$) (Fig.3b,c). Within the blood immune cell population there was reduced CD4+ T helper cells in the SAD group ($t(34)=-2.049$, $p<0.05$) (Fig.3d). These data indicate that the SAD microbiota transfer reduced circulating stress hormone and peripheral immunity.

Next, to discern how central immunity was affected, neuroinflammatory- and blood brain barrier-related gene expression was measured in the bed nucleus of the stria terminalis (BNST), medial amygdala (MeA), and medial prefrontal cortex (MePFC). Arginase 1 (*Arg1*) expression was depleted across all three regions tested (BNST, MeA, and MePFC) following SAD FMT (t(43)=-3.927, $p<0.001$; t(43)=-3.241, $p<0.01$, t(42)=-3.55, $p<0.001$ respectively) (Fig.3e). In the MeA, tumour necrosis factor alpha (*Tnf-α*; t(35)= -2.081, $p<0.05$), interleukin 10 (*Il-10;* t(36)= -2.342, $p<0.05$), and chemokine C-X-C ligand 15 (*Cxcl15;* t(38)=-2.137, $p<0.05$) were all reduced (Fig.3e). In the MePFC Toll-like receptor 4 (*Tlr4*) was also reduced (t(40)= -2.839, $p<0.05$) (Fig.3e). Then, blood brain barrier-related genes were measured and the MeA showed the most significant reductions in tight junction protein 1 (*Tjp1*; t(43)= -3.033, $p<0.01$), claudin 5 (*Cldn5*; t(41)=-2.601, $p<0.05$), and occludin (*Ocln*; t(42)=-1.811, $p=0.08$) (Fig.3f). There was an additional trend for reduced *Ocln* in the BNST (t(43)=-1.901, $p=0.06$) and a reduction of *Tjp1* expression in the MePFC (t(41)= -2.473, $p<0.05$) (Fig.3f). These data show that neuroinflammatory markers are altered and blood brain barrier function is impaired by SAD FMT. This further demonstrates that the SAD microbiota is capable of far-reaching immunomodulatory effects.

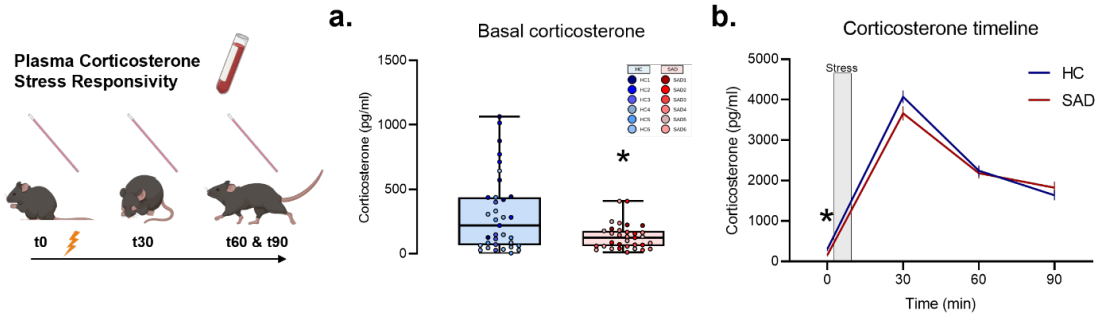


Fig. 2 SAD FMT modulates basal stress hormone corticosterone plasma levels.

(a.) *Basal plasma corticosterone is significantly reduced in the SAD group compared to HC ($t(64)=-1.858$, $p<0.05$) ($n=35$ HC, $n=33$ SAD).* ***(b.)*** *The stress response timeline measured by plasma corticosterone collected at 30-minute intervals over 90 minutes. The forced swim test (stress stimulus) took place from 5 minutes to 11 minutes (total duration of stress was 6 minutes). There was a significantly lower concentration of plasma corticosterone at the basal timepoint (0 minutes) in the SAD compared to HC group and no significant effects at the 30-, 60-, or 90-minute time points.*

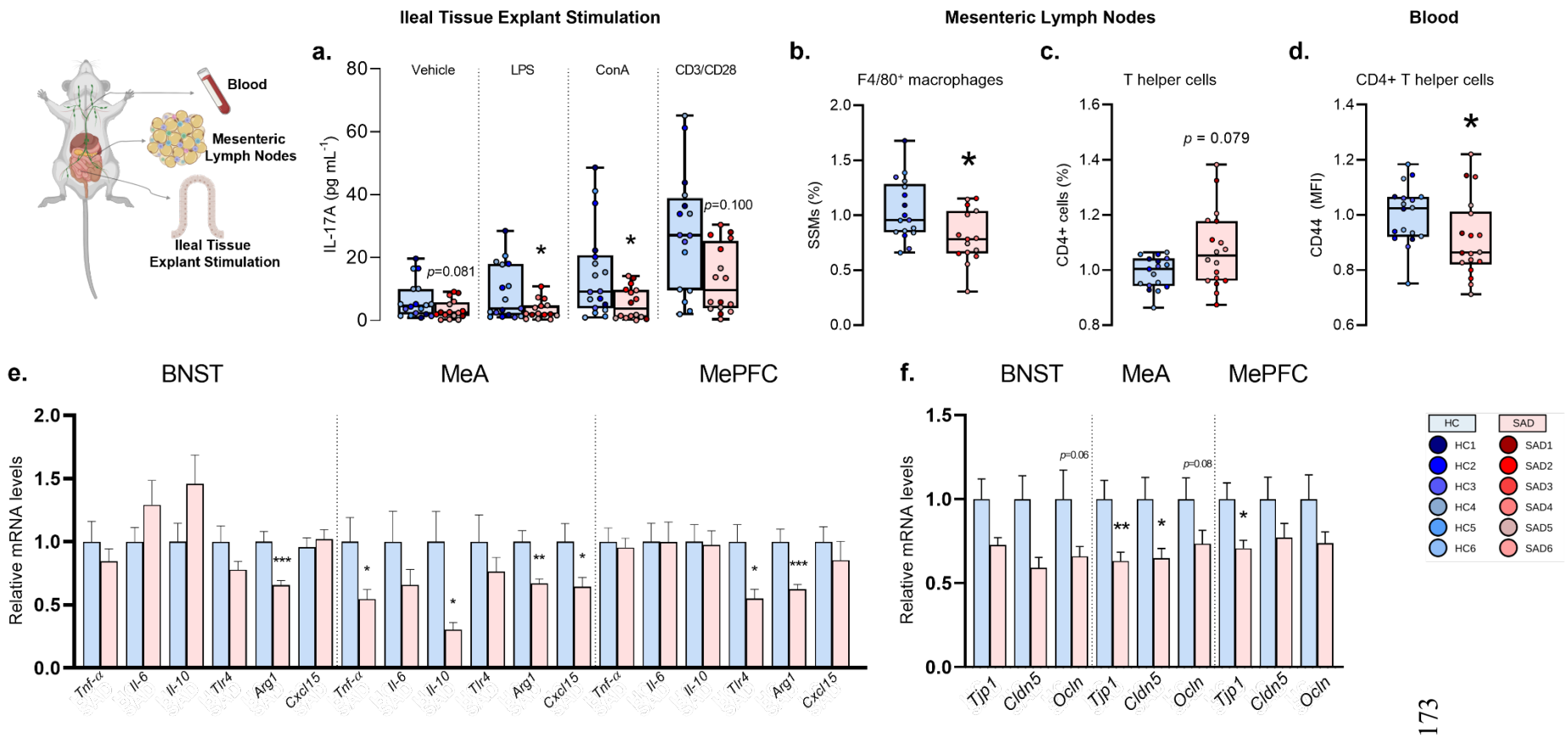

Blood
Mesenteric Lymph Nodes
Ileal Tissue Explant Stimulation
Ileal Tissue Explant Stimulation
a.
IL-17A (pg mL-1)
Vehicle
LPS
ConA
CD3/CD28
p=0.081
p=0.100
Mesenteric Lymph Nodes
b.
F4/80+ macrophages
SSMs (%)
c.
T helper cells
CD4+ cells (%)
p = 0.079
Blood
d.
CD4+ T helper cells
CD44 (MFI)
e.
BNST
MeA
MePFC
Relative mRNA levels
Tnf-α
Il-6
Il-10
Tlr4
Arg1
Cxcl15
f.
BNST
MeA
MePFC
Relative mRNA levels
Tjp1
Cldn5
Ocln
p=0.06
p=0.08
HC
SAD
HC1
HC2
HC3
HC4
HC5
HC6
SAD1
SAD2
SAD3
SAD4
SAD5
SAD6

Fig. 3 SAD FMT modulates ileal IL-17A, immune cell population composition, and gene expression markers related to neuroinflammation and blood brain barrier integrity.

(a.) *SAD FMT reduces IL-17A cytokines produced by ileal explants following stimulation with vehicle (buffer; $t(32)=-1.804$, $p=0.081$), lipopolysaccharide (LPS; $t(30)=-2.297$, $p<0.05$), concanavalin A (ConA; $t(32)=-2.457$, $p<0.05$) and CD3/CD28 ($t(30)=-1.813$, $p=0.100$) (n=16-18 per group).* ***(b.)*** *$F4/80^+$ macrophages in the mesenteric lymph nodes (MLNs) were significantly reduced in the SAD group compared to the HC group ($t(30)=-2.602$, $p<0.05$) (n=17 HC, n=15 SAD).* ***(c.)*** *There was a trend for increased $CD4^+$ T helper cells in the MLNs of the SAD group compared to the HC group ($t(10)=1.953$, $p=0.079$) (n=17 HC, n=18 SAD).* ***(d.)*** *The CD44 median fluorescent intensity was reduced in blood $CD4^+$ T helper cells in the SAD group compared to the HC group ($t(34)=-2.049$, $p<0.05$) (n=18 per group).* ***(e.)*** *Neuroinflammatory- and neuroimmune-related gene expression measured in the bed nucleus of the stria terminalis (BNST), medial amygdala (MeA), and medial prefrontal cortex (MePFC). In the BNST arginase 1 (Arg1) was reduced by SAD microbiota transfer ($t(43)=-3.927$, $p<0.001$). In the MeA there were reductions in expression of tumour necrosis factor alpha (TNF-α; $t(35)=-2.081$, $p<0.05$), interleukin 10 (Il-10; $t(36)=-2.342$, $p<0.05$), Arg1 ($t(43)=-3.241$, $p<0.01$), and chemokine C-X-C ligand 15 (Cxcl15; $t(38)=-2.137$, $p<0.05$). In the MePFC there were reductions in Toll-like receptor 4 (Tlr4; $t(40)=-2.839$, $p<0.05$) and Arg1 ($t(42)=-3.55$, $p<0.001$) following SAD microbiota transfer (n= 17-23 per group).* ***(f.)*** *Blood brain barrier-related gene expression measured in the BNST, MeA, and MePFC. In the BNST there was a trend for reduced occludin (Ocln) in the SAD microbiota transfer recipient group ($t(43)=-1.901$, $p=0.06$). In the MeA there were reductions in expression of tight junction protein 1 (Tjp1; $t(43)=-3.033$, $p<0.01$), claudin 5 (Cldn5; $t(41)=-2.601$, $p<0.05$), and Ocln ($t(42)=-1.811$, $p=0.08$). In the MePFC there was a reduction of expression of Tjp1 ($t(41)=-2.473$, $p<0.05$) following SAD microbiota transfer (n=20-23 per group).*

Reduced neuronal oxytocin in the bed nucleus of the stria terminalis and oxytocin-related gene expression in the medial amygdala and prefrontal cortex are associated with increased social fear.

Oxytocin, an extensive neuropeptide governing social behaviour, was measured in the paraventricular nucleus (PVN), supraoptic nucleus (SON), and the BNST by

immunohistochemistry. These brain regions have been shown to play key roles in directing social behaviour through oxytocin generation and signalling. The regions were stained for oxytocin (Oxt) containing neurons (NeuN) in HC and SAD FMT recipients (representative images of the BNST are shown in Fig.4a,b, PVN Fig.S4a,b, and SON Fig.S4d,e). No differences were observed in either the PVN or SON (Fig.S4c,f), but there was a significant reduction in Oxt neurons in the BNST ($t(17)=-2.369$, $p<0.05$) (Fig.3c). This result indicates that the BNST is sensitive to the SAD microbiota transfer and is associated with social fear behaviour.

Next, oxytocin- and vasopressin-related gene expression was measured in the BNST, MeA, and MePFC to assess potential transcription level alterations between SAD and HC FMT recipient groups. No statistically significant effects were identified in oxytocin gene (*Oxt*) or receptor expression (*Oxtr*) in the BNST, but there were reductions in both genes in the MeA ($t(34)=-2.455$, $p<0.05$; $t(40)= -2.143$, $p<0.05$, respectively) and reduced *Oxtr* in the MePFC ($t(40)= -2.419$, $p<0.05$). There was reduced vasopressin receptor 1a (*Avpr1a*) in the MePFC ($t(42)= -3.184$, $p<0.01$) in addition to trends for reduced *Avpr1a* in the MeA ($t(41)=-1.895$, $p=0.07$) and reduced vasopressin receptor 1b (*Avpr1b*) in the BNST ($t(41)=-2.115$, $p=0.06$). Taken together, these data reveal alterations in oxytocin- and vasopressin-related gene expression across these brain regions following SAD microbiota transfer to mice.

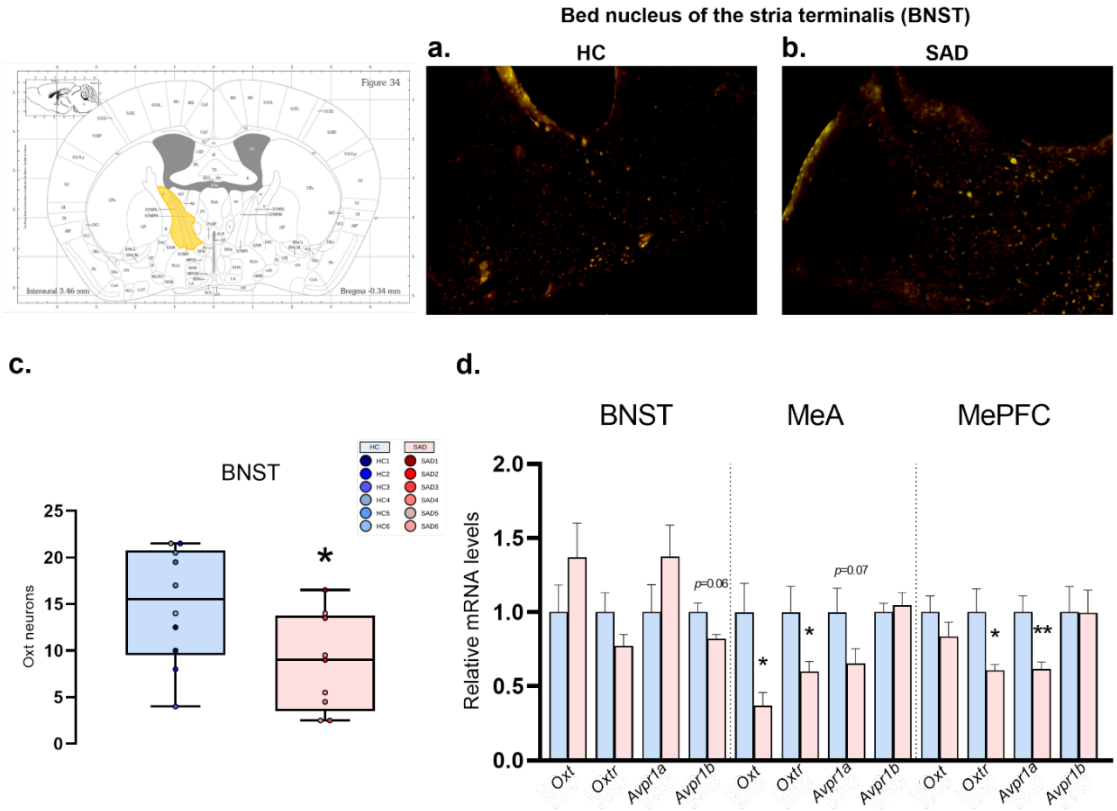


Fig. 4 SAD FMT modulates neurons containing oxytocin in the bed nucleus of the stria terminalis (BNST) and oxytocin- and vasopressin-related genes in the medial amygdala (MeA) and medial prefrontal cortex (MePFC).

Representative illustration of the bed nucleus of the stria terminalis (BNST)[67] and immunohistochemistry microscopy images of oxytocin (Oxt) staining in BNST neurons from HC ***(a.)*** *and SAD* ***(b.)*** *FMT recipients (0.02 and -0.08mm from Bregma; NeuN Alexa555, Oxt Alexa488).* ***(c.)*** *There was a significant reduction in the number of Oxt containing neurons in the BNST of the SAD group compared to the HC group ($t(17)=-2.369$, $p<0.05$) (n=10 HC, n=9 SAD).* ***(d.)*** *BNST, MeA, and MePFC expression of oxytocin- and vasopressin-related genes in the HC and SAD microbiota recipient groups. There was a trend for reduced vasopressin receptor 1b (Avpr1b) in the BNST ($t(41)=-2.115$, $p=0.06$) (n=22 per group). In the MeA there were reductions in oxytocin (Oxt; $t(34)=-2.455$, $p<0.05$), oxytocin receptor (Oxtr; $t(40)=-2.143$, $p<0.05$), and vasopressin receptor 1a (Avpr1a; $t(41)=-1.895$, $p=0.07$; n=20-22 per group). In the MePFC there were reductions in Oxtr ($t(40)= -2.419$, $p<0.05$) and Avpr1a ($t(42)= -3.184$, $p<0.01$; n=21-22 per group).*

4.4 Discussion

Understanding the biological basis of complex disorders such as SAD is an important endeavor in psychiatric research. Here we build on correlational observational studies to causally implicate a role for the microbiome in behaviours relevant to SAD.

At the microbiome level we show that the beta-diversity microbiota composition alterations observed in human patients with SAD are similar to the beta-diversity found to be different in recipient mice administered SAD or HC faecal microbiota from the selected human donors. Additionally, there were bacterial species that were differentially abundant across the murine groups. *Bacteroides nordii* was reduced in SAD compared to HC. Previously this species has been negatively correlated with neurodevelopmental behaviour syndromes[505]. *Bacteroides cellulosilyticus* was reduced in SAD compared to HC, and accompanying *B. nordii*, higher relative abundances have been associated with fewer symptoms in hyperactivity, impulsivity, and inattention (DSM- HD and AD scores)[506]. *Phocaeicola massiliensis* (formerly *Bacteroides massiliensis*) was increased in SAD compared to HC and has been linked with post-traumatic stress disorder[507] and prolonged social isolation stress[508]. These microbiota alterations indicate that there are microbial community and specific bacterial taxa differentially transferred to recipient mice by FMT from SAD compared to HC donors, resulting in transfer of a social fear sensitive phenotype to the recipients.

Social fear conditioning and extinction is a rodent behavioural test specifically designed to model the development and treatment of SAD. Pavlovian conditioning is used to first induce social-specific fear and then measure the rate at which fear diminishes in response

to repeated exposure to different social cues[336]. Following social fear conditioning there was a significant reduction in social interaction in the SAD group compared to the HC group (as measured the next day, during social fear extinction), indicating that a SAD microbiota transfer is capable of intensifying the social fear response. These effects are specific to social fear as there was no difference between groups in sociability or social novelty preference measured in the three-chamber test. This fits well with recent research indicating that a substantial proportion of individuals with SAD report normal (or even high) levels of extraversion and novelty-seeking/openness to new experiences, despite their anxiety about social situations[509,510]. Given that the hypothalamic pituitary adrenal (HPA) axis, immune and oxytocin systems have been implicated in social fear responses[340,511,512] we next assessed if the SAD recipient group also exhibited changes in these systems as a result of the FMT.

There was a significant reduction in plasma corticosterone measured before stress in the SAD group, but no difference in the stress hormone at timepoints following stress. In the SAD patient cohort, there was also a reduction of circulating anti-inflammatory cytokine Il-10 compared to HCs[325]. To assess gut immune function following activation, we stimulated ileal explants with LPS, ConA, and CD3/CD28, the latter two (ConA and CD3/CD28) induce T cell activation. We observed that interleukin-17A (IL-17A) was reduced in the SAD group ileal tissue explants stimulated with LPS and ConA, and there were trends for reduction following vehicle and CD3/CD28 stimulation compared to the HC group. IL-17A is a proinflammatory cytokine that is induced by infection, stress, and trauma[513]. Following perturbation, IL-17A is involved in sensory response, T cell

activation, and neutrophil mobilisation in various tissues[514-516]. Moreover, IL-17A has been shown to rescue sociability deficits in mice exposed to maternal immune activation during embryogenesis[517]. In the SAD FMT recipient animal MLNs, there was a significant reduction in F4/80$^+$ macrophages and a trend for an increase in the relative number of CD4$^+$ T helper cells. This fits with the migration of macrophages away from the MLNs previously observed following chronic stress and microbiota perturbation[309]. Furthermore, there was a reduction of CD44 receptors on circulating CD4$^+$ T helper cells in the SAD group, indicating inadequate immune memory and activation following SAD microbiota transplant. CD44 is a T cell activation marker indicating memory and effector populations from naïve T cell populations and has been linked with enhanced IL-17 production from T helper cells[518]. Taken together, these data indicate that the SAD microbiota drives HPA-axis dysfunction coupled with a reduction of IL-17A and circulating effector and memory T helper cells, leading to diminished immune signalling as a driving contributor to the SAD phenotype.

The neuropeptide oxytocin is a key modulator within the limbic system and has been shown to be critically involved in the circuitry mediating various social behaviours, including stress-induced defensive and social coping responses[519-521]. Oxytocin can elicit diverse effects in various brain regions mediated by circuit-specific actions which are further complicated by differences across sex, species, and models[522-526]. Oxytocin receptors in the BNST are activated by PVN and SON projections which have been shown to play a role in fear learning and memory[527]. Therefore, using immunohistochemistry, we next investigated the levels of the oxytocin within the hypothalamic PVN, SON, as

well as the BNST connecting the limbic forebrain to hypothalamic and brainstem regions. No differences in oxytocin containing neurons were observed in the PVN and SON, however, a significant reduction was observed in the BNST.

In addition to immunohistochemistry, we also measured genes responsible for oxytocin, oxytocin receptor (*Oxtr*), and vasopressin receptors 1a and 1b (*Avpr1a* and *Avpr1b*) in the BNST and other brain areas related to social fear behaviour- the MeA and MePFC. Oxytocin and vasopressin are both well known for playing roles in social behaviour and interestingly, we found a trend for a reduction of *Avpr1b* expression in the BNST. Disruption of Avpr1b has specifically been shown to reduce social memory and aggression in mice[528-530]. Furthermore, broad inhibition of Avpr1b with the antagonist SSR149415 partially attenuated the effects of social defeat on social anxiogenic behaviour indicating complex regional responsiveness and effectiveness[531]. Since oxytocin and vasopressin have been shown to modulate pro- and anti-social behaviour respectively, our data suggests that the BNST is a particularly sensitive region to SAD microbiota transfer to mice. However, the BNST is a complex structure that orchestrates emotional and behavioural responses to stress[532] by connecting to other brain regions involved in social circuitry and has been linked to responses to unpredictability that can worsen social anxiety[533]. It is a heterogenous brain area with many subregions and thus it is perhaps not unsurprising that there is disconnect between the data on oxytocin at the protein level in slices observed by immunohistochemistry versus the levels of gene expression in relatively crude tissue punch collections.

Importantly, oxytocin released in the MeA has been shown to facilitate social memory formation during social encounters[534]. Here we found reductions in both oxytocin and oxytocin receptor gene expression in the MeA in addition to a trend for reduced *Avpr1a*. Moreover, it has been shown that activation of neurons expressing *Oxtr* in the MePFC have been shown to increase activity of neurons in the BNST[535] indicating region-specific circuitry capable of modulating neural activity. Our MePFC data shows reductions in SAD microbiota recipient *Oxtr* and *Avpr1a* receptor gene expression, indicating that oxytocin and vasopressin receptor neural activity may be responsible for regional differences that can lead to increased sensitivity to social fear.

Next, we explored the mechanism by which this gut derived FMT treatment may be exerting a behavioural effect, and as we have observed immune modulation in ileal explants, MLNs, and blood. We thus chose to measure expression of neuroinflammation and blood brain barrier related genes in the brain regions (BNST, MeA, and MePFC). Alterations in such genes have been shown with antibiotic or dietary interventions targeting the microbiome previously[536,537]. Again, we noticed regional effects with the only shared gene being significantly reduced in the SAD microbiota recipient group across all regions was arginase 1 (*Arg1*), a marker in the brain of cellular repair activation following inflammation[538,539]. In the MeA there was a reduction in expression of inflammatory cytokine *Tnf-α* and *Cxcl15* in addition to a reduction in anti-inflammatory cytokine *IL-10*, indicating a modulation of the neuroinflammatory response by SAD compared to HC microbiota transfer. Additionally, we observed a reduction in *Tlr4* expression in the MePFC in the SAD FMT recipient group. This receptor is classically

known for mediating inflammatory responses following endotoxin activation and knockout of this gene has been shown to increase anxiety-like behaviour and reduce social interaction in mice[540]. Additionally, pharmacological blockade of Tlr4 in murine prefrontal cortex has been shown to modulate visceral hypersensitivity, further indicating it as a key marker of microbiota-gut-brain axis activity[541]. Last, we measured blood brain barrier related gene markers *Tjp1*, *Cldn5*, and *Ocln*. Interestingly, we observed reductions in *Cldn5* in the MeA, and *Tjp1* in both the MeA and MePFC. Previously it has been shown that social stress can reduce blood brain barrier integrity and *Cldn5* downregulation in the nucleus accumbens, another region in the limbic system linked with social and emotional behaviours[345,542]. These results indicate that there was a reduction in tight junction network and compromised barrier integrity following SAD microbiota transfer. Overall, these gene expression data provide a picture of neuroinflammatory and immune modulation that was associated with oxytocin and vasopressin alterations.

We next assessed the specificity of the behaviour alterations transferred by SAD FMT. There were no significant changes in anxiety-like behaviour in terms of time spent and entries into the open arms of the elevated plus maze, nor were there significant changes in stress-coping behaviour (measured as time spent immobile in the forced swim test). Gastrointestinal transit, measured by timing the duration of passage of carmine red following oral gavage, was also not different between groups. These outcomes further show that the SAD FMT recipients harbored very specific behavioural changes relevant to social fear domains with no distinguishable differences in other distinct social nor stress-coping behaviours, or in gastrointestinal function.

Taken together, our findings provide novel evidence that the microbiota in individuals with SAD can generate increased social fear that is associated with impaired peripheral immune activation and neuronal oxytocin within the BNST in mice. This suggests that the microbiota can play a causal role in heightened social fear responses in the disorder. Moving forward, the microbiota-gut-brain axis is an ideal target for identifying novel therapeutics to improve symptoms in SAD.

4.5 Methods Summary

Here, we provide a summary of the methods important to understand our study. Further details are given in *SI Appendix, Extended methods*.

Participants (FMT donors)

FMT donors were a subset of participants (18-65 years of age, male and female) recruited for our earlier descriptive study of the microbiota in SAD[274]. Briefly, the SAD group was recruited through local health practitioners and support groups or via an online website, and a primary clinical diagnosis of SAD was required for inclusion. The HC group were recruited through University College Cork and were required to have no past or current psychiatric diagnosis. For both groups, significant acute or chronic medical illness, other psychiatric illness, presence of any potentially confounding condition or medication, pregnancy or breastfeeding, and strict specific diets were considered exclusion criteria (see Butler et al., 2023 for further details[274]). The final subset of FMT donors (n=6 per group) were selected based on microbiota metrics, Liebowitz Social Anxiety Scale score, age, body mass index, sex, and an absence of psychotropic or microbiota medications (*i.e.*, antibiotics, probiotics, prebiotics, *etc.*; Table S2). All study procedures involving human participants were approved by the Clinical Research Ethics Committee of the Cork Teaching Hospitals (Study number APC085) and the study was conducted in accordance with the ICH Guidelines on Good Clinical Practice, and the Declaration of Helsinki. All participants provided written informed consent.

Animals (FMT recipients)

This study used male C57Bl/6J mice (N=72; 8 weeks of age on arrival; Envigo, UK; *n*=6 per donor and *n*=36 per group). Animals were habituated for 2 weeks after which treatments began. The holding room was under a 12-hour light/dark cycle (7:00-19:00), with a temperature of 21°C and humidity of 10%. Standard rodent chow (Teklad Global 18% Protein Rodent Diet, sterilized) and water were available *ad libitum* throughout the experiments. An examination of the literature, our own publications, and in-house data were carried out to determine probable effect sizes for behavioural readouts as a consequence of social fear conditioning and faecal microbiota transplantation. Comprehensive power analyses ($\alpha = 0.05$, power = 80%) were performed to determine the minimum number of animals required for each of the studies in this project to ensure pre-clinically and clinically relevant findings. All procedures involving animals were conducted in accordance with the European Directive 2010/63/EC, the requirements of the S.I. No 543 of 2012 and approved by the Animal Experimentation Ethics Committee of University College Cork and the Health Products Regulatory Authority (HPRA AE19130 P118). Procedures are reported in line with the Guidelines for Reporting on Animal Fecal Transplantation (GRAFT) Framework[9].

Antibiotic treatment

At the start of the study, mice were placed on an antibiotic cocktail consisting of ampicillin (1g/L), vancomycin (0.5g/L), imipenem (0.25g/L), and vancomycin (1g/L; all from Discovery Fine Chemicals, UK). This was prepared fresh every second day and administered to all animals *ad libitum* in the drinking water for seven days to deplete the resident microbiota (see Fig.1c for experimental timeline).

Faecal microbiota transplant (FMT)

SAD and HC faecal inocula were prepared for FMT within four hours of production. Samples were stored in an airtight container with an AnaeroGen sachet (Oxoid AGS AnaeroGen Compact, Fischer Scientific, Ireland) to maintain an anaerobic environment during transport. Upon arrival samples were immediately placed within an anaerobic cabinet, mixed with sterile reduced phosphate buffered saline 1% (PBS)/20% glycerol as cryoprotectant (final faecal inocula concentration: 100mg/mL), and manually passed through a 70µm stomacher filter to remove large particulates. Then samples were aliquoted and stored at -80ºC until administered to animals. Animals were randomised to a specific donor and received their respective FMT treatment via oral gavage (100µl) daily for three successive days followed by two booster FMTs per subsequent week for the remainder of the study (10 total FMTs).

Behavioural testing

Ten days after the start of FMT treatments, mice began behavioural testing comprising of the elevated plus maze (EPM), three chamber sociability test (3CT), carmine red gastrointestinal transit and motility (CR), social fear conditioning (SFC), and the forced swim test (FST), with a three to four-day interval between each test. Details regarding each behavioural test are given in *SI Appendix, Materials and Methods*. Three days after the end of testing, mice were euthanised by rapid decapitation (n=4 per donor) or perfusion (n=2 per donor, randomly allocated) and tissues were harvested to assess the microbiota, brain, and immune system function (Fig.1c). The allocation of samples was determined by power calculations described above.

Flow cytometry

Flow cytometry was performed as previously described[364,410]. Trunk blood samples collected during euthanasia were processed on the same day before flow cytometry analysis. Details regarding flow cytometry immune targets, staining, and analysis are given in *SI Appendix, Materials and Methods*.

Immunohistochemistry and microscopy

The paraventricular nucleus of the hypothalamus (PVN), supraoptic nucleus (SON), and bed nucleus of the stria terminalis (BNST) were sectioned and stained to visualize oxytocin (Oxt) containing neurons (NeuN). Details regarding collection, immunohistochemistry, and microscopy are given in *SI Appendix, Materials and Methods*.

Repeated blood sampling for stress and immune measures

Plasma from each animal was sampled by tail tip five minutes prior to the forced swim test, then thirty, sixty, and ninety minutes after the start of the test. The tail was securely restrained, and a diagonal incision was made approximately 1-2mm from the tip of the tail. Approximately 40µl of whole blood was collected in an EDTA-lined capillary tube (Fisher Scientific, 749311) per timepoint. Samples were deposited in an Eppendorf and centrifuged for 10min at 3500g at 4^{o}C. Plasma was collected and stored at -80^{o}C for later corticosterone quantification.

Corticosterone stress response timeline

Corticosterone quantification of plasma samples (10µl) collected during FST was performed using a corticosterone ELISA and carried out according to manufacturer's guidelines (Enzo Life Sciences, ADI-901-097). Samples were analysed in duplicate in a single assay, the threshold detection was less than 32pg/mL; coefficient of variation limit=20%; the concentration units are expressed in ng/mL. Light absorbance was read with a multi-mode plate reader (Synergy HT, BioTek Instruments, Inc.) at 405nm.

Ileal explant stimulations

Ileal tissue explants were collected during tissue harvest, trimmed of fat, and placed in RPMI medium (R8758, supplemented with 10% Foetal Bovine Serum (F7524, Sigma), and 1% penicillin-streptomycin-glutamine 100x (10378-016, Biosciences Ltd.). They were then treated with Red Blood Cell Lysis Buffer (R7757, Sigma), passed through a 70µm filter, and then resuspended in fresh supplemented RPMI medium. Next, 4mL of cells were seeded in 6-well plates at a concentration of 16x106 cells/well. After a 2.5hr rest period, cells were stimulated with lipopolysaccharide (2µg/mL, tlrl-eblps, Invivogen), concanavalin A (2.5µg/mL, C5275, Sigma), or CD3/CD28 (CD3 - 100238, CD28 - 102116, Biolegend) for 24hr. Then, cell suspensions were harvested and centrifuged (300g, 5min), and supernatants were collected for further analysis.

Inflammatory cytokine analysis

Cytokine levels from plasma and splenocyte supernatant samples was collected during euthanasia and were quantified using the V-PLEX Proinflammatory Panel 1 Mouse Kit (K15048D, Meso Scale Discovery, USA) measuring IFN-γ, IL-6, IL-12/IL-23p40, TNF-α, IP-10. Cytokine quantification was carried out according to the manufacturer's

guidelines. Samples below the detection limit of each assay were excluded. The lower threshold detection limits for each cytokine were: IFN-γ= 0.04 pg/mL, TNF-α= 0.13pg/mL, IL-1β= 0.11pg/mL, IL-4= 0.11pg/mL, IL-5= 0.06pg/mL, IL-6= 0.61pg/mL, IL-10= 0.94pg/mL, IL-13= 2.7pg/mL, IL-17A= 0.30pg/mL, IL-17E/IL-25= 1.6pg/mL.

Faecal microbiome collection, sequencing, and analysis

Human donor and murine recipient faecal microbiotas were analysed to assess the differences in community level composition between SAD and HC. Human donor microbiomes were assessed by 16S rRNA sequencing to identify target candidates to transfer to mice. Murine microbiomes were assessed by full metagenomic sequencing at the beginning of the study before any treatments and at the end of the study the day before euthanasia. Details regarding the collection, sequencing, and analysis of bacteriomes and viromes from human donor and murine recipient faecal microbiotas are given in *SI Appendix, Materials and Methods*.

Bioinformatics and statistical analysis of microbiome data

Data-handling of microbiome measures was undertaken in R (version 4.2.2) using the Rstudio GUI (version 2022.7.2.576) or Python (v3.11.0). Principal component analysis was performed on centred log-ratio transformed (clr) values as a visual companion to the beta diversity analysis. Alpha-diversity metrics were calculated using scikit-bio (v0.5.8; http://scikit-bio.org/). For all analysis beyond alpha-diversity, taxa with a prevalence of < 5% (at the species level for bacteria and vOTU level for viruses) were excluded from analysis as ratios are invariant to sub-setting and this study employs compositional data analysis techniques[432,433]. Zero values were then imputed for using the 'const'

approach[434]. Count data were then centred log-ratio (clr) transformed using scikit-bio. Differential abundance estimates were computed using the analysis of composition of microbiomes (ANCOM)[455] method within scikit-bio. Beta diversity was computed in terms of Aitchison distance (Euclidean distance of clr-transformed counts) and differences in beta diversity were assessed using the PERMANOVA implementation from the vegan library using 1000 permutations[456]. Plotting was handled using ggplot2 and the Python implementation of plotly (https://plotly.com/).

Gene expression of brain regions

The BNST, medial amygdala (MeA), and medial prefrontal cortex (MePFC) were dissected from frozen whole brain tissue using mouse brain matrices and a micropunch approach following mouse brain atlas coordinates[543]. Total RNA was extracted using the RNeasy® Plus Universal Mini Kit (catalogue no. 73404; Qiagen®, Germany) according to manufacturer's instructions. RNA concentrations were quantified using a Nanodrop™ spectrophotometer (Thermofisher Scientific®, USA). Complementary DNA (cDNA) was then synthesized using High-Capacity cDNA Reverse Transcription Kit (catalogue no. 4368814; Thermofisher Scientific®, USA).

Genes that were selected for analysis were chosen based on their role in oxytocin signalling, neuroinflammation, and tight junction proteins. Oxytocin signalling genes analysed were for oxytocin generation (*Oxt*), oxytocin receptor (*Oxtr*), vasopressin receptor 1a (*Avpr1a*), and vasopressin receptor 1b (*Avpr1b*). Neuroinflammation genes analysed were tumour necrosis factor alpha (*Tnf-α*), interleukin 6 (*Il-6*), interleukin 10 (*Il-10*), toll-like receptor 4 (*Tlr4*), arginase 1 (*Arg1*), and chemokine C-X-C ligand 15

(*Cxcl15*). Tight junction-related genes selected were tight junction protein 1 (*Tjp1*), claudin 5 (*Cldn5*), and occludin (*Ocln*). Then RT-qPCR was performed using SYBR® Green real-time PCR on the cDNA samples using SYBR green (KAPA SYBR® FAST Kit; catalogue no. KK4602; Sigma, USA) to evaluate gene expression levels. Gene expression levels were then analysed on an AB7300 system (Applied Biosystems, Thermofisher®, USA). Expression levels were calculated as the average of three replicates for each biological sample from both groups and all donors (n=23 per group) relative to β-actin expression. Then fold changes were calculated using the $2^{-\Delta\Delta CT}$ method[452].

Statistics

Behavioural, immune, and gene expression data were assessed for outliers defined as being outside of 2.5x standard deviations of the mean and were subsequently excluded from analysis. Further statistical analysis was handled in R (v4.2.2) using the R Studio GUI (version 2022.7.2.576) and in Python with SciPy (v1.9.3). To account for the nested donor structure, we used the linear mixed-effects modelling framework provided in the lme4 package in R[436], with the following model: feature ~ Treatment + (1|donor_ID). In all cases, an alpha threshold of 0.05 was used to denote significance.

Data availability

Human 16S rRNA sequencing data can be found in European Nucleotide Archive (ENA) under accession PRJEB68191. Murine metagenomic sequencing data can be found on figshare via the following link (https://figshare.com/projects/Social_Anxiety_Disorder-Associated_Gut_Microbiota_Increases_Social_Fear/185134). Other source data that

support the findings of this study are available from the corresponding author upon request.

Extended methods

Elevated plus maze

The elevated plus maze test (EPM) was used to assess anxiety-like behaviour and was conducted as previously described[2] (Fig.S3a,b). The maze apparatus was elevated 1m above ground and consisted of a grey plus (+) shaped maze with two opposing open arms and closed arms (50x5cm arm length, 15cm closed wall height, 1 cm open wall height). Experiments and habituation were conducted in red light (5lux). Mice were habituated to the room for 1hr prior to the test, then placed in the centre of the maze (facing an open arm) and allowed to explore for 5min. The maze was cleaned with 70% ethanol between each animal. Behaviour was videotaped from a ceiling-mounted camera and videos were scored blind for time spent in open arms and open arm entries (entrance defined as all paws in arm).

Three-chamber sociability test

The three-chamber sociability test (3CT) was used to assess sociability and social novelty preference and was conducted as previously described[3] (Fig.1h-j). The test apparatus was a rectangular box (20x40x22cm) divided into three chambers connected by small circular openings (5cm diameter). The two outer chambers contained wire stimulus cages (10cm diameter, 13cm height), allowing for visual, auditory, and olfactory interaction, but not physical contact. The test was conducted in a single session over three 10min phases,

consisting of habituation, sociability, and social novelty. During habituation, mice were allowed to explore the entire box with both wire cages left empty. In the sociability phase, one wire cage contained a novel, age-matched, conspecific, male mouse, whereas the other cage contained an object (rubber duck). In the social novelty phase, the original conspecific remained in the wire cage (familiar mouse), while the object was replaced with a novel conspecific mouse. Between phases, the test mouse was enclosed in the middle chamber. The whole apparatus and wire cages were cleaned with 70% ethanol after each test. To reduce potential anxiogenic factors, all mice were habituated to the testing room 60min before the test, the floor of the testing arena was covered with sawdust and testing was performed under dim light (60 lux). All experiments were videotaped using a ceiling camera and were scored blind for the time spent interacting with the wire cages.

Carmine red gastrointestinal transit and motility

To assess whole gastrointestinal transit and motility, test mice were administered carmine red dye (CR) by oral gavage and the latency to excretion of the first red-coloured faecal pellet was recorded (Fig.S3d).

Social fear conditioning

Social fear learning and social fear extinction were assessed in the social fear conditioning (SFC) test (Fig.1f,g)[4]. One week prior to SFC, mice were individually housed and remained in individual cages for the remainder of the study. The SFC consisted of a single conditioning session on the first day, followed by a single extinction session on the following day. The conditioning chamber consisted of a transparent box (29x25x25cm) enclosed in a wooden chamber to reduce external noise and visual stimulation. The floor

consisted of a removable stainless-steel grid connected to a shock delivery unit used for manual application of foot shocks. A video camera at the top of the chamber enabled recording.

During conditioning, mice were placed in the conditioning chamber with an empty wire mesh cage (10x8x7cm) placed in the corner as a non-social stimulus. Mice were allowed to freely explore the chamber and the non-social stimulus for 3min, before it was replaced by an identical cage containing an unfamiliar conspecific (the social stimulus). After 2s of interaction (defined by sniffing of the social stimulus), the experimental mouse was manually given a 1s electric foot shock (0.6mA). This was repeated each time the experimental animal returned to interact with the social stimulus. When no further social contact was made for a 2min period, mice were returned to their home cage. The first social contact and food shock occurred within 30s for all experimental mice, and all mice received between 2- and 5-foot shocks over a maximum 5min interval. The time mice spent investigating the non-social stimulus, as a pre-conditioning measure of anxiety, was analysed using an automated tracking program and no differences were observed (Ethovision 11.5, Noldus, the Netherlands). Wire mesh cages were cleaned with Trigene disinfectant between each extinction session.

On the next day, social fear extinction was assessed in the home cage of each experimental mouse. There was a total of 9 trials in the extinction session, each consisting of a 3min exposure to a social or non-social stimulus (placed on a short wall of the home cage), with a 3min inter-trial interval. For the first 3 trials, experimental mice were exposed to three non-social stimuli identical to the cage used during conditioning. Then mice were exposed

to six novel conspecifics (social stimuli) enclosed within the wire mesh cages. To reduce conditioned fear responses to the non-social stimulus, a clean wire mesh cage was placed in the home cage overnight between conditioning and extinction days. Wire mesh cages were cleaned with 70% ethanol between each extinction session. Stimulus investigation, defined as time spent interacting within 7cm of social stimulus, was analysed using an automated tracking program (Ethovision 11.5, Noldus, the Netherlands) and assessed as a readout of social fear during each trial of extinction.

Forced swim test

The forced swim test (FST) was used to assess stress-coping behaviour as previously described[5] (Fig.S3c). A glass cylinder (21cm diameter) was filled with 24+1ºC water to a height of 15cm, water was emptied and replaced after each individual. Experimental animals were placed in the water for 6min while being recorded by a ceiling-mounted camera. After each test, animals were gently dried with a towel and placed back in their home cage. The last 4min of the 6min test was manually scored for immobility behaviour by a researcher blinded to the experimental groups. Mice were judged to be immobile when only making movements necessary to keep its head above water.

Flow cytometry

Flow cytometry was performed as previously described[6,7]. MLNs and trunk blood samples collected during euthanasia were processed on the same day before flow cytometry analysis. Blood was resuspended in 10mL of red blood cell lysis buffer for 3min (15.5mM

NH4Cl, 1.2mM NaHCO3, 0.01mM tetrasodium EDTA, diluted in deionised water). Samples were then centrifuged (1500g, 5min, 20ºC), and resuspended in 45µl staining buffer (autoMACS Rinsing Solution, Miltenyi 130-091-222, supplemented with MACS BSA stock solution, Miltenyi 130-091-376) for staining procedure. Then, 5µl of FcR blocking reagent (Miltenyi, 130-092-575) was added to each sample. Next, samples were incubated with a mix of antibodies either for blood samples (CD11b VFITC Miltenyi 130-113-234, LY6G PerCP/Cy5.5 Biolegend 127615, LY6C APC Miltenyi 130-111-917, CD62L PE-Cy7 Biolegend 104417, MHC-II BV421 Biolegend 107632, CD4 BV605 Biolegend 100548, CD44 BV786 BD Biosciences 563736, CD69 PE Miltenyi 130-115-575) or MLNs (CD11b VFITC Miltenyi 130-113-234, LY6C APC Miltenyi 130-111-917, MHC-II BV421 Biolegend 107632, CD4 BV605 Biolegend 100548, CD44 BV786 BD Biosciences 563736, CD69 PE Miltenyi 130-115-575, CD11c PerCP-Vio700 Miltenyi 130-110-842, F4/80 PE-Cy7 Biolegend 123113) and incubated for 30min on ice. After, samples were fixed in 4% PFA for 30min on ice. Fixed samples were resuspended in staining buffer and analysed the next day on the BD FACSCelesta flow cytometer. Data were analysed using FlowJo (version 10). Live single cells were gated based FSC-height and SSC-height; subsequently LY6Chi monocytes ($CD11b^{+}$, $LY6C^{hi}$), neutrophils ($CD11b^{+}$, $LY6C^{+}$, $LY6G^{+}$), and T helper cells ($CD11b^{-}$, $LY6G^{-}$, $CD4^{+}$) were selected. Next, $LY6C^{hi}$ monocytes and neutrophils that contained CD62L or MHC-II were assessed in their relative proportion to the respective parent population. Then, T helper cells that were either $CD69^{+}$ or $CD44^{hi}$ were similarly assessed in their relative proportion of the total parent cell population.

Immunohistochemistry and microscopy

Mice were deeply anaesthetised with sodium pentobarbital (90mg/kg) and transcardially perfused with PBS followed by 4% PFA. Brains were post fixed in PFA for a minimum of 4hrs at 4°C and cryoprotected in a sucrose gradient for 48hrs at 4°C before being snap frozen and stored at -80°C. The brains were sectioned on a cryostat (Leica CM1900) at -20°C into coronal slices (40um thickness) and placed in -20°C in cryoprotectant solution until further processing. 7 representative sections per mouse between -0.28 and -1.155mm from Bregma (according to the 3rd edition of The Mouse Brain in Stereotaxic Coordinates[8]) were mounted on slides. Brain slices were washed 2x5min with 1xPBS and blocked for 1h at room temperature in 1xPBS with 0.3% TritonX-100 and 10% donkey serum. Next, sections were incubated overnight in 4°C with an anti-oxytocin antibody (1:3000; Immunostar, ref: 20068) in a carrier solution (1xPBS with 0.3% TritonX-10 and 2.5% donkey serum). After washing (2x5min with1xPBS), sections were incubated for 2h at room temperature with a secondary antibody (Alexa Fluor 488 donkey anti-rabbit, 1:500, Invitrogen, ref: A-21206) in the carrier solution. The slices were washed (3x10min in 1xPBS) and incubated for 2h at room temperature with NeuN, Alexa Fluor 555 conjugate (1:200, Abcam, ab2072281) in the carrier solution and for 10min with DAPI (286nM in 1xPBS with 0.1% Tween). After washing (2x5min in 1xPBS), coverslips were added using Immu-Mount (Epredia, USA).

Images of BNST, PVN and SON were collected under the fluorescence microscope (Olympus bx51) using a 10x and a 20x objective. SON (20x images; analysed area: from

-0.28 to -1.055mm from Bregma) oxytocin positive cells were counted manually in ImageJ using the Cell Counter function. In BNST there were few oxytocin positive neurons visible on the level of 0.02 and -0.08mm from Bregma. To count oxytocin cells in PVN (10x images; analysed area: from -0.48 to -1.155mm from Bregma), an ImageJ macro was written.

Faecal bacteriome collection and sequencing

16S sequencing of human donor faeces

The QIAamp DNA Stool Mini Kit (Qiagen, Hilden, Germany) was used to extract bacterial DNA using the manufacturer's handbook (Second Edition 2012) Isolation of DNA from Stool for Pathogen Detection protocol. Samples were prepared for 16S sequencing using the Nextera XT DNA Library Prep Kit (Illumina, San Diego, CA, USA), as described in the Illumina 16S library preparation workflow. 16S bacterial rRNA gene was amplified using primers targeting the V3-V4 hypervariable region (Forward: 5'TCGTCGGCAGCGTCAGATGTGTATAAGAGACAGCCTACGGGNGGCWG-CAG; Reverse: 5'GTCTCGTGGGCTCGGAGATGTGTATAAGAGACAGGAC-TACHVGGGTATCTAATCC) (Sigma Aldrich Ireland ltd., Wicklow, Ireland). The Illumina V3–V4 primers were selected for their high coverage (94.5% bacteria) while remaining in the amplicon size necessary for sequencing[9]. 16S rRNA amplicons were sequenced on the Illumina MiSeq platform (Teagasc, Moorepark, Ireland).

Metagenomic sequencing of murine recipient faeces

The QIAamp Fast DNA Stool Mini Kit (Qiagen, Hilden, Germany) was used to extract DNA from faecal pellets. This was performed following the manufacturer's guidelines.

Before extraction, however, 20µL the ZymobIOMICs spike-in control 1 (Zymo Research, Irvine, CA, United States) was added to aid in calculating absolute abundances. DNA concentrations were then measured using the Qubit High Sensitivity assay (Thermo Fisher Scientific) before performing reverse transcription, Superscript IV (Invitrogen/Thermo Fisher Scientific) following the manufacturer's guidelines on 22µL of sample to incorporate RNA viruses within the microbiome. Samples were then adjusted to a volume of 52.5µL sheared with a M220 Focused-Ultrasonicator (Covaris) applying the 350bp DNA fragment length settings (peak power 50W, duty factor 20%, 200 cycles per burst, total duration of 65s). Sequencing libraries were subsequently created using the xGen ssDNA & Low-Input DNA Library Prep Kit (IDT). Library quality was assessed using the 4200 Agilent Tapestation (Agilent Technologies, Santa Clara, CA, United States) using the High Sensitivity D1000 ScreenTape assay (Agilent Technologies) before whole metagenomic sequencing was performed on an Illumina Novaseq 6000 platform using 2 × 150nt paired-end chemistry (Genewiz, Germany).

Faecal virome collection and sequencing

For faecal samples, a single faecal sample from each mouse was pooled per donor group (*n*=12 donors) in 650µl of SM buffer. Fresh 0.5M dithiothreitol was prepared in 1mL of SM buffer. A volume of 16µl of the dithiothreitol stock was added to samples to achieve a final concentration of 12mM, and samples were incubated at 37°C for 30min. Centrifugation at 4,000g for 30min at room temperature was used to pellet debris and bacterial cells. Subsequently, 400µl of liquid was removed and treated with 40µl of DNase/RNase buffer (50mM MgCl2, 10mM CaCl2), 12µl (24U) of Turbo DNase (Thermo Fisher) and

4µl (40U) of Fermentas RNase I (Fisher Scientific) at 37°C for 1h. Nucleases were inactivated by incubating at 65°C for 10min. With free nucleic acids now removed virus like particles (VLPs) were lysed using the QIAgen Blood and Tissue Kit following the manufacturer's guidelines. However, an elution volume of 30µl of Qiagen AE elution buffer (10mM Tris-HCl, 0.5mM EDTA, pH 9.0) was used to increase the final concentration of nucleic acid obtained.

Prior to library preparation, 22µl of each sample underwent reverse transcription using the Superscript IV kit (Invitrogen/Thermo Fisher Scientific) and sonicated to fragment DNA as described above. Samples were then concentrated using the Genomic DNA Clean and Concentrator kit from Zymo Research and eluted in 16µl. Library preparation was then carried out using xGen ssDNA and Low-Input DNA Library Prep Kit (IDT) according to the manufacturer's instructions. However, a final and additional bead clean-up step of 0.8 DNA/AMPure beads v/v ratio was included. Library QC to determine fragment length distribution and quantitation was performed using the 4200 Agilent Tapestation (Agilent Technologies, Santa Clara, CA, United States) using the High Sensitivity D1000 ScreenTape assay (Agilent Technologies) and Invitrogen Qubit. The normalised pooled library was then sequenced using 2 × 150 nucleotide paired-end sequencing chemistry on the Illumina NovaSeq 6000 platform at Genewiz (Leipzig, Germany).

Analysis of bacteriome sequencing data

For reads generated from whole-metagenome sequencing, reads pre-processing was conducted to remove adaptors, trim low-quality bases, and filter reads for quality and length

using fastp v0.23.2[10] with the flags '*--length_required 60 --detect_adapter_for_pe --trim_tail1 15 --trim_front2 15*'. Eukaryotic reads were then identified and removed by mapping reads to the *Mus musculus* and *Homo sapien* genomes (GCF_000001635.27_GRCm39 and GCF_009914755.1_T2T-CHM13v2.0 respectively) using Kraken v2.1.2[11]. Reads corresponding to the common Illumina sequencing internal control phiX-174 were removed using bbduk from the BBMap suite of tools (v39.01; https://sourceforge.net/projects/bbmap/) with options '*k=31 hdist=1*'. At each step read quality was assessed using FastQC v0.11.9 (https://www.bioinformatics.babraham.ac.uk/projects/fastqc/), with all read-QC outputs collated using MultiQC v1.13[12]. Taxanomic profiling of the microbial community within each sample was determined using the MetaPhlan4 v4.0.3[13] with the '*mpa_vJan21_CHOCOPhlAnSGB_202103*' database.

Analysis of total viral sequences within the bulk metagenomic sequencing data

Reads obtained from virome sequencing were pre-processed using the same steps applied to the whole metagenome sequencing reads, *i.e.*, trimming and filtering using fastp, eukaryotic decontamination using Kraken2, and phiX-174 removal using bbduk, with quality assessed using FastQC and MultiQC. Reads passing these steps were then assembled for each sample using metaSPAdes v3.15.5[14]. Reads were also assembled in groups by donor wherein the reads for each donor virome sample (*i.e.*, pre- and post-FMT mouse viromes were combined along with their donor virome) and assembled using MEGAHIT v1.2.9[15]. The contigs from all assemblies were then pooled and filtered to retain only contigs ≥ 3Kbp in length using the '*reformat.sh'* script from the BBMap suite. Redundancy

among the contigs was then removed by retaining only unique contigs or the longest contigs from hits with ≥ 95% identity over ≥ 95% of the shortest contig's length via an all-vs-all comparison of the contigs using BLASTn v2.13.0+ (e-value cut-off of ≤ 1 x 10^{-20})[16].

Putative viral sequences were then identified using a combination of geNomad[17] with the following paramaters '*end-to-end --splits 12 --cleanup --composition virome --enable-score-calibration*', and BLASTn comparisons (e-value cut-off of ≤ 1 x 10^{-10}) against the National Center for Biotechnology Information (NCBI) RefSeq viral database release 215, the Joint Genome Institute (JGI) IMG/VR v4.1 database[17], our in-house crAss-like bacteriophage genome database, and those bacteriophages listed in the International Committee on Taxonomy of Viruses (ICTV) Virus Metadata Resource (VMR) table that were available within GenBank. For the BLASTn comparisons, contigs were deemed as potentially viral if the contig had at least 50% identity ≥ 85% of its length to a known virus in any of these databases. Putative viral contigs were then examined with CheckV v1.0.1[18] and its sequence database v1.5. Where a sequence was defined as proviral by CheckV the trimmed proviral sequence suggested by CheckV was then used instead of the original sequence. As this refinement altered the contig lengths, contigs were again filtered to remove contigs ≤ 3Kbp. Viral sequences were then subset into viral operational taxonomic units (vOTUs) based on sharing 95% average nucleotide identity over at least 85% of the aligned fraction of the shortest of the 2 contigs[19].

The vOTUs were then again examined using CheckV to retain only contigs that matched the following criteria: 1) contig < 100kb in length, viral gene count > 0 and bacterial gene

count < viral gene count (likely a known virus with minimal host contamination); 2) contig ≥ 100kb, viral gene count > 0 and host gene count < 20 % contigs total gene count (potential large virus with minimal host contamination); 3) Contigs where viral gene count = 0 and bacterial gene count = 0 (potential novel viral contig). In all cases only contigs with at least 5 putative genes and either ≥ 50% completeness by CheckV or where an estimation of completeness could not be assigned (*i.e.*, potentially novel viral sequence) were considered further.

Quantitative analysis was achieved by mapping the trimmed/filtered reads per sample against the viral contig database using Bowtie2 v2.5.0[20] in '*--end-to-end*' mode. Mapping information was then processed using SAMTools v1.16.1[21] to obtain read coverages and mapping counts. Cases of spurious mapping were eliminated from the count data by assigning the read count value to 0 for any contig found to have at least 1x coverage over < 75% of its length. The abundance of each of the viral contigs within the viral contig database was estimated using 'total-sum scaling'[22], wherein read counts are normalised by contig length and the total number of reads used for mapping in a sample (*i.e.*, contig read count / contig length / sample read count).

Taxonomy was assigned to each of the vOTUs by resubmission to geNomad to obtain updated taxonomic information (mainly in case the vOTU was represented by a sequence previously designated a proviral element, and therefore trimmed as this may have altered the initial geNomad taxonomy). Taxonomy was further assigned by comparing the final vOTU set to the RefSeq viral, IMG/VR, ICTV, and our in-house crAss virus database using BLASTn ('*-evalue 1e-10*') and clustering all hits into vOTUs as described earlier.

Any assembled sequence that clustered into a vOTU with a reference virus was then assigned the taxonomic designation of the reference virus.

Acknowledgements

The authors would like to thank the volunteer donors who participated in the study as well as Drs. C. Fulling, K.E. Guzzetta, A. Lannon, J. Pereira-Cruz, S.J. Leigh, C.M.K. Lynch, M. Segalla, E. Myers, M. Neto, M. van de Wouw, and J. Nagpal for their technical assistance and knowledge sharing with the study, as well as P. Fitzgerald, C. Manley, J. Riley, and A. Markewinski for their assistance with mouse husbandry. The authors acknowledge the use of the APC Microbiome Ireland Flow Cytometry Platform. APC Microbiome Ireland is a research centre funded by Science Foundation Ireland (SFI), through the Irish Governments' national development plan (grant no. 12/RC/2273_P2). A.N.S. was supported by a Wellcome Trust Research Career Development Fellowship [220646/Z/20/Z], and the European Research Council (ERC) under the European Union's Horizon 2020 research and innovation programme (grant agreement No 101001684). Illustrations were adapted, in part, using graphics created with BioRender.com (DH261LA17M), Servier Medical Art, and Inkscape Project.

Author contributions

N.L.R., M.I.B., C.C., L.A.D, V.T., L.M., M.R.A., G.M.M., C.H., G.C., D.A.S., T.G.D, and J.F.C. designed the studies. N.L.R. and M.B. performed the experiments with animals. N.L.R., M.B., M.I.B., C.C., C.B., L.A.D., V.T., L.M., D.C., C.E.G., A.R., V.S., A.G., and G.M.M. performed assays, sample collection, and processing. C.T., A.N.S., and T.F.S.B.

generated metagenomic and virome sequencing analyses. N.L.R., C.T., and T.F.S.B. analysed the data. N.L.R. and J.F.C. wrote the paper with contributions made from all the authors.

4.6 Supplemental Figures

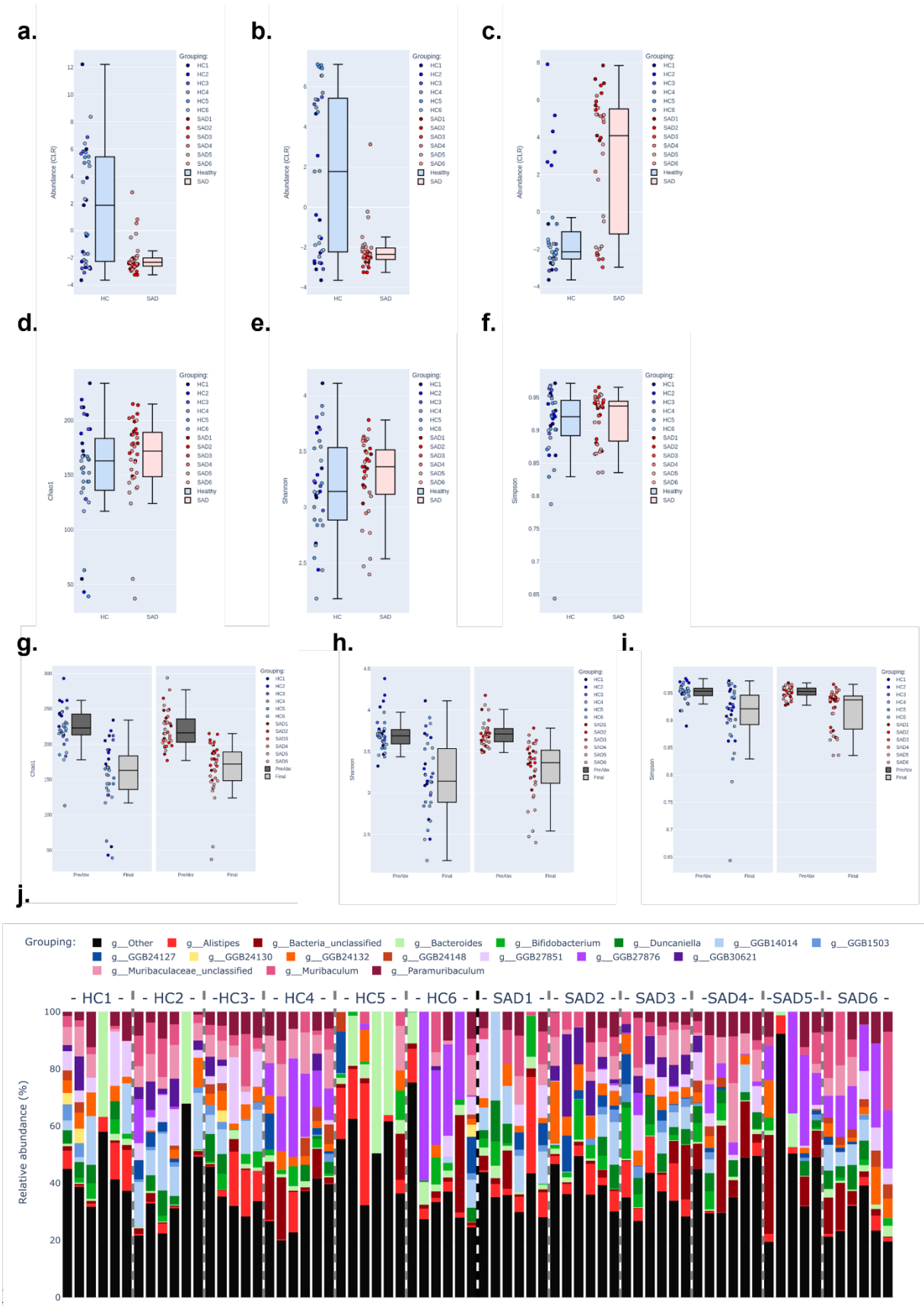

a.
b.
c.
d.
e.
f.
g.
h.
i.
j.
Grouping:
HC1
HC2
HC3
HC4
HC5
HC6
SAD1
SAD2
SAD3
SAD4
SAD5
SAD6
Healthy
SAD
Abundance (CLR)
Chao1
Shannon
Simpson
HC
SAD
PreAbx
Final
g__Other
g__Alistipes
g__Bacteria_unclassified
g__Bacteroides
g__Bifidobacterium
g__Duncaniella
g__GGB14014
g__GGB1503
g__GGB24127
g__GGB24130
g__GGB24132
g__GGB24148
g__GGB27851
g__GGB27876
g__GGB30621
g__Muribaculaceae_unclassified
g__Muribaculum
g__Paramuribaculum
- HC1 -
- HC2 -
-HC3-
- HC4 -
- HC5 -
- HC6 -
- SAD1 -
- SAD2 -
- SAD3 -
-SAD4-
-SAD5-
- SAD6 -
Relative abundance (%)

Fig. S1 Bacteriome measures.

*(**a.**) Bacteroides nordii is reduced in SAD compared to HC (W=273, p<0.05; ANCOM). (**b.**) Bacteroides cellulosiyticus is reduced in SAD compared to HC (W=246, p<0.05; ANCOM). (**c.**) Phocaeicola massiliensi is increased in SAD compared to HC (W=274, p<0.05; ANCOM). (**d.-f.**) There is no statistical difference between the SAD and HC recipient groups in bacteriome alpha diversity metric comparisons measured at end of study (**d.** Chao1; **e.** Shannon; **f.** Simpson). (**g.-i.**) Before treatment (PreAbx) and end of study (Final) alpha diversity measures of the bacteriome (**g.** Chao1; **h.** Shannon; **i.** Simpson), the alpha diversity scores of each group are significantly reduced at end of study compared to the beginning (p<0.05) (n=35 mice per group). (**j.**) Stacked bar plots displaying bacteriome genus community profile at end of study for each individual mouse separated by donor and group. For each bacteriome figure n=35 mice per group.*

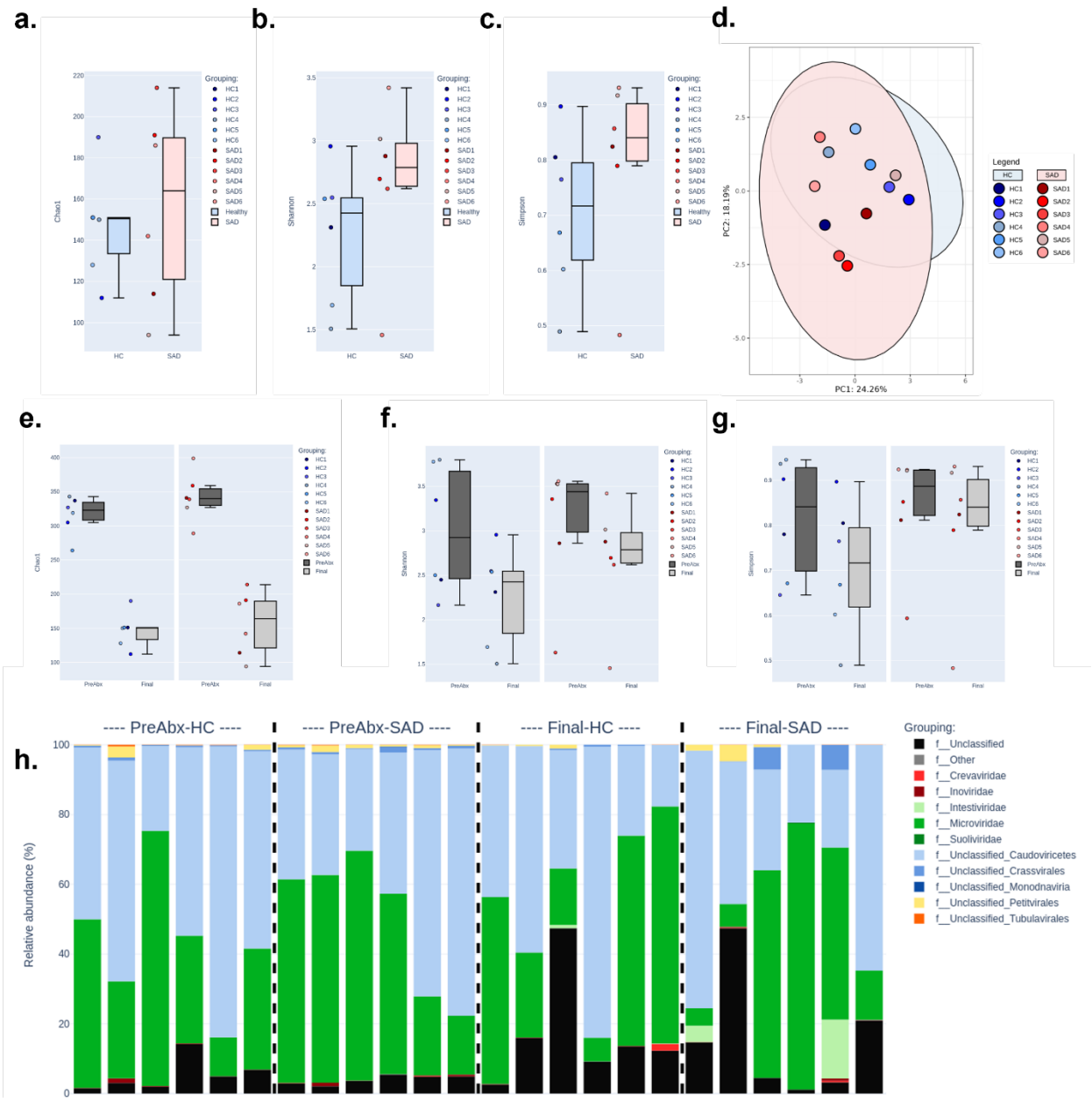


Fig. S2 Virome measures.

*(**a.-c.**) There is no statistical difference between the SAD and HC recipient groups in virome alpha diversity metric comparisons at end of study (**a.** Chao1; **b.** Shannon; **c.** Simpson). (**d.**) There was no significant shift in viral Aitchison beta diversity between groups. (**e.-g.**) Before treatment (PreAbx) and end of study (Final) alpha diversity measures of the virome (**e.** Chao1; **f.** Shannon; **g.** Simpson), (**e.**) Chao1 virome richness was significantly reduced at end of study compared to the beginning ($p<0.05$), but there were no differences in (**f.**) Shannon or (**g.**) Simpson. (**h.**) Viral family composition of each*

donor-recipient group before treatment and at end of study, respectively. Donor group viromes were pooled to ensure adequate nucleic acid concentration (n=35 mice per group, 5-6 per donor).

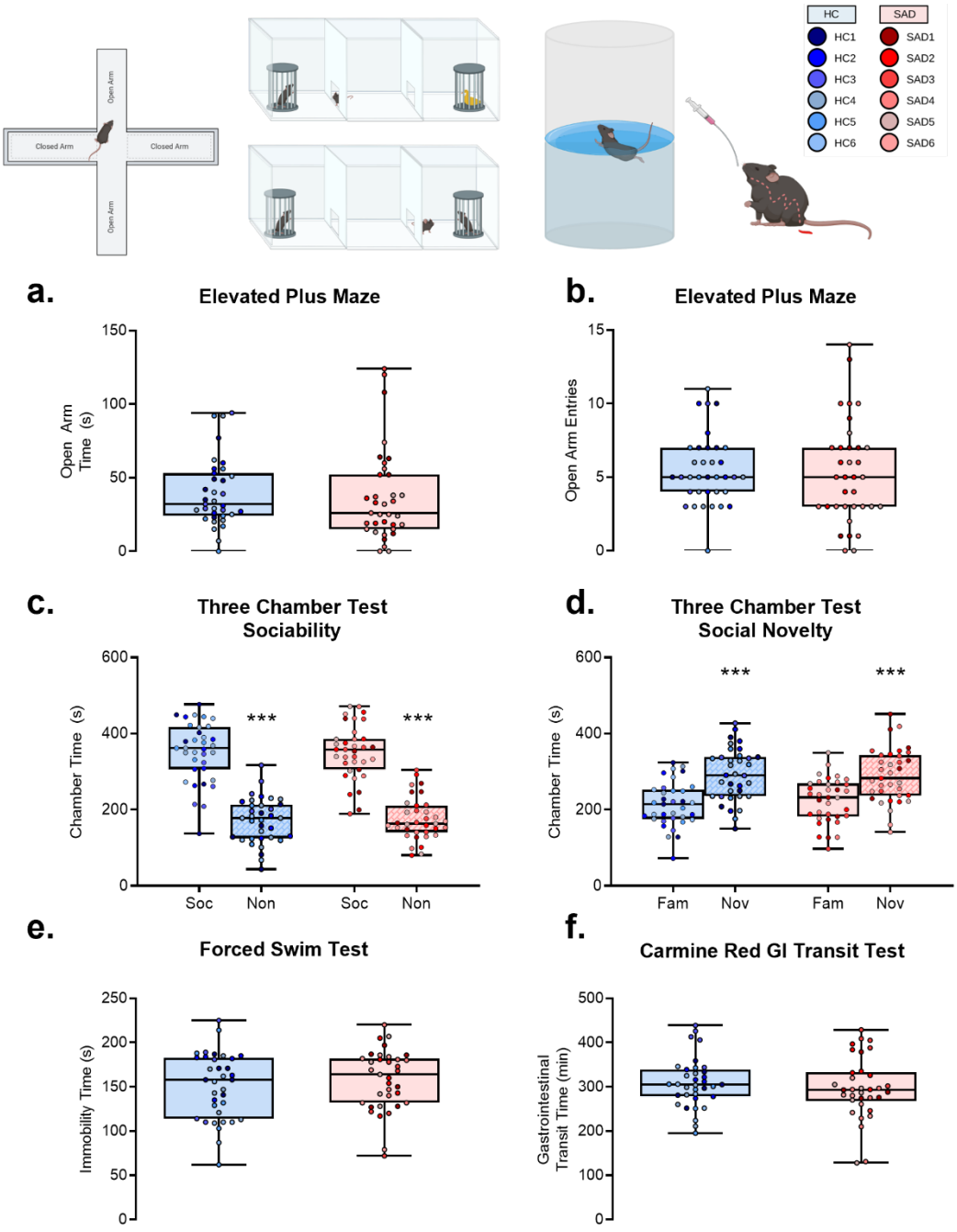


Fig. S3 General anxiety-like, social, and stress-coping behaviours, and gastrointestinal (GI) transit time are not affected by faecal microbiota transplantation (FMT) from social anxiety disorder (SAD) patients, compared to FMT from healthy controls (HC).

*(**a.**) General anxiety-like behaviour was measured by total time spent in open arms of elevated plus maze and (**b.**) total number of entries into open arms. (**c.**) Following habituation, sociability was assessed by preference for a novel social stimulus over an inanimate, non-social object (rubber duck), then social novelty preference was assessed by preference for a novel conspecific over the now-familiar conspecific used in the sociability phase. There were no significant group differences in sociability; both groups spent significantly more time interacting with the social (Soc) stimulus over the non-social (Non) stimulus ($t(68)=9.202, 8.861, p<0.001$). (**d.**) There were no significant group differences in social novelty preference; both groups spent significantly more time interacting with the novel (Nov) over the familiar (Fam) social stimulus ($t(68)=3.895, 3.193, p<0.001$) ($n=35$ per group). (**e.**) Stress coping behaviour measured by total time spent immobile in the forced swim test. (**f.**) Gastrointestinal transit and motility was measured by the total time elapsed for carmine red dye to be expelled after oral gavage in the carmine red gastrointestinal transit test ($n=35$ per group).*

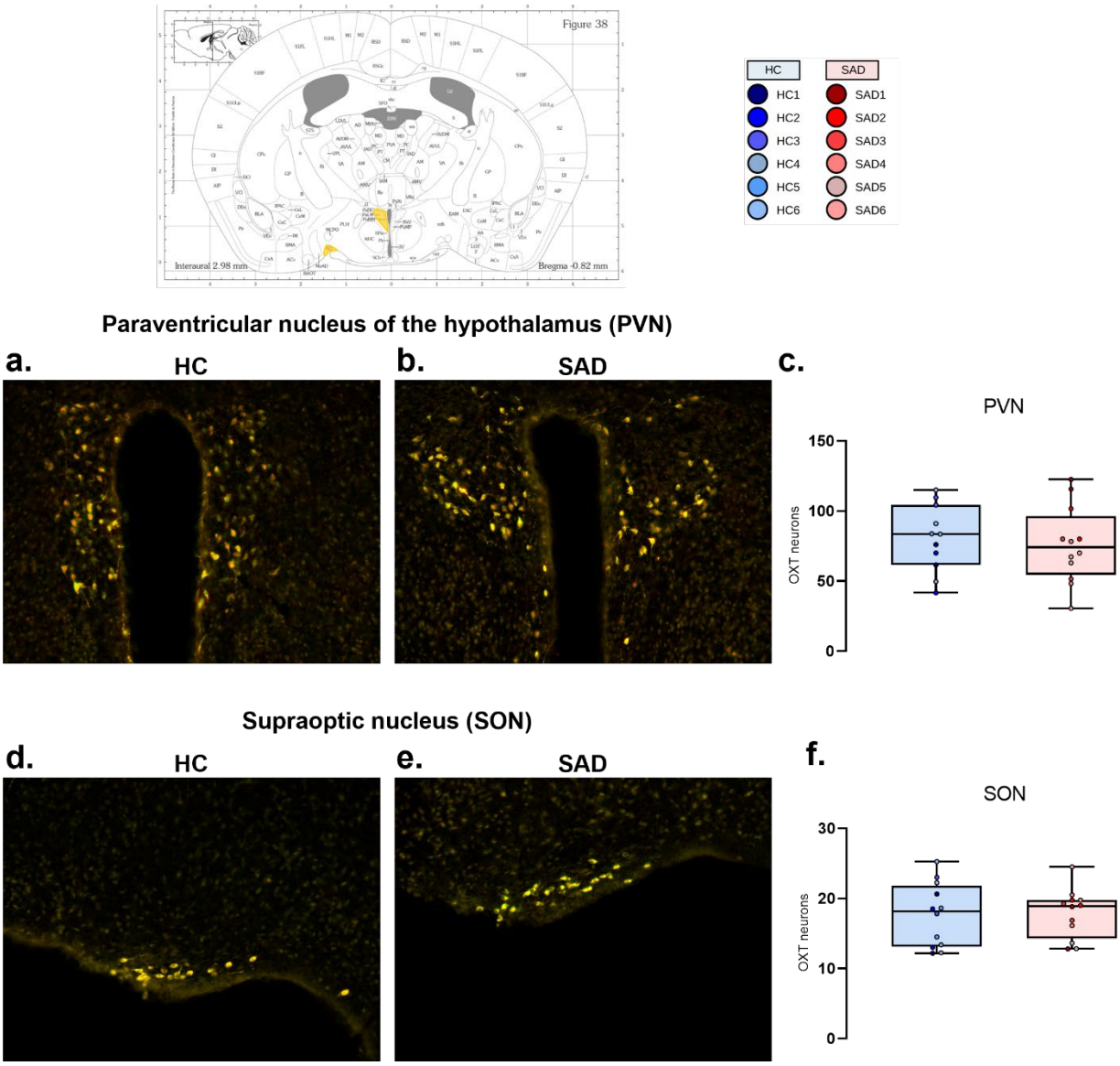


Fig. S4 Oxytocin levels are not modulated in the paraventricular nucleus and supraoptic nucleus by social anxiety disorder FMT.

Representative illustration of the paraventricular nucleus of the hypothalamus (PVN) and supraoptic nucleus (SON)[67] and immunohistochemistry microscopy images of oxytocin (Oxt) staining in PVN neurons from HC ***(a.)*** *and SAD* ***(b.)*** *FMT recipients (NeuN Alexa555, Oxt Alexa488).* ***(c.)*** *There was no statistically significant difference observed in Oxt containing neurons in the paraventricular nucleus (PVN). Representative immunohistochemistry microscopy images of Oxt staining in SON neurons from HC* ***(d.)*** *and SAD* ***(e.)*** *FMT recipients (NeuN Alexa555, Oxt Alexa488).* ***(f.)*** *There was no*

significant difference observed in Oxt containing neurons in the supraoptic nucleus (SON) ***(d.)*** *(n = 12/group).*

Table S1 Inflammatory cytokine and flow cytometry immune measures.

(a) *Inflammatory cytokine ileal explant stimulation and basal blood plasma of healthy control (HC) and social anxiety disorder (SAD) groups.* ***(b)*** *Immune cell population data of SAD blood and mesenteric lymph nodes (MLNs) relative to HC. Mean percent of parent population or median fluorescence intensity data presented with general linear mixed effects model comparison between HC and SAD (*p<0.05, #p<0.1) (n=35 per group).*

Table S1a

	Ileal Explant Stimulations								Blood Plasma	
	Vehicle		LPS		ConA		CD3/CD28		Basal	
Inflammatory Cytokines (pg/ml)	HC	SAD	HC	SAD	HC	SAD	HC	SAD	HC	SAD
IFN-γ	0.84	1.08	2.41	1.40	2.53	1.79	3.84	2.15	0.64	0.66
TNF-α	5.41	5.87	13.19	13.19	5.35	4.72	6.95	5.84	6.53	5.68
IL-1β	2.44	2.96	5.41	5.15	3.58	3.56	3.32	2.83	0.67	0.76
IL-4	0.39	0.16	0.32	0.24	0.21	0.19	0.76	0.35	-	-
IL-5	19.7	30.7	22.33	22.00	26.42	16.30	26.46	22.16	-	-
IL-6	2156.25	2999.64	3339.97	3473.91	2087.59	1914.00	2179.37	2240.43	4.41	9.67
IL-10	9.76	9.97	31.96	33.87	9.72	8.50	12.34	12.12	9.69	8.86
IL-13	-	-	-	-	5.66	4.23	-	-	-	-
IL-17A	6.40	3.48#	8.89	3.46*	14.83	5.52*	27.85	13.05#	-	-
IL-17E/IL-25	1.20	1.07	0.60	1.02	1.68	1.27	0.87	1.12	-	-

Table S1b

Flow Cytometry

	Blood		Blood		MLNs		MLNs	
	Percent of parent population		Median fluorescence intensity		Percent of parent population		Median fluorescence intensity	
Immune cell populations	HC	SAD	HC	SAD	HC	SAD	HC	SAD
LY6Chi Monocytes (CD11b+, LY6G-, LY6Chi)	1.00	0.92	-	-	-	-	-	-
CD62L+ LY6Chi Monocytes	1.00	0.90	1.00	0.97	-	-	-	-
CD11b+ LY6Chi Monocytes	-	-	1.04	1.06	-	-	-	-
MHC-II+ LY6Chi Monocytes	-	-	1.05	0.97	-	-	-	-
Neutrophils (CD11b+, LY6G+)	1.00	0.98	-	-	-	-	-	-
CD62L+ Neutrophils	1.00	1.03	1.00	0.89	-	-	-	-
MHC-II+ Neutrophils	1.00	1.38	1.00	1.00	-	-	-	-
CD11b+ Neutrophils	-	-	1.04	1.18	-	-	-	-
T helper cells (CD4+)	1.00	0.95	1.00	1.04	0.99	1.07#	1.00	1.02
CD44hi T helper cells	1.00	0.95	1.00	0.91*	1.00	1.08	1.00	1.14
CD69+ T helper cells	1.00	1.11	1.00	1.05	1.02	1.13	1.00	1.06
Macrophages (CD11b+, LY6C-, F4_80+)	-	-	-	-	1.05	0.85*	-	-
CD11b+ Macrophages	-	-	-	-	-	-	1.02	0.98
CD11c+ Macrophages	-	-	-	-	-	-	1.00	1.13
F4_80+ Macrophages	-	-	-	-	-	-	1.05	1.15
Dendritic cells (MHC-II+, CD11c+)	-	-	-	-	1.04	0.93	1.00	0.98
CD11b+ Dendritic cells	-	-	-	-	1.00	1.01	1.00	0.98
CD11c+ Dendritic cells	-	-	-	-	-	-	1.00	1.05
MHC-II+ Dendritic cells	-	-	-	-	-	-	1.00	0.92

Table S2 Demographic characteristics of faecal microbiota donors.

	SAD (*n*=6)	**HC (*n*=6)**	***p*-value**
Age (years); mean (SEM)	37.8 (2.6)	41.8 (5.2)	0.54
Sex; % female (*n*)	50 (3)	50 (3)	0.50
Race; % Caucasian (*n*)	100 (6)	83.3 (5)	0.36
Years of education (SEM)	18.7 (0.9)	19.8 (2.0)	0.63
Delivery mode at birth %			0.41
• Vaginal	66.7	83.3	
• Caesarean section	16.7	16.7	
• Unknown	16.7	0	
BMI (kg/m^2); mean (SEM)	26.4 (1.5)	25.3 (2.5)	0.56
Alcohol (units per wk); mean (SEM)	9.3 (4.3)	2.8 (0.7)	0.20
Alcohol categories; % (*n*)			0.30
• 0-3 units/wk	50 (3)	66.7 (4)	
• 4-9 units/wk	16.7 (1)	33.3 (2)	
• ≥10 units/wk	33.3 (2)	0 (0)	
Smoking status; % smokers (*n*)	16.7 (1)	0 (0)	
Exercise (IPAQ score); mean (SEM)	1230.8 (528.0)	4945.5 (996.3)	0.02
Exercise (IPAQ category); % (*n*)			0.10
• Low	50 (3)	0 (0)	
• Moderate	33.3 (2)	16.7 (1)	
• High	16.7 (1)	66.7 (4)	
Psychotropic medication% (*n*)			
• No medication	100 (6)	100 (6)	
• Taking medication	0 (0)	0 (0)	

Chapter 5

Discussion and conclusions

5.1 Summary

In this thesis, we have explored the role of the gut bacteriome and virome in chronic stress and social fear behaviour (Table 5.1). The gut microbiota is made up of tremendous microbial diversity that we are, as of yet, only now realizing the depth and potential impact of unexplored microbes. Bacteriophage viruses have increasingly been implicated for their role in the microbiota and health and disease, and this work further supports their capability as a potential microbiota-based treatment for stress and suggests their candidacy for future work in other disorders linked to the microbiota-gut-brain axis. The role of the gut virome is less clear in social fear and social anxiety disorder (SAD), likely due to large unknown and undefined populations of viruses and phages. There is, however, a clear association between social fear response variability and bacteriome Aitchison beta diversity distance from the centroid. Moreover, by use of microbiota transfer from human donors with SAD to mouse recipients, we show that the SAD microbial community can elicit heightened sensitivity to social fear in addition to immune, basal forebrain oxytocin, and gene expression in multiple central regions.

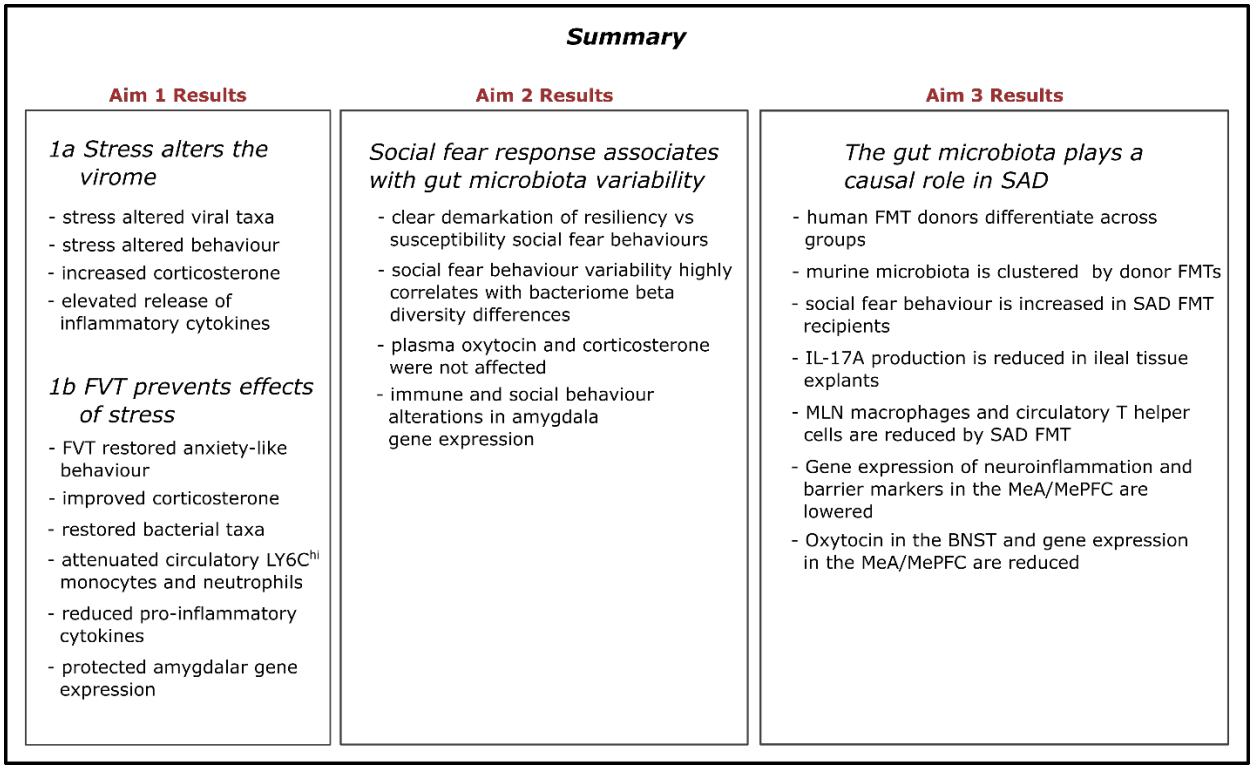
The results presented in the first data chapter (Ch. 2) show that the gut virome can attenuate stress-induced changes in behaviour and immunity in mice. The effects of the FVT administered during stress protected against many stress-related effects observed in the control stress group. The FVT improved stress-associated reductions in behaviour (locomotor and anxiety-like behaviours), immune cells (circulating monocytes and neutrophils), inflammatory cytokines (IP-10, TNF-α, IL-6, and IL-12), and restored gene expression in the amygdala. The alterations in the immune system in central and

peripheral tissues suggest that the virome transfer restored the microbiota from a stressed and inflammatory state to one of homeostasis which then resulted in diminished pro-inflammatory and immune effects in the host. These data demonstrate that the gut virome is altered by stress and that returning it to the stressed host in the form of an autochthonous FVT is capable of protecting against stress-related brain and behaviour sequelae.

In the second data chapter (Ch. 3) we demonstrate that the response to social fear conditioning is associated with microbiome variability. While there are various risk factors for SAD, the biological mechanisms underpinning social fear resiliency and susceptibility are a topic of active research. We approached this question in the context of the microbiota-gut-brain axis and identified inherent differences in how mice respond to social fear conditioning. Interestingly, there is a strong correlation between social fear extinction behaviour and bacteriome Aitchison beta diversity variability. While there have been many links between the microbiota and social behaviour in the past[313], this is the first association between the microbiota and social fear. We also observed a trend for virome variability to correlate with social fear, but it appears that bacteriome composition is more important here. We explored corticosterone and inflammatory cytokines in the periphery and oxytocin markers in the periphery and the brain but did not find any differences between groups. However, with transcriptomic analysis we found differential gene expression in the amygdala of mice between resilient, susceptible, and control extinction social fear profiles. Many of these genes have been previously associated with social behaviour, inflammation, immunity, and microbe-host interaction.

The final data chapter (Ch. 4) explores the causal mechanisms underlying SAD and social fear in the context of the microbiota-gut-brain axis. In this translational study we found that individuals with SAD and matched healthy controls (HC) had different microbiota compositions by Aitchison beta diversity. We then identified and selected microbiota transplant donors based on microbiota composition, Liebowitz Social Anxiety Scale score, not taking any psychotropic or microbiota medications, and otherwise demographic matched between SAD and HC. After FMT to mouse recipients we found that the microbiota alterations observed in humans were similarly transplanted to mice. We also found that mice that received the SAD FMT had increased sensitivity to social fear, but not other social, anxiety-like, or depressive-like behaviours. This was particularly intriguing as it shows that the microbiota transfer specifically altered social fear behaviour, but not others, even those that would be frequently comorbid with SAD. We also found reductions in immune cell populations (mesenteric lymph node macrophages and T helper cells in circulation), the inflammatory cytokine IL-17A produced by stimulation of ileal tissue explants, and inflammatory cytokine and blood brain barrier - related expression of genes which were both reduced in the medial amygdala and medial prefrontal cortex. Then, we explored neuronal oxytocin in the bed nucleus of the stria terminalis and oxytocin-related gene expression in the medial amygdala and medial prefrontal cortex and found that overall oxytocin and vasopressin related genes in these regions was downregulated following SAD FMT. These differences indicate that the microbiota in SAD can play a causal role in driving the progression of the disorder through immune and oxytocin pathways downregulation in the brain and periphery.

Table 5.1 Summary of thesis findings. *In this work we have successfully tested the three aims to assess the role of the virome in stress, find associations between the microbiota and social fear, and show that the social anxiety disorder (SAD) microbiota plays a causal role in the condition.*



5.2 Faecal virome transplant as a tool to elucidate the role of the stressed gut virome

Chronic social stress was shown to modulate the bacteriome and virome as well as behaviour, the HPA axis, and immunity. This led us to question whether a phage-based treatment would be sufficient to restore these components of the microbiota-gut-brain axis during stress. Ideally, identifying the phages modulated by stress would provide candidate treatment strains to test for efficacy. However, the lack of identification and resolution

capacity of viral sequences, and the inability to culture many gut microbes with current techniques, creates arduous hurdles to overcome at this time. Fortunately, there is an elegant solution by transplanting the entire population of free phages through a faecal virome transplant (FVT).

The process to create an FVT requires the collection of faeces from specified donors followed by separating the viral content from the rest of the faecal microbiota, compounds, and particulate primarily through the use of size stratification techniques[151]. These processes include centrifugation, filtration, and dialysis followed by gradient reconcentration to provide a biologically active dose. An important consideration of this technique is that, as discussed in the introduction, phages are present in multiple forms in the gut environment. FVT methods primarily isolate the free form of phages that are fully intact and ready to infect specific hosts upon encounter. However, most phages in the gut are temperate, meaning that they can be virulent (*i.e.*, lytic) and lysogenic. Indeed, temperate viruses are predominantly lysogenized prophages which would not be collected in FVT preparations[103,151].

By using this FVT model we can then introduce a large number of phages to infect gut bacteria of the host while undergoing chronic social stress. Another important consideration though is that while viromes within an individual are highly stable over time, they are highly divergent between individuals[123]. This means that the phageome from one individual has a high likelihood of discordancy for infection of the bacteriome of another individual. For this reason, we designed an autochthonous FVT study whereby each animal that received an FVT had an individual-specific transfer generated from their

own microbiota from a pre-stress (*i.e.*, healthy) timepoint to assure highest concordance between phage predators and their bacterial hosts.

5.3 Limitations of faecal virome transplant studies

There are many subjects related to this work that need more tools and approaches for researchers to design more elegant studies and solutions. Viral and particularly phage sequencing databases need more characterization and novel insights in how to measure the many taxa comprised within. The human virome is largely unknown, and yet, the murine virome is even less characterized. The direct and indirect activity of phages is difficult to decipher due to their various infection pathways (virulent, lysogenic, temperate, pseudolysogeny, chronic infection, *etc*.). At this time, we can correlate species that are altered by FVT and phage infection but the environment is too complex to definitively describe individual phage-host interactions. These questions would be best answered by *in vitro* and reconstituted GF limited consortia animal models. More expansive gut microbe culturing techniques are also needed so that we can directly characterize phage-host dynamics and subsequently deliver specific microbes identified with different diseases and disorders. Last, more control groups would always be ideal to test hypotheses more comprehensively (such as an unstressed FVT, a stressed donor FVT, an inactivated FVT, *etc*.). However, it was our goal to design the most efficient and effective experiments to replace, reduce, and refine the use of live animals in scientific research.

5.4 Future of virome therapeutics

There is an exciting future ahead for virome-based therapies. Phage-therapy for infectious pathogens has already been in use for decades, but going forward we have the potential to design virome-therapies to confer optimal microbiota health. FVT provides a top-down approach to modulate large swaths of the microbial community, but in coming years we will see more targeted approaches to eliminate, or render less virulent, pathobionts and microbes associated with pro-inflammatory cascades. There is also the potential to design phage cocktails to enhance probiotic strain function by arming them with greater metabolic range, protection from microbial predation, and production of key compounds. Virome, and specifically phage, therapies are advantageous because they are more resistant to our aerobic atmosphere, cryopreservation, and have high target specificity (reducing side effects). One potential issue is the very same high target specificity, in that phages usually target specific strains of bacteria that may or may not be present in many individuals. Another issue is that viruses have a very high mutation rate, so divergent effects cannot be ruled out. Regardless, more research is needed to see where virome transfers can be beneficial and much more research is needed in categorizing the gut virome so that we may better characterize their role and function in the microbiome.

In many ways there is an exciting future in phage therapy. Not only will there be more attainable and widespread use for phages targeting infectious pathogens, but there will be the capability to use phages to improve microbiota health. As we continue to elucidate phage biology in the gut, we will be able to design therapeutics with highly specific

targeting of pathobiont and commensal species. While delivering virulent phages offer the most direct mechanism of lysing unwanted microbes, temperate phages will allow a more nuanced approach where we be able to edit the microbiota through horizontal gene transfer. With this method we could improve the function of beneficial members of the microbiota by extending their metabolic range, increasing niche-colonization, and even protecting them from microbial competitors.

Already the virome and phage therapy are being tested in gut diseases like inflammatory bowel disease[544], irritable bowel syndrome[354], colorectal cancer[545], and of course *C. difficile*[151]. There is also clear potential to increase phage therapeutics outside of the gut. Phages can be delivered to other organs that have a microbiota including the skin[546], oral cavity[547], respiratory tract[548], urogenital tract[549], mammary gland[550], and cancer[545,551,552] as well as diseases and disorders associated with other organs but can be affected through the gut microbiota such as liver disease[553,554], hypertension[555], and diabetes[556].

To accomplish this more preclinical research and tools need to be developed that will help us design and enable more options for hijacking the microbiota to optimize human health.

5.5 The social fear conditioning paradigm in the context of the microbiota-gut-brain axis

The social fear conditioning behavioural test has proven to be a robust model of social anxiety disorder[336]. It has proven to be an effective paradigm to elicit and measure social fear. Interestingly, we found no sociability or social novelty preference differences

between SAD and HC groups in Ch. 4, further underscoring how testing a response to a negative stimulus is more powerful than testing without the appropriate context to the disease or disorder being modeled. In Ch. 3 and Ch. 4 we also measured how social fear extinction behaviour was affected in an acute time scale (one day between conditioning and extinction), but there is also the potential to test behaviour after an extended period of time[451]. The shorter timescale worked well for our study aims, but in the future it would be interesting to see how social fear behaviour is affected after a longer duration, as this long-term effect is seen in some individuals with SAD. Microbiota-based treatments to stabilize variability should be sought to increase normal fear extinction behaviour and resiliency. Probiotic and short chain fatty acid treatments have already been shown to alleviate stress-related effects and would make ideal candidates to bolster social fear sensitivity[27,557]. This study links social fear behaviour differences with variability in the gut microbiota and alterations in amygdalar gene expression, however further work is needed to characterize the mechanistic pathways driving these changes.

5.6 Social anxiety disorder humanized mice to assess microbiota driving social fear causality

In our translational model we first showed that there are inherent microbiota alterations between individuals with SAD and matched healthy controls. Then we designed a preclinical microbiota transfer study to humanize mice with microbiota from donors selected to represent each condition and then test disorder specific effects for behaviour, HPA axis, immune, and oxytocin pathways. Six representative donors were selected for

each group (SAD and HC) to FMT into their own specific subgroups, so that each donor FMT was administered to six mice (n=36 per group). This allowed for a donor covariate to be included in the statistical linear model to assess differences between treatments, which is an important feature in establishing microbiota causality in donor/recipient studies[150,501,502]. To increase engraftment of donor microbiota, mice were administered a cocktail of antibiotics for microbiota-depletion prior to FMT. Using this method, we show the causal role of the microbiota in SAD. This is a comprehensive translational approach to establish the role of the microbiota in a microbiota-gut-brain axis disorder. It requires a full team of experts in clinical psychiatry, preclinical neuroscience animal models, bioinformatics, and molecular and microbiological techniques. This has potential to serve as a template for assigning causality in the microbiome field.

5.7 Limitations of microbiota-gut-brain axis and social fear

We found no microbiota differences between male and female SAD FMT donors and transferred all microbiotas into male mice. This decision was made since there were no microbiota sex effects observed, despite some differences being reported in males and females with the disorder[558]. We also made this decision to increase the robustness of the model and the statistical approach, as well as reduce the total number of animals needed to complete the study. However, we do advocate for increased female testing, especially when there is a biological basis for expecting differentiation between the sexes[559]. SAD

also typically arises in individuals during adolescence[560]. This may indicate that beginning the FMT to adolescent rather than adult mice may increase the effects we observed. In this regard, recolonizing GF mice with SAD or HC microbiotas and then testing the F_1 progeny (to reduce GF developmental differences) is an alternative approach. While we considered this option, we resolved that working in a GF model could potentially add confounding variables and logistical hurdles that in some cases cannot be overcome, thus we decided to utilize the antibiotic-depletion model.

5.8 Social anxiety and microbiota: Where are we going

The work described herein lays fundamental groundwork linking SAD and the microbiota-gut-brain axis. We have established that the microbiota can play a causal role in increased sensitivity of social fear, a major component of SAD, and that reductions in immune function, oxytocin signalling, and the HPA axis are capable of being transferred across species, via the microbiota. However, important questions remain in how we use this newfound knowledge to design microbiota-treatments for SAD.

The next steps will first be to look to current therapies being used within the microbiota-gut-brain axis. Probiotics, prebiotics, and even FMT from healthy cohabitants and family are at the forefront of this field and there is good rationale to begin the next phase of testing here. Healthy lifestyle, particularly including diet and exercise, are often overlooked but play a fundamental role in health and well-being[561]. Personalized diets for individuals who are susceptible to social fear could be a viable option to improve

resiliency[562]. There is also the potential of specifically designing probiotics and prebiotics to supplement the microbes that are reduced in SAD[274] or perhaps targeting microbes elevated in SAD with FVT or specific cocktail of phages.

Here we show that the microbiota plays a causal role in SAD. Moving forward, this approach should be used to assess microbiota involvement in other neuropsychiatric disorders like obsessive compulsive disorder, other anxiety disorders (generalized anxiety disorder, panic disorder, phobia-related disorders, agoraphobia, *etc*.), schizophrenia, substance abuse, bipolar disorder and attention deficit hyperactivity disorder. More research is necessary but there is now evidence that supports these approaches going forward.

5.9 Conclusions

The microbiota is intricately involved in social and stress-related disorders. Through the work described herein we have extended this to include characterisation of the bacteriome and the virome. Microbiota research as a whole is largely built on associations observed but we have been able to use models of microbiota transplant to specifically test and infer causality in stress and social fear. Furthermore, we have characterized the role of different systems in the microbiota-gut-brain axis including the microbial community, immune system, HPA axis, oxytocin pathways, and brain transcriptomics. Based on our findings, we have proposed and laid the foundation for future research to continue to build upon microbiota-based stress and social anxiety disorder therapeutics. As this field continues to grow, we will further construct the mechanisms and pathways that connect the microbiota-gut-brain axis and mental health to improve health and well-being.

Uncategorized References

1 Turnbaugh, P. J. *et al.* The human microbiome project. *Nature* **449**, 804-810, doi:10.1038/nature06244 (2007).

2 Gaulke, C. A. *et al.* Ecophylogenetics clarifies the evolutionary association between mammals and their gut microbiota. *MBio* **9**, 10.1128/mbio. 01348-01318 (2018).

3 Rosenberg, E. & Zilber-Rosenberg, I. The hologenome concept of evolution after 10 years. *Microbiome* **6**, 78, doi:10.1186/s40168-018-0457-9 (2018).

4 Bordenstein, S. R. & Theis, K. R. Host biology in light of the microbiome: ten principles of holobionts and hologenomes. *PLoS biology* **13**, e1002226 (2015).

5 Nagpal, J. & Cryan, J. F. Host genetics, the microbiome & behaviour-a 'Holobiont' perspective. *Cell Res* **31**, 832-833, doi:10.1038/s41422-021-00512-x (2021).

6 Sender, R., Fuchs, S. & Milo, R. Revised estimates for the number of human and bacteria cells in the body. *PLoS biology* **14**, e1002533 (2016).

7 Qin, J. *et al.* A human gut microbial gene catalogue established by metagenomic sequencing. *Nature* **464**, 59-65, doi:10.1038/nature08821 (2010).

8 Cryan, J. F. *et al.* The microbiota-gut-brain axis. *Physiological reviews* (2019).

9 Erny, D. *et al.* Host microbiota constantly control maturation and function of microglia in the CNS. *Nature neuroscience* **18**, 965-977 (2015).

10 Williamson, L. L. *et al.* Got worms? Perinatal exposure to helminths prevents persistent immune sensitization and cognitive dysfunction induced by early-life infection. *Brain, behavior, and immunity* **51**, 14-28 (2016).

11 Hoban, A. E. *et al.* Behavioural and neurochemical consequences of chronic gut microbiota depletion during adulthood in the rat. *Neuroscience* **339**, 463-477 (2016).

12 Hoban, A. E. *et al.* Regulation of prefrontal cortex myelination by the microbiota. *Translational psychiatry* **6**, e774-e774 (2016).

13 Stilling, R. M. *et al.* Social interaction-induced activation of RNA splicing in the amygdala of microbiome-deficient mice. *Elife* **7**, e33070 (2018).

14 Hoban, A. E. *et al.* Microbial regulation of microRNA expression in the amygdala and prefrontal cortex. *Microbiome* **5**, 1-11 (2017).

15 Bravo, J. A. *et al.* Ingestion of Lactobacillus strain regulates emotional behavior and central GABA receptor expression in a mouse via the vagus nerve. *Proceedings of the National Academy of Sciences* **108**, 16050-16055 (2011).

16 Stenman, L. K., Patterson, E., Meunier, J., Roman, F. J. & Lehtinen, M. J. Strain specific stress-modulating effects of candidate probiotics: A systematic screening in a mouse model of chronic restraint stress. *Behavioural Brain Research* **379**, 112376 (2020).

17 Nobile, V., Giardina, S. & Puoci, F. The effect of a probiotic complex on the gut-brain axis: a translational study. *Neuropsychobiology* **81**, 116-126 (2022).

18 Zheng, P. *et al.* Gut microbiome remodeling induces depressive-like behaviors through a pathway mediated by the host's metabolism. *Molecular psychiatry* **21**, 786-796 (2016).

19 Kelly, J. R. *et al.* Transferring the blues: depression-associated gut microbiota induces neurobehavioural changes in the rat. *Journal of psychiatric research* **82**, 109-118 (2016).
20 Sharon, G. *et al.* Human gut microbiota from autism spectrum disorder promote behavioral symptoms in mice. *Cell* **177**, 1600-1618. e1617 (2019).
21 Boehme, M. *et al.* Microbiota from young mice counteracts selective age-associated behavioral deficits. *Nature Aging* **1**, 666-676 (2021).
22 Burokas, A. *et al.* Targeting the microbiota-gut-brain axis: prebiotics have anxiolytic and antidepressant-like effects and reverse the impact of chronic stress in mice. *Biological psychiatry* **82**, 472-487 (2017).
23 Grimaldi, R. *et al.* A prebiotic intervention study in children with autism spectrum disorders (ASDs). *Microbiome* **6**, 133 (2018).
24 Liu, Q. *et al.* Mannan oligosaccharide attenuates cognitive and behavioral disorders in the 5xFAD Alzheimer's disease mouse model via regulating the gut microbiota-brain axis. *Brain, Behavior, and Immunity* **95**, 330-343 (2021).
25 Cruz-Pereira, J. S. *et al.* Prebiotic supplementation modulates selective effects of stress on behavior and brain metabolome in aged mice. *Neurobiology of Stress* **21**, 100501 (2022).
26 Fischer, C. N. *et al.* Metabolite exchange between microbiome members produces compounds that influence Drosophila behavior. *Elife* **6**, e18855 (2017).
27 Van de Wouw, M. *et al.* Short-chain fatty acids: microbial metabolites that alleviate stress-induced brain–gut axis alterations. *The Journal of physiology* **596**, 4923-4944 (2018).
28 Needham, B. D. *et al.* A gut-derived metabolite alters brain activity and anxiety behaviour in mice. *Nature* **602**, 647-653 (2022).
29 Weiner, A., Turjeman, S. & Koren, O. Gut microbes and host behavior: the forgotten members of the gut-microbiome. *Neuropharmacology*, 109453 (2023).
30 Rojo, D. *et al.* Exploring the human microbiome from multiple perspectives: factors altering its composition and function. *FEMS microbiology reviews* **41**, 453-478 (2017).
31 Peterson, J. *et al.* The NIH human microbiome project. *Genome research* **19**, 2317-2323 (2009).
32 Johnson, A. J. *et al.* Daily sampling reveals personalized diet-microbiome associations in humans. *Cell host & microbe* **25**, 789-802. e785 (2019).
33 Asnicar, F. *et al.* Microbiome connections with host metabolism and habitual diet from 1,098 deeply phenotyped individuals. *Nature medicine* **27**, 321-332 (2021).
34 Armet, A. M. *et al.* Rethinking healthy eating in light of the gut microbiome. *Cell Host & Microbe* **30**, 764-785 (2022).
35 Cattaneo, A. *et al.* Association of brain amyloidosis with pro-inflammatory gut bacterial taxa and peripheral inflammation markers in cognitively impaired elderly. *Neurobiology of aging* **49**, 60-68 (2017).
36 Barichella, M. *et al.* Unraveling gut microbiota in Parkinson's disease and atypical parkinsonism. *Movement Disorders* **34**, 396-405 (2019).

37 De Palma, G. *et al.* Transplantation of fecal microbiota from patients with irritable bowel syndrome alters gut function and behavior in recipient mice. *Science translational medicine* **9**, eaaf6397 (2017).
38 Valles-Colomer, M. *et al.* The neuroactive potential of the human gut microbiota in quality of life and depression. *Nature microbiology* **4**, 623-632 (2019).
39 Heijtz, R. D. *et al.* Normal gut microbiota modulates brain development and behavior. *Proceedings of the National Academy of Sciences* **108**, 3047-3052 (2011).
40 Neufeld, K., Kang, N., Bienenstock, J. & Foster, J. A. Reduced anxiety-like behavior and central neurochemical change in germ-free mice. *Neurogastroenterology & Motility* **23**, 255-e119 (2011).
41 Lomasney, K. *et al.* Selective influence of host microbiota on cAMP-mediated ion transport in mouse colon. *Neurogastroenterology & Motility* **26**, 887-890 (2014).
42 Knox, E. G. *et al.* The gut microbiota is important for the maintenance of blood–cerebrospinal fluid barrier integrity. *European Journal of Neuroscience* **57**, 233-241 (2023).
43 Ogbonnaya, E. S. *et al.* Adult hippocampal neurogenesis is regulated by the microbiome. *Biological psychiatry* **78**, e7-e9 (2015).
44 Janik, R. *et al.* Magnetic resonance spectroscopy reveals oral Lactobacillus promotion of increases in brain GABA, N-acetyl aspartate and glutamate. *Neuroimage* **125**, 988-995 (2016).
45 Helgeland, L., Vaage, J., Rolstad, B., Midtvedt, T. & Brandtzaeg, P. Microbial colonization influences composition and T-cell receptor Vβ repertoire of intraepithelial lymphocytes in rat intestine. *Immunology* **89**, 494-501 (1996).
46 Atarashi, K. *et al.* Induction of colonic regulatory T cells by indigenous Clostridium species. *Science* **331**, 337-341, doi:10.1126/science.1198469 (2011).
47 Zheng, D., Liwinski, T. & Elinav, E. Interaction between microbiota and immunity in health and disease. *Cell research* **30**, 492-506 (2020).
48 Erny, D., Hrabě de Angelis, A. L. & Prinz, M. Communicating systems in the body: how microbiota and microglia cooperate. *Immunology* **150**, 7-15 (2017).
49 Dupraz, L. *et al.* Gut microbiota-derived short-chain fatty acids regulate IL-17 production by mouse and human intestinal γδ T cells. *Cell Reports* **36**, 109332 (2021).
50 Wu, S. *et al.* Interleukin-6 absence triggers intestinal microbiota dysbiosis and mucosal immunity in mice. *Cytokine* **153**, 155841 (2022).
51 Fasano, A. & Shea-Donohue, T. Mechanisms of disease: the role of intestinal barrier function in the pathogenesis of gastrointestinal autoimmune diseases. *Nature clinical practice Gastroenterology & hepatology* **2**, 416-422 (2005).
52 Abdel-Haq, R., Schlachetzki, J. C., Glass, C. K. & Mazmanian, S. K. Microbiome–microglia connections via the gut–brain axis. *Journal of Experimental Medicine* **216**, 41-59 (2019).
53 Macpherson, A. J., Pachnis, V. & Prinz, M. Boundaries and integration between microbiota, the nervous system, and immunity. *Immunity* **56**, 1712-1726 (2023).
54 Kawai, T. & Akira, S. Toll-like receptors and their crosstalk with other innate receptors in infection and immunity. *Immunity* **34**, 637-650 (2011).

55 Cavaillon, J.-M. Exotoxins and endotoxins: Inducers of inflammatory cytokines. *Toxicon* **149**, 45-53 (2018).
56 Harden, L., Kent, S., Pittman, Q. & Roth, J. Fever and sickness behavior: friend or foe? *Brain, behavior, and immunity* **50**, 322-333 (2015).
57 Rosadini, C. V. & Kagan, J. C. Early innate immune responses to bacterial LPS. *Current opinion in immunology* **44**, 14-19 (2017).
58 Lester, S. N. & Li, K. Toll-like receptors in antiviral innate immunity. *Journal of molecular biology* **426**, 1246-1264 (2014).
59 Gogokhia, L. *et al.* Expansion of bacteriophages is linked to aggravated intestinal inflammation and colitis. *Cell host & microbe* **25**, 285-299. e288 (2019).
60 Turner, M. D., Nedjai, B., Hurst, T. & Pennington, D. J. Cytokines and chemokines: At the crossroads of cell signalling and inflammatory disease. *Biochimica et Biophysica Acta (BBA)-Molecular Cell Research* **1843**, 2563-2582 (2014).
61 Al Bander, Z., Nitert, M. D., Mousa, A. & Naderpoor, N. The gut microbiota and inflammation: an overview. *International journal of environmental research and public health* **17**, 7618 (2020).
62 Maciel-Fiuza, M. F. *et al.* Role of gut microbiota in infectious and inflammatory diseases. *Frontiers in Microbiology* **14**, 1098386 (2023).
63 Schirmer, M. *et al.* Linking the human gut microbiome to inflammatory cytokine production capacity. *Cell* **167**, 1125-1136. e1128 (2016).
64 Carvalho, F. A. *et al.* Transient inability to manage proteobacteria promotes chronic gut inflammation in TLR5-deficient mice. *Cell host & microbe* **12**, 139-152 (2012).
65 Wang, T. & He, C. Pro-inflammatory cytokines: The link between obesity and osteoarthritis. *Cytokine & growth factor reviews* **44**, 38-50 (2018).
66 Kany, S., Vollrath, J. T. & Relja, B. Cytokines in inflammatory disease. *International journal of molecular sciences* **20**, 6008 (2019).
67 Wang, J., Chen, W.-D. & Wang, Y.-D. The relationship between gut microbiota and inflammatory diseases: the role of macrophages. *Frontiers in microbiology* **11**, 1065 (2020).
68 McNeil, N. I., Cummings, J. & James, W. Short chain fatty acid absorption by the human large intestine. *Gut* **19**, 819-822 (1978).
69 Baxter, N. T. *et al.* Dynamics of human gut microbiota and short-chain fatty acids in response to dietary interventions with three fermentable fibers. *MBio* **10**, 10.1128/mbio. 02566-02518 (2019).
70 Gill, P., Van Zelm, M., Muir, J. & Gibson, P. Short chain fatty acids as potential therapeutic agents in human gastrointestinal and inflammatory disorders. *Alimentary pharmacology & therapeutics* **48**, 15-34 (2018).
71 Maltz, R. M. *et al.* Prolonged restraint stressor exposure in outbred CD-1 mice impacts microbiota, colonic inflammation, and short chain fatty acids. *PloS one* **13**, e0196961 (2018).
72 Dai, Z.-L., Wu, G. & Zhu, W.-Y. Amino acid metabolism in intestinal bacteria: links between gut ecology and host health. *Frontiers in Bioscience-Landmark* **16**, 1768-1786 (2011).

73 Blachier, F., Mariotti, F., Huneau, J.-F. & Tomé, D. Effects of amino acid-derived luminal metabolites on the colonic epithelium and physiopathological consequences. *Amino acids* **33**, 547-562 (2007).
74 Schaible, U. E. & Kaufmann, S. H. A nutritive view on the host–pathogen interplay. *Trends in microbiology* **13**, 373-380 (2005).
75 D'Antona, G. *et al.* Branched-chain amino acid supplementation promotes survival and supports cardiac and skeletal muscle mitochondrial biogenesis in middle-aged mice. *Cell metabolism* **12**, 362-372 (2010).
76 Clarke, T. B. *et al.* Recognition of peptidoglycan from the microbiota by Nod1 enhances systemic innate immunity. *Nature medicine* **16**, 228-231 (2010).
77 Arentsen, T. *et al.* The bacterial peptidoglycan-sensing molecule Pglyrp2 modulates brain development and behavior. *Molecular psychiatry* **22**, 257-266 (2017).
78 Neuman, H., Debelius, J. W., Knight, R. & Koren, O. Microbial endocrinology: the interplay between the microbiota and the endocrine system. *FEMS microbiology reviews* **39**, 509-521 (2015).
79 Margolis, K. G., Cryan, J. F. & Mayer, E. A. The Microbiota-Gut-Brain Axis: From Motility to Mood. *Gastroenterology* (2021).
80 Foster, J. A., Rinaman, L. & Cryan, J. F. Stress & the gut-brain axis: regulation by the microbiome. *Neurobiology of stress* **7**, 124-136 (2017).
81 Woźniak, D., Cichy, W., Przysławski, J. & Drzymała-Czyż, S. The role of microbiota and enteroendocrine cells in maintaining homeostasis in the human digestive tract. *Advances in medical sciences* **66**, 284-292 (2021).
82 Latorre, R., Sternini, C., De Giorgio, R. & Greenwood-Van Meerveld, B. Enteroendocrine cells: a review of their role in brain–gut communication. *Neurogastroenterology & Motility* **28**, 620-630 (2016).
83 Mawe, G. M. & Hoffman, J. M. Serotonin signalling in the gut—functions, dysfunctions and therapeutic targets. *Nature reviews Gastroenterology & hepatology* **10**, 473-486 (2013).
84 Rao, M. & Gershon, M. D. The bowel and beyond: the enteric nervous system in neurological disorders. *Nature reviews Gastroenterology & hepatology* **13**, 517-528 (2016).
85 Breit, S., Kupferberg, A., Rogler, G. & Hasler, G. Vagus Nerve as Modulator of the Brain-Gut Axis in Psychiatric and Inflammatory Disorders. *Front Psychiatry* **9**, 44, doi:10.3389/fpsyt.2018.00044 (2018).
86 Fülling, C., Dinan, T. G. & Cryan, J. F. Gut Microbe to Brain Signaling: What Happens in Vagus…. *Neuron* **101**, 998-1002, doi:10.1016/j.neuron.2019.02.008 (2019).
87 Vazquez, E. *et al.* Dietary 2'-Fucosyllactose Enhances Operant Conditioning and Long-Term Potentiation via Gut-Brain Communication through the Vagus Nerve in Rodents. *PLoS One* **11**, e0166070, doi:10.1371/journal.pone.0166070 (2016).
88 Sgritta, M. *et al.* Mechanisms Underlying Microbial-Mediated Changes in Social Behavior in Mouse Models of Autism Spectrum Disorder. *Neuron* **101**, 246-259.e246, doi:10.1016/j.neuron.2018.11.018 (2019).

89 Rhee, S. H., Pothoulakis, C. & Mayer, E. A. Principles and clinical implications of the brain–gut–enteric microbiota axis. *Nature reviews Gastroenterology & hepatology* **6**, 306-314 (2009).
90 Chey, W. Y., Jin, H. O., Lee, M. H., Sun, S. W. & Lee, K. Y. Colonic motility abnormality in patients with irritable bowel syndrome exhibiting abdominal pain and diarrhea. *The American journal of gastroenterology* **96**, 1499-1506 (2001).
91 Hsiao, E. Y. *et al.* Microbiota modulate behavioral and physiological abnormalities associated with neurodevelopmental disorders. *Cell* **155**, 1451-1463, doi:10.1016/j.cell.2013.11.024 (2013).
92 Lyte, M. Microbial endocrinology in the microbiome-gut-brain axis: how bacterial production and utilization of neurochemicals influence behavior. *PLoS pathogens* **9**, e1003726 (2013).
93 Wall, R. *et al.* Bacterial neuroactive compounds produced by psychobiotics. *Microbial endocrinology: The microbiota-gut-brain axis in health and disease*, 221-239 (2014).
94 Roth, W., Zadeh, K., Vekariya, R., Ge, Y. & Mohamadzadeh, M. Tryptophan metabolism and gut-brain homeostasis. *International journal of molecular sciences* **22**, 2973 (2021).
95 Clarke, G. *et al.* The microbiome-gut-brain axis during early life regulates the hippocampal serotonergic system in a sex-dependent manner. *Molecular psychiatry* **18**, 666-673 (2013).
96 Kennedy, P. J., Cryan, J. F., Dinan, T. G. & Clarke, G. Kynurenine pathway metabolism and the microbiota-gut-brain axis. *Neuropharmacology* **112**, 399-412 (2017).
97 Barr, J. J. *et al.* Bacteriophage adhering to mucus provide a non–host-derived immunity. *Proceedings of the National Academy of Sciences* **110**, 10771-10776 (2013).
98 Lourenço, M. *et al.* The Spatial Heterogeneity of the Gut Limits Predation and Fosters Coexistence of Bacteria and Bacteriophages. *Cell Host & Microbe* (2020).
99 Gama, J. A. *et al.* Temperate bacterial viruses as double-edged swords in bacterial warfare. *PLoS One* **8**, e59043, doi:10.1371/journal.pone.0059043 (2013).
100 Wommack, K. E. & Colwell, R. R. Virioplankton: viruses in aquatic ecosystems. *Microbiology and molecular biology reviews : MMBR* **64**, 69-114, doi:10.1128/mmbr.64.1.69-114.2000 (2000).
101 Reyes, A. *et al.* Viruses in the faecal microbiota of monozygotic twins and their mothers. *Nature* **466**, 334-338 (2010).
102 Lim, E. S. *et al.* Early life dynamics of the human gut virome and bacterial microbiome in infants. *Nature medicine* **21**, 1228 (2015).
103 Shkoporov, A. N., Turkington, C. J. & Hill, C. Mutualistic interplay between bacteriophages and bacteria in the human gut. *Nature Reviews Microbiology* **20**, 737-749 (2022).
104 Howard-Varona, C., Hargreaves, K. R., Abedon, S. T. & Sullivan, M. B. Lysogeny in nature: mechanisms, impact and ecology of temperate phages. *The ISME journal* **11**, 1511 (2017).

105 Koskella, B. & Meaden, S. Understanding bacteriophage specificity in natural microbial communities. *Viruses* **5**, 806-823 (2013).
106 Liang, G. & Bushman, F. D. The human virome: assembly, composition and host interactions. *Nature Reviews Microbiology* **19**, 514-527 (2021).
107 Hoyles, L. *et al.* Characterization of virus-like particles associated with the human faecal and caecal microbiota. *Research in microbiology* **165**, 803-812 (2014).
108 Lepage, P. *et al.* Dysbiosis in inflammatory bowel disease: a role for bacteriophages? *Gut* **57**, 424-425, doi:10.1136/gut.2007.134668 (2008).
109 Shkoporov, A. N. *et al.* The human gut virome is highly diverse, stable, and individual specific. *Cell host & microbe* **26**, 527-541. e525 (2019).
110 Dalmasso, M., Hill, C. & Ross, R. P. Exploiting gut bacteriophages for human health. *Trends Microbiol* **22**, 399-405, doi:10.1016/j.tim.2014.02.010 (2014).
111 Carding, S. R., Davis, N. & Hoyles, L. The human intestinal virome in health and disease. *Alimentary pharmacology & therapeutics* **46**, 800-815 (2017).
112 Manrique, P. *et al.* Healthy human gut phageome. *Proceedings of the National Academy of Sciences* **113**, 10400-10405 (2016).
113 Reyes, A., Wu, M., McNulty, N. P., Rohwer, F. L. & Gordon, J. I. Gnotobiotic mouse model of phage–bacterial host dynamics in the human gut. *Proceedings of the National Academy of Sciences* **110**, 20236-20241 (2013).
114 Shkoporov, A. N. *et al.* Reproducible protocols for metagenomic analysis of human faecal phageomes. *Microbiome* **6**, 1-17 (2018).
115 Horvath, P. & Barrangou, R. CRISPR/Cas, the immune system of bacteria and archaea. *Science* **327**, 167-170 (2010).
116 Seed, K. D., Lazinski, D. W., Calderwood, S. B. & Camilli, A. A bacteriophage encodes its own CRISPR/Cas adaptive response to evade host innate immunity. *Nature* **494**, 489 (2013).
117 Chevallereau, A. *et al.* Next-Generation "-omics" Approaches Reveal a Massive Alteration of Host RNA Metabolism during Bacteriophage Infection of Pseudomonas aeruginosa. *PLoS genetics* **12**, e1006134, doi:10.1371/journal.pgen.1006134 (2016).
118 Wahida, A., Ritter, K. & Horz, H. P. The Janus-Face of Bacteriophages across Human Body Habitats. *PLoS Pathog* **12**, e1005634, doi:10.1371/journal.ppat.1005634 (2016).
119 Hsu, B. B. *et al.* Dynamic modulation of the gut microbiota and metabolome by bacteriophages in a mouse model. *Cell host & microbe* **25**, 803-814. e805 (2019).
120 Zhernakova, A. *et al.* Population-based metagenomics analysis reveals markers for gut microbiome composition and diversity. *Science* **352**, 565-569, doi:10.1126/science.aad3369 (2016).
121 Catel-Ferreira, M., Tnani, H., Hellio, C., Cosette, P. & Lebrun, L. Antiviral effects of polyphenols: development of bio-based cleaning wipes and filters. *Journal of virological methods* **212**, 1-7, doi:10.1016/j.jviromet.2014.10.008 (2015).
122 Marantos, A., Mitarai, N. & Sneppen, K. From kill the winner to eliminate the winner in open phage-bacteria systems. *PLoS Comput Biol* **18**, e1010400, doi:10.1371/journal.pcbi.1010400 (2022).

123 Sutcliffe, S. G., Reyes, A. & Maurice, C. F. Bacteriophages Playing Nice: Lysogenic bacteriophage replication stable in the human gut microbiota. *Iscience* **26** (2023).
124 Chen, X., Ma, R., Yang, Y., Jiao, N. & Zhang, R. Viral Regulation on Bacterial Community Impacted by Lysis-Lysogeny Switch: A Microcosm Experiment in Eutrophic Coastal Waters. *Front Microbiol* **10**, 1763, doi:10.3389/fmicb.2019.01763 (2019).
125 Maslov, S. & Sneppen, K. Population cycles and species diversity in dynamic Kill-the-Winner model of microbial ecosystems. *Sci Rep* **7**, 39642, doi:10.1038/srep39642 (2017).
126 Silveira, C. B. & Rohwer, F. L. Piggyback-the-Winner in host-associated microbial communities. *npj Biofilms and Microbiomes* **2**, 1-5 (2016).
127 Stern, A. & Sorek, R. The phage-host arms race: shaping the evolution of microbes. *Bioessays* **33**, 43-51, doi:10.1002/bies.201000071 (2011).
128 Shkoporov, A. N. & Hill, C. Bacteriophages of the human gut: the "known unknown" of the microbiome. *Cell host & microbe* **25**, 195-209 (2019).
129 Silpe, J. E. & Bassler, B. L. Phage-encoded LuxR-type receptors responsive to host-produced bacterial quorum-sensing autoinducers. *MBio* **10**, e00638-00619 (2019).
130 Hatfull, G. F. Complete genome sequences of 138 mycobacteriophages. *Journal of virology* **86**, 2382-2384, doi:10.1128/jvi.06870-11 (2012).
131 Turner, D. *et al.* Abolishment of morphology-based taxa and change to binomial species names: 2022 taxonomy update of the ICTV bacterial viruses subcommittee. *Archives of virology* **168**, 74, doi:10.1007/s00705-022-05694-2 (2023).
132 Roux, S., Krupovic, M., Poulet, A., Debroas, D. & Enault, F. Evolution and diversity of the Microviridae viral family through a collection of 81 new complete genomes assembled from virome reads. *PLoS One* **7**, e40418, doi:10.1371/journal.pone.0040418 (2012).
133 Dutilh, B. E. *et al.* A highly abundant bacteriophage discovered in the unknown sequences of human faecal metagenomes. *Nat Commun* **5**, 4498, doi:10.1038/ncomms5498 (2014).
134 Shkoporov, A. N. *et al.* ΦCrAss001 represents the most abundant bacteriophage family in the human gut and infects Bacteroides intestinalis. *Nat Commun* **9**, 4781, doi:10.1038/s41467-018-07225-7 (2018).
135 Yutin, N. *et al.* Discovery of an expansive bacteriophage family that includes the most abundant viruses from the human gut. *Nat Microbiol* **3**, 38-46, doi:10.1038/s41564-017-0053-y (2018).
136 Cruz-Pereira, J. S. & Cryan, J. F. In Need of a Quorum: From Microbes to Mood Via the Immune System. *The American journal of psychiatry* **177**, 895-897, doi:10.1176/appi.ajp.2020.20081182 (2020).
137 Schluter, J. *et al.* The gut microbiota is associated with immune cell dynamics in humans. *Nature*, 1-5 (2020).
138 Federici, S., Nobs, S. P. & Elinav, E. Phages and their potential to modulate the microbiome and immunity. *Cellular & Molecular Immunology*, 1-16 (2020).

238

139 Barr, J. J. A bacteriophages journey through the human body. *Immunological reviews* **279**, 106-122, doi:10.1111/imr.12565 (2017).
140 Karimi, M. *et al.* Bacteriophages and phage-inspired nanocarriers for targeted delivery of therapeutic cargos. *Advanced drug delivery reviews* **106**, 45-62, doi:10.1016/j.addr.2016.03.003 (2016).
141 Tian, Y. *et al.* Probing the endocytic pathways of the filamentous bacteriophage in live cells using ratiometric pH fluorescent indicator. *Advanced healthcare materials* **4**, 413-419, doi:10.1002/adhm.201400508 (2015).
142 Nieth, A., Verseux, C., Barnert, S., Süss, R. & Römer, W. A first step toward liposome-mediated intracellular bacteriophage therapy. *Expert opinion on drug delivery* **12**, 1411-1424, doi:10.1517/17425247.2015.1043125 (2015).
143 Nguyen, S. *et al.* Bacteriophage transcytosis provides a mechanism to cross epithelial cell layers. *MBio* **8**, e01874-01817 (2017).
144 Tetz, G. & Tetz, V. Bacteriophage infections of microbiota can lead to leaky gut in an experimental rodent model. *Gut Pathog* **8**, 33, doi:10.1186/s13099-016-0109-1 (2016).
145 Tetz, G. V. *et al.* Bacteriophages as potential new mammalian pathogens. *Scientific reports* **7**, 1-9 (2017).
146 Norman, J. M. *et al.* Disease-specific alterations in the enteric virome in inflammatory bowel disease. *Cell* **160**, 447-460 (2015).
147 Duerkop, B. A. *et al.* Murine colitis reveals a disease-associated bacteriophage community. *Nat Microbiol* **3**, 1023-1031, doi:10.1038/s41564-018-0210-y (2018).
148 Galtier, M. *et al.* Bacteriophages targeting adherent invasive Escherichia coli strains as a promising new treatment for Crohn's disease. *Journal of Crohn's and Colitis* **11**, 840-847 (2017).
149 Duerkop, B. A. Bacteriophages shift the focus of the mammalian microbiota. *PLoS Pathog* **14**, e1007310, doi:10.1371/journal.ppat.1007310 (2018).
150 Walter, J. & Shanahan, F. Fecal microbiota-based treatment for recurrent Clostridioides difficile infection. *Cell* **186**, 1087, doi:10.1016/j.cell.2023.02.034 (2023).
151 Ott, S. J. *et al.* Efficacy of sterile fecal filtrate transfer for treating patients with Clostridium difficile infection. *Gastroenterology* **152**, 799-811. e797 (2017).
152 Draper, L. A. *et al.* Long-term colonisation with donor bacteriophages following successful faecal microbial transplantation. *Microbiome* **6**, 220, doi:10.1186/s40168-018-0598-x (2018).
153 Zuo, T. *et al.* Bacteriophage transfer during faecal microbiota transplantation in Clostridium difficile infection is associated with treatment outcome. *Gut* **67**, 634-643 (2018).
154 Broecker, F., Klumpp, J. & Moelling, K. Long-term microbiota and virome in a Zürich patient after fecal transplantation against Clostridium difficile infection. *Ann N Y Acad Sci* **1372**, 29-41, doi:10.1111/nyas.13100 (2016).
155 Abedon, S. T., Danis-Wlodarczyk, K. M. & Alves, D. R. Phage Therapy in the 21st Century: Is There Modern, Clinical Evidence of Phage-Mediated Efficacy? *Pharmaceuticals (Basel, Switzerland)* **14**, doi:10.3390/ph14111157 (2021).

156 Rasmussen, T. S. *et al.* Faecal virome transplantation decreases symptoms of type 2 diabetes and obesity in a murine model. *Gut* (2020).
157 Draper, L. A. *et al.* Autochthonous faecal virome transplantation (FVT) reshapes the murine microbiome after antibiotic perturbation. (2019).
158 Lin, D. M. *et al.* Transplanting Fecal Virus-Like Particles Reduces High-Fat Diet-Induced Small Intestinal Bacterial Overgrowth in Mice. *Frontiers in cellular and infection microbiology* **9**, 348 (2019).
159 Nash, A. K. *et al.* The gut mycobiome of the Human Microbiome Project healthy cohort. *Microbiome* **5**, 1-13 (2017).
160 Huffnagle, G. B. & Noverr, M. C. The emerging world of the fungal microbiome. *Trends Microbiol* **21**, 334-341, doi:10.1016/j.tim.2013.04.002 (2013).
161 Hoffmann, C. *et al.* Archaea and fungi of the human gut microbiome: correlations with diet and bacterial residents. *PLoS One* **8**, e66019, doi:10.1371/journal.pone.0066019 (2013).
162 Strati, F. *et al.* Altered gut microbiota in Rett syndrome. *Microbiome* **4**, 41 (2016).
163 Strati, F. *et al.* Age and Gender Affect the Composition of Fungal Population of the Human Gastrointestinal Tract. *Front Microbiol* **7**, 1227, doi:10.3389/fmicb.2016.01227 (2016).
164 Odamaki, T. *et al.* Age-related changes in gut microbiota composition from newborn to centenarian: a cross-sectional study. *BMC Microbiol* **16**, 90, doi:10.1186/s12866-016-0708-5 (2016).
165 Hallen-Adams, H. E. & Suhr, M. J. Fungi in the healthy human gastrointestinal tract. *Virulence* **8**, 352-358, doi:10.1080/21505594.2016.1247140 (2017).
166 Yapar, N. Epidemiology and risk factors for invasive candidiasis. *Therapeutics and clinical risk management* **10**, 95-105, doi:10.2147/tcrm.s40160 (2014).
167 Takata, K. *et al.* Dietary Yeasts Reduce Inflammation in Central Nerve System via Microflora. *Annals of clinical and translational neurology* **2**, 56-66, doi:10.1002/acn3.153 (2015).
168 Rizzetto, L. *et al.* Fungal chitin induces trained immunity in human monocytes during cross-talk of the host with Saccharomyces cerevisiae. *Journal of Biological Chemistry* **291**, 7961-7972 (2016).
169 Qamar, A. *et al.* Saccharomyces boulardii stimulates intestinal immunoglobulin A immune response to Clostridium difficile toxin A in mice. *Infect Immun* **69**, 2762-2765, doi:10.1128/iai.69.4.2762-2765.2001 (2001).
170 Castagliuolo, I., Riegler, M. F., Valenick, L., LaMont, J. T. & Pothoulakis, C. Saccharomyces boulardii protease inhibits the effects of Clostridium difficile toxins A and B in human colonic mucosa. *Infect Immun* **67**, 302-307, doi:10.1128/iai.67.1.302-307.1999 (1999).
171 Buts, J. P. *et al.* Saccharomyces boulardii produces in rat small intestine a novel protein phosphatase that inhibits Escherichia coli endotoxin by dephosphorylation. *Pediatr Res* **60**, 24-29, doi:10.1203/01.pdr.0000220322.31940.29 (2006).
172 Jones, L. *et al.* The transformative possibilities of the microbiota and mycobiota for health, disease, aging, and technological innovation. *Biomedicines* **7**, 24 (2019).

173 Zou, R. *et al.* Dysbiosis of gut fungal microbiota in children with autism spectrum disorders. *Journal of Autism and Developmental Disorders* **51**, 267-275 (2021).
174 Voropaeva, E. A. [Resistance to antibiotics and histamine production at the bacteria, isolated from the stomatopharynx of the children with bronchial asthma]. *Antibiotiki i khimioterapiia = Antibiotics and chemoterapy [sic]* **47**, 8-13 (2002).
175 Reyes-García, M. G., García-Tamayo, F. & Hernández-Hernández, F. Gamma-aminobutyric acid (GABA) increases in vitro germ-tube formation and phospholipase B1 mRNA expression in Candida albicans. *Mycoscience* **53**, 36-39, doi:https://doi.org/10.1007/s10267-011-0130-7 (2012).
176 Mayr, A., Hinterberger, G., Dierich, M. P. & Lass-Flörl, C. Interaction of serotonin with Candida albicans selectively attenuates fungal virulence in vitro. *International journal of antimicrobial agents* **26**, 335-337, doi:10.1016/j.ijantimicag.2005.07.006 (2005).
177 De Angelis, M. *et al.* Fecal microbiota and metabolome of children with autism and pervasive developmental disorder not otherwise specified. *PLoS One* **8**, e76993, doi:10.1371/journal.pone.0076993 (2013).
178 Kantarcioglu, A. S., Kiraz, N. & Aydin, A. Microbiota-Gut-Brain Axis: Yeast Species Isolated from Stool Samples of Children with Suspected or Diagnosed Autism Spectrum Disorders and In Vitro Susceptibility Against Nystatin and Fluconazole. *Mycopathologia* **181**, 1-7, doi:10.1007/s11046-015-9949-3 (2016).
179 Strati, F. *et al.* New evidences on the altered gut microbiota in autism spectrum disorders. *Microbiome* **5**, 24 (2017).
180 Burrus, C. J. A biochemical rationale for the interaction between gastrointestinal yeast and autism. *Medical hypotheses* **79**, 784-785, doi:10.1016/j.mehy.2012.08.029 (2012).
181 Botschuijver, S. *et al.* Intestinal fungal dysbiosis is associated with visceral hypersensitivity in patients with irritable bowel syndrome and rats. *Gastroenterology* **153**, 1026-1039 (2017).
182 Zou, R. *et al.* Changes in the gut microbiota of children with autism spectrum disorder. *Autism Research* **13**, 1614-1625 (2020).
183 Gouba, N., Raoult, D. & Drancourt, M. Gut microeukaryotes during anorexia nervosa: a case report. *BMC research notes* **7**, 33 (2014).
184 Severance, E. G. *et al.* Candida albicans exposures, sex specificity and cognitive deficits in schizophrenia and bipolar disorder. *NPJ schizophrenia* **2**, 1-7 (2016).
185 Severance, E. G. *et al.* Probiotic normalization of Candida albicans in schizophrenia: a randomized, placebo-controlled, longitudinal pilot study. *Brain, behavior, and immunity* **62**, 41-45 (2017).
186 Jiang, H. Y. *et al.* Altered gut bacterial-fungal interkingdom networks in patients with current depressive episode. *Brain and behavior*, e01677, doi:10.1002/brb3.1677 (2020).
187 Severance, E. G. *et al.* Gastrointestinal inflammation and associated immune activation in schizophrenia. *Schizophrenia research* **138**, 48-53 (2012).
188 Zou, R. *et al.* Dysbiosis of Gut Fungal Microbiota in Children with Autism Spectrum Disorders. *Journal of Autism and Developmental Disorders* (2020).

189 Peleg, A. Y., Hogan, D. A. & Mylonakis, E. Medically important bacterial-fungal interactions. *Nature reviews. Microbiology* **8**, 340-349, doi:10.1038/nrmicro2313 (2010).
190 Sam, Q. H., Chang, M. W. & Chai, L. Y. The Fungal Mycobiome and Its Interaction with Gut Bacteria in the Host. *Int J Mol Sci* **18**, doi:10.3390/ijms18020330 (2017).
191 Zhu, F. *et al.* Transplantation of microbiota from drug-free patients with schizophrenia causes schizophrenia-like abnormal behaviors and dysregulated kynurenine metabolism in mice. *Molecular psychiatry* **25**, 2905-2918 (2020).
192 Obrenovich, M. E. M. Leaky Gut, Leaky Brain? *Microorganisms* **6**, doi:10.3390/microorganisms6040107 (2018).
193 Iliev, I. D. & Leonardi, I. Fungal dysbiosis: immunity and interactions at mucosal barriers. *Nature reviews. Immunology* **17**, 635-646, doi:10.1038/nri.2017.55 (2017).
194 Iliev, I. D. & Cadwell, K. Effects of Intestinal Fungi and Viruses on Immune Responses and Inflammatory Bowel Diseases. *Gastroenterology* **160**, 1050-1066, doi:10.1053/j.gastro.2020.06.100 (2021).
195 Carter, C. J. Genetic, Transcriptome, Proteomic, and Epidemiological Evidence for Blood-Brain Barrier Disruption and Polymicrobial Brain Invasion as Determinant Factors in Alzheimer's Disease. *Journal of Alzheimer's disease reports* **1**, 125-157, doi:10.3233/adr-170017 (2017).
196 Pisa, D., Alonso, R. & Carrasco, L. Parkinson's disease: a comprehensive analysis of fungi and bacteria in brain tissue. *International Journal of Biological Sciences* **16**, 1135 (2020).
197 Forbes, J. D. *et al.* A comparative study of the gut microbiota in immune-mediated inflammatory diseases-does a common dysbiosis exist? *Microbiome* **6**, 221, doi:10.1186/s40168-018-0603-4 (2018).
198 Iliev, I. D. *et al.* Interactions between commensal fungi and the C-type lectin receptor Dectin-1 influence colitis. *Science* **336**, 1314-1317, doi:10.1126/science.1221789 (2012).
199 Wheeler, M. L. *et al.* Immunological Consequences of Intestinal Fungal Dysbiosis. *Cell Host Microbe* **19**, 865-873, doi:10.1016/j.chom.2016.05.003 (2016).
200 McKenzie, H., Main, J., Pennington, C. R. & Parratt, D. Antibody to selected strains of Saccharomyces cerevisiae (baker's and brewer's yeast) and Candida albicans in Crohn's disease. *Gut* **31**, 536-538, doi:10.1136/gut.31.5.536 (1990).
201 Seibold, F., Stich, O., Hufnagl, R., Kamil, S. & Scheurlen, M. Anti-Saccharomyces cerevisiae antibodies in inflammatory bowel disease: a family study. *Scand J Gastroenterol* **36**, 196-201, doi:10.1080/003655201750065960 (2001).
202 Murdoch, T. B. *et al.* Pattern recognition receptor and autophagy gene variants are associated with development of antimicrobial antibodies in Crohn's disease. *Inflamm Bowel Dis* **18**, 1743-1748, doi:10.1002/ibd.22884 (2012).

203 Farias, E. S. K. *et al.* Serum 1,3-beta-D-glucan as a noninvasive test to predict histologic activity in patients with inflammatory bowel disease. *World journal of gastroenterology* **27**, 866-885, doi:10.3748/wjg.v27.i9.866 (2021).
204 He, S. *et al.* A systematic review and meta-analysis of diagnostic accuracy of serum 1,3-β-d-glucan for invasive fungal infection: Focus on cutoff levels. *Journal of Microbiology, Immunology and Infection* **48**, 351-361, doi:https://doi.org/10.1016/j.jmii.2014.06.009 (2015).
205 Abautret-Daly, Á., Dempsey, E., Parra-Blanco, A., Medina, C. & Harkin, A. Gut-brain actions underlying comorbid anxiety and depression associated with inflammatory bowel disease. *Acta neuropsychiatrica* **30**, 275-296, doi:10.1017/neu.2017.3 (2018).
206 Wang, L. *et al.* Investigation into archaeal extremophilic lifestyles through comparative proteogenomic analysis. *Journal of biomolecular structure & dynamics* **39**, 7080-7092, doi:10.1080/07391102.2020.1808531 (2021).
207 Pereira, S. L. & Reeve, J. N. Histones and nucleosomes in Archaea and Eukarya: a comparative analysis. *Extremophiles : life under extreme conditions* **2**, 141-148, doi:10.1007/s007920050053 (1998).
208 Koga, Y. & Morii, H. Biosynthesis of ether-type polar lipids in archaea and evolutionary considerations. *Microbiology and molecular biology reviews : MMBR* **71**, 97-120, doi:10.1128/mmbr.00033-06 (2007).
209 Liu, Y. & Whitman, W. B. Metabolic, phylogenetic, and ecological diversity of the methanogenic archaea. *Ann N Y Acad Sci* **1125**, 171-189, doi:10.1196/annals.1419.019 (2008).
210 Matarazzo, F. *et al.* The domain Archaea in human mucosal surfaces. *Clinical microbiology and infection : the official publication of the European Society of Clinical Microbiology and Infectious Diseases* **18**, 834-840, doi:10.1111/j.1469-0691.2012.03958.x (2012).
211 Nakamura, N., Lin, H. C., McSweeney, C. S., Mackie, R. I. & Gaskins, H. R. Mechanisms of microbial hydrogen disposal in the human colon and implications for health and disease. *Annual review of food science and technology* **1**, 363-395, doi:10.1146/annurev.food.102308.124101 (2010).
212 Rey, F. E. *et al.* Metabolic niche of a prominent sulfate-reducing human gut bacterium. *Proceedings of the National Academy of Sciences of the United States of America* **110**, 13582-13587, doi:10.1073/pnas.1312524110 (2013).
213 Bernalier-Donadille, A. Fermentative metabolism by the human gut microbiota. *Gastroentérologie Clinique et Biologique* **34**, S16-S22, doi:https://doi.org/10.1016/S0399-8320(10)70016-6 (2010).
214 Pimentel, M. *et al.* Methane, a gas produced by enteric bacteria, slows intestinal transit and augments small intestinal contractile activity. *American journal of physiology. Gastrointestinal and liver physiology* **290**, G1089-1095, doi:10.1152/ajpgi.00574.2004 (2006).
215 Million, M., Lagier, J. C., Yahav, D. & Paul, M. Gut bacterial microbiota and obesity. *Clinical microbiology and infection : the official publication of the European Society of Clinical Microbiology and Infectious Diseases* **19**, 305-313, doi:10.1111/1469-0691.12172 (2013).

216 Dridi, B., Henry, M., El Khéchine, A., Raoult, D. & Drancourt, M. High prevalence of Methanobrevibacter smithii and Methanosphaera stadtmanae detected in the human gut using an improved DNA detection protocol. *PLoS One* **4**, e7063, doi:10.1371/journal.pone.0007063 (2009).
217 Knobbe, T. J. *et al.* Altered Gut Microbial Fermentation and Colonization with Methanobrevibacter smithii in Renal Transplant Recipients. *J Clin Med* **9**, doi:10.3390/jcm9020518 (2020).
218 Stewart, J. A., Chadwick, V. S. & Murray, A. Carriage, quantification, and predominance of methanogens and sulfate-reducing bacteria in faecal samples. *Lett Appl Microbiol* **43**, 58-63, doi:10.1111/j.1472-765X.2006.01906.x (2006).
219 Pochart, P. *et al.* Pyxigraphic sampling to enumerate methanogens and anaerobes in the right colon of healthy humans. *Gastroenterology* **105**, 1281-1285, doi:10.1016/0016-5085(93)90129-z (1993).
220 Nava, G. M. *et al.* Hydrogenotrophic microbiota distinguish native Africans from African and European Americans. *Environmental microbiology reports* **4**, 307-315, doi:10.1111/j.1758-2229.2012.00334.x (2012).
221 Samuel, B. S. & Gordon, J. I. A humanized gnotobiotic mouse model of host-archaeal-bacterial mutualism. *Proceedings of the National Academy of Sciences of the United States of America* **103**, 10011-10016, doi:10.1073/pnas.0602187103 (2006).
222 Mihajlovski, A., Doré, J., Levenez, F., Alric, M. & Brugère, J. F. Molecular evaluation of the human gut methanogenic archaeal microbiota reveals an age-associated increase of the diversity. *Environmental microbiology reports* **2**, 272-280, doi:10.1111/j.1758-2229.2009.00116.x (2010).
223 Dridi, B., Fardeau, M. L., Ollivier, B., Raoult, D. & Drancourt, M. Methanomassiliicoccus luminyensis gen. nov., sp. nov., a methanogenic archaeon isolated from human faeces. *International journal of systematic and evolutionary microbiology* **62**, 1902-1907, doi:10.1099/ijs.0.033712-0 (2012).
224 Hwang, L. *et al.* Evaluating breath methane as a diagnostic test for constipation-predominant IBS. *Dig Dis Sci* **55**, 398-403, doi:10.1007/s10620-009-0778-4 (2010).
225 Blais Lecours, P. *et al.* Increased prevalence of Methanosphaera stadtmanae in inflammatory bowel diseases. *PLoS One* **9**, e87734 (2014).
226 Mbakwa, C. A. *et al.* Gut colonization with methanobrevibacter smithii is associated with childhood weight development. *Obesity (Silver Spring, Md.)* **23**, 2508-2516, doi:10.1002/oby.21266 (2015).
227 Peled, Y. Methane excretion in man. *Gut* **26**, 1270-1271, doi:10.1136/gut.26.11.1270 (1985).
228 Kandler, O. & König, H. Cell wall polymers in Archaea (Archaebacteria). *Cellular and molecular life sciences : CMLS* **54**, 305-308, doi:10.1007/s000180050156 (1998).
229 Dridi, B., Raoult, D. & Drancourt, M. Archaea as emerging organisms in complex human microbiomes. *Anaerobe* **17**, 56-63, doi:10.1016/j.anaerobe.2011.03.001 (2011).

230 Woodmansey, E. J., McMurdo, M. E., Macfarlane, G. T. & Macfarlane, S. Comparison of compositions and metabolic activities of fecal microbiotas in young adults and in antibiotic-treated and non-antibiotic-treated elderly subjects. *Appl Environ Microbiol* **70**, 6113-6122, doi:10.1128/aem.70.10.6113-6122.2004 (2004).
231 Stams, A. J. & Plugge, C. M. Electron transfer in syntrophic communities of anaerobic bacteria and archaea. *Nature reviews. Microbiology* **7**, 568-577, doi:10.1038/nrmicro2166 (2009).
232 Siddiqui, R., Ali, I. K. M., Cope, J. R. & Khan, N. A. Biology and pathogenesis of Naegleria fowleri. *Acta tropica* **164**, 375-394, doi:10.1016/j.actatropica.2016.09.009 (2016).
233 Worth, A. R., Andrew Thompson, R. C. & Lymbery, A. J. Reevaluating the evidence for Toxoplasma gondii-induced behavioural changes in rodents. *Advances in parasitology* **85**, 109-142, doi:10.1016/b978-0-12-800182-0.00003-9 (2014).
234 Berdoy, M., Webster, J. P. & Macdonald, D. W. Fatal attraction in rats infected with Toxoplasma gondii. *Proceedings. Biological sciences* **267**, 1591-1594, doi:10.1098/rspb.2000.1182 (2000).
235 Vyas, A., Kim, S. K. & Sapolsky, R. M. The effects of toxoplasma infection on rodent behavior are dependent on dose of the stimulus. *Neuroscience* **148**, 342-348, doi:10.1016/j.neuroscience.2007.06.021 (2007).
236 Bercik, P. *et al.* Chronic gastrointestinal inflammation induces anxiety-like behavior and alters central nervous system biochemistry in mice. *Gastroenterology* **139**, 2102-2112. e2101 (2010).
237 Gregory, A. C., Zablocki, O., Howell, A., Bolduc, B. & Sullivan, M. B. The human gut virome database. *BioRxiv*, 655910 (2019).
238 Gregory, A. C. *et al.* The gut virome database reveals age-dependent patterns of virome diversity in the human gut. *Cell host & microbe* **28**, 724-740. e728 (2020).
239 Cain, C. W., Lohse, M. B., Homann, O. R., Sil, A. & Johnson, A. D. A conserved transcriptional regulator governs fungal morphology in widely diverged species. *Genetics* **190**, 511-521, doi:10.1534/genetics.111.134080 (2012).
240 Petitjean, C., Deschamps, P., López-García, P., Moreira, D. & Brochier-Armanet, C. Extending the conserved phylogenetic core of archaea disentangles the evolution of the third domain of life. *Mol Biol Evol* **32**, 1242-1254, doi:10.1093/molbev/msv015 (2015).
241 Gouba, N., Raoult, D. & Drancourt, M. Plant and fungal diversity in gut microbiota as revealed by molecular and culture investigations. *PLoS One* **8**, e59474, doi:10.1371/journal.pone.0059474 (2013).
242 Lagier, J. C. *et al.* Culture of previously uncultured members of the human gut microbiota by culturomics. *Nat Microbiol* **1**, 16203, doi:10.1038/nmicrobiol.2016.203 (2016).
243 Morais, L. H., Schreiber IV, H. L. & Mazmanian, S. K. The gut microbiota–brain axis in behaviour and brain disorders. *Nature Reviews Microbiology* **19**, 241-255 (2021).

245

244 Cowan, C. S., Dinan, T. G. & Cryan, J. F. Annual Research Review: Critical windows–the microbiota–gut–brain axis in neurocognitive development. *Journal of Child Psychology and Psychiatry* **61**, 353-371 (2020).
245 Horvath, K. & Perman, J. A. Autism and gastrointestinal symptoms. *Current gastroenterology reports* **4**, 251-258 (2002).
246 Buie, T. *et al.* Evaluation, diagnosis, and treatment of gastrointestinal disorders in individuals with ASDs: a consensus report. *Pediatrics* **125**, S1-S18 (2010).
247 Luna, R. A. *et al.* Distinct microbiome-neuroimmune signatures correlate with functional abdominal pain in children with autism spectrum disorder. *Cellular and molecular gastroenterology and hepatology* **3**, 218-230 (2017).
248 McElhanon, B. O., McCracken, C., Karpen, S. & Sharp, W. G. Gastrointestinal symptoms in autism spectrum disorder: a meta-analysis. *Pediatrics* **133**, 872-883, doi:10.1542/peds.2013-3995 (2014).
249 Neuhaus, E., Bernier, R. A., Tham, S. W. & Webb, S. J. Gastrointestinal and Psychiatric Symptoms Among Children and Adolescents With Autism Spectrum Disorder. *Front Psychiatry* **9**, 515, doi:10.3389/fpsyt.2018.00515 (2018).
250 Kang, D.-W. *et al.* Microbiota transfer therapy alters gut ecosystem and improves gastrointestinal and autism symptoms: an open-label study. *Microbiome* **5**, 1-16 (2017).
251 Marrs, T. & Walter, J. Pros and cons: Is faecal microbiota transplantation a safe and efficient treatment option for gut dysbiosis? *Allergy* **76**, 2312-2317, doi:10.1111/all.14750 (2021).
252 Meltzer, A. & Van de Water, J. The Role of the Immune System in Autism Spectrum Disorder. *Neuropsychopharmacology* **42**, 284-298, doi:10.1038/npp.2016.158 (2017).
253 Finegold, S. M. *et al.* Gastrointestinal microflora studies in late-onset autism. *Clinical infectious diseases : an official publication of the Infectious Diseases Society of America* **35**, S6-s16, doi:10.1086/341914 (2002).
254 Parracho, H. M., Bingham, M. O., Gibson, G. R. & McCartney, A. L. Differences between the gut microflora of children with autistic spectrum disorders and that of healthy children. *Journal of medical microbiology* **54**, 987-991, doi:10.1099/jmm.0.46101-0 (2005).
255 Kang, D. W. *et al.* Reduced incidence of Prevotella and other fermenters in intestinal microflora of autistic children. *PLoS One* **8**, e68322, doi:10.1371/journal.pone.0068322 (2013).
256 Finegold, S. M., Downes, J. & Summanen, P. H. Microbiology of regressive autism. *Anaerobe* **18**, 260-262, doi:10.1016/j.anaerobe.2011.12.018 (2012).
257 Adams, J. B., Johansen, L. J., Powell, L. D., Quig, D. & Rubin, R. A. Gastrointestinal flora and gastrointestinal status in children with autism--comparisons to typical children and correlation with autism severity. *BMC Gastroenterol* **11**, 22, doi:10.1186/1471-230x-11-22 (2011).
258 Finegold, S. M. *et al.* Pyrosequencing study of fecal microflora of autistic and control children. *Anaerobe* **16**, 444-453, doi:10.1016/j.anaerobe.2010.06.008 (2010).

259 Li, Z., Zhu, H., Guo, Y., Du, X. & Qin, C. Gut microbiota regulate cognitive deficits and amyloid deposition in a model of Alzheimer's disease. *Journal of neurochemistry* **155**, 448-461 (2020).
260 Grabrucker, S. *et al.* Microbiota from Alzheimer's patients induce deficits in cognition and hippocampal neurogenesis. *Brain*, awad303 (2023).
261 Hill-Burns, E. M. *et al.* Parkinson's disease and Parkinson's disease medications have distinct signatures of the gut microbiome. *Movement disorders : official journal of the Movement Disorder Society* **32**, 739-749, doi:10.1002/mds.26942 (2017).
262 Tan, A. H., Lim, S. Y. & Lang, A. E. The microbiome–gut–brain axis in Parkinson disease—from basic research to the clinic. *Nature Reviews Neurology* **18**, 476-495 (2022).
263 Romano, S. *et al.* Meta-analysis of the Parkinson's disease gut microbiome suggests alterations linked to intestinal inflammation. *npj Parkinson's Disease* **7**, 27 (2021).
264 Gérard, H. C. *et al.* Chlamydophila (Chlamydia) pneumoniae in the Alzheimer's brain. *FEMS immunology and medical microbiology* **48**, 355-366, doi:10.1111/j.1574-695X.2006.00154.x (2006).
265 Roubaud-Baudron, C., Krolak-Salmon, P., Quadrio, I., Mégraud, F. & Salles, N. Impact of chronic Helicobacter pylori infection on Alzheimer's disease: preliminary results. *Neurobiol Aging* **33**, 1009.e1011-1009, doi:10.1016/j.neurobiolaging.2011.10.021 (2012).
266 Liang, X. *et al.* Gut microbiome, cognitive function and brain structure: a multi-omics integration analysis. *Translational neurodegeneration* **11**, 49, doi:10.1186/s40035-022-00323-z (2022).
267 Sampson, T. R. *et al.* Gut Microbiota Regulate Motor Deficits and Neuroinflammation in a Model of Parkinson's Disease. *Cell* **167**, 1469-1480.e1412, doi:10.1016/j.cell.2016.11.018 (2016).
268 Tetz, G., Brown, S. M., Hao, Y. & Tetz, V. Parkinson's disease and bacteriophages as its overlooked contributors. *Sci Rep* **8**, 10812, doi:10.1038/s41598-018-29173-4 (2018).
269 Yang, J. *et al.* Landscapes of bacterial and metabolic signatures and their interaction in major depressive disorders. *Science advances* **6**, eaba8555 (2020).
270 Müller, B. *et al.* Fecal Short-Chain Fatty Acid Ratios as Related to Gastrointestinal and Depressive Symptoms in Young Adults. *Psychosom Med* **83**, 693-699, doi:10.1097/psy.0000000000000965 (2021).
271 Zhou, M. *et al.* Microbiome and tryptophan metabolomics analysis in adolescent depression: roles of the gut microbiota in the regulation of tryptophan-derived neurotransmitters and behaviors in human and mice. *Microbiome* **11**, 145, doi:10.1186/s40168-023-01589-9 (2023).
272 Dong, Z. *et al.* Gut Microbiome: A Potential Indicator for Differential Diagnosis of Major Depressive Disorder and General Anxiety Disorder. *Front Psychiatry* **12**, 651536, doi:10.3389/fpsyt.2021.651536 (2021).
273 Kossewska, J., Bierlit, K. & Trajkovski, V. Personality, Anxiety, and Stress in Patients with Small Intestine Bacterial Overgrowth Syndrome. The Polish

Preliminary Study. *Int J Environ Res Public Health* **20**, doi:10.3390/ijerph20010093 (2022).
274 Butler, M. I. *et al.* The gut microbiome in social anxiety disorder: evidence of altered composition and function. *Translational Psychiatry* **13**, 95 (2023).
275 Coretti, L. *et al.* Gut Microbiota Features in Young Children With Autism Spectrum Disorders. *Front Microbiol* **9**, 3146, doi:10.3389/fmicb.2018.03146 (2018).
276 Kang, D.-W. *et al.* Long-term benefit of Microbiota Transfer Therapy on autism symptoms and gut microbiota. *Scientific Reports* **9**, 5821, doi:10.1038/s41598-019-42183-0 (2019).
277 Li, S. *et al.* The gut microbiome is associated with brain structure and function in schizophrenia. *Sci Rep* **11**, 9743, doi:10.1038/s41598-021-89166-8 (2021).
278 Tap, J. *et al.* Identification of an Intestinal Microbiota Signature Associated With Severity of Irritable Bowel Syndrome. *Gastroenterology* **152**, 111-123.e118, doi:10.1053/j.gastro.2016.09.049 (2017).
279 Mars, R. A. T. *et al.* Longitudinal Multi-omics Reveals Subset-Specific Mechanisms Underlying Irritable Bowel Syndrome. *Cell* **182**, 1460-1473.e1417, doi:10.1016/j.cell.2020.08.007 (2020).
280 Tap, J. *et al.* Diet and gut microbiome interactions of relevance for symptoms in irritable bowel syndrome. *Microbiome* **9**, 74, doi:10.1186/s40168-021-01018-9 (2021).
281 Halfvarson, J. *et al.* Dynamics of the human gut microbiome in inflammatory bowel disease. *Nat Microbiol* **2**, 17004, doi:10.1038/nmicrobiol.2017.4 (2017).
282 Vich Vila, A. *et al.* Gut microbiota composition and functional changes in inflammatory bowel disease and irritable bowel syndrome. *Sci Transl Med* **10**, doi:10.1126/scitranslmed.aap8914 (2018).
283 Clooney, A. G. *et al.* Ranking microbiome variance in inflammatory bowel disease: a large longitudinal intercontinental study. *Gut* **70**, 499-510, doi:10.1136/gutjnl-2020-321106 (2021).
284 Petrov, V. A. *et al.* Analysis of Gut Microbiota in Patients with Parkinson's Disease. *Bulletin of experimental biology and medicine* **162**, 734-737, doi:10.1007/s10517-017-3700-7 (2017).
285 Zhuang, Z. Q. *et al.* Gut Microbiota is Altered in Patients with Alzheimer's Disease. *Journal of Alzheimer's disease : JAD* **63**, 1337-1346, doi:10.3233/jad-180176 (2018).
286 Fagundes, C. P. *et al.* Attachment anxiety is related to Epstein–Barr virus latency. *Brain, behavior, and immunity* **41**, 232-238 (2014).
287 Jones-Brando, L. *et al.* Atypical immune response to Epstein-Barr virus in major depressive disorder. *Journal of affective disorders* **264**, 221-226 (2020).
288 Al-Beltagi, M. *et al.* Viruses and autism: A Bi-mutual cause and effect. *World journal of virology* **12**, 172-192, doi:10.5501/wjv.v12.i3.172 (2023).
289 Karlsson, H., Sjöqvist, H., Brynge, M., Gardner, R. & Dalman, C. Childhood infections and autism spectrum disorders and/or intellectual disability: a register-based cohort study. *Journal of neurodevelopmental disorders* **14**, 12, doi:10.1186/s11689-022-09422-4 (2022).

290 Clooney, A. G. *et al.* Whole-Virome Analysis Sheds Light on Viral Dark Matter in Inflammatory Bowel Disease. *Cell Host Microbe* **26**, 764-778.e765, doi:10.1016/j.chom.2019.10.009 (2019).
291 Zuo, T. *et al.* Gut mucosal virome alterations in ulcerative colitis. *Gut* **68**, 1169-1179, doi:10.1136/gutjnl-2018-318131 (2019).
292 Allnutt, M. A. *et al.* Human Herpesvirus 6 Detection in Alzheimer's Disease Cases and Controls across Multiple Cohorts. *Neuron* **105**, 1027-1035.e1022, doi:10.1016/j.neuron.2019.12.031 (2020).
293 Hur, J. Y. *et al.* The innate immunity protein IFITM3 modulates γ-secretase in Alzheimer's disease. *Nature* **586**, 735-740, doi:10.1038/s41586-020-2681-2 (2020).
294 Ling, Z. *et al.* Structural and Functional Dysbiosis of Fecal Microbiota in Chinese Patients With Alzheimer's Disease. *Frontiers in cell and developmental biology* **8**, 634069, doi:10.3389/fcell.2020.634069 (2020).
295 Nagpal, R. *et al.* Gut mycobiome and its interaction with diet, gut bacteria and alzheimer's disease markers in subjects with mild cognitive impairment: A pilot study. *EBioMedicine* **59**, 102950 (2020).
296 Ye, T. *et al.* Effect of Probiotic Fungi against Cognitive Impairment in Mice via Regulation of the Fungal Microbiota-Gut-Brain Axis. *Journal of agricultural and food chemistry* **70**, 9026-9038, doi:10.1021/acs.jafc.2c03142 (2022).
297 Hong, G. *et al.* Gut fungal dysbiosis and altered bacterial-fungal interaction in patients with diarrhea-predominant irritable bowel syndrome: An explorative study. *Neurogastroenterology & Motility* **32**, e13891 (2020).
298 van Thiel, I. A. M. *et al.* Genetic and phenotypic diversity of fecal Candida albicans strains in irritable bowel syndrome. *Sci Rep* **12**, 5391, doi:10.1038/s41598-022-09436-x (2022).
299 Qiu, X. *et al.* Alterations in the mucosa-associated fungal microbiota in patients with ulcerative colitis. *Oncotarget* **8**, 107577 (2017).
300 Chiaro, T. R. *et al.* A member of the gut mycobiota modulates host purine metabolism exacerbating colitis in mice. *Sci Transl Med* **9**, doi:10.1126/scitranslmed.aaf9044 (2017).
301 Li, X. V. *et al.* Immune regulation by fungal strain diversity in inflammatory bowel disease. *Nature* **603**, 672-678, doi:10.1038/s41586-022-04502-w (2022).
302 Alookaran, J. *et al.* Fungi: Friend or Foe? A Mycobiome Evaluation in Children With Autism and Gastrointestinal Symptoms. *Journal of Pediatric Gastroenterology and Nutrition* **74**, 377-382 (2022).
303 Wang, T. *et al.* Methanogen Levels Are Significantly Associated with Fecal Microbiota Composition and Alpha Diversity in Healthy Adults and Irritable Bowel Syndrome Patients. *Microbiology Spectrum* **10**, e01653-01622 (2022).
304 Villanueva-Millan, M. J. *et al.* Methanogens and Hydrogen Sulfide Producing Bacteria Guide Distinct Gut Microbe Profiles and Irritable Bowel Syndrome Subtypes. *Official journal of the American College of Gastroenterology | ACG* **117** (2022).

305 Ghavami, S. B. *et al.* Alterations of the human gut Methanobrevibacter smithii as a biomarker for inflammatory bowel diseases. *Microbial pathogenesis* **117**, 285-289 (2018).
306 Coker, O. O., Wu, W. K. K., Wong, S. H., Sung, J. J. Y. & Yu, J. Altered Gut Archaea Composition and Interaction With Bacteria Are Associated With Colorectal Cancer. *Gastroenterology* **159**, 1459-1470.e1455, doi:https://doi.org/10.1053/j.gastro.2020.06.042 (2020).
307 Collaborators, G. M. D. Global, regional, and national burden of 12 mental disorders in 204 countries and territories, 1990–2019: a systematic analysis for the Global Burden of Disease Study 2019. *The Lancet Psychiatry* **9**, 137-150 (2022).
308 Santomauro, D. F. *et al.* Global prevalence and burden of depressive and anxiety disorders in 204 countries and territories in 2020 due to the COVID-19 pandemic. *The Lancet* **398**, 1700-1712 (2021).
309 Gao, X. *et al.* Chronic stress promotes colitis by disturbing the gut microbiota and triggering immune system response. *Proceedings of the National Academy of Sciences* **115**, E2960-E2969 (2018).
310 Krupa-Kotara, K., Gwioździk, W., Nandzik, S. & Grajek, M. The Role of Microbiota Pattern in Anxiety and Stress Disorders—A Review of the State of Knowledge. *Psych* **5**, 602-618 (2023).
311 Sudo, N. *et al.* Postnatal microbial colonization programs the hypothalamic–pituitary–adrenal system for stress response in mice. *The Journal of physiology* **558**, 263-275 (2004).
312 Willing, B. P., Vacharaksa, A., Croxen, M., Thanachayanont, T. & Finlay, B. B. Altering host resistance to infections through microbial transplantation. *PloS one* **6**, e26988 (2011).
313 Sherwin, E., Bordenstein, S. R., Quinn, J. L., Dinan, T. G. & Cryan, J. F. Microbiota and the social brain. *Science* **366**, eaar2016 (2019).
314 Desbonnet, L., Clarke, G., Shanahan, F., Dinan, T. G. & Cryan, J. Microbiota is essential for social development in the mouse. *Molecular psychiatry* **19**, 146-148 (2014).
315 Parracho, H. M. *et al.* A double-blind, placebo-controlled, crossover-designed probiotic feeding study in children diagnosed with autistic spectrum disorders. *International Journal of Probiotics & Prebiotics* **5**, 69 (2010).
316 Sharon, G. *et al.* Commensal bacteria play a role in mating preference of Drosophila melanogaster. *Proceedings of the National Academy of Sciences* **107**, 20051-20056 (2010).
317 Buffington, S. A. *et al.* Microbial reconstitution reverses maternal diet-induced social and synaptic deficits in offspring. *Cell* **165**, 1762-1775 (2016).
318 Alberoni, D. *et al.* Impact of beneficial bacteria supplementation on the gut microbiota, colony development and productivity of Apis mellifera L. *Beneficial microbes* **9**, 269-278 (2018).
319 Shaaban, S. Y. *et al.* The role of probiotics in children with autism spectrum disorder: A prospective, open-label study. *Nutritional neuroscience* **21**, 676-681 (2018).

320 Wu, W.-L. *et al.* Microbiota regulate social behaviour via stress response neurons in the brain. *Nature*, 1-6 (2021).
321 Agranyoni, O. *et al.* Gut microbiota determines the social behavior of mice and induces metabolic and inflammatory changes in their adipose tissue. *NPJ biofilms and microbiomes* **7**, 28 (2021).
322 Kessler, R. C. *et al.* Lifetime prevalence and age-of-onset distributions of DSM-IV disorders in the National Comorbidity Survey Replication. *Archives of general psychiatry* **62**, 593-602 (2005).
323 Ruscio, A. M. *et al.* Social fears and social phobia in the USA: results from the National Comorbidity Survey Replication. *Psychological medicine* **38**, 15-28 (2008).
324 Sarmiento, C. & Lau, C. Diagnostic and statistical manual of mental disorders: DSM-5. *The Wiley Encyclopedia of Personality and Individual Differences: Personality Processes and Individual Differences*, 125-129 (2020).
325 Butler, M. I. *et al.* The immune-kynurenine pathway in social anxiety disorder. *Brain, behavior, and immunity* **99**, 317-326 (2022).
326 Wigger, A. & Neumann, I. D. Periodic maternal deprivation induces gender-dependent alterations in behavioral and neuroendocrine responses to emotional stress in adult rats. *Physiol Behav* **66**, 293-302, doi:10.1016/s0031-9384(98)00300-x (1999).
327 Bale, T. L. *et al.* Mice deficient for corticotropin-releasing hormone receptor-2 display anxiety-like behaviour and are hypersensitive to stress. *Nat Genet* **24**, 410-414, doi:10.1038/74263 (2000).
328 Reber, S., Obermeier, F., Straub, R., Falk, W. & Neumann, I. Chronic intermittent psycho-social stress in mice increases the severity of an acute DSS-induced colitis and additionally impairs regeneration. *Endocrinology* **147**, 4968-4976 (2006).
329 Ait-Belgnaoui, A. *et al.*
330 Bharwani, A., Mian, M. F., Surette, M. G., Bienenstock, J. & Forsythe, P. Oral treatment with Lactobacillus rhamnosus attenuates behavioural deficits and immune changes in chronic social stress. *BMC Med* **15**, 7, doi:10.1186/s12916-016-0771-7 (2017).
331 Ávila, P. R. M. *et al.* Effects of microbiota transplantation and the role of the vagus nerve in gut–brain axis in animals subjected to chronic mild stress. *Journal of Affective Disorders* **277**, 410-416 (2020).
332 Cai, T. *et al.* Therapeutic effect of fecal microbiota transplantation on chronic unpredictable mild stress-induced depression. *Frontiers in Cellular and Infection Microbiology* **12**, 900652 (2022).
333 Werbner, M. *et al.* Social-stress-responsive microbiota induces stimulation of self-reactive effector T helper cells. *MSystems* **4**, e00292-00218 (2019).
334 Turk, C. L., Heimberg, R. G. & Magee, L. Social anxiety disorder. *Clinical handbook of psychological disorders: A step-by-step treatment manual* **3**, 114-153 (2001).
335 Gould, R. A., Buckminster, S., Pollack, M. H., Otto, M. W. & Yap, L. Cognitive-behavioral and pharmacological treatment for social phobia: a meta-analysis. *Clinical Psychology: Science and Practice* **4**, 291 (1997).

336 Toth, I., Neumann, I. D. & Slattery, D. A. Social fear conditioning: a novel and specific animal model to study social anxiety disorder. *Neuropsychopharmacology* **37**, 1433 (2012).
337 Hidaka, B. H. Depression as a disease of modernity: explanations for increasing prevalence. *J Affect Disord* **140**, 205-214, doi:10.1016/j.jad.2011.12.036 (2012).
338 Shah, S. M. A., Mohammad, D., Qureshi, M. F. H., Abbas, M. Z. & Aleem, S. Prevalence, Psychological Responses and Associated Correlates of Depression, Anxiety and Stress in a Global Population, During the Coronavirus Disease (COVID-19) Pandemic. *Community mental health journal* **57**, 101-110, doi:10.1007/s10597-020-00728-y (2021).
339 Cryan, J. F. & Mazmanian, S. K. Microbiota–brain axis: Context and causality. *Science* **376**, 938-939, doi:10.1126/science.abo4442 (2022).
340 Zoicas, I., Slattery, D. A. & Neumann, I. D. Brain oxytocin in social fear conditioning and its extinction: involvement of the lateral septum. *Neuropsychopharmacology* **39**, 3027 (2014).
341 Zoicas, I., Menon, R. & Neumann, I. D. Neuropeptide S reduces fear and avoidance of con-specifics induced by social fear conditioning and social defeat, respectively. *Neuropharmacology* **108**, 284-291, doi:10.1016/j.neuropharm.2016.03.054 (2016).
342 Royer, M. *et al.* Transcriptome and chromatin alterations in social fear indicate association of MEG3 with successful extinction of fear. *Molecular Psychiatry* **27**, 4064-4076, doi:10.1038/s41380-022-01481-2 (2022).
343 Fehm, L., Pelissolo, A., Furmark, T. & Wittchen, H. U. Size and burden of social phobia in Europe. *European neuropsychopharmacology : the journal of the European College of Neuropsychopharmacology* **15**, 453-462, doi:10.1016/j.euroneuro.2005.04.002 (2005).
344 Kessler, R. C., Petukhova, M., Sampson, N. A., Zaslavsky, A. M. & Wittchen, H. U. Twelve-month and lifetime prevalence and lifetime morbid risk of anxiety and mood disorders in the United States. *International journal of methods in psychiatric research* **21**, 169-184 (2012).
345 Menard, C. *et al.* Social stress induces neurovascular pathology promoting depression. *Nature neuroscience* **20**, 1752-1760 (2017).
346 Lozupone, C. A., Stombaugh, J. I., Gordon, J. I., Jansson, J. K. & Knight, R. Diversity, stability and resilience of the human gut microbiota. *Nature* **489**, 220-230 (2012).
347 Brunse, A. *et al.* Fecal filtrate transplantation protects against necrotizing enterocolitis. *The ISME journal* **16**, 686-694 (2022).
348 Lin, D. M. *et al.* Transplanting fecal virus-like particles reduces high-fat diet-induced small intestinal bacterial overgrowth in mice. *Frontiers in Cellular and Infection Microbiology* **9**, 348 (2019).
349 Draper, L. A. *et al.* Autochthonous faecal viral transfer (FVT) impacts the murine microbiome after antibiotic perturbation. *BMC Biology* **18**, 1-14 (2020).
350 Foster, J. A. & Neufeld, K.-A. M. Gut–brain axis: how the microbiome influences anxiety and depression. *Trends in neurosciences* **36**, 305-312 (2013).

351 Chong, H. *et al.* Lactobacillus plantarum DR7 alleviates stress and anxiety in adults: a randomised, double-blind, placebo-controlled study. *Beneficial microbes* **10**, 355-373 (2019).
352 Bastiaanssen, T. F. *et al.* Volatility as a Concept to Understand the Impact of Stress on the Microbiome. *Psychoneuroendocrinology* **124**, 105047 (2021).
353 Minot, S. *et al.* The human gut virome: inter-individual variation and dynamic response to diet. *Genome research* **21**, 1616-1625 (2011).
354 Coughlan, S. *et al.* The gut virome in irritable bowel syndrome differs from that of controls. *Gut Microbes* **13**, 1887719 (2021).
355 Mayneris-Perxachs, J. *et al.* Caudovirales bacteriophages are associated with improved executive function and memory in flies, mice, and humans. *Cell Host & Microbe* **30**, 340-356. e348 (2022).
356 Finger, B., Dinan, T. & Cryan, J. High-fat diet selectively protects against the effects of chronic social stress in the mouse. *Neuroscience* **192**, 351-360 (2011).
357 Kinsey, S. G., Bailey, M. T., Sheridan, J. F., Padgett, D. A. & Avitsur, R. Repeated social defeat causes increased anxiety-like behavior and alters splenocyte function in C57BL/6 and CD-1 mice. *Brain, behavior, and immunity* **21**, 458-466 (2007).
358 Merlot, E., Moze, E., Dantzer, R. & Neveu, P. J. Cytokine production by spleen cells after social defeat in mice: activation of T cells and reduced inhibition by glucocorticoids. *Stress* **7**, 55-61 (2004).
359 Vieira-Silva, S. *et al.* Species–function relationships shape ecological properties of the human gut microbiome. *Nature microbiology* **1**, 1-8 (2016).
360 Wu, X. *et al.* Gut microbiota contributes to the methionine metabolism in host. *Frontiers in Microbiology* **13**, 1065668 (2022).
361 Ullah, H. *et al.* The Efficacy of S-Adenosyl Methionine and Probiotic Supplementation on Depression: A Synergistic Approach. *Nutrients* **14**, 2751 (2022).
362 Baldessarini, R. J. Neuropharmacology of S-adenosyl-L-methionine. *The American journal of medicine* **83**, 95-103 (1987).
363 Bottiglieri, T. *et al.* S-adenosylmethionine influences monoamine metabolism. *The Lancet* **324**, 224 (1984).
364 van de Wouw, M., Boehme, M., Dinan, T. G. & Cryan, J. F. Monocyte mobilisation, microbiota & mental illness. *Brain, Behavior, and Immunity* **81**, 74-91 (2019).
365 Niraula, A., Witcher, K. G., Sheridan, J. F. & Godbout, J. P. Interleukin-6 induced by social stress promotes a unique transcriptional signature in the monocytes that facilitate anxiety. *Biological psychiatry* **85**, 679-689 (2019).
366 Hodes, G. E. *et al.* Individual differences in the peripheral immune system promote resilience versus susceptibility to social stress. *Proceedings of the National Academy of Sciences* **111**, 16136-16141 (2014).
367 Wohleb, E. S., Powell, N. D., Godbout, J. P. & Sheridan, J. F. Stress-induced recruitment of bone marrow-derived monocytes to the brain promotes anxiety-like behavior. *Journal of Neuroscience* **33**, 13820-13833 (2013).
368 Dhabhar, F. S., Malarkey, W. B., Neri, E. & McEwen, B. S. Stress-induced redistribution of immune cells—From barracks to boulevards to battlefields: A

tale of three hormones–Curt Richter Award Winner. *Psychoneuroendocrinology* **37**, 1345-1368 (2012).
369 Swirski, F. K. *et al.* Identification of splenic reservoir monocytes and their deployment to inflammatory sites. *Science* **325**, 612-616 (2009).
370 Xu, H., Manivannan, A., Crane, I., Dawson, R. & Liversidge, J. Critical but divergent roles for CD62L and CD44 in directing blood monocyte trafficking in vivo during inflammation. *Blood, The Journal of the American Society of Hematology* **112**, 1166-1174 (2008).
371 Sharvin, B. L., Aburto, M. R. & Cryan, J. F. Decoding the neurocircuitry of gut feelings: Region-specific microbiome-mediated brain alterations. *Neurobiology of Disease* **179**, 106033 (2023).
372 Cowan, C. S. *et al.* Gutsy moves: the amygdala as a critical node in microbiota to brain signaling. *BioEssays* **40**, 1700172 (2018).
373 Guzzetta, K. E., Cryan, J. F. & O'Leary, O. F. Microbiota-gut-brain axis regulation of adult hippocampal neurogenesis. *Brain Plasticity* **8**, 97-119 (2022).
374 Blake, J. A. *et al.* Mouse Genome Database (MGD): Knowledgebase for mouse–human comparative biology. *Nucleic Acids Research* **49**, D981-D987 (2021).
375 Cheng, H.-W., Jiang, S. & Hu, J. in *Oral Health by Using Probiotic Products* (IntechOpen, 2019).
376 Zhang, T. *et al.* Alleviation of Neuronal Cell Death and Memory Deficit with Chungkookjang Made with Bacillus amyloliquefaciens and Bacillus subtilis Potentially through Promoting Gut–Brain Axis in Artery-Occluded Gerbils. *Foods* **10**, 2697 (2021).
377 Feng, S., Meng, C., Hao, Z. & Liu, H. Bacillus licheniformis Reshapes the Gut Microbiota to Alleviate the Subhealth. *Nutrients* **14**, 1642 (2022).
378 Wang, Y. *et al.* Bacillus amyloliquefaciens SC06 attenuated high-fat diet induced anxiety-like behavior and social withdrawal of male mice by improving antioxidant capacity, intestinal barrier function and modulating intestinal dysbiosis. *Behavioural Brain Research*, 114172 (2022).
379 Forbes, J. D., Van Domselaar, G. & Bernstein, C. N. The gut microbiota in immune-mediated inflammatory diseases. *Frontiers in microbiology* **7**, 1081 (2016).
380 Stilling, R. M. *et al.* The neuropharmacology of butyrate: the bread and butter of the microbiota-gut-brain axis? *Neurochemistry international* **99**, 110-132 (2016).
381 Kaakoush, N. O. Vol. 5 84 (Frontiers Media SA, 2015).
382 Dey, N., Soergel, D. A., Repo, S. & Brenner, S. E. Association of gut microbiota with post-operative clinical course in Crohn's disease. *BMC gastroenterology* **13**, 1-11 (2013).
383 Gevers, D. *et al.* The treatment-naive microbiome in new-onset Crohn's disease. *Cell host & microbe* **15**, 382-392 (2014).
384 Labbé, A., Ganopolsky, J. G., Martoni, C. J., Prakash, S. & Jones, M. L. Bacterial bile metabolising gene abundance in Crohn's, ulcerative colitis and type 2 diabetes metagenomes. *PloS one* **9**, e115175 (2014).
385 Craven, M. *et al.* Inflammation drives dysbiosis and bacterial invasion in murine models of ileal Crohn's disease. *PloS one* **7**, e41594 (2012).

386 Schaubeck, M. *et al.* Dysbiotic gut microbiota causes transmissible Crohn's disease-like ileitis independent of failure in antimicrobial defence. *Gut* **65**, 225-237 (2016).
387 Han, H. *et al.* Effects of ammonia on gut microbiota and growth performance of broiler chickens. *Animals* **11**, 1716 (2021).
388 Maura, D., Elmekki, N. & Goddard, C. A. The ammonia oxidizing bacterium Nitrosomonas eutropha blocks T helper 2 cell polarization via the anti-inflammatory cytokine IL-10. *Scientific reports* **11**, 1-10 (2021).
389 Fan, P., Lavoie, J., Le, N., Szerb, J. & Butterworth, R. Neurochemical and electrophysiological studies on the inhibitory effect of ammonium ions on synaptic transmission in slices of rat hippocampus: evidence for a postsynaptic action. *Neuroscience* **37**, 327-334 (1990).
390 Grady, E. N., MacDonald, J., Liu, L., Richman, A. & Yuan, Z.-C. Current knowledge and perspectives of Paenibacillus: a review. *Microbial cell factories* **15**, 1-18 (2016).
391 Yao, Z.-Y. *et al.* Maternal sleep deprivation induces gut microbial dysbiosis and neuroinflammation in offspring rats. *Zoological Research* **43**, 380 (2022).
392 Gu, J. *et al.* The potential mechanism of BPF-induced neurotoxicity in adult zebrafish: Correlation between untargeted metabolomics and gut microbiota. *Science of The Total Environment*, 156221 (2022).
393 Pu, Y. *et al.* A role of the subdiaphragmatic vagus nerve in depression-like phenotypes in mice after fecal microbiota transplantation from Chrna7 knock-out mice with depression-like phenotypes. *Brain, Behavior, and Immunity* **94**, 318-326 (2021).
394 Fitzgerald, C. B. *et al.* Probing the "Dark Matter" of the Human Gut Phageome: Culture Assisted Metagenomics Enables Rapid Discovery and Host-Linking for Novel Bacteriophages. *Frontiers in Cellular and Infection Microbiology* **11** (2021).
395 Roux, S. *et al.* iPHoP: an integrated machine-learning framework to maximize host prediction for metagenome-assembled virus genomes. *bioRxiv* (2022).
396 Latka, A. *et al.* Engineering the modular receptor-binding proteins of Klebsiella phages switches their capsule serotype specificity. *MBio* **12**, 10.1128/mbio. 00455-00421 (2021).
397 Beamud, B. *et al.* Genetic determinants of host tropism in Klebsiella phages. *Cell Reports* **42** (2023).
398 Scanlan, P. D. Bacteria–bacteriophage coevolution in the human gut: implications for microbial diversity and functionality. *Trends in microbiology* **25**, 614-623 (2017).
399 Dhabhar, F. S. & Mcewen, B. S. Acute stress enhances while chronic stress suppresses cell-mediated immunityin vivo: A potential role for leukocyte trafficking. *Brain, behavior, and immunity* **11**, 286-306 (1997).
400 Joshi, A., Punke, E. B., Mehmetoglu-Gurbuz, T., Peralta, D. P. & Garg, H. TLR9 polymorphism correlates with immune activation, CD4 decline and plasma IP10 levels in HIV patients. *BMC infectious diseases* **19**, 1-13 (2019).

401 Hayney, M. S. *et al.* Serum IFN-γ-induced protein 10 (IP-10) as a biomarker for severity of acute respiratory infection in healthy adults. *Journal of Clinical Virology* **90**, 32-37 (2017).
402 Carroll-Portillo, A. & Lin, H. C. Bacteriophage and the innate immune system: access and signaling. *Microorganisms* **7**, 625 (2019).
403 Hoban, A. E. *et al.* The microbiome regulates amygdala-dependent fear recall. *Molecular psychiatry* **23**, 1134-1144 (2018).
404 Lima-Junior, D. S. *et al.* Endogenous retroviruses promote homeostatic and inflammatory responses to the microbiota. *Cell* **184**, 3794-3811. e3719 (2021).
405 Borin, J. M. *et al.* Fecal virome transplantation is sufficient to alter fecal microbiota and drive lean and obese body phenotypes in mice. *BioRxiv*, 2023.2002. 2003.527064 (2023).
406 Mao, X. *et al.* A reproducible enteric phage community improves blood glucose regulation in an obesity mouse model. *BioRxiv*, 2023.2003. 2020.532903 (2023).
407 Rasmussen, T. S. *et al.* Bacteriophage-mediated manipulation of the gut microbiome-promises and presents limitations. *FEMS Microbiology Reviews* (2020).
408 Wu, D. *et al.* Beyond faecal microbiota transplantation, the non-negligible role of faecal virome or bacteriophage transplantation. *Journal of Microbiology, Immunology and Infection* (2023).
409 Raeisi, H. *et al.* Emerging applications of phage therapy and fecal virome transplantation for treatment of Clostridioides difficile infection: challenges and perspectives. *Gut Pathogens* **15**, 1-20 (2023).
410 Gururajan, A. *et al.* Resilience to chronic stress is associated with specific neurobiological, neuroendocrine and immune responses. *Brain, behavior, and immunity* **80**, 583-594 (2019).
411 Tsankova, N. M. *et al.* Sustained hippocampal chromatin regulation in a mouse model of depression and antidepressant action. *Nature neuroscience* **9**, 519-525 (2006).
412 Klindworth, A. *et al.* Evaluation of general 16S ribosomal RNA gene PCR primers for classical and next-generation sequencing-based diversity studies. *Nucleic acids research* **41**, e1-e1 (2013).
413 Shkoporov, A. N. *et al.* Viral biogeography of the mammalian gut and parenchymal organs. *Nature microbiology* **7**, 1301-1311 (2022).
414 Chen, S., Zhou, Y., Chen, Y. & Gu, J. fastp: an ultra-fast all-in-one FASTQ preprocessor. *Bioinformatics* **34**, i884-i890 (2018).
415 Wood, D. E., Lu, J. & Langmead, B. Improved metagenomic analysis with Kraken 2. *Genome biology* **20**, 1-13 (2019).
416 Andrews, S. (Babraham Bioinformatics, Babraham Institute, Cambridge, United Kingdom, 2010).
417 Li, D., Liu, C.-M., Luo, R., Sadakane, K. & Lam, T.-W. MEGAHIT: an ultra-fast single-node solution for large and complex metagenomics assembly via succinct de Bruijn graph. *Bioinformatics* **31**, 1674-1676 (2015).

418 Roux, S. *et al.* IMG/VR v3: an integrated ecological and evolutionary framework for interrogating genomes of uncultivated viruses. *Nucleic acids research* **49**, D764-D775 (2021).
419 Cao, Q. *et al.* Effects of rare microbiome taxa filtering on statistical analysis. *Frontiers in microbiology* **11**, 607325 (2021).
420 Hyatt, D. *et al.* Prodigal: prokaryotic gene recognition and translation initiation site identification. *BMC bioinformatics* **11**, 1-11 (2010).
421 Terzian, P. *et al.* PHROG: families of prokaryotic virus proteins clustered using remote homology. *NAR Genomics and Bioinformatics* **3**, lqab067 (2021).
422 Roux, S. *et al.* Cryptic inoviruses revealed as pervasive in bacteria and archaea across Earth's biomes. *Nature microbiology* **4**, 1895-1906 (2019).
423 Guo, J. *et al.* VirSorter2: a multi-classifier, expert-guided approach to detect diverse DNA and RNA viruses. *Microbiome* **9**, 1-13 (2021).
424 Ren, J. *et al.* Identifying viruses from metagenomic data using deep learning. *Quantitative Biology* **8**, 64-77 (2020).
425 Nayfach, S. *et al.* CheckV assesses the quality and completeness of metagenome-assembled viral genomes. *Nature biotechnology* **39**, 578-585 (2021).
426 Bin Jang, H. *et al.* Taxonomic assignment of uncultivated prokaryotic virus genomes is enabled by gene-sharing networks. *Nature biotechnology* **37**, 632-639 (2019).
427 Hockenberry, A. J. & Wilke, C. O. BACPHLIP: predicting bacteriophage lifestyle from conserved protein domains. *PeerJ* **9**, e11396 (2021).
428 Langmead, B. & Salzberg, S. L. Fast gapped-read alignment with Bowtie 2. *Nature methods* **9**, 357-359 (2012).
429 Li, H. *et al.* The sequence alignment/map format and SAMtools. *Bioinformatics* **25**, 2078-2079 (2009).
430 Roux, S., Emerson, J. B., Eloe-Fadrosh, E. A. & Sullivan, M. B. Benchmarking viromics: an in silico evaluation of metagenome-enabled estimates of viral community composition and diversity. *PeerJ* **5**, e3817 (2017).
431 McLaren, M. R., Willis, A. D. & Callahan, B. J. Consistent and correctable bias in metagenomic sequencing experiments. *Elife* **8**, e46923 (2019).
432 Gloor, G. B., Macklaim, J. M., Pawlowsky-Glahn, V. & Egozcue, J. J. Microbiome datasets are compositional: and this is not optional. *Frontiers in microbiology* **8**, 2224 (2017).
433 Aitchison, J. The statistical analysis of compositional data. *Journal of the Royal Statistical Society: Series B (Methodological)* **44**, 139-160 (1982).
434 Lubbe, S., Filzmoser, P. & Templ, M. Comparison of zero replacement strategies for compositional data with large numbers of zeros. *Chemometrics and Intelligent Laboratory Systems* **210**, 104248 (2021).
435 Hsieh, T., Ma, K. & Chao, A. iNEXT: an R package for rarefaction and extrapolation of species diversity (H ill numbers). *Methods in Ecology and Evolution* **7**, 1451-1456 (2016).
436 Bates, D., Kliegl, R., Vasishth, S. & Baayen, H. Parsimonious mixed models. *arXiv preprint arXiv:1506.04967* (2015).

437 Patel, A. *et al.* Virus and prokaryote enumeration from planktonic aquatic environments by epifluorescence microscopy with SYBR Green I. *Nature protocols* **2**, 269 (2007).
438 Simon 3, E. B. I. B. E. G. N. K. A. M. E. R. A. G. S. G. S. A. U.-V. A. W. *et al.* Initial sequencing and comparative analysis of the mouse genome. *Nature* **420**, 520-562 (2002).
439 Bray, N. L., Pimentel, H., Melsted, P. & Pachter, L. Near-optimal probabilistic RNA-seq quantification. *Nature biotechnology* **34**, 525-527 (2016).
440 Bastiaanssen, T. F., Quinn, T. P. & Loughman, A. Bugs as features (part 1): concepts and foundations for the compositional data analysis of the microbiome–gut–brain axis. *Nature Mental Health*, doi:https://doi.org/10.1038/s44220-023-00148-3 (2023).
441 Bastiaanssen, T. F., Quinn, T. P. & Loughman, A. Bugs as features (part 2): a perspective on enriching microbiome–gut–brain axis analyses. *Nature Mental Health*, doi:https://doi.org/10.1038/s44220-023-00149-2 (2023).
442 Bourgon, R., Gentleman, R. & Huber, W. Independent filtering increases detection power for high-throughput experiments. *Proceedings of the National Academy of Sciences* **107**, 9546-9551 (2010).
443 Xie, Z. *et al.* Gene set knowledge discovery with enrichr. *Current protocols* **1**, e90 (2021).
444 The Gene Ontology resource: enriching a GOld mine. *Nucleic acids research* **49**, D325-D334 (2021).
445 Bastiaanssen, T. F., Quinn, T. P. & Cryan, J. F. Knowledge-based Integration of Multi-Omic Datasets with Anansi: Annotation-based Analysis of Specific Interactions. *arXiv preprint arXiv:2305.10832* (2023).
446 Stein, M. B. & Stein, D. J. Social anxiety disorder. *The lancet* **371**, 1115-1125 (2008).
447 Baldwin, D. S. *et al.* Evidence-based pharmacological treatment of anxiety disorders, post-traumatic stress disorder and obsessive-compulsive disorder: a revision of the 2005 guidelines from the British Association for Psychopharmacology. *Journal of Psychopharmacology* **28**, 403-439 (2014).
448 Tanelian, A., Nankova, B., Miari, M., Nahvi, R. J. & Sabban, E. L. Resilience or susceptibility to traumatic stress: Potential influence of the microbiome. *Neurobiology of Stress* **19**, 100461 (2022).
449 Feder, A., Nestler, E. J. & Charney, D. S. Psychobiology and molecular genetics of resilience. *Nature Reviews Neuroscience* **10**, 446-457 (2009).
450 Bagot, R. C. *et al.* Circuit-wide transcriptional profiling reveals brain region-specific gene networks regulating depression susceptibility. *Neuron* **90**, 969-983 (2016).
451 Toth, I., Neumann, I. D. & Slattery, D. A. Social fear conditioning as an animal model of social anxiety disorder. *Current protocols in neuroscience* **63**, 9.42. 41-49.42. 13 (2013).
452 Livak, K. J. & Schmittgen, T. D. Analysis of relative gene expression data using real-time quantitative PCR and the 2− ΔΔCT method. *methods* **25**, 402-408 (2001).

453 Sato, R. G. E. R. G. P. I. T. C. P. H. N. H.-K. T. K. H. N. M. S. N., 13, M. G. S. C. W. R. L. E. R. J. B. E. & 6, S. m. H. Y. Analysis of the mouse transcriptome based on functional annotation of 60,770 full-length cDNAs. *Nature* **420**, 563-573 (2002).
454 Bastiaanssen, T. F., Quinn, T. P. & Loughman, A. Bugs as Features (Part II): A Perspective on Enriching Microbiome-Gut-Brain Axis Analyses with Multidisciplinary Techniques. *arXiv preprint arXiv:2305.11703* (2023).
455 Mandal, S. *et al.* Analysis of composition of microbiomes: a novel method for studying microbial composition. *Microbial ecology in health and disease* **26**, 27663 (2015).
456 Aitchison, J., Barceló-Vidal, C., Martín-Fernández, J. A. & Pawlowsky-Glahn, V. Logratio analysis and compositional distance. *Mathematical geology* **32**, 271-275 (2000).
457 Johnson, K. V.-A. & Foster, K. R. Why does the microbiome affect behaviour? *Nature reviews microbiology* **16**, 647-655 (2018).
458 Sarkar, A. *et al.* The role of the microbiome in the neurobiology of social behaviour. *Biological Reviews* **95**, 1131-1166 (2020).
459 Olsson, A. & Phelps, E. A. Social learning of fear. *Nature neuroscience* **10**, 1095-1102 (2007).
460 Irle, E. *et al.* Reduced amygdalar and hippocampal size in adults with generalized social phobia. *Journal of psychiatry and neuroscience* **35**, 126-131 (2010).
461 Machado-de-Sousa, J. P. *et al.* Increased amygdalar and hippocampal volumes in young adults with social anxiety. *PloS one* **9**, e88523 (2014).
462 Qi, C.-C. *et al.* Interaction of basolateral amygdala, ventral hippocampus and medial prefrontal cortex regulates the consolidation and extinction of social fear. *Behavioral and Brain Functions* **14**, 1-13 (2018).
463 Ruiz-Opazo, N. & Tonkiss, J. Genome-wide scan for quantitative trait loci influencing spatial navigation and social recognition memory in Dahl rats. *Physiological genomics* **26**, 145-151 (2006).
464 Gunturkun, M. H. *et al.* Genome-wide association study on three behaviors tested in an open field in heterogeneous stock rats identifies multiple loci implicated in psychiatric disorders. *Frontiers in Psychiatry* **13**, 790566 (2022).
465 Tennant-Eyles, A. J., Moffitt, H., Whitehouse, C. A. & Roberts, R. G. Characterisation of the FAM69 family of cysteine-rich endoplasmic reticulum proteins. *Biochemical and Biophysical Research Communications* **406**, 471-477 (2011).
466 Dudkiewicz, M., Lenart, A. & Pawłowski, K. A novel predicted calcium-regulated kinase family implicated in neurological disorders. *PLoS One* **8**, e66427 (2013).
467 Fergusson, D. M., Boden, J. M., Horwood, L. J., Miller, A. L. & Kennedy, M. A. MAOA, abuse exposure and antisocial behaviour: 30-year longitudinal study. *The British Journal of Psychiatry* **198**, 457-463 (2011).
468 Fergusson, D. M., Boden, J. M., Horwood, L. J., Miller, A. & Kennedy, M. A. Moderating role of the MAOA genotype in antisocial behaviour. *The British Journal of Psychiatry* **200**, 116-123 (2012).

469 Campbell, D. B., Warren, D., Sutcliffe, J. S., Lee, E. B. & Levitt, P. Association of MET with social and communication phenotypes in individuals with autism spectrum disorder. *American Journal of Medical Genetics Part B: Neuropsychiatric Genetics* **153**, 438-446 (2010).
470 Lubke, G. *et al.* Genome-wide analyses of borderline personality features. *Molecular psychiatry* **19**, 923-929 (2014).
471 Iqbal, Z. *et al.* Homozygous SLC6A17 mutations cause autosomal-recessive intellectual disability with progressive tremor, speech impairment, and behavioral problems. *The American Journal of Human Genetics* **96**, 386-396 (2015).
472 Arenella, M. *et al.* Potential role for immune-related genes in autism spectrum disorders: Evidence from genome-wide association meta-analysis of autistic traits. *Autism* **26**, 361-372 (2022).
473 Cartoni, R. *et al.* The mammalian-specific protein Armcx1 regulates mitochondrial transport during axon regeneration. *Neuron* **92**, 1294-1307 (2016).
474 Li, B. & Yang, L. Creatine in T Cell antitumor immunity and cancer immunotherapy. *Nutrients* **13**, 1633 (2021).
475 Datler, C. *et al.* CKMT1 regulates the mitochondrial permeability transition pore in a process that provides evidence for alternative forms of the complex. *Journal of Cell Science* **127**, 1816-1828 (2014).
476 Pei, L. & Wallace, D. C. Mitochondrial etiology of neuropsychiatric disorders. *Biological psychiatry* **83**, 722-730 (2018).
477 McConnell, B. B. & Yang, V. W. Mammalian Krüppel-like factors in health and diseases. *Physiological reviews* **90**, 1337-1381 (2010).
478 Yin, K.-J., Hamblin, M., Fan, Y., Zhang, J. & Chen, Y. E. Krüpple-like factors in the central nervous system: novel mediators in Stroke. *Metabolic brain disease* **30**, 401-410 (2015).
479 McConnell, B. B., Klapproth, J. M. A., Sasaki, M., Nandan, M. O. & Yang, V. W. Krüppel-like factor 5 mediates transmissible murine colonic hyperplasia caused by Citrobacter rodentium infection. *Gastroenterology* **134**, 1007-1016. e1002 (2008).
480 Wang, J. *et al.* Genome-wide association analysis identifies variation in vitamin D receptor and other host factors influencing the gut microbiota. *Nature genetics* **48**, 1396-1406 (2016).
481 Cathcart, M. K. & Bhattacharjee, A. Monoamine oxidase A (MAO-A): a signature marker of alternatively activated monocytes/macrophages. *Inflammation and cell signaling* **1** (2014).
482 Mentis, A.-F. A., Dardiotis, E., Katsouni, E. & Chrousos, G. P. From warrior genes to translational solutions: novel insights into monoamine oxidases (MAOs) and aggression. *Translational psychiatry* **11**, 130 (2021).
483 Sun, X. *et al.* The MAOA gene influences the neural response to psychosocial stress in the human brain. *Frontiers in Behavioral Neuroscience* **14**, 65 (2020).
484 Siu, M., Sengupta Ghosh, A. & Lewcock, J. W. Dual Leucine Zipper Kinase Inhibitors for the Treatment of Neurodegeneration: Miniperspective. *Journal of Medicinal Chemistry* **61**, 8078-8087 (2018).

485 Guan, J., Fan, Y., Wang, S. & Zhou, F. Functions of MAP3Ks in antiviral immunity. *Immunologic Research*, 1-19 (2023).
486 Dixit, E. *et al.* Peroxisomes are signaling platforms for antiviral innate immunity. *Cell* **141**, 668-681 (2010).
487 Di Cara, F., Sheshachalam, A., Braverman, N. E., Rachubinski, R. A. & Simmonds, A. J. Peroxisome-mediated metabolism is required for immune response to microbial infection. *Immunity* **47**, 93-106. e107 (2017).
488 Vijayan, V. *et al.* A new immunomodulatory role for peroxisomes in macrophages activated by the TLR4 ligand lipopolysaccharide. *The Journal of Immunology* **198**, 2414-2425 (2017).
489 Timilsina, U. & Stavrou, S. SERINC5: One antiviral factor to bind them all. *PLoS pathogens* **19**, e1011076 (2023).
490 Nguyen, T. A. *et al.* SIDT1 localizes to endolysosomes and mediates double-stranded RNA transport into the cytoplasm. *The Journal of Immunology* **202**, 3483-3492 (2019).
491 Morell, M. *et al.* SIDT1 plays a key role in type I IFN responses to nucleic acids in plasmacytoid dendritic cells and mediates the pathogenesis of an imiquimod-induced psoriasis model. *EBioMedicine* **76** (2022).
492 Masola, V., Greco, N., Tozzo, P., Caenazzo, L. & Onisto, M. The role of SPATA2 in TNF signaling, cancer, and spermatogenesis. *Cell Death & Disease* **13**, 977 (2022).
493 Ren, Y. *et al.* Spata2 knockdown exacerbates brain inflammation via NF-κB/P38MAPK signaling and NLRP3 inflammasome activation in cerebral ischemia/reperfusion rats. *Neurochemical Research* **46**, 2262-2275 (2021).
494 Babb, J. A., Carini, L. M., Spears, S. L. & Nephew, B. C. Transgenerational effects of social stress on social behavior, corticosterone, oxytocin, and prolactin in rats. *Hormones and behavior* **65**, 386-393 (2014).
495 Harvey, B. H., Regenass, W., Dreyer, W. & Möller, M. Social isolation rearing-induced anxiety and response to agomelatine in male and female rats: role of corticosterone, oxytocin, and vasopressin. *Journal of Psychopharmacology* **33**, 640-646 (2019).
496 Lukas, M. *et al.* The neuropeptide oxytocin facilitates pro-social behavior and prevents social avoidance in rats and mice. *Neuropsychopharmacology* **36**, 2159-2168 (2011).
497 Donaldson, Z. R. & Young, L. J. Oxytocin, vasopressin, and the neurogenetics of sociality. *Science* **322**, 900-904 (2008).
498 Stein, M. B. & Kean, Y. M. Disability and quality of life in social phobia: epidemiologic findings. *American Journal of Psychiatry* **157**, 1606-1613 (2000).
499 Keller, M. The lifelong course of social anxiety disorder: a clinical perspective. *Acta Psychiatrica Scandinavica* **108**, 85-94 (2003).
500 Patel, A., Knapp, M., Henderson, J. & Baldwin, D. The economic consequences of social phobia. *Journal of affective disorders* **68**, 221-233 (2002).
501 Gheorghe, C. E. *et al.* Investigating causality with fecal microbiota transplantation in rodents: applications, recommendations and pitfalls. *Gut microbes* **13**, 1941711 (2021).

502 Secombe, K. *et al.* Guidelines For Reporting On Animal Faecal Transplantation (GRAFT) Studies: Recommendations From A Systematic Review of Murine Transplantation Protocols. (2021).
503 Li, D. *et al.* 3β-Hydroxysteroid dehydrogenase expressed by gut microbes degrades testosterone and is linked to depression in males. *Cell Host & Microbe* **30**, 329-339. e325 (2022).
504 Li, D. *et al.* Gut-microbiome-expressed 3β-hydroxysteroid dehydrogenase degrades estradiol and is linked to depression in premenopausal females. *Cell Metabolism* **35**, 685-694. e685 (2023).
505 Zhang, W. *et al.* Preliminary evidence for an influence of exposure to polycyclic aromatic hydrocarbons on the composition of the gut microbiota and neurodevelopment in three-year-old healthy children. *BMC pediatrics* **21**, 1-13 (2021).
506 Li, Y. *et al.* Gut metagenomic characteristics of ADHD reveal low Bacteroides ovatus-associated host cognitive impairment. *Gut Microbes* **14**, 2125747 (2022).
507 Zeamer, A. *et al.* Pilot study of the association between microbiome and the development of adverse posttraumatic neuropsychiatric sequelae after traumatic stress exposure. *medRxiv*, 2023.2003. 2001.23286577 (2023).
508 Nuccio, D. A., Normann, M. C., Zhou, H., Grippo, A. J. & Singh, P. Microbiome and Metabolome Variation as Indicator of Social Stress in Female Prairie Voles. *International Journal of Molecular Sciences* **24**, 1677 (2023).
509 Binelli, C. *et al.* New evidence of heterogeneity in social anxiety disorder: Defining two qualitatively different personality profiles taking into account clinical, environmental and genetic factors. *European Psychiatry* **30**, 160-165 (2015).
510 Costache, M. E. *et al.* Higher-and lower-order personality traits and cluster subtypes in social anxiety disorder. *PloS one* **15**, e0232187 (2020).
511 Condren, R., O'Neill, A., Ryan, M., Barrett, P. & Thakore, J. HPA axis response to a psychological stressor in generalised social phobia. *Psychoneuroendocrinology* **27**, 693-703 (2002).
512 Azzinnari, D. *et al.* Mouse social stress induces increased fear conditioning, helplessness and fatigue to physical challenge together with markers of altered immune and dopamine function. *Neuropharmacology* **85**, 328-341 (2014).
513 Zenobia, C. & Hajishengallis, G. Basic biology and role of interleukin-17 in immunity and inflammation. *Periodontology 2000* **69**, 142-159 (2015).
514 Ye, P. *et al.* Requirement of interleukin 17 receptor signaling for lung CXC chemokine and granulocyte colony-stimulating factor expression, neutrophil recruitment, and host defense. *The Journal of experimental medicine* **194**, 519-528 (2001).
515 Gaffen, S. L. Structure and signalling in the IL-17 receptor family. *Nature Reviews Immunology* **9**, 556-567 (2009).
516 Chen, C. *et al.* IL-17 is a neuromodulator of Caenorhabditis elegans sensory responses. *Nature* **542**, 43-48 (2017).
517 Reed, M. D. *et al.* IL-17a promotes sociability in mouse models of neurodevelopmental disorders. *Nature* **577**, 249-253 (2020).

518 Schumann, J., Stanko, K., Schliesser, U., Appelt, C. & Sawitzki, B. Differences in CD44 surface expression levels and function discriminates IL-17 and IFN-γ producing helper T cells. *PLoS One* **10**, e0132479 (2015).
519 Neumann, I. D. & Slattery, D. A. Oxytocin in general anxiety and social fear: a translational approach. *Biological psychiatry* **79**, 213-221 (2016).
520 Hasan, M. T. *et al.* A fear memory engram and its plasticity in the hypothalamic oxytocin system. *Neuron* **103**, 133-146. e138 (2019).
521 Triana-Del Rio, R. *et al.* The modulation of emotional and social behaviors by oxytocin signaling in limbic network. *Frontiers in Molecular Neuroscience* (2022).
522 Dölen, G., Darvishzadeh, A., Huang, K. W. & Malenka, R. C. Social reward requires coordinated activity of nucleus accumbens oxytocin and serotonin. *Nature* **501**, 179-184 (2013).
523 Dumais, K. M., Alonso, A. G., Immormino, M. A., Bredewold, R. & Veenema, A. H. Involvement of the oxytocin system in the bed nucleus of the stria terminalis in the sex-specific regulation of social recognition. *Psychoneuroendocrinology* **64**, 79-88 (2016).
524 Bredewold, R. & Veenema, A. H. Sex differences in the regulation of social and anxiety-related behaviors: insights from vasopressin and oxytocin brain systems. *Current opinion in neurobiology* **49**, 132-140 (2018).
525 Caldwell, H. K. Oxytocin and sex differences in behavior. *Current opinion in behavioral sciences* **23**, 13-20 (2018).
526 Duque-Wilckens, N. *et al.* Extrahypothalamic oxytocin neurons drive stress-induced social vigilance and avoidance. *Proceedings of the National Academy of Sciences* **117**, 26406-26413 (2020).
527 Martinon, D. *et al.* Oxytocin receptors in the dorsolateral bed nucleus of the stria terminalis (BNST) bias fear learning toward temporally predictable cued fear. *Translational Psychiatry* **9**, 140 (2019).
528 DeVito, L. M. *et al.* Vasopressin 1b receptor knock-out impairs memory for temporal order. *Journal of Neuroscience* **29**, 2676-2683 (2009).
529 Wersinger, S. R., Caldwell, H. K., Christiansen, M. & Young III, W. Disruption of the vasopressin 1b receptor gene impairs the attack component of aggressive behavior in mice. *Genes, Brain and Behavior* **6**, 653-660 (2007).
530 Wersinger, S., Ginns, E. I., O'carroll, A., Lolait, S. & Young Iii, W. Vasopressin V1b receptor knockout reduces aggressive behavior in male mice. *Molecular psychiatry* **7**, 975-984 (2002).
531 Litvin, Y., Murakami, G. & Pfaff, D. W. Effects of chronic social defeat on behavioral and neural correlates of sociality: vasopressin, oxytocin and the vasopressinergic V1b receptor. *Physiology & behavior* **103**, 393-403 (2011).
532 Gururajan, A., Bastiaanssen, T. F., Ventura Silva, A. P., Moloney, G. M. & Cryan, J. F. The impact of psychosocial defeat stress on the bed nucleus of the stria terminalis transcriptome in adult male mice. *European Journal of Neuroscience* **55**, 67-77 (2022).

533 Clauss, J. A., Avery, S. N., Benningfield, M. M. & Blackford, J. U. Social anxiety is associated with BNST response to unpredictability. *Depression and anxiety* **36**, 666-675 (2019).
534 Ferguson, J. N., Aldag, J. M., Insel, T. R. & Young, L. J. Oxytocin in the medial amygdala is essential for social recognition in the mouse. *Journal of Neuroscience* **21**, 8278-8285 (2001).
535 Tan, Y. *et al.* Oxytocin receptors are expressed by glutamatergic prefrontal cortical neurons that selectively modulate social recognition. *Journal of Neuroscience* **39**, 3249-3263 (2019).
536 Leclercq, S. *et al.* Low-dose penicillin in early life induces long-term changes in murine gut microbiota, brain cytokines and behavior. *Nature communications* **8**, 1-12 (2017).
537 Fülling, C. *et al.* Adolescent Dietary Manipulations Differentially Affect Gut Microbiota Composition and Amygdala Neuroimmune Gene Expression in Male Mice in Adulthood. *Brain, Behavior, and Immunity* (2020).
538 Morris Jr, S. M. Arginine metabolism: boundaries of our knowledge. *The Journal of nutrition* **137**, 1602S-1609S (2007).
539 Greenhalgh, A. D. *et al.* Arginase-1 is expressed exclusively by infiltrating myeloid cells in CNS injury and disease. *Brain, behavior, and immunity* **56**, 61-67 (2016).
540 Femenia, T., Qian, Y., Arentsen, T., Forssberg, H. & Heijtz, R. D. Toll-like receptor-4 regulates anxiety-like behavior and DARPP-32 phosphorylation. *Brain, Behavior, and Immunity* **69**, 273-282 (2018).
541 Tramullas, M. *et al.* Toll-like receptor 4 regulates chronic stress-induced visceral pain in mice. *Biological psychiatry* **76**, 340-348 (2014).
542 Jackson, M. E. & Moghaddam, B. Amygdala regulation of nucleus accumbens dopamine output is governed by the prefrontal cortex. *Journal of neuroscience* **21**, 676-681 (2001).
543 Keith, B., Franklin, G. P. & Paxinos, G. The mouse brain in stereotaxic coordinates. *California: Academic* (2008).
544 Federici, S. *et al.* Targeted suppression of human IBD-associated gut microbiota commensals by phage consortia for treatment of intestinal inflammation. *Cell* **185**, 2879-2898.e2824, doi:10.1016/j.cell.2022.07.003 (2022).
545 Zheng, D. W. *et al.* Phage-guided modulation of the gut microbiota of mouse models of colorectal cancer augments their responses to chemotherapy. *Nature biomedical engineering* **3**, 717-728, doi:10.1038/s41551-019-0423-2 (2019).
546 Natarelli, N., Gahoonia, N. & Sivamani, R. K. Bacteriophages and the microbiome in dermatology: The role of the phageome and a potential therapeutic strategy. *International Journal of Molecular Sciences* **24**, 2695 (2023).
547 Shlezinger, M. *et al.* Phage Therapy: A New Horizon in the Antibacterial Treatment of Oral Pathogens. *Current topics in medicinal chemistry* **17**, 1199-1211, doi:10.2174/1568026616666160930145649 (2017).
548 Man, W. H., de Steenhuijsen Piters, W. A. A. & Bogaert, D. The microbiota of the respiratory tract: gatekeeper to respiratory health. *Nature Reviews Microbiology* **15**, 259-270, doi:10.1038/nrmicro.2017.14 (2017).

549 Zalewska-Piątek, B. & Piątek, R. Phage Therapy as a Novel Strategy in the Treatment of Urinary Tract Infections Caused by E. Coli. *Antibiotics (Basel, Switzerland)* **9**, doi:10.3390/antibiotics9060304 (2020).
550 Liang, B. *et al.* Effective of phage cocktail against Klebsiella pneumoniae infection of murine mammary glands. *Microb Pathog* **182**, 106218, doi:10.1016/j.micpath.2023.106218 (2023).
551 Kabwe, M., Dashper, S., Bachrach, G. & Tucci, J. Bacteriophage manipulation of the microbiome associated with tumour microenvironments-can this improve cancer therapeutic response? *FEMS Microbiol Rev* **45**, doi:10.1093/femsre/fuab017 (2021).
552 Meng, X. *et al.* Optimization of CRISPR-Cas system for clinical cancer therapy. *Bioengineering & translational medicine* **8**, e10474, doi:10.1002/btm2.10474 (2023).
553 Gan, L. *et al.* Bacteriophage targeting microbiota alleviates non-alcoholic fatty liver disease induced by high alcohol-producing Klebsiella pneumoniae. *Nat Commun* **14**, 3215, doi:10.1038/s41467-023-39028-w (2023).
554 Fujiki, J. & Schnabl, B. Phage Therapy: Targeting Intestinal Bacterial Microbiota for Treatment of Liver Diseases. *JHEP Reports*, 100909 (2023).
555 Han, M., Yang, P., Zhong, C. & Ning, K. The Human Gut Virome in Hypertension. *Front Microbiol* **9**, 3150, doi:10.3389/fmicb.2018.03150 (2018).
556 Chen, Q. *et al.* Enteric Phageome Alterations in Patients With Type 2 Diabetes. *Front Cell Infect Microbiol* **10**, 575084, doi:10.3389/fcimb.2020.575084 (2020).
557 Yang, C. *et al.* Bifidobacterium in the gut microbiota confer resilience to chronic social defeat stress in mice. *Sci Rep* **7**, 45942, doi:10.1038/srep45942 (2017).
558 Asher, M., Asnaani, A. & Aderka, I. M. Gender differences in social anxiety disorder: A review. *Clinical psychology review* **56**, 1-12, doi:10.1016/j.cpr.2017.05.004 (2017).
559 Rechlin, R. K., Splinter, T. F. L., Hodges, T. E., Albert, A. Y. & Galea, L. A. M. An analysis of neuroscience and psychiatry papers published from 2009 and 2019 outlines opportunities for increasing discovery of sex differences. *Nature Communications* **13**, 2137, doi:10.1038/s41467-022-29903-3 (2022).
560 Stein, M. B. *et al.* Social anxiety disorder and the risk of depression: a prospective community study of adolescents and young adults. *Arch Gen Psychiatry* **58**, 251-256, doi:10.1001/archpsyc.58.3.251 (2001).
561 Nota, M. H., Nicolas, S., O'Leary, O. F. & Nolan, Y. M. Outrunning a bad diet: interactions between exercise and a Western-style diet for adolescent mental health, metabolism and microbes. *Neuroscience & Biobehavioral Reviews*, 105147 (2023).
562 Magzal, F. *et al.* A personalized diet intervention improves depression symptoms and changes microbiota and metabolite profiles among community-dwelling older adults. *Frontiers in nutrition* **10**, 1234549, doi:10.3389/fnut.2023.1234549 (2023).